

**Molecular characterisation of poliovirus
inactivation with formaldehyde or other
alternative chemical compounds**

Thomas Wilton

**Imperial College London
Department of Medicine
Division of Infectious Diseases**

**A thesis submitted in partial fulfilment of the
requirements for the degree of Doctor of Philosophy
under the discipline of Virology**

2012

ABSTRACT

As the Global Polio Eradication Initiative progresses towards its conclusion inactivated poliovirus vaccine (IPV) is increasingly being used on a routine basis to ensure that any re-introduced viruses do not spread. However the current administration of conventional IPV (cIPV) includes a risk of wild seed viruses escaping from manufacturing facilities. To address this risk IPVs could instead be prepared from Sabin live attenuated strains. However Sabin IPV (sIPV) type 2 has been found to induce a lower level of antibodies than type 2 cIPV. The reason (s) for this difference is not clear as little is known about the molecular mechanisms that underpin the formaldehyde inactivation process. To investigate the process of inactivation and its consequences, this study has analysed the effect of inactivation on different aspects of poliovirus biology. As serotype 2 shows the greatest differences between sIPV and cIPV, a range of type 2 poliovirus strains with varied antigenic and biological properties have been inactivated using formaldehyde and alternative chemicals. The effect of inactivation on the viral antigenicity and immunogenicity of the poliovirus strains has been assessed using methods for the pre-release control of vaccine batches and various novel techniques including a biosensor-based technique and immunisation-challenge experiments in transgenic mice. Both the virus strain and inactivation chemical affected the potency of inactivated preparations. The effect of inactivation on the functionality of the viral RNA and the ability of inactivated virus to bind and undergo the conformational changes necessary to enter the target cell have been investigated using real-time RT-PCR and FACS flow cytometry. Inactivation modified the viral RNA and prevented poliovirus virions from undergoing necessary conformational changes. This research will contribute to better understanding the differences between sIPV and cIPV and will help to develop new/modified inactivation protocols to produce IPVs with improved immunogenicity.

CONTENTS

SECTION	PAGE
Abstract	2
Contents list	3
Declaration	4
List of figures and table	5
Acknowledgements	11
List of abbreviations	12
Chapter 1 Introduction	17
Chapter 2 Materials and Methods	68
Chapter 3 Characterisation of serotype 2 poliovirus strains inactivated with formaldehyde	100
Chapter 4 Inactivation of poliovirus with alternative chemicals	128
Chapter 5 Immunogenicity of poliovirus inactivated with beta-propiolactone, binary ethyleneimine or formaldehyde	161
Chapter 6 Molecular properties of inactivated poliovirus	179
Chapter 7 General discussion	231
Chapter 8 Conclusions and recommendations	241
References	244

DECLARATION

I declare that this thesis is my own work and the research described here was performed by myself unless otherwise stated.

Thomas Wilton

October 2012

LIST OF FIGURES AND TABLES

CHAPTER 1	PAGE
Figure 1.1	Genomic structure of serotype 1 poliovirus (Mahoney strain) and proteolytic processing of its polypeptide..... 21
Figure 1.2	Secondary structure of 5' non-coding region of serotype 1 poliovirus (Mahoney strain)..... 22
Figure 1.3	Stereo space-filling representation of the three-dimensional structure of poliovirus particle (Mahoney strain)..... 24
Figure 1.4	Simplified diagram showing the wedge-like structure of the core structure common to capsid proteins..... 25
Figure 1.5	Antigenic sites depicted on a space-filling model of the poliovirus particle..... 27
Figure 1.6	Proposed closed loop model of poliovirus negative-strand RNA synthesis..... 30
Figure 1.7	Assembly of poliovirus particles..... 32
Figure 1.8	Seasonal variation in poliomyelitis incidence and relative humidity in New England during 1942-1951..... 34
Figure 1.9	Lymphatic model of poliovirus pathogenesis..... 36
Figure 1.10	Mucosal model of poliovirus pathogenesis..... 37
Figure 1.11	Formaldehyde inactivation curves of wild-type strains, Mahoney, MEF-1, and Saukett..... 39
Figure 1.12	Location of principal attenuating nucleotide and amino acid substitutions in each of the three Sabin oral poliovirus vaccine strains..... 45
Figure 1.13	Flow chart of poliovirus isolation in RD and L20B cells..... 53
Figure 1.14	Circulation of wild-type poliovirus, as of January 2012..... 55
Figure 1.15	Location of poliovirus outbreaks associated with circulating vaccine-derived polioviruses..... 60
Table 1.1	Classification of genus <i>Enterovirus</i> 20
Table 1.2	Location of antigenic sites of poliovirus serotypes 1, 2, and 3..... 26
Table 1.3A	Passage history of serotype 2 Sabin strain..... 43

Table 1.3B	Passage history of serotype 3 Sabin strain.....	44
CHAPTER 2		
Figure 2.1	Layout of serum test plates for neutralisation assay.....	87
Figure 2.2	Real-time reverse transcription-polymerase chain reaction assay conditions.....	98
Figure 2.3	Regions of poliovirus genome analysed by real-time reverse transcription-polymerase chain reactions.....	99
Table 2.1	M-13-tagged primers used to sequence serotype 2 poliovirus strains.....	70
Table 2.2	Sequences of oligonucleotide primers used in real-time reverse transcription-polymerase chain reaction.....	71
Table 2.3	Serotype 2 poliovirus strains analysed throughout this project.....	75
Table 2.4	Inactivation conditions of each chemical.....	80
Table 2.5	Optimised inactivation conditions of each chemical.....	82
Table 2.6	Antigenic-site-specific serotype 2 poliovirus monoclonal antibodies.....	85
CHAPTER 3		
Figure 3.1	Neighbour-joining tree showing phylogenetic relationships between the serotype 2 strains and Mahoney of poliovirus serotype 1.....	108
Figure 3.2	Proportion of non-synonymous nucleotide changes in serotype 2 poliovirus strains.....	110
Figure 3.3	Antigenic structure of live serotype 2 poliovirus strains.....	113
Figure 3.4	Antigenic structure of formaldehyde-inactivated serotype 2 poliovirus strains.....	115
Figure 3.5	Immunogenicity of inactivated serotype 2 polioviruses against challenge virus strains.....	119
Figure 3.6	Specificity of immune response of rats immunised with inactivated poliovirus.....	121
Figure 3.7	Immunogenicity of live and inactivated poliovirus strains against challenge viruses.....	123

Table 3.1	A representative collection of serotype 2 poliovirus strains.....	106
Table 3.2	Nucleotide and amino acid differences between the serotype 2 strains.....	108
Table 3.3	Amino acid difference between the serotype 2 poliovirus strains at antigenic sites 1, 2a, 2b, 3a and 3b.....	111
Table 3.4	The D-Antigen content of live and inactivated poliovirus.....	116
Table 3.5	Infectious titre / D-Antigen ratio of serotype 2 poliovirus strains.....	118
 CHAPTER 4		
Figure 4.1	Chemical structure of beta-propiolactone, binary ethyleneimine, and iodoacetamide.....	130
Figure 4.2	Schematic of the Kretschmann configuration of surface plasmon resonance.....	132
Figure 4.3	Inactivation of viral infectivity with iodoacetamide.....	135
Figure 4.4	Loss of viral infectivity during inactivation with iodoacetamide.....	135
Figure 4.5	Effect of inactivation with iodoacetamide on viral antigenicity.....	136
Figure 4.6	Effect of inactivation with beta-propiolactone, binary ethyleneimine, and formaldehyde on viral infectivity of MEF-1 strain.....	140
Figure 4.7	Effect of inactivation with beta-propiolactone, binary ethyleneimine, and formaldehyde on viral infectivity.....	146
Figure 4.8	Effect of inactivation with beta-propiolactone, binary ethyleneimine, and formaldehyde on viral antigenicity.....	148
Figure 4.9	Antigenic structure of beta-propiolactone-, binary ethyleneimine- and formaldehyde-inactivated poliovirus strains.....	150
Figure 4.10	Correlation of D-Antigen estimates of inactivated poliovirus vaccines determined by biosensor and ELISA protocols.....	155
Table 4.1	Effect of inactivation with beta-propiolactone, binary ethyleneimine, and formaldehyde on viral antigenicity of MEF-1 strain.....	142
Table 4.2	Binding of serotype 2-specific monoclonal antibodies to immobilised rabbit anti-mouse immunoglobulins.....	153

CHAPTER 5

Figure 5.1	Immunogenicity of beta-propiolactone-, binary ethyleneimine- and formaldehyde-inactivated MEF-1 against challenge viruses.....	167
Figure 5.2	Protection conferred by inactivated poliovirus preparations to transgenic mice.....	169
Table 5.1	Neutralisation titre from the sera of immunised transgenic mice against challenge viruses.....	171
Table 5.2	Reduction of viral immunogenicity of inactivated poliovirus following heat-treatment.....	173
Table 5.3	Immunogenicity of untreated and heat-treated formaldehyde-inactivated poliovirus in transgenic mice.....	175

CHAPTER 6

Figure 6.1	Schematic diagram of human CD155 α	181
Figure 6.2	Schematic of poliovirus entry into a host cell.....	183
Figure 6.3	Optimisation of CD155-AP secretion by confluent 293-CD155-AP cells.....	187
Figure 6.4	Reduction of plaque forming units by neutralisation with CD155-AP.....	189
Figure 6.5	Analysis of the interaction between poliovirus and poliovirus receptor by an alkaline phosphatase assay.....	190
Figure 6.6	Analysis of the interaction between live or inactivated poliovirus and poliovirus receptor.....	191
Figure 6.7	Determination of virus-receptor binding by surface plasmon resonance.....	193
Figure 6.8	Binding of poliovirus to L20B cells analysed by fluorescence-activated cell sorting flow cytometry.....	196
Figure 6.9	Quantification of the binding of poliovirus to L20B cells analysed by fluorescence-activated cell sorting flow cytometry.....	197
Figure 6.10	Inhibition of poliovirus binding to L20B cells by pre-incubation with soluble poliovirus receptor analysed by fluorescence-activated cell sorting flow cytometry.....	198

Figure 6.11	Binding of live and inactivated poliovirus to L20B cells analysed by fluorescence-activated cell sorting flow cytometry.....	199
Figure 6.12	Real-time reverse transcription-polymerase chain reaction analysis of interaction between live poliovirus and murine cell lines.....	200
Figure 6.13	Real-time reverse transcription-polymerase chain reaction analysis of the interaction between live / inactivated poliovirus and L20B / Ltk-cells.....	202
Figure 6.14	Reduction of poliovirus binding to L20B cells following incubation with monoclonal antibodies and CD155-AP.....	204
Figure 6.15	Amount of live and formaldehyde-inactivated poliovirus within cells post incubation.....	209
Figure 6.16	Reverse transcription-polymerase chain reaction products of viral RNA extracted from live and inactivated poliovirus.....	216
Figure 6.17	Calibration curve used to assess the genome copy number of extracted viral RNA.....	218
Figure 6.18	Effect of inactivation on functionality of viral RNA extracted from live MEF-1 and beta-propiolactone-, binary ethyleneimine- and formaldehyde-inactivated MEF-1.....	219
Figure 6.19	Visualisation of RNA extracted from inactivated poliovirus vaccine preparations using an electrophoresis system.....	224
Table 6.1	Neutralisation of infectious poliovirus by expressed CD155-AP.....	188
Table 6.2	Reduction in poliovirus binding to L20B cells following pre-incubation with different agents.....	201
Table 6.3	Effect of pre-incubation with CD155-AP and monoclonal antibodies on the interaction between poliovirus and L20B cells.....	205
Table 6.4	Antigenic and binding ability and presence of viral RNA of heated poliovirus.....	207
Table 6.5	Biological activity of poliovirus RNA transfected using DEAE-dextran.....	212
Table 6.6	Biological activity of poliovirus RNA transfected using electroporation.....	214

Table 6.7	Effect of inactivation on concentration and functionality of viral RNA extracted from live and inactivated MEF-1.....	221
Table 6.8	Genome copy number of RNA extracted using different techniques.....	223

ACKNOWLEDGEMENTS

I would like to thank my colleagues at the National Institute for Biological Standards and Control who provided assistance and encouragement during this PhD. Particularly I would like to thank Dr Philip D. Minor for allowing me to use the facilities in the Virology department for my PhD. I would also like to thank members of the Poliovirus group who provided guidance and advice, in particular Dr Andrew Macadam, Glynis Dunn and Lindsay Forrest. Thanks should also go to the Biological Services Division at the National Institute for Biological Standards and Control who assisted with the rat and mice studies and to Alan Heath who provided guidance with statistical analyses.

I am also indebted to my supervisor at Imperial College London, Professor Myra McClure. I am grateful for the support and guidance you gave me and for our helpful discussions. Finally I would like to thank my primary supervisor Dr Javier Martín for his guidance, patience and support throughout this PhD. The advice and encouragement you provided to me have been invaluable to me and I have been privileged to have had you as a supervisor.

This PhD was supported financially by a grant from the National Institute for Biological Standards and Control.

LIST OF ABBREVIATIONS

°C	Degree Celsius
μ	Micro
AEI	N-acetyleneimine
AFP	Acute flaccid paralysis
AmpB	Amphotericin B
AP	Alkaline phosphatase
APCs	Antigen-presenting cells
aVDPV	Ambiguous vaccine-derived poliovirus
BCR	B-cell receptor
BEI	Binary ethyleneimine
BEV	Bovine enterovirus
bOPV	Bivalent oral poliovirus vaccine
BPL	Beta-propiolactone
BSL	Biosafety level
cDNA	Complementary DNA
cIPV	Conventional inactivated poliovirus vaccine
CLIP	Class II-associated invariant chain peptide
CNS	Central nervous system
CPE	Cytopathic effect
<i>cre</i>	<i>cis</i> -acting replication element
Cryo-EM	Cryo-electron microscopy
Cryo-ET	Cryo-electron tomography
CV	Coxsackievirus
cVDPV	Circulating vaccine-derived poliovirus
D-Ag	D-Antigen
DMEM	Dulbecco's modified Eagle's medium
ED ₅₀	Effective dose
eIF	Eukaryotic translation initiation factor
eIPV	Enhanced-potency inactivated poliovirus vaccine
ELISA	Enzyme-linked immunosorbent assay
ES	Environmental surveillance
EV	Enterovirus

FACS	Fluorescence-activated cell sorting
FCS	Foetal calf serum
FDA	US food and drug administration
FMD	Foot-and-mouth-disease
FITC	Fluorescein isothiocyanate
GPEI	Global polio eradication initiative
GPLN	Global polio laboratory network
h	Hour
HBME	Human brain microvascular endothelial
HCHO	Formaldehyde
HEV	Human enterovirus
HRV	Human rhinovirus
IAN	Iodoacetamide
Ig	Immunoglobulin
IFN	Interferon
Ii	Invariant chain
IPV	Inactivated poliovirus vaccine
IRES	Internal ribosome entry site
ITD	Intratypic differentiation
iVDPV	Immunodeficient vaccine-derived poliovirus
LD ₅₀	Lethality dose
L-glu	L-glutamine
MAb	Monoclonal antibody
MDA5	Melanoma differentiation-associated gene 5
MEM	Eagle's minimum essential medium
MHC	Major histocompatibility complex
min	Minute
MKTC	Monkey kidney tissue culture
mOPV	Monovalent oral poliovirus vaccine
NCR	Non-coding region
NIBSC	National Institute for Biological Standards and Control
NIDs	National immunisation days
nt	Nucleotide
OD	Optical density

OPV	Oral poliovirus vaccine
ORF	Open reading frame
PABP	poly (A)-binding protein
PAHO	Pan American health organisation
PAMPs	Pathogen associated molecular patterns
PBS	Phosphate buffered saline
PCBP	poly r(C) binding protein
PCR	Polymerase chain reaction
PD ₅₀ / 50PD ₅₀	Paralysing dose
PFB	PBS flow buffer
PFU	Plaque forming units
PEV	Porcine enterovirus
Pol	Polymerase
Pro	Proteinase
PRRs	Pattern recognition receptors
P-S	Penicillin-Streptomycin
PV	Poliovirus
PVR	Poliovirus receptor
RT-PCR	Reverse transcription-polymerase chain reaction
RU	Resonance units
SNIDs	Subnational immunisation days
sIPV	Sabin inactivated poliovirus vaccine
SO	Sabin original
SPR	Surface plasmon resonance
sPVR	Soluble poliovirus receptor
TCID ₅₀	Tissue culture 50 % infectious dose
TCR	T-helper cell receptor
Tg	Transgenic
TgPVR mice	Transgenic mice expressing human poliovirus receptor
TLR	Toll-like receptor
tOPV	Trivalent oral poliovirus vaccine
VAPP	Vaccine associated paralytic poliomyelitis
VDPV	Vaccine-derived poliovirus
VP	Viral protein

WHO

World Health Organisation

AMINO ACID ABBREVIATIONS

A	Alanine
C	Cysteine
D	Aspartic acid
F	Phenylalanine
G	Glycine
H	Histidine
I	Isoleucine
K	Lysine
L	Leucine
M	Methionine
N	Asparagine
Q	Glutamine
R	Arginine
S	Serine
T	Threonine
Y	Tyrosine

NUCLEOTIDE ABBREVIATIONS

A	Adenine
C	Cytosine
G	Guanine
U	Uracil

CHAPTER 1

INTRODUCTION

Poliovirus (PV) is a non-enveloped positive strand RNA virus which can cause paralytic poliomyelitis by infecting the motor neurones of the central nervous system (CNS). The tropism of the virus to infect the anterior horn of the spinal cord (the grey matter of the spinal cord) give the disease its name, from *polios* and *myelos*, Greek for ‘grey’ and ‘matter’, respectively. The earliest documented case of poliomyelitis was the funerary stele of Rom from about 1300 BCE which showed the characteristic downflexed foot and withered limb associated with muscle atrophy following the loss of motor nerve innervations of the leg. Although reports of poliomyelitis were rare until the late 19th and early 20th centuries, it had become one of the most-feared diseases in developed countries by the mid-20th century (262, 338). In 1908 Landsteiner and Popper reported that a filterable agent (i.e., virus) was the cause of poliomyelitis on the basis of microscopic examination of spinal cords from two monkeys that had been injected intraperitoneally with a suspension of ground-up cord from a fatal human case (283). The virus which caused poliomyelitis was termed PV. Findings of cross-immunity and serologic tests by Burnet and Macnamara showed that more than one strain of PV could cause poliomyelitis and that immunity to one strain did not confer immunity to another strain (72). Following research to determine the number of distinct PV strains the Committee on Typing of the National Foundation for Infantile Paralysis reported that there were three serotypes of PV, designated types I, II and III (110). Subsequently it was found that PV could be grown in nervous, human embryonic tissue (152). These findings, along with the later research which showed that circulating antibodies had a protective effect against poliomyelitis were essential requirements for the development of effective PV vaccines (62, 195, 219, 319, 363, 485, 486). Two vaccines were developed: inactivated PV vaccine (IPV) and live attenuated oral PV vaccine (OPV). Both of these vaccines have been used to control, eliminate and subsequently eradicate PV and paralytic poliomyelitis.

1.1 PROPERTIES OF POLIOVIRUSES

1.1.1 Taxonomy

Poliovirus is a member of genus *Enterovirus* of family *Picornaviridae*. Currently the *Picornaviridae* family consists of 28 species grouped into 12 genera, including, *Enterovirus*, *Cardiovirus*, *Aphthovirus*, *Hepatovirus*, *Parechovirus*, *Erbovirus*, *Kobuvirus*, *Teschovirus*, *Sapelovirus*, *Senecavirus*, *Tremovirus* and *Avihepatovirus*. As table 1.1 shows, genus *Enterovirus* is made up of 10 species, including, Human enterovirus A, Human enterovirus B, Human enterovirus C, Human enterovirus D, Simian enterovirus A, Bovine enterovirus, Porcine enterovirus B, Human rhinovirus A, Human rhinovirus B, Human rhinovirus C and unassigned simian enteroviruses. Based on neutralisation reactions with immune sera, PVs are classified into three serotypes (1, 2 and 3) (46, 552). The inability of antisera raised against the other two serotypes to neutralise infectivity is used to define the serotype. Serologically distinct strains have been identified by specific antisera prepared by cross adsorption with heterologous strains or by monoclonal antibodies (MAbs) (161). Until recently the three PV serotypes existed as a separate PV species within genus *Enterovirus*. However to solve phylogenetic inconsistencies the PV species was abolished and the PV serotypes were moved to the Human enterovirus C species (263).

Species	No. of serotypes	Examples
Human enterovirus A (HEV-A)	22	Coxsackievirus A2 (CV-A2), CV-A3, CV-A4, CV-A5, CV-A6, CV-A7, CV-A8, CV-A10, CV-A12, CV-A14, CV-A16, enterovirus A71 (EV-A71), EV-A76, EV-A89, EV-A90, EV-A91, EV-114 and the simian enteroviruses EV-A92, SV19, SV43, SV46 and A13
Human enterovirus B (HEV-B)	60	coxsackievirus B1 (CV-B1), CV-B2, CV-B3, CV-B4, CV-B5 (incl. swine vesicular disease virus [SVDV]), CV-B6, CV-A9, echovirus 1 (E-1; incl. E-8), E-2, E-3, E-4, E-5, E-6, E-7, E-9 (incl. CV-A23), E-11, E-12, E-13, E-14, E-15, E-16, E-17, E-18, E-19, E-20, E-21, E-24, E-25, E-26, E-27, E-29, E-30, E-31, E-32, E-33, enterovirus B69 (EV-B69), EV-B73, EV-B74, EV-B75, EV-B77, EV-B78, EV-B79, EV-B80, EV-B81, EV-B82, EV-B83, EV-B84, EV-B85, EV-B86, EV-B87, EV-B88, EV-B93, EV-B97, EV-B98, EV-B100, EV-B101, EV-B106, EV-B107, EV-B110 (from a chimpanzee) and the simian enterovirus SA5
Human enterovirus C (HEV-C)	21	Poliovirus (PV) 1, PV-2, PV-3, coxsackievirus A1 (CV-A1), CV-A11, CV-A13, CV-A17, CV-A19, CV-A20, CV-A21, CV-A22, CV-A24, EV-C95, EV-C96, EV-C99, EV-C102, EV-C104, EV-C105, EV-C109, EV-C113 and EV-C116
Human enterovirus D (HEV-D)	4	EV-D68, EV-D70, EV-D94 & EV-D111 (from both humans & chimpanzees)
Simian enterovirus A	1	SV4, SV28 and SA4 and A-2 plaque virus
Bovine enterovirus (BEV)	2	BEV 1 and BEV-2
Porcine enterovirus B (PEV-B)	2	PEV-9 and PEV-10
Human rhinovirus A (HRV-A)	77	HRV-A1, A2, A7, A8, A9, A10, A11, A12, A13, A15, A16, A18, A19, A20, A21, A22, A23, A24, A25, A28, A29, A30, A31, A32, A33, A34, A36, A38, A39, A40, A41, A43, A44, A45, A46, A47, A49, A50, A51, A53, A54, A55, A56, A57, A58, A59, A60, A61, A62, A63, A64, A65, A66, A67, A68, A71, A73, A74, A75, A76, A77, A78, A80, A81, A82, A85, A88, A89, A90, A94, A95, A96, A98, A100, A101, A102 and A103
Human rhinovirus B (HRV-B)	25	HRV-B3, B4, B5, B6, B14, B17, B26, B27, B35, B37, B42, B48, B52, B69, B70, B72, B79, B83, B84, B86, B91, B92, B93, B97 and B99
Human rhinovirus C (HRV-C)	49?	There are at present 49 types – a proposal for the designation of HRV-C types 1-33 has been published (440)

Table 1.1. Classification of genus *Enterovirus*.

Classification of enteroviruses (EVs) based on biological and molecular properties (230, 473).

1.1.2 Poliovirus genomic structure and function

The PV genome is approximately 7441 nucleotides (nts) in length and composed of single-stranded RNA of positive-sense polarity. It consists of a 5' non-coding region (NCR), a single open reading frame (ORF) encoding the viral polyprotein and a 3' NCR followed by a virus-encoded poly (A) tract (figure 1.1) (117, 134, 261, 415, 481, 571).

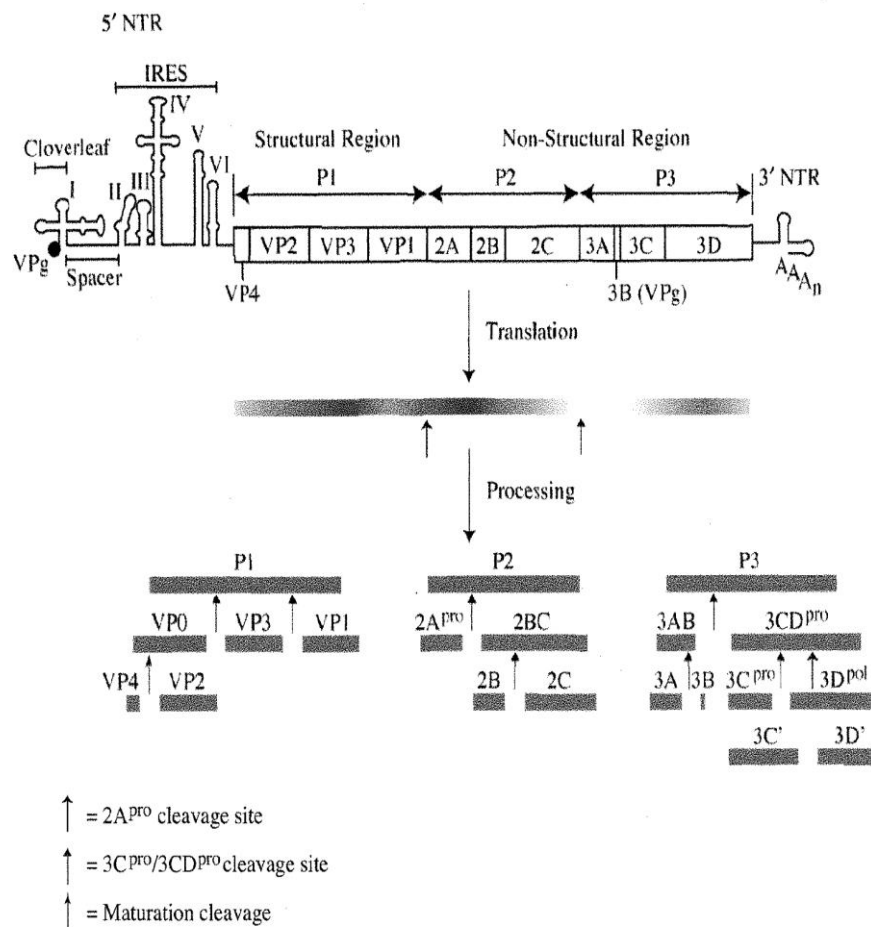


Figure 1.1. Genomic structure of serotype 1 poliovirus (Mahoney strain) and proteolytic processing of its polypeptide.

Poliovirus genome is composed of single-stranded RNA molecule of positive-sense polarity which encodes a single polyprotein. A cloverleaf and internal ribosome entry site domains make up the 5' NCR region. The 3' NCR is poly-adenylated. Cleavage of the polyprotein by virally encoded proteinases 2A^{pro} and 3C^{pro} / 3CD^{pro} releases the P1, P2 and P3 precursor polypeptides. Further proteolytic processing by these virally encoded proteinases releases eleven mature viral proteins (117). Non-translated region is abbreviated as NTR; internal ribosome entry site is abbreviated as IRES.

The 5'NCR is covalently linked to a virus-encoded VPg protein of 22 amino acids (290, 538). Important for viral RNA and protein synthesis, the 5'NCR is conserved in all three serotypes and comprises 10 % (742 nts) of the genome (117). The 5'NCR can be divided into the 5'terminal cloverleaf and the internal ribosome entry site (IRES). The 5' terminal cloverleaf is an essential *cis*-acting element in viral RNA replication and regulates the initiation of translation (15, 302, 388, 392). By facilitating initiation of translation independent of a capping group and a free 5' end the IRES mediates cap-independent translation of the viral RNA (96, 235, 236, 392, 398, 399). Computer analysis has predicated the 5'NCR to harbour a complex secondary structure divided into six domains (I-VI) (figure 1.2) (6, 405, 475). Many of these predicted domains have been validated by genetic and biochemical analyses and visualised by electron microscopy (32, 147).

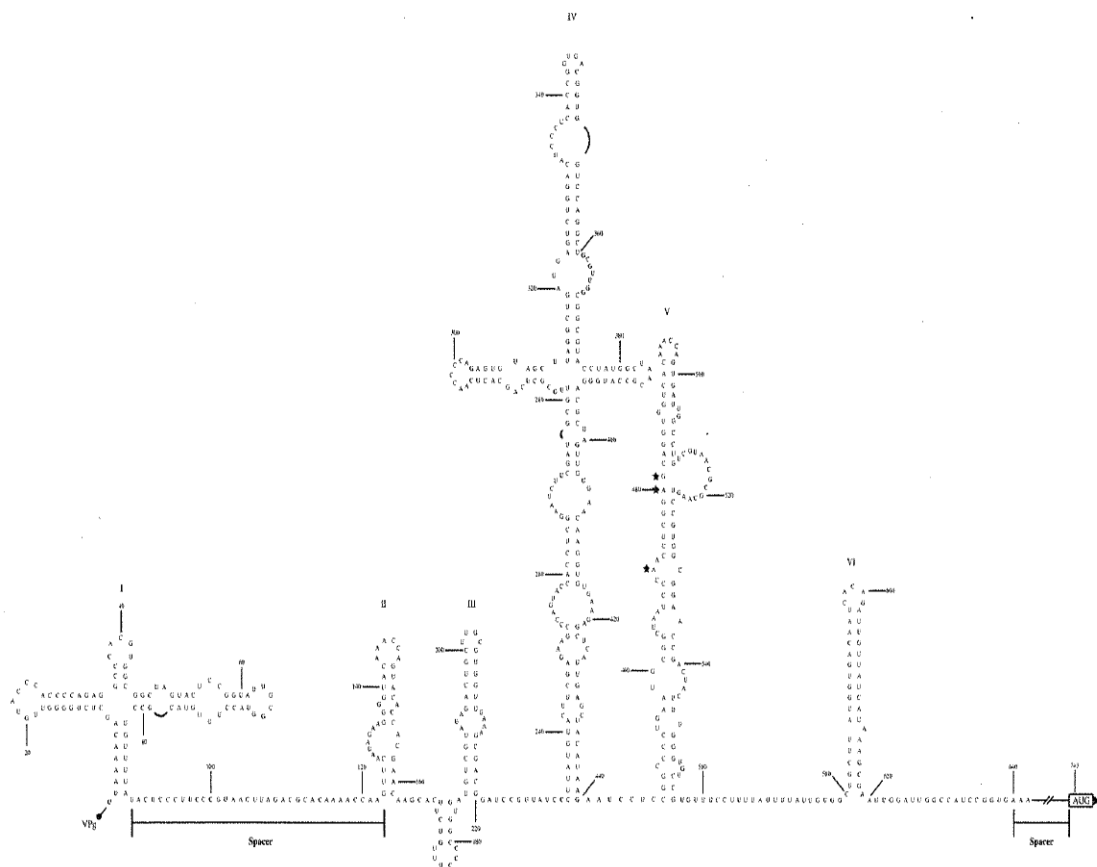


Figure 1.2. Secondary structure of 5'non-coding region of serotype 1 poliovirus (Mahoney strain)

Six domains make up the 5'NCR. Domain 1 constitutes the cloverleaf, while the remaining domains comprise the IRES. Between the cloverleaf and the IRES and between the IRES and the initiation codon there are spacer

sequences which lack a complex secondary domain. Stars denote attenuation mutations of the Sabin PV serotype 1, 2, and 3 vaccine strains at nts 480 (A to G), 481 (A to G), and 472 (C to U) (respectively) (117).

The polyprotein encoded by the single ORF can be divided into P1, P2 and P3 regions (figure 1.1). The P1 region encodes the structural viral capsid proteins VP1, VP3 and VP0. VP0 is later cleaved to release VP2 and VP4. These capsid proteins are responsible for binding to the PV receptor (PVR) and harbour the antigenic sites. The P2 and P3 region encodes the non-structural proteins. The P2 region encodes the 2A proteinase ($2A^{pro}$), the processing intermediate 2BC and subsequently the 2B and 2C ATPase ($2C^{ATPase}$) proteins. The $2A^{pro}$ cleaves the nascent polyprotein *in cis* at the p1/2A junction to release the P1 precursor polypeptide (385). During infection the $2A^{pro}$ cleaves several host factors to shut-off the host translation and transcription (573). The 2B and the $2C^{ATPase}$ proteins and their precursor 2BC have been associated with the production of membranous vesicular replication structures (98). The 2B protein is also involved with membrane permeabilisation, blockade of the cellular secretory system and disintegration of the Golgi apparatus (9, 130, 454). The $2C^{ATPase}$ protein has ATPase and RNA-binding activities (346, 435).

The P3 region encodes the 3A, $3B^{VPg}$, $3C^{pro}$, 3CD and 3D polymerase ($3D^{pol}$) proteins, all of which are involved with RNA replication. The 3A protein and its precursor 3AB have multiple roles in RNA replication and stimulate the polymerase activity of $3D^{pol}$ (348, 385, 393, 428). The $3C^{pro}$ and its precursor $3CD^{pro}$ carry out the majority of the secondary processing steps. The $3D^{pol}$ is a template and primer dependent RNA polymerase essential for the replication of RNA genome (385). The poly-adenylated 3'NCR comprises 1-3 % (70 nts) of the genome and is predicted to exhibit secondary structures consisting of two hairpins (234, 407). It has been indicated to have a functional role in RNA replication (58, 59, 143, 234, 330, 404, 406, 407).

1.1.3 Poliovirus morphology and structure

Poliovirus virions are spherical with a diameter of 27-30 nm and consist of a protein shell surrounding the naked RNA genome (414). X-ray diffraction studies and the molecular structure of PV have shown that the virus capsid consists of 60 protomers with each being made up of one molecule of each of the four capsid viral proteins. Protomers are arranged with icosahedral symmetry (figure 1.3) (209).

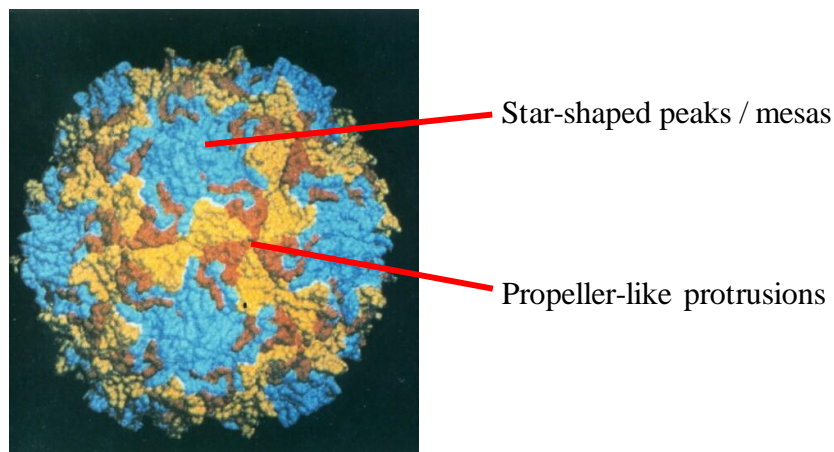


Figure 1.3. Stereo space-filling representation of the three-dimensional structure of poliovirus particle (Mahoney strain).

Virus particle consists of 60 protomers. Each protomer contains a single copy of VP1 (blue), VP2 (yellow) and VP3 (red) (209).

Three protomers make up the 20 faces of the icosahedron and are orientated so the 12 apices of the icosahedron are composed of 5 copies of VP1. The centre of each face is made of 3 copies each of VP2 and VP3 alternating around the 3-fold axis (333). Protomers are orientated so the VP4 lies on the inner surface of the capsid (414).

The icosahedron's apices at the 5-fold axis are elevated forming star-shaped peaks or mesas at the surface of the virion (figure 1.3). The face of the icosahedron at the 3-fold axis is elevated forming propeller-like protrusions (figure 1.3). These elevations are separated by deep depressions ("canyon") which surround the peaks at the 5-fold axis of symmetry. Saddle-shaped depressions crossing the two-fold axis of symmetry link the canyons together (162, 208, 209). A hydrocarbon-binding pocket is located beneath the canyon (162, 208). The

floor of the canyon has been mapped as the virus-receptor binding site by genetic, mutational and structural studies (34, 38, 108, 172, 200, 296).

The largest virion proteins (VP1, VP2 and VP3) have a similar core structure in which the peptide backbone of the protein loops back on itself to form a barrel of eight strands held together by hydrogen bonds (the β -barrel). A wedge-like structure is formed by this core (figure 1.4).

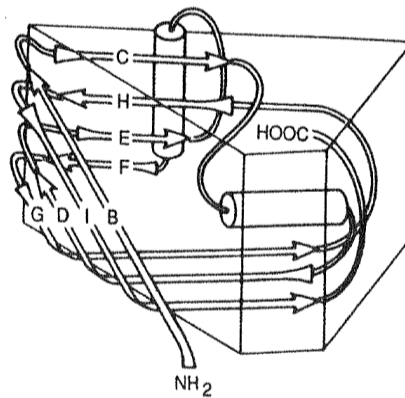


Figure 1.4. Simplified diagram showing the wedge-like structure of the core structure common to capsid proteins.

Wedge-like structure is formed by folding pattern of eight β -strands (209).

Amino acid sequences between the sequences making up the β -barrel and the sequences at the N- and C- terminal portions of the protein contain elaborations which include the main antigenic sites involved in the neutralisation of viral infectivity (344).

1.1.3.1 Antigenic structure of poliovirus

Four neutralising antigenic sites have been identified by the isolation of antigenic variants resistant to MAbs which are able to neutralise the parental strain, and then characterised by sequencing the genomic RNA. Table 1.2 shows these antigenic sites for the three PV serotypes. A BC loop in VP1 forms the continuous antigenic site 1. The remaining antigenic sites are discontinuous and formed from loops contributed by different capsid proteins (291, 382). The locations of the antigenic sites on the viral proteins that make up the viral capsid are shown in figure 1.5.

Serotype	Antigenic site					
	Site 1	Site 2a	Site 2b	Site 3a	Site 3b	Site 4
PV1	VP1 90-102, 144	VP1 221-226	VP2 164-173		VP3 58-60	VP2 72, VP3 76
PV2	VP1 93- 101, 174	VP1 217-221, 140	VP2 167-168	VP2 72-73, 158, 239, 244	VP2 158, VP3 56, 61, 66	
PV3	VP1 89-101, 166, 253	VP1 220-222	VP2 164-173	VP1 286-290	VP3 58-60	VP3 77, 79

Table 1.2. Location of antigenic sites of poliovirus serotypes 1, 2, and 3.

Four antigenic sites were identified using MAbs (342, 343, 357-359). Sites 2 and 3 are subdivided.

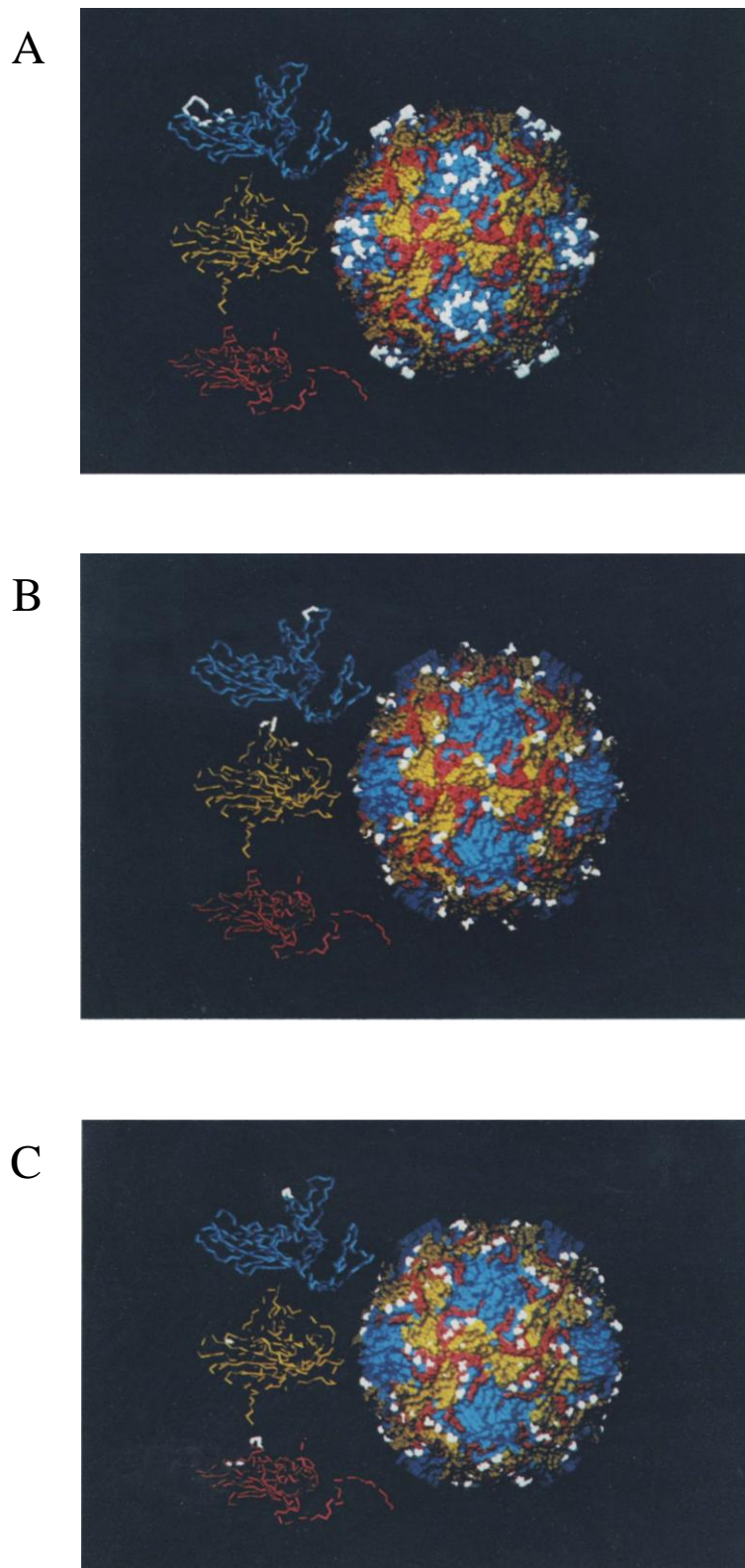


Figure 1.5. Antigenic sites depicted on a space-filling model of the poliovirus particle.

Plates A, B and C contain isolated copies of VP1, VP2 and VP3 on the left and an intact particle on the right. VP1 is blue, VP2 is yellow, and VP3 is red. The sites of mutations which confer resistance to neutralising MAbs are highlighted in white. Using spatial considerations and cross neutralisation studies the mutations have been grouped into three sites: Site 1 (A), Site 2 (B) and Site 3 (C) (210).

Neutralising antigenic sites vary within each serotype. However, possibly due to steric requirements for interactions with the PVR, the range of this variation is limited (201). Two types of antigenicities (D and C) are shown by PV preparations, depending on their sedimentation coefficient in sucrose gradients. Intact infectious virions sediment at 155-160S in sucrose gradients and show D-antigenicity, while empty capsids or denatured PVs sediment at 70-80S in sucrose gradients and show C-antigenicity (344). D-Antigen (D-Ag) units are considered the protective antigens as they stimulate neutralising antibodies. Treatment of infectious PV virions with heat or ultraviolet radiation can denature the PVs and result in a conversion from D to C antigenicity (289).

1.1.4 Replication and cellular life cycle of poliovirus

The cellular life cycle of PV is initiated by the binding of a PV virion to the N-terminal V-type immunoglobulin-like domain of the human PVR or CD155 (266, 329, 461). The exact mechanism by which the PV virion releases its RNA genome into the cytoplasm of the cell is not clear. Current research indicates following binding to the PVR the PV virion undergoes a series of conformational changes releasing myristoylated capsid protein VP4 and the N-terminal amphipathic helix of VP1 before the viral RNA. The myristoylated VP4 and amphipathic helix of VP1 are thought to insert into the cell membrane creating pores through which the virus RNA can enter into the cytoplasm (117, 511).

Receptor-mediated endocytosis has been proposed as an alternative explanation for the entry of the virus (117). Two recent studies have explored this mechanism of entry for PV by using fluorescence microscopy to trace the movement of virions, and a combination of approaches to correlate the movement of virions with the pathway of productive infection (54, 112). Brandenburg *et al.* (54) used live cell microscopy of HeLa cells infected with virus labelled with separate fluorescence dyes bound to the capsid protein and the viral genome (511). This study found that a receptor-mediated conversion to 135S or A particle conformation (see Chapter 6) was required for internalisation. RNA release was rapid and occurred within 100-200 nm of the cell surface. Infection of HeLa cells by PV was found to be independent of clathrin, caveolin, flotillin, microtubules, and pinocytosis. The infection of these cells was dependent on actin, ATP, and an unidentified tyrosine (54, 511). The findings

of this study indicate that RNA release occurs within clathrin- and caveolin-independent vesicles in the cell periphery (35). In the second study Coyne *et al.* (112) examined the entry pathway of PV in Human Brain Microvascular Endothelial (HBME) cells, a highly polarised cultured cell line which serves as a model for the blood-brain barrier. In contrast to the findings of previous studies where infection of HeLa cells was fast and independent of both dynamin and caveolin (54, 128), Coyne *et al.* (112) showed that PV infection of HBME cells is very slow and utilizes dynamin-dependent caveolar endocytosis. The differences between the two studies indicate that PV has high flexibility in that it is able to use multiple mechanisms to enter different cell types (511)

After entry, an unknown cellular phosphodiesterase is believed to cleave the VPg viral protein from the RNA genome. Host ribosomes bind to the IRES (within the 5'NCR) and initiate translation of the RNA genome (117). The single translated polyprotein contains two sequences which serve as proteolytic enzymes, digesting the polyprotein at specific positions during translation (344). The first is the 2A^{pro} which catalyses the cleavage of the genomic polyprotein at a tyrosine-glycine dipeptide, resulting in the release of the P1 precursor polypeptide (507). The second is the 3C^{pro} / 3CD^{pro} which catalyse the cleavage of P2 and P3 precursors at glutamine-glycine dipeptides into non-structural proteins, including, 2A^{pro}, 2B, 2BC, 2C, 3A, 3AB, 3B^{VPg}, 3C^{pro} / 3CD^{pro} and 3D^{pol} (197). At the same time the 2A^{pro} mediates the cleavage of the eukaryotic translation initiation factor (eIF)-4G subunit of the eIF-4F complex to shut off the cap-dependent host cell translation (275, 480, 523). This cleavage results in a modified eIF-4G which lacks the N-terminal domain required for interaction with the cap binding protein eIF-4E and poly (A)-binding protein (PABP). Therefore this cleavage inhibits cap-dependent translation initiation and PABP-mediated enhancement and reinitiation of translation on cellular mRNAs (114). Poly (A)-binding protein is also cleaved by PV proteinases and this is hypothesised to contribute to the shut down of cap-dependent translation (114, 240, 278). Host cell transcription is inhibited by 3C^{pro} which inactivates transcription factor TFIIC and cleaves the TATA box binding protein (107, 565).

The 2B and 2C viral proteins and their precursor 2BC, induce the formation of viral replication complexes in the cytoplasm by stimulating the rearrangement of endoplasmic reticulum derived intracellular membranes into vesicular structures (41, 98, 344, 496). Replication of the RNA genome is complex involving the formation of intermediates,

including, a replicative intermediate consisting of a negative strand partially hybridised to multiple nascent positive-strands, and a replicative form that has a double stranded structure, composed of one full length copy of the positive and negative strands each (117).

Replication of PV RNA begins with the synthesis of a negative-RNA strand. A closed loop model which involves both viral and host cellular proteins has been proposed and is shown in figure 1.6.

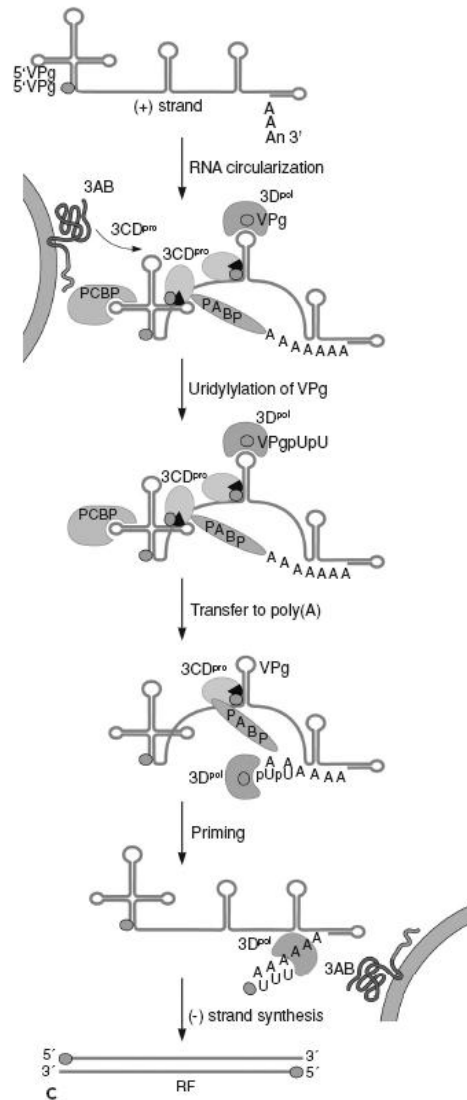


Figure 1.6. Proposed closed loop model of poliovirus negative-strand RNA synthesis.

The positive (+) strand is at the top, showing the 5' cloverleaf structure, the internal *cis*-acting replication element (*cre*) sequence, and 3' pseudoknot. The host poly r(C) binding protein (PCBP) and viral 3CD^{pro} bind the cloverleaf structure forming a ribonucleoprotein complex. This complex interacts with the host cell protein PABP, which is bound to the 3'-poly (A) sequence, producing a circular loop. Membrane bound 3AB is cleaved by 3CD^{pro} to release 3A and VPg. The VPg, 3D^{pol} and 3CD^{pro} bind to the *cre* sequence within the RNA genome.

The 3D^{pol} catalyses the uridylation of the VPg, using the sequence AAACA of *cre* as the template. The complex is transferred to the 3' end of the genome, and the VPG-pUpU is used by 3D^{pol} to prime synthesis of a negative RNA strand, thus resulting in the double stranded replicative form (414).

In this model a ribonucleoprotein complex is formed when the host cell protein PCBP2 and viral protein 3CD^{pro} bind to stem-loop I at the 5'NCR (443). This ternary complex interacts with the host cell protein PABP1, which is bound to the 3'-poly (A) sequence, producing a circular loop. Membrane bound 3AB is cleaved by 3CD^{pro} to release 3A and VPg (414). During replication of PV RNA the synthesis of both negative- and positive-sense strands is primed by a uridylated form of the genome linked viral protein VPg (VPg-pUpU) (395). The *cre* is a position-independent stem-loop RNA structure essential for picornavirus RNA replication which has variable location in the genome of different virus types. The *cre* is thought to act as the site for the uridylation of VPg by 3D^{pol} (114). The uridylation of VPg results in a covalent linkage between the single tyrosine in VPg and the PV negative- and positive- RNA strands (14, 168, 261, 290, 373, 374, 401, 438). The VPg, 3D^{pol} and 3CD^{pro} bind to the *cre* sequence within the RNA genome. The 3D^{pol} catalyses the uridylation of the VPg, using the sequence AAACA of *cre* as the template. The complex is transferred to the 3' end of the genome, and the VPG-pUpU is used by 3D^{pol} to prime synthesis of a negative RNA strand, thus resulting in the double stranded replicative form (344, 395, 414). This associates with the vesicular structures to form the replication intermediate complexes (344). The negative-strand of this complex acts as a template for synthesis of multiple positive-strand RNAs. The increasing excess of VPg-pU-pU over VPg favours this and results in asymmetric levels of positive- versus negative-strand viral RNAs in the infected cell (344, 395). The positive strand RNA molecules either serve as templates for additional rounds of translation or negative-strand RNA synthesis or are covalently linked to VPg triggering encapsidation in progeny PV virions (374, 443). It should be noted that due to the frequent single base misincorporations and lack of proofreading the replication of the PV genome is prone to errors.

The cleavage of the P1 precursor polypeptide by 3CD^{pro} releases the VP0, VP1 and VP3 proteins. After cleavage, considerable movement of the amino termini and carboxyl termini of these viral proteins occurs. In the mature capsid, the carboxyl termini of VP1, VP2, and VP3 are on the outer surface of the capsid, whereas the amino termini are on the interior, where

they engage in an extensive network of interactions amongst protomers (414). This process allows one copy of VP0, VP1 and VP3 to assemble to form the 5S protomer (534). A pentamer which sediments at 14S is formed by the assembly of five protomers (figure 1.7) (117, 403, 414).

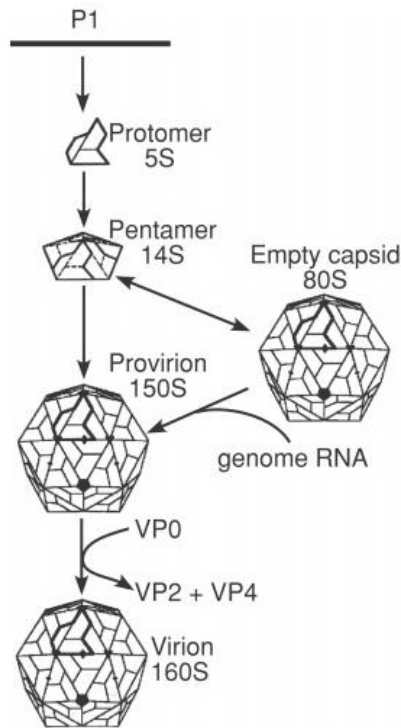


Figure 1.7. Assembly of poliovirus particles.

P1 precursor polypeptide is cleaved from P2 precursor polypeptide. P1 precursor polypeptide is further cleaved by 3CD^{pro} to release VP0, VP1 and VP3. One copy each of VP0, VP1 and VP3 assemble to form the protomer. Five protomers assemble to form a pentamer. Pentamers assemble into an empty capsid into which the RNA genome is threaded in to create a provirion. Alternatively the pentamers assemble around the RNA genome to form the provirion. Cleavage of VP0 to release VP2 and VP4 is the final morphogenic step that produces the infectious 160S virion (414).

Subsequently 12 pentamers assemble about the viral RNA genome to form the provirion (233, 403). Alternatively the pentamers assemble into an empty capsid into which the viral RNA genome is incorporated, forming the provirion (233, 402, 414). The provirion is converted into a mature infectious virion by the cleavage of VP0 into VP2 and VP4, possibly by an autolytic mechanism (208, 212, 233). Mature infectious PV virions are then released by the lysis of the infected cell (117).

1.2 INFECTION AND DISEASE

1.2.1 Epidemiology

Polioviruses are transmitted from person to person by the faecal-oral route or oral-oral route following excretion in faeces and pharyngeal secretions (255, 364). There are no known extrahuman reservoirs as the PVR is only expressed on the cells of humans and a few subhuman primate species (355, 413). Although there is consensus that poliomyelitis has been occurring for millennia, few cases were reported until the late 19th century. Epidemic poliomyelitis began around 1880 with a series of outbreaks in several Scandinavian countries and the United States (287). An increase in the age at which PV infection was occurring has been proposed as a possible hypothesis for these epidemics of poliomyelitis (369). Prior to these epidemics enteric infections were very common and many infants were infected within 6-12 months. At this time they had circulating antibodies derived from their nursing mothers which prevented viremia, thus avoiding invasion of the CNS and paralysis. However as personal hygiene and public sanitation were improved the transmission of enteric infections was delayed so that some infants were first infected after 12 months of age, when the level of passive antibodies had fallen. This allowed for the infection of the CNS and the development of paralytic poliomyelitis in infants or as it was known then, “infantile paralysis” (364).

As a result of this improvement in hygiene the age distribution of patients with poliomyelitis increased. Adults had a higher probability than infants of developing paralytic poliomyelitis than nonparalytic CNS infections, abortive illness or asymptomatic infection (218). Data regarding the distributions of the three PV serotypes in the USA during this epidemic era suggests that the virulence (paralytogenicity) varies between the serotypes. Serotype 1 was found to be more virulent than the other serotypes which showed similar virulence to one another (465).

Prior to the introduction of vaccines poliomyelitis was a seasonal disease in cooler temperate climates with the incidence of infection peaking in the summer and autumn months (figure 1.8).

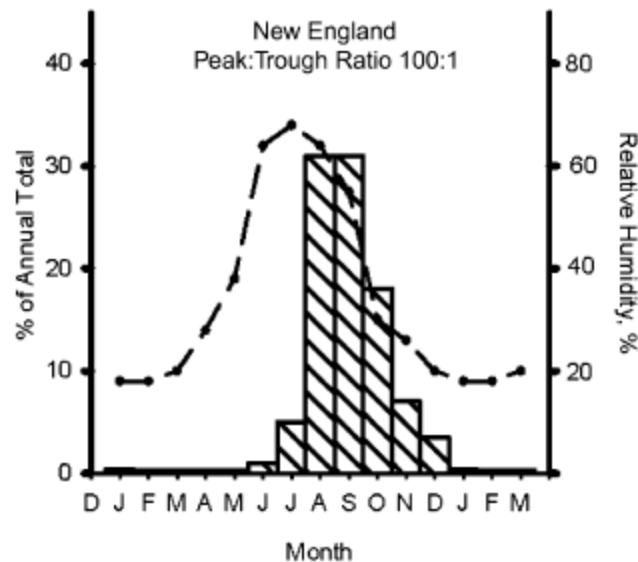


Figure 1.8. Seasonal variation in poliomyelitis incidence (striped bars) and relative humidity (dashed line) in New England during 1942-1951.

The degree of seasonal variation in poliomyelitis incidence is shown by the ratio (370, 462).

The degree of seasonality decreases towards the equator, with poliomyelitis being prevalent all year-round in tropical regions. It has been hypothesised that this seasonality is due to the humidity level which affect PV survival (figure 1.8) (364, 369, 445).

The incidence of poliomyelitis fell significantly when IPV and live attenuated OPV were introduced in 1955 and 1960, respectively. The use of these vaccines in the seasonal trough allowed for PV to fade out of individual regions, particularly if it was not reintroduced (364). This fall has increased further worldwide since the Global Polio Eradication Initiative (GPEI) began in 1988. However the GPEI has changed the ecology of PV. For most of the world immunity to PV is now conferred solely by vaccination rather than through natural infection.

Although the GPEI has been successful, there are still epidemiological barriers to the eradication of PV in the remaining areas of the world where wild-type PVs remain endemic,

which encompasses Nigeria, Afghanistan, Pakistan and northern India. These include a lack of seasonality and a higher incidence of enteric infections in tropical climates (390). The inability to vaccinate in conflict areas of Afghanistan and Pakistan represents a single epidemiologic block, with ongoing large population movements between the two countries accompanied by cross-border transmission. In addition the high population densities and poor sanitation, which occurs in Uttar Pradesh and Bihar in India, Nigeria and Pakistan, enhances the transmission of PV (364).

1.2.2 Clinical and pathological aspects

Poliovirus can cause minor illness typical of a systemic infection or it can cause major illness such as poliomyelitis, the most serious disease caused by any of the EVs. As described above PV transmits via the faecal-oral route. Several models of PV pathogenesis have been described, one of which is the lymphatic model of Bodian (43) (figure 1.9).

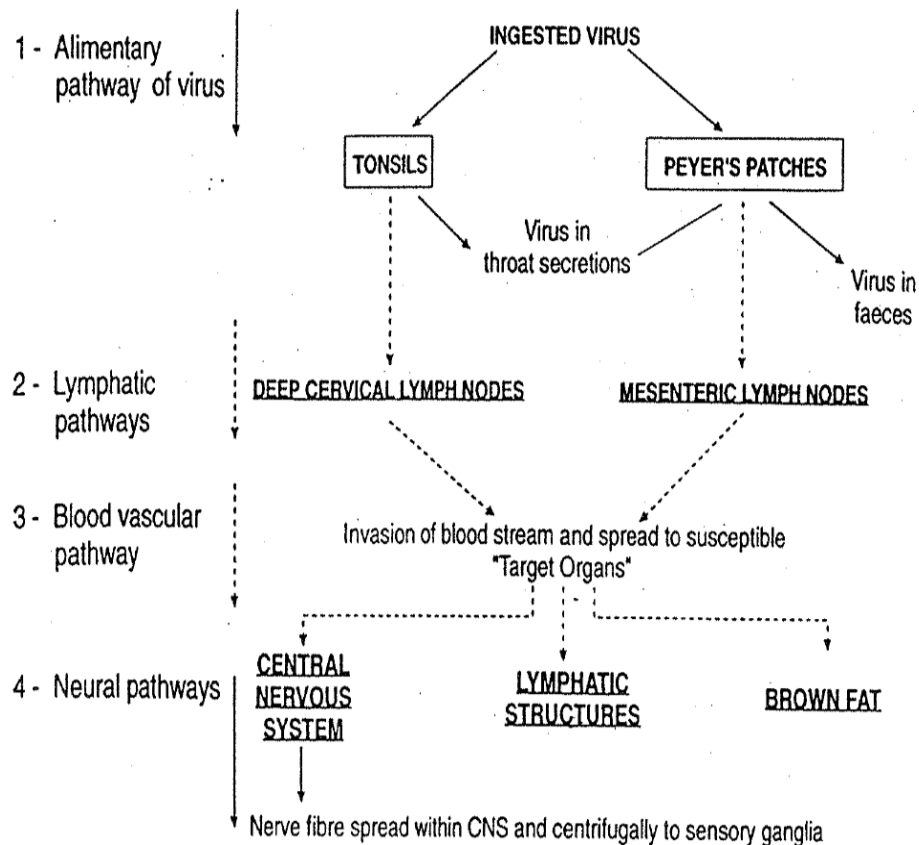


Figure 1.9. Lymphatic model of poliovirus pathogenesis.

Model of PV pathogenesis, showing the progression from the alimentary to lymphatic sites, viremia, and neuronal infection (43, 340).

The lymphatic tissue of the gastrointestinal tract, including the tonsils and the Peyer's patches of the ileum, act as the primary sites of replication for PV. Poliovirus shed in the faeces is sourced from the Peyer's patches. Before the viremic phase occurs the deep cervical and mesenteric lymph nodes become infected by drainage from the gastrointestinal lymphoid tissues. Blood-borne PV might originate from these local lymph nodes. Poliovirus then disseminates independently to brown fat, other lymphatic structures and the CNS (340).

An alternative mucosal model has been proposed by Sabin (446) (figure 1.10).

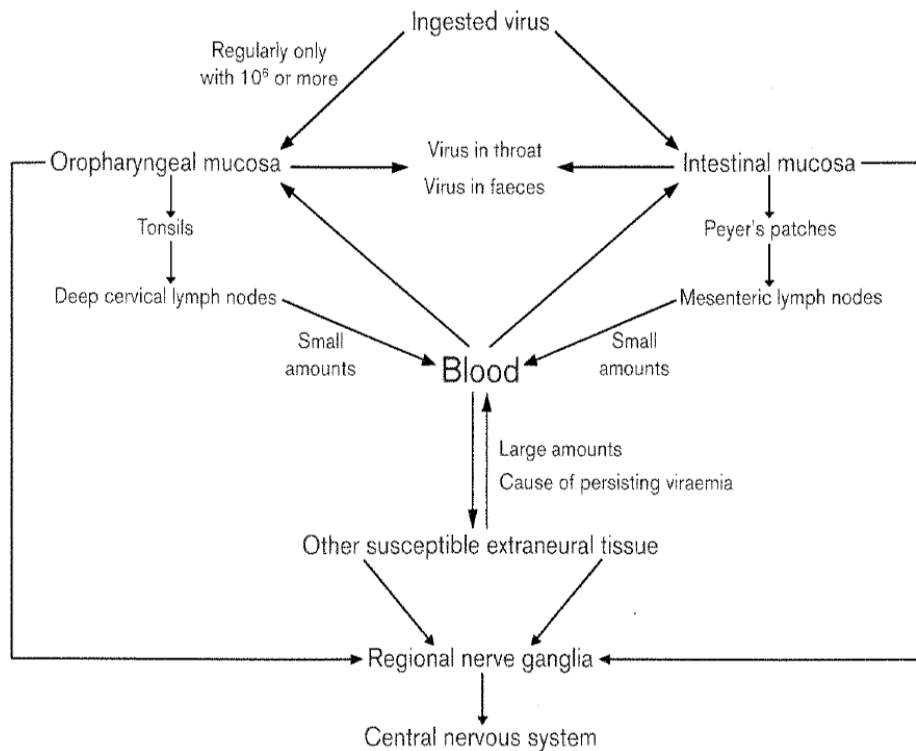


Figure 1.10. Mucosal model of poliovirus pathogenesis.

Model of PV pathogenesis, showing the interchange between oropharyngeal and intestinal mucosa, extraneural tissue, and regional nerve ganglia (338, 446).

In this model PV becomes present in the throat or faeces as result of ingested virus replicating in the oropharyngeal or intestinal mucosa. Subsequently the local lymphatic tissue (tonsils and the Peyer's patches) accumulates PV without necessarily being the replication site. As described above the deep cervical or mesenteric lymphoid nodes are infected by these lymphatic tissues. Small amounts of PV can leak from these nodes into the blood and disseminate to other susceptible extraneural replication sites. Through a number of routes regional nerve ganglia may be infected, and PV can then migrate to the CNS (340). The precise mechanism (s) by which PV invades the CNS is not well understood (117). However experimental evidence from research in non-human primates (43, 45) and CD155 transgenic (Tg) mice (378, 422) strongly suggest that PV invades the CNS by retrograde axonal transport (192, 377, 378). Replication of PV within the CNS triggers the major illness associated with PV.

For the great majority of PV infections (approximately 95 %) a minor viremia develops and they are asymptomatic. For some infected individuals (4-8 %) a major viremia develops that is associated with minor illness (117). Clinical symptoms of this minor illness include malaise, diarrhoea, fever and sore throat (117, 340). If the symptoms resolve then the infected individual is said to have suffered abortive paralysis (340). A small number of patients who experience major viremia develop non-paralytic aseptic meningitis or paralytic poliomyelitis, indicating that PV has invaded CNS (117). In 1-2 % of PV infections non-paralytic aseptic meningitis develops, characterised by rigidity of the neck, back and lower limbs (85). Depending on the serotype 0.1-1 % of PV infections develop into paralytic poliomyelitis (369). The severity of the paralytic poliomyelitis depends on the areas of the CNS affected and the extent of damage to the neuronal tissue. In spinal poliomyelitis the motor nerves are destroyed and associated skeletal musculature is denervated (117). This results in hemilateral paralysis, more prominent in the lower limbs. Clinical signs of bulbar poliomyelitis include paralysis of the respiratory muscle, and it is characterised by paralysis of the cranial nerves associated with the control of breathing. Both the spinal cord and the brain stem are affected in bulbospinal poliomyelitis (44, 85).

1.3 VACCINES AGAINST POLIOVIRUS

In the late 19th century the improvement of hygiene led to delayed transmission of PV until maternal antibodies had waned. This changed the pattern of poliomyelitis from uncommon and endemic to the occurrence of large epidemics. In response research focussed on developing vaccines. Several scientific discoveries allowed the development of PV vaccines. These included the isolation of PV by Landsteiner and Popper (284), which allowed research to begin. The definition of three serotypes allowed the conclusion to be made that no cross-protection was conferred (46). Viremia was found to precede paralysis and neutralising antibodies were confirmed to protect against poliomyelitis (196, 219). Finally it was demonstrated that PV could propagate in human cells (152). Subsequent studies found that PV could propagate in a range of cells from tissues of human and nonhuman primate origin. The monkey kidney became the source of tissue for vaccine production (430). Two vaccines have been developed; an injectable (killed) IPV; and a live attenuated OPV by Drs Salk *et al.* (451) and Dr Sabin (448), respectively.

1.3.1 Inactivated poliovirus vaccine

Following several technical developments, such as the propagation of the monolayer form of monkey kidney and testicular cells, Salk and colleagues were able to grow large quantities of the three PV serotypes (178, 409). The kinetics of inactivation with formaldehyde (HCHO) were analysed and it was concluded that if filtration was able to remove aggregates of PV, the virus could be inactivated at a constant first-order rate, allowing complete elimination of infectivity if sufficient time was allowed (figure 1.11) (409).

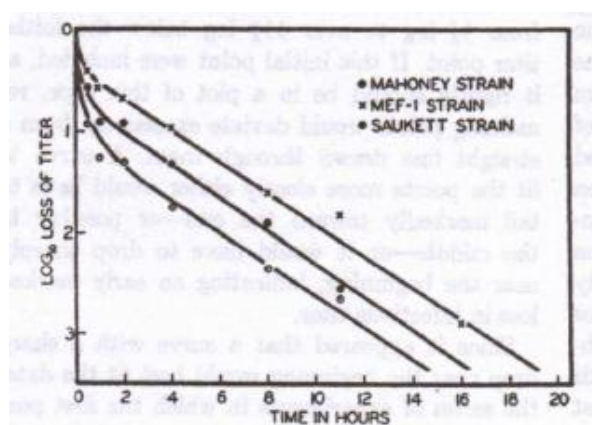


Figure 1.11. Formaldehyde inactivation curves of wild-type strains, Mahoney, MEF-1, and Saukett.

Strains were inactivated at pH 7.0 with 1:4000 HCHO. Averaged data from four to five inactivation experiments was used to plot the curves for each strain (503).

Several trivalent vaccine pools were prepared and found to be safe and immunogenic in monkeys and humans (430). Based on these laboratory findings large-scale field trials in humans were conducted by Thomas Francis and his associates in 1954. The vaccine was found to be safe and effective at 60-70 % for serotype 1 and 90 % for serotype 2 and 3 (170, 178). Potency (antibody response in children) correlated with effectiveness of the vaccine (178). IPV was licenced shortly after (430).

However paralytic cases began to appear shortly after IPV became available. Two vaccine pools from one manufacturer, Cutter Laboratories Inc., were traced to be the source of these cases by an epidemiological investigation. The Cutter vaccine was found to have caused 260 cases of poliomyelitis (366-368). Inactivated PV vaccine vaccination was

suspended, the Cutter vaccine was recalled and the US Public Health Service launched an intensive investigation. The Cutter incident was attributed to two problems with IPV production. The first was that there was a failure to remove viral clumps which could hide infectious particles. Secondly, virus inactivation was not linear as there was a “tailing-off” of viral inactivation at lower concentrations of infectious PV (409). A filtration step was added to the production process, midway during HCHO inactivation which removed the virus clumps. While this improved the safety of the preparation, it also diminished the antigenicity (326). The PV inactivation period was extended and the volume of vaccine doses was significantly increased in the test for residual infectivity in monkey kidney cultures after virus inactivation. Between the late 1950s and early 1960s this first generation IPV was widely used in the USA, Canada, Netherlands, Sweden, France and Finland. However in the early 1960s many of the countries in the Americas and Europe switched to OPV when it was licenced (178).

Following several technical advances in the late 1960s and 1970s, enhanced-potency IPV (eIPV) was developed. This second generation IPV differed from the first generation IPV as the virus harvest was concentrated and purified before inactivation by ultrafiltration and column chromatography. In addition to increase the density of cells they were grown on microbeads in large fermenters. In 1967 van Wezel developed a microcarrier system which could be applied to 100 L fermenters (521). Either secondary or tertiary subcultures of kidneys from pathogen-free monkeys or human diploid cell strains or the Vero African green monkey kidney cell line were used as the cell substrate. The use of well characterised cells ensures that the IPV is free of extraneous contaminating agents. This trivalent eIPV acts as the conventional IPV (cIPV) and is administered either alone or in combination with other vaccines, including diphtheria, tetanus and acellular pertussis, hepatitis B and / or *Hemophilus influenzae* b. Both preparations are highly immunogenic in infants following three doses at two, three and four months of age (178).

The wild-type PV strains used by Salk *et al.* for the first generation IPV are still used by most modern manufacturers. These include Mahoney (serotype 1; Brunenders is used in Sweden and Denmark); MEF-1 (serotype 2) and Saukett (serotype 3) (409). Although HCHO inactivation has been noted to modify the antigenic site 1 of PV serotypes 2 and 3 (160), immunisation with IPV can induce high titres of neutralising antibodies protective against all PV strains. However local (intestinal) immunity is not induced, which allows the virus to still

multiply in the intestinal tract of the vaccinee and thus to be shed in faeces and become a source of infection to others (321). Other problems with the IPV include the cost for needle and syringe and the need for trained health workers to administer the vaccine (546). However IPV has been used exclusively in Sweden, Finland and the Netherlands and has virtually eliminated poliomyelitis (344). Finally as it is a killed vaccine it does not carry the risk of causing vaccine associated paralytic poliomyelitis (VAPP).

1.3.2 Oral poliovirus vaccine

In 1946 Theiler (500) developed the first attenuated variant of the serotype 2 strain Lansing by serial passage of the virus. This approach was adopted by others and in 1952 Koprowski *et al.* (270) reported the first successful immunisation of volunteers with an attenuated rodent-adapted serotype 2 PV strain. The principle attenuated vaccine candidates were developed by three key research groups led by Sabin (448), Koprowski (270), and Cox (75). Between 1950 and 1960 these candidate vaccines were developed and tested in large field-trials held in a number of countries under various conditions. Many of these trials in humans involved the sequential administration of monovalent preparations of the three serotypes. The results of these trials were assessed in two conferences held by the Pan American Health Organisation (PAHO) in 1959 and 1960 (386, 387). In 1958, a detailed comparison of candidate strains was carried out at Baylor College of Medicine in Houston and at the Division of Biologics Standards of the National Institutes of Health (322-324, 327, 362).

Throughout all of these field trials and laboratory comparisons the candidate vaccines were evaluated for their immunogenicity, genetic stability on passage in humans, lack of paralytic properties in humans, restricted capacity to spread from man to man, and low neuropathogenicity in monkeys (255). Research at Baylor College of Medicine in Houston and at the Division of Biologics Standards of the National Institutes of Health concluded that the Koprowski and Cox candidate vaccine strains were more neurotropic for monkeys than the Sabin strains. As a result the Sabin vaccine strains were licenced and manufactured. The strains have been used almost universally since then (485). Oral PV vaccine was licenced as a

monovalent preparation sequentially between 1961 and 1963 (396). Following a successful field trial in Canada a trivalent formulation was licenced in 1963 (485).

The Sabin OPV strains were developed from circulating strains that had been adapted to laboratory conditions (339). In 1941 Drs Francis and Mack isolated the serotype 1 Mahoney strain from which the Sabin 1 strain is derived. After Salk made 14 monkey kidney tissue culture (MKTC) and 2 monkey testicular passages Li and Schaeffer made 11 MKTC passages to yield the partially attenuated LS strain. The further attenuated LS-c strain was yielded by additional passages in monkey kidney and skin. The LS-c, 2ab was obtained when Sabin carried the LS-c strain through terminal dilutions and single plaque passages and selected subsequent strains by neurovirulence testing. Two further passages in cynomolgus MKTC yielded the Sabin original (SO) or the LS-c, 2ab/KP₂ strain. A further passage of the SO at Merck Sharp and Dome in rhesus MKTC yielded the SO+1 (LS-c, 2ab/KP₃) strain. The current vaccine is four passages from the SO and thus is termed SO+4. After five passages earlier (grandmother) seeds must be thawed and used to prepare new mother seeds (485).

Sabin also developed attenuated Sabin strains for serotypes 2 and 3. A low neurovirulence PV strain (P712) isolated from a healthy child was used to derive the Sabin 2 (P712, Ch, 2ab/KP₃) strain. The Sabin 3 (Leon 12ab/KP₄) strain was derived by passage of a highly neurovirulent PV strain (Leon) isolated from the spinal cord of a child who had died of bulbospinal poliomyelitis (255, 485). The passage history of these strains is summarised in tables 1.3A and B.

Year	Manipulation	Designation
–	Fox and Gelfand: Isolated P 712 strain	P 712
1954	Sabin: 4 passages in cynomolgus MKTC 3 serial passages of plaque isolates Selection by neurovirulence testing <ul style="list-style-type: none"> - Fed to chimpanzees - 3 single-plaque passages 	P 712, Ch P 712, Ch, 2ab
1956	Sabin: 2 passages in cynomolgus MKTC	P 712, Ch, 2ab/KP ₂ = SO
1956	Merck, Sharp & Dohme: 1 passage in rhesus MKTC	P 712, Ch, 2ab/KP ₃ = SO+1

Table 1.3A. Passage history of serotype 2 Sabin strain.

Sabin 2 strain was derived by passage of low neurovirulent PV strain (P712). Adapted from (448, 485).

Year	Manipulation	Designation
1951	Kessel and Stimpert: Isolated Leon strain 20 intracerebral passages in rhesus monkeys	Leon
1952	Melnick: 8 passages in rhesus testicular tissue culture	
1953	Sabin: 3 passages in cynomolgus MKTC 30 rapid passages at low dilution in cynomolgus MKTC 3 terminal dilution passages 1 low-dilution passage 9 plaques isolated, single-plaques passed 3 times Selection by neurovirulence testing	Leon 12a,b
1956	Sabin: 3 passages in cynomolgus MKTC	Leon 12a,b/KP ₃ = SO
1956	Merck, Sharp & Dohme: 1 passage in rhesus MKTC	Leon 12a,b/KP ₄ = SO+1

Table 1.3B. Passage history of serotype 3 Sabin strain.

Sabin 3 strain was derived by passage of highly neurovirulent PV strain (Leon). Adapted from (448, 485).

With greater understanding of the molecular biology of PV and the advent of recombinant DNA technology it was possible to identify the genetic determinants of attenuation. The publication of the complete nt sequences of PV genomes allowed the sequences of the Sabin strains and their neurovirulent wild-type parent (serotypes 1 and 3) or neurovirulent revertents (serotypes 2 and 3), from VAPP cases, to be compared. The development of infectious complementary DNA (cDNA) clones allowed the contribution of specific nt substitutions to attenuation to be assessed (485).

Sabin 1 has 57 nt substitutions throughout its genome which distinguish it from the Mahoney strain (375). Six are found in the 5'NCR, 49 map to the coding region (of which 21 code for amino acid substitutions), and two are located in the 3'NCR (255). Infectious cDNA constructs identified that the A-G substitution at position 480 in the IRES of the 5'NCR was the most important attenuating mutation (figure 1.12) (250). The attenuated phenotype was also due to four other substitutions within the viral capsid proteins (one in VP4, one in VP3, two in VP1). These substitutions have also contributed to the temperature sensitive phenotype of the Sabin 1 strain. A substitution mapped to the 3D^{pol} region contributes to the temperature sensitive but not attenuated phenotype (52, 99, 318, 379, 394, 494).

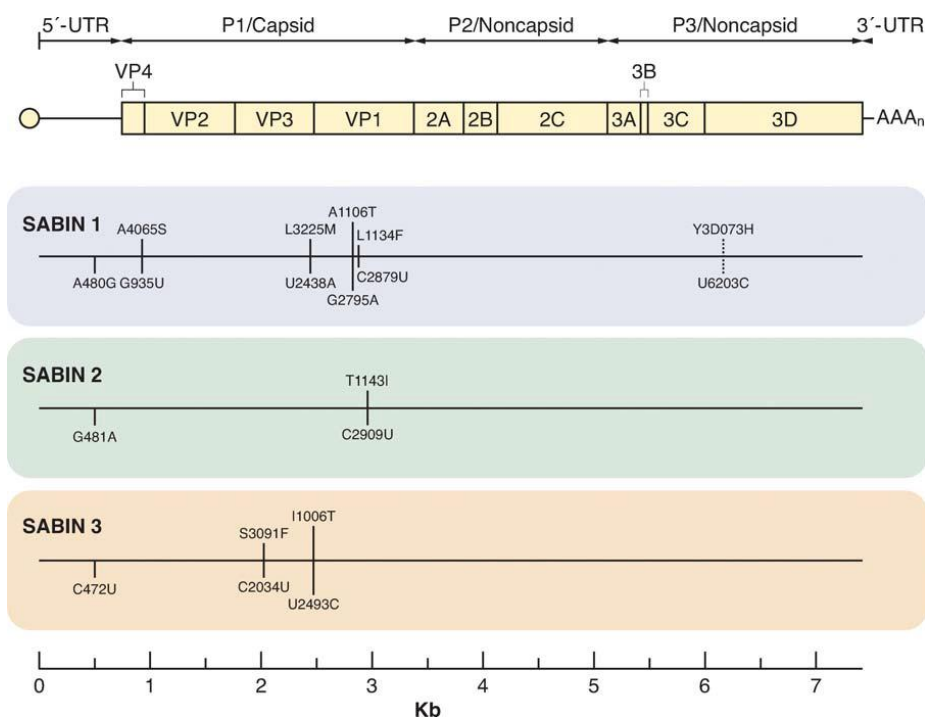


Figure 1.12. Location of principal attenuating nucleotide (lower bars) and amino acid (upper bar) substitutions in each of the three Sabin oral poliovirus vaccine strains.

Nucleotide residue abbreviations: A, adenine; C, cytosine; G, guanine; U, uracil. Amino acid abbreviations: A, alanine; C, cysteine; F, phenylalanine; H, histidine; I, isoleucine; L, leucine; M, methionine; S, serine; T, threonine; Y, tyrosine. Substitutions are shown as nonattenuated parent-position-Sabin strain (255). From residue 1 of RNA genome, nts are numbered consecutively. Amino acids are numbered consecutively from residue 1 of each viral protein. Abbreviated name of viral protein (4, VP4; 2, VP2; 3, VP3; 1, VP1; 3D, 3D-polymerase) indicates position of amino acids. Untranslated region is abbreviated as UTR (52, 250, 255, 305, 424, 494, 533).

The attenuated and temperature sensitive phenotype of the Sabin 2 strain was found to be due to two nt substitutions. These included a G-A substitution at position 481 in the IRES, and the C2909U substitution which encodes a T-I substitution at position 143 of VP1 (figure 1.12) (305, 424). Three substitutions determine the attenuated and temperature sensitive phenotype of the Sabin 3 strain. These include a C-U at position 472 in the IRES, C2034U encoding an S-F substitution at position 91 of VP3 and U2493C encoding an I-T substitution at position 6 of VP1 (figure 1.12) (255, 303, 336, 533). The attenuated phenotype of the Sabin strains is conferred by multiple substitutions, as described above (255). Substitutions within domain V of the IRES (figure 1.2) of the 5'NCR have been associated with deficiencies in viral replication in the CNS and neuroblastoma cells and a reduction in the efficiency of the initiation of translation of the PV RNA template (279-281, 487-489).

A series of animal models and cell culture assays have been developed to analyse the biological properties of OPV strains. The neurovirulence of OPV strains has been tested in both monkeys and Tg mice which express human PVR (269, 543). Poliovirus sensitive Tg mice were developed by introducing the gene encoding the human PVR into the mouse genome. The expression of the receptor mRNAs in tissues of the Tg mice was analysed by RNA blot hybridisation and polymerase chain reaction (PCR). The Tg mice were found to be susceptible to all three serotypes of PV (269). The temperature sensitivity of an OPV strain is assessed by comparing plaque formation on HEp-2C cells at different temperatures (264, 380).

Another assay used in the quality control of OPV strains is the mutant analysis by PCR and restriction enzyme cleavage. This is a molecular biological assay for quantitation of the trace amount of revertant sequence (s) in monovalent Sabin bulks (105, 543). This assay involves the extraction of RNA from virions, reverse transcription and amplification of a target stretch of the cDNA by PCR. Restriction enzymes then digest the amplified products with enzymes which cut either attenuated or virulent sequence. Following polyacrylamide gel electrophoresis the cut and uncut bands are quantified (543). This assay allows the position of reversion to be quantified and has been used to estimate the ratio of neurovirulence in a virus population correlated to the revertants (104, 427).

Oral poliovirus vaccine is administered orally and parallels the natural infection by replicating in the gastrointestinal tract. This stimulates both local secretory immunoglobulin

A (IgA) in the pharynx and gastrointestinal tract and circulating IgG. The virus is excreted in the faeces for several weeks and possibly in pharyngeal secretions for days (344). In areas with a high incidence of PV and low hygiene and sanitation, OPV immunisation can lead to the passive immunisation of close contacts through the spread of the vaccine shed in the faeces and pharyngeal secretions. Unlike IPV, which only elicit serum humoral immunity, OPV is able to induce gut immunity as well. This imitation of the natural infection results in OPV breaking the transmission of PV (338). In addition OPV is cheap to produce in the large quantities required for national immunisation days (NIDs). Finally as OPV is orally administered, no sterile injection equipment or specially trained health workers are required (255). For the reasons stated above OPV became the choice vaccine to be used in the GPEI.

A major flaw with OPV is that it is genetically unstable (117). As discussed above, following immunisation OPV strains replicate in the gastrointestinal tract of immunocompetent individuals for a limited time before the vaccine is excreted for periods of up to 30-60 days (3, 311). During this period, the attenuating mutations of the vaccine can rapidly revert and the OPV can change through a range of mechanisms. These include recombination, site suppression mutations, back mutations and a steady drift in molecular sequence. The loss of the attenuation mutations is selected for during replication in the gut as it improves the growth characteristics of the OPV strains. VAPP is caused by this reversion of the attenuation mutations during OPV replication in humans.

The World Health Organisation (WHO) defines VAPP as poliomyelitis which occurs in a vaccinee between 7 and 30 days after a dose or in a person in close contact with a vaccinee between 7 and 60 days after that dose was received (335). Viruses isolated from healthy OPV recipients / contacts often show biological and chemical properties which are indistinguishable from viruses isolated from patients with VAPP (255). Vaccine associated paralytic poliomyelitis occurs at a low rate, estimated at between 1 per 500,000 and 1 per 750, 000 vaccinees following the first vaccination; and 1 in 12 million vaccinees after the second dose (440). People with primary B-cell immunodeficiency are at much higher risk of developing VAPP (~3000 fold) (255). The ability of OPV strains to revert to virulence and to spread to contacts has implications for the GPEI.

1.4 GLOBAL POLIOVIRUS ERADICATION INITIATIVE

1.4.1 Disease eradication

Less than 20 years since the introduction of OPV, the transmission of wild-type PV was halted in the United States of America (85). This success prompted the PAHO to use OPV as its weapon of choice against poliomyelitis. Successes in OPV vaccination programmes run throughout South America resulted in the PAHO meeting its goal of eradicating wild-type PV in the Western Hemisphere by 1990. The transmission of wild-type PV in the Americas was certified to be discontinued three years later by the International Commission for the Certification of Poliomyelitis Eradication. Two decades prior to this the WHO had committed itself to vaccinate the entire world's population as a means to aid the eradication of variola virus which caused smallpox. This mass vaccination strategy eventually eliminated the virus and in 1980, the 33rd World Health Assembly announced the first successful eradication of a major human disease – smallpox (117, 158). Both the success of the PAHO eradication campaigns in the Americas and the eradication of smallpox encouraged the WHO to commit itself to the eradication of poliomyelitis by the year 2000.

There are three levels of interventions to prevent infectious disease (135). These include control, which means to reduce the morbidity of the disease to a socially acceptable level through various measures (including vaccination). If successful this leads to the next level, disease elimination, which is the reduction of morbidity to zero by applying measures used to control the disease. By creating universal immunity in the human population this can be achieved even if the agent is still present in the environment. Eradication is the final level which leads to the permanent elimination of the disease from circulation and the prevention of any reintroduction. The difference between elimination and eradication is that the former requires rigorous control measures to maintain zero morbidity, while eradication would mean that such measures could be discontinued, conserving public health resources for other needs. Therefore if it is possible, it is better to eradicate rather than eliminate a disease. It is biologically possible to eradicate poliomyelitis as humans are the only natural reservoir host of PV (103). Consequently the decision was made to eradicate rather than eliminate poliomyelitis.

The eradication of PV requires a number of biological principles to be met. These include, the spread of the virus by person-to-person transmission; the absence of a persistent carrier state; the interruption of virus transmission by immunisation; a finite virus survival time in the environment; and the absence of any nonhuman reservoir hosts for the virus (136). In addition there must be a political will to enforce the eradication campaign. The GPEI has been dependent on the strong alliance among national governments, international agencies (e.g. UNICEF) and private partners (including Rotary International, the Bill and Melinda Gates Foundation and the UN Foundation) (255).

1.4.2 Strategies for poliovirus eradication

A combination of routine immunisation and supplementary campaigns guided by surveillance has been used to stop PV transmission. The four key strategies have been employed include, a high routine immunisation coverage of infants with four doses of trivalent OPV (tOPV) in the first year of life; supplementary immunisation through mass OPV campaigns, such as NIDs and subnational immunisation days (SNIDs) which target children younger than five years of age; targeted door-to-door “mop-up” OPV immunisations in high-risk areas; and surveillance for cases of acute flaccid paralysis (AFP) in children under 15 years of age with virological investigations of clinical specimens from AFP patients (103, 228, 255).

1.4.2.1 Immunisation

One of the key strategies of PV eradication is the high routine immunisation coverage of infants of less than one year of age with tOPV. Although routine coverage specifically protect individuals, if used in high coverage it can be used to interrupt the circulation of OPV. However routine immunisation coverage is low in many parts of the developing world. In addition in tropical countries routine immunisation is not very effective in blocking PV transmission. This could be due to problems with the storage of the vaccine in hot climates, where it is likely to lose potency if not stored at low temperatures. In addition the level of coverage that can be consistently achieved over several years and the epidemiology of PV

circulation in tropical countries might affect the effectiveness of routine immunisation (339). As described above there is a lack of seasonality in PV circulating in tropical countries and this may contribute to difference in the effectiveness of routine immunisation in temperate and tropical countries. For example if individuals in tropical countries are routinely immunised in the winter, as they might be in temperate countries, it is more likely that they will be infected with wild-type PV before they are immunised (339).

For the reasons described above routine immunisation is used in conjunction with supplementary immunisation and “mopping-up” strategies in developing and tropical countries. In developing countries supplementary immunisation is an essential part of the eradication strategy as it can, in combination with routine immunisation, raise population immunity rates above the thresholds required to block PV transmission (556). Supplementary immunisation often takes the form of NIDs and SNIDs. The aim of NIDs is to immunise all children under the age of five in a country or region in a short period of time (normally a few days) and then to repeat the process a few weeks later. Subnational immunisation days are similar, but only immunise all the children under five in areas smaller than a country or region. National immunisation days and SNIDs are designed to interrupt PV transmission in a population by abruptly reducing the number of susceptible individuals. By preventing all transmission, even the silent transmission which does not lead to disease, the virus dies out (339).

For some regions a synchronous immunity barrier to all three PV serotypes has been achieved by coordinating NIDs of neighbouring countries (103). Surveillance is used to drive supplementary immunisation campaigns. For example surveillance can guide SNIDs and “mop-up” campaigns to reservoirs communities where chains of PV transmission continue to survive and propagate (255).

1.4.2.2 Surveillance

Poliovirus surveillance is an essential cornerstone to the GPEI. The WHO established a global network of laboratories (the Global Polio Laboratory Network, GPLN) in 97 countries to support PV surveillance for all countries. The 144 GPLN laboratories are divided into three tiers which include, 121 national laboratories; 16 regional reference laboratories; and 7

global specialised reference laboratories (84, 103). The GPLN isolates PV from clinical specimens and in some settings environmental samples, and identifies them using various laboratory techniques (103).

Nucleotide sequence analysis is used to further characterise vaccine-derived PV (VDPV, see below) and wild-type PV isolates. This analysis can be used to generate phylogenetic trees of current wild-type PV and VDPV isolates, which along with spot maps of different genetic groups of PVs, are dispatched monthly from the GPLN to the WHO and reinfected countries and to those in endemic areas. High-risk endemic areas which require intensified immunisation activities are identified using this genetic data (103).

Poliovirus surveillance can be based on two separate approaches, including, clinical case-driven surveillance, and direct virus targeted surveillance. The WHO gold standard of the former approach is AFP surveillance which is based on the assumption that if wild-type PV is circulating in a population, it is likely to be found in patients with a disease typically caused by PV. The view that all PV infected individuals, whether symptomatic or not, excrete relatively large amounts of the virus into stools for several weeks forms the basis of the direct virus targeted surveillance (220).

Acute flaccid paralysis surveillance encompasses a number of steps. These include an active search for acutely paralytic children in the community; virological examination of faeces from these children; and centralised data collection and analysis (220). To avoid extensive neurologic examinations, which are not feasible in many developing countries, AFP was chosen as a clinical measure of paralytic poliomyelitis. However AFP surveillance alone is not highly specific or sensitive for detecting wild-type PV infections (16). As AFP has multiple etiologies (including Guillian-Barré syndrome, transverse myelitis, and traumatic neuropathy) this surveillance reports many other diseases in addition to poliomyelitis. The background rate of AFP from etiologies other than wild-type PV infection is at least 1 case per 100,000 persons younger than 15 years of age (254, 383, 485). Thus, the detection of an AFP case does not necessarily indicate infection with wild-type PV (254). For this reason, clinical specimens of AFP cases should be analysed by virologic techniques to investigate the etiologic role of wild-type PVs (255).

While AFP surveillance can detect endemic PV circulation in a population, its sensitivity is judged to be low as approximately only 1 in 200 nonimmune children infected with wild-type PV shows signs of AFP (16, 164, 255, 384). Acute flaccid paralysis may appear in fewer than 1 of 10,000 wild-type PV infections when the population shows high levels of immunity (255, 410). To increase the sensitivity for detecting wild-type PV circulation environmental surveillance (ES) of PV is being used as a supplementary surveillance. Environmental surveillance refers to monitoring PV transmission in human populations by examining environmental specimens supposedly contaminated by human faeces. It is based on the fact that PV-infected individuals, whether presenting with disease symptoms or not, shed large amounts of PV in the faeces for several weeks (223). Following successful examples in Europe (222) and Israel (308) ES has been introduced to in Egypt (221), India (127), and Pakistan (103). Environmental surveillance has been able to detect PV lineages which were undetected by AFP. In most cases, strains closely related to the environmental isolates were found in the same country by AFP surveillance. However in some cases imported wild-type PV (Israel, India, and Switzerland) and otherwise-undetected highly divergent VDPVs have been found by ES (90, 91, 103).

1.4.2.3 Laboratory diagnosis

The GPLN laboratories carry out a number of virologic assays and techniques to aid PV surveillance. The use of recombinant murine cells which express CD155 (L20B cells), has enhanced standard methods for PV isolation in cultured cells (224, 408, 552). As these cells express CD155 they are selectively susceptible to PV and will produce a characteristic EV cytopathic effect (CPE). Although some non-PVs might be able to infect L20B cells, their CPE is usually different from that of PV. A small number of non-PV EVs can infect and grow in L20B cells, producing EV characteristic CPE. RD cells are derived from a human rhabdomyosarcoma and are permissive to PV, many ECHO viruses and some other EVs, all of which produce a characteristic EV CPE (552). A combination of passages in these two cell lines is used to isolate PV (figure 1.13).

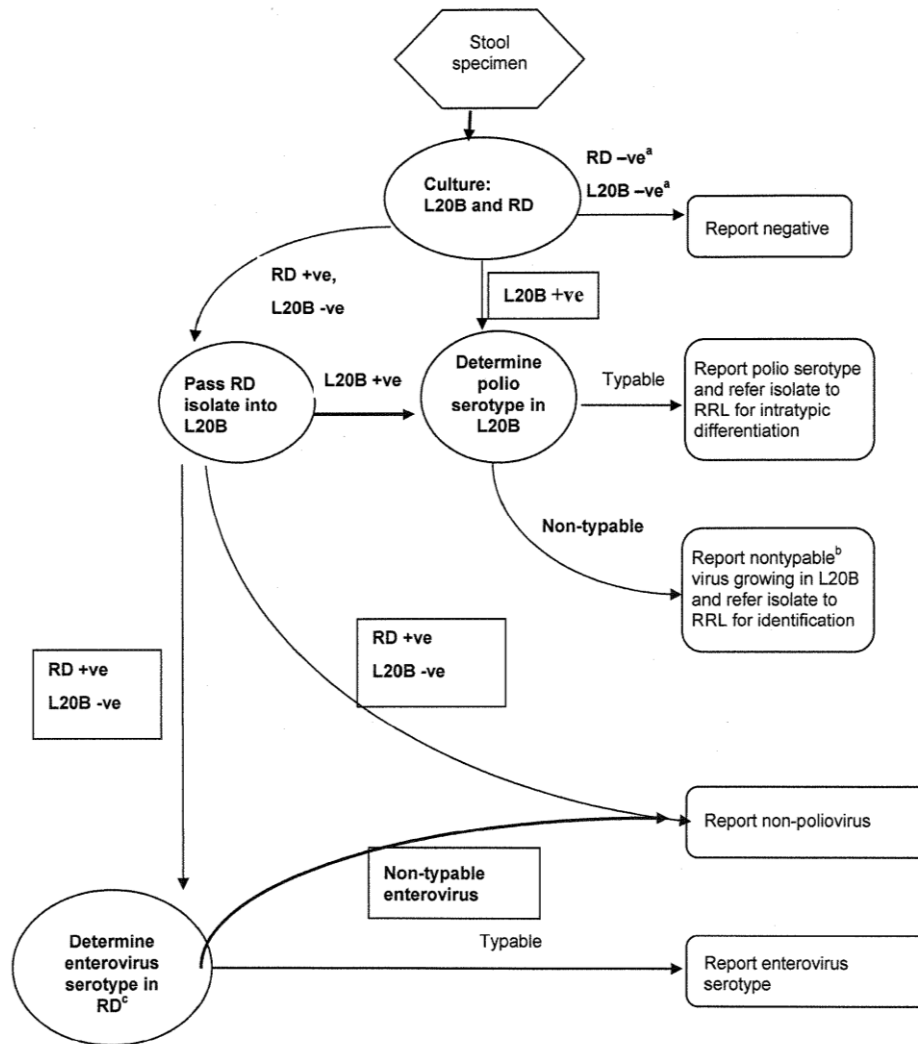


Figure 1.13. Flow chart of poliovirus isolation in RD and L20B cells.

^a: Passaged two times for a minimum of 14 days in total; ^b: If a nontypable isolate is obtained in L20B cells from samples from a non-endemic or recently endemic country, a regional reference laboratory coordinator and the national programme should be informed; ^c: Non-polio EVs are only typed at the request of the Expanded Programme on Immunisation (552).

Standard typing assays or PCR using PV group-specific or serotype-specific primer sets can be used to distinguish PV from non-PV EVs (258, 259, 552). Poliovirus typing is performed on the L20B culture of a clinical sample, while non-PV EV typing is carried out on the RD culture of a clinical sample (552). Intratypic differentiation (ITD) of PV is carried out by regional reference laboratories of the GPLN to determine whether it is vaccine-related or a wild-type. Methods assessing the antigenic and molecular properties of PV are used to

perform the ITD of PV (83). The antigenic ITD method incorporates an ELISA system with preparations of highly specific cross-adsorbed antisera (517, 522). Alternatively this method is based on MAb neutralisation using Sabin-specific MAbs in a cell culture-based neutralisation (517). Either genotype-specific nucleic acid probes, genotype-specific PCR primers, or PCR-restriction fragment length polymorphism are used in the molecular ITD methods (24, 118, 119, 298, 568, 569).

Oral poliovirus vaccine-like PVs which are unlikely to be of current epidemiologic importance are screened out by ITD, while VDPVs and wild-type PV are screened for. The complete VP1 region (~900 nts, ~15 % of total genome) of VDPV and wild-type PV has been sequenced by the GPLN since 2001. Different alignment algorithms, tree-building methods, estimation of genetic distances, and testing models of evolution can be used to compare nt sequences (309). This sequenced region is used to compare isolates as several serotype-specific antigenic sites are encoded in this part of the genome and nt substitutions are successively fixed in this area as the PV strains evolve (255, 337). Comparative VP1 sequence data can generally afford sufficient phylogenetic resolution for individual chains of transmission and identification of local endemic reservoirs to be reconstructed as the PV sequence evolves rapidly (1 to 2 nt substitutions per week over the entire genome) (467). If higher resolution is required the sequencing window can be widened to cover the entire PV genome (253, 299, 466, 567). Phylogenetic trees and lineage maps are used to summarise sequence relationships (33, 42, 149, 253-255, 314, 466, 467, 570).

1.5 CURRENT STATUS OF POLIOVIRUS ERADICATION

1.5.1 Progress between 1988 and 2011

In 1988 the GPEI was launched with the intention of eradicating poliomyelitis by the year 2000 (18). Global cases had decreased 99 % from an estimated 350, 000 cases in 124 countries in 1988 to 719 cases in 23 nations by the year 2000 (18, 551). In addition the last case of serotype 2 wild-type PV was reported in Uttar Pradesh, India, in October 1999 (79). Between 1988 and 2002 three WHO regions were certified to be free of indigenous wild-type PV circulation. These included the Americas in 1994 (81); the Western Pacific Region in

2000 (82); and the European region in 2002 (80). In 2001 the fewest reports of PV were recorded, with 483 cases across 15 countries (551).

However following difficulties in eradicating PV in Nigeria, India, Pakistan and Afghanistan, which still retain an endemic circulation of PV (figure 1.14), the number of wild-type PV cases rose, peaking at 1651 cases in 18 countries in 2008 (17, 551). Although most of the population in these countries are protected transmission still continues from some of the highest-risk areas (103). Indeed these persistent reservoir countries have served as the main source of infection for a series of imported PV outbreaks that have affected countries in Africa, Southeast and Central Asia, and Europe (figure 1.14) (89, 92, 483, 553). Innovations in the vaccination campaigns and the type of OPV used have since led to a decrease in the number of PV cases, at 650 cases in 2011 (551).

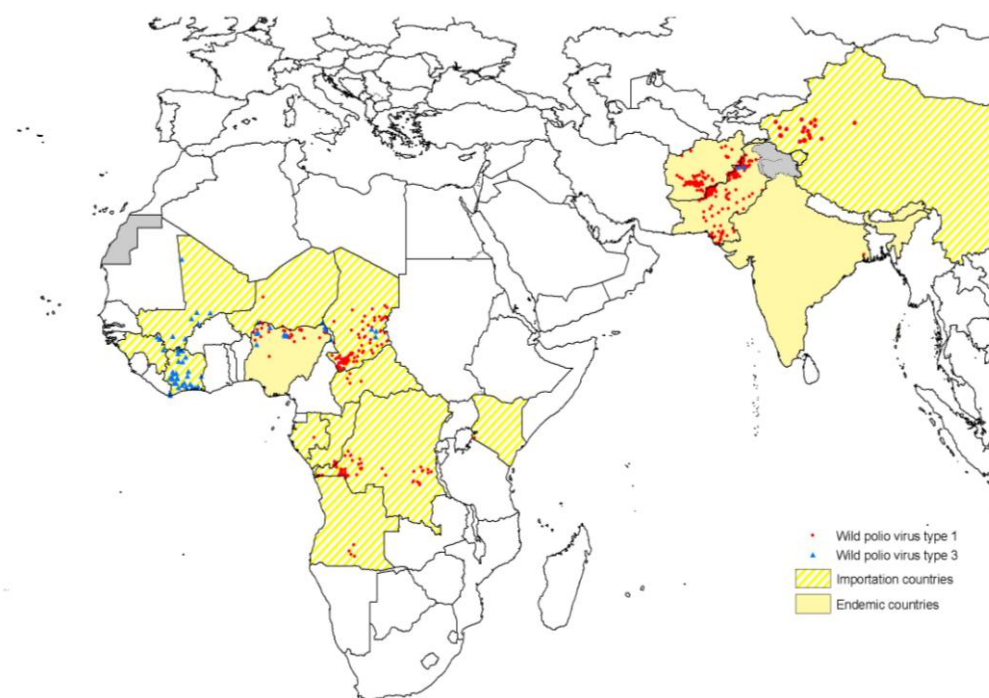


Figure 1.14. Circulation of wild-type poliovirus, as of January 2012.

Nigeria, India, Afghanistan and Pakistan retain endemic circulation of PV. These persistent reservoir countries have served as the main source of infection for a series of imported PV outbreaks that have affected countries in Southeast and Central Asia and Africa. Adapted from (499).

Poliovirus remains endemic in these four persistent reservoir countries for different reasons. In 2003 and 2004 unfounded concerns about OPV safety led to the suspension of mass immunisation campaigns in the northern states of Nigeria (103). Due to a shortage of funds at the same time there was a reduction in immunisation activities in the surrounding countries. The combination of these two events led to an increase in the number of cases in Nigeria and the spread of PV across Central Africa (338). In addition PV was introduced into Yemen and Indonesia from Nigeria as a result of the pilgrimage to Mecca (344). Following greatly improved vaccine coverage in door-to-door immunisation campaigns in the Northern states, where previously less than 40 % of young children had been immunised, the 798 wild-type PV cases in 2008 decreased to 388 and 21 cases in 2009 and 2010, respectively (17).

In India wild-type PV has been eliminated from all but the two most populous states of Uttar Pradesh and Bihar (combined population, ~275 million; combined monthly birth cohort, >600,000). There is extremely high potential for PV transmission in these areas, and despite a well-run program, focal serotype 1 and 3 wild-type PV circulation had continued in the highest-risk communities. The lower per-dose efficacy of tOPV in the settings of high population density, poor hygiene and sanitation, inadequate nutrition, competing enteric pathogens, and high rates of diarrhoeal diseases is one aspect of this eradication problem (103). It is not clear why the vaccine shows reduced efficacy in this region. Either interference from other circulating EVs (449) or environmental or nutritional factors could contribute to this reduced vaccine efficacy by compromising the immune competence of the population. Due to interference from the robust Sabin 2 strain the tOPV efficacy might be lower for the Sabin 1 and 3 strains (103). In response the GPEI has switched to using serotype 1 and 3 monovalent OPVs (mOPV). This decision was taken as modelling had shown improved-per-dose efficacy (103, 189). In addition following administration of serotype 1 mOPV, improved seroconversion rates in newborns have been found by serologic studies (148).

Substantial progress towards PV eradication in India was made in 2010 and 2011. The last confirmed serotype 3 and 1 wild-type PV strains were detected in October 2010 and January 2011, respectively. Environmental surveillance of sewage last detected wild-type PV in Mumbai in November 2010. It is likely that wild-type PV transmission has been interrupted as there has been no detection of PV in any of the sewage sampling sites since November 2010. In addition no wild-type PV has been detected in the previously polio-

endemic states of Uttar Pradesh and Bihar for >17 and >12 months, respectively (88). The simultaneous reduction in serotype 1 and 3 wild-type PV cases in India is likely to have largely been due to the introduction of bivalent OPV (bOPV) in supplementary immunisation activities from January 2010 onwards. The levels of immunity required to stop wild-type PV transmission could have been reached and sustained by the focussed vaccination coverage on children in high-risk endemic areas and migrant populations since 2010 (88).

Access to some communities in Afghanistan and Pakistan, which were previously open to immunisation activities, has been restricted by conflicts since 2001. In the southern states of Afghanistan and the insecure Federally Administered Tribal Areas of Pakistan along the northern border with Afghanistan, serotype 1 and 3 wild-type PV persist. The spread of PV from these reservoir areas to communities which have immunity gaps has been facilitated by heightened mobility of the population in these areas. This has led to outbreaks and re-established transmission (86, 103). During January to September 2011 increased numbers of wild-type PV cases were reported in Afghanistan and Pakistan, compared to a similar period in 2010. While serotype 1 wild-type PV transmission was widespread and uncontrolled throughout Pakistan, transmission in Afghanistan primarily occurred in conflict-affected areas in the south region. In both countries the transmission of serotype 3 wild-type PV was significantly reduced, with transmission only present in the Federally Administered Tribal Areas of Pakistan during 2011 (87).

The success of eradicating indigenous wild-type PV from many countries raises the risk that imported wild-type PV will spread unless high rates of PV vaccine coverage are maintained. Following the successful eradication of the indigenous wild-type PV, the immunisation activities of many resource-poor and conflict-affected countries have deteriorated. This has led to growing immunity gaps in populations, increasing the risk of outbreaks. For example in northern Nigeria the suspension of immunisation campaigns led to outbreaks of serotype 1 wild-type PV which spread to 27 other countries in 2005 to 2007, from Guinea in West Africa to Indonesia in Southeast Asia (89, 103).

Apart from its intrinsic biological limitations, global AFP surveillance has developed gaps in critical areas (103). Phylogenetic trees can be analysed to identify orphan lineages. Orphan lineages are isolates whose sequences appear at the tips of trees and do not appear closely related to other sequences. Orphan isolates are most often related to strains that were

previously isolated in the same region but that were believed to have been eliminated. The presence of wild-type PV orphan lineages, which in some cases have not been detected for up to five years, might indicate that some AFP cases are being missed. This problem is particularly prevalent in areas with conflict or under-resourced countries. In the African region an extension of the period of reporting “no wild-type PV-associated cases” beyond the three years requirement that was applied for the certification of eradication in the Americas, Western Pacific and European Regions, may be required as orphan lineages have been detected in sub-Saharan Africa (103).

1.5.2 Vaccine-derived poliovirus

Oral poliovirus vaccine is genetically unstable and as discussed above, the attenuation mutations can revert during replication within the gut (117). Following recombination, site suppression mutations, back mutations and a steady drift in molecular sequence the loss of attenuation mutations can result in the development of VAPP (335). Reversion of an OPV strain can progress further resulting in the development of VDPV. Vaccine-derived poliovirus isolates have a higher genetic divergence from OPV strains than do isolates from most VAPP cases (255).

Two types of vaccine-related isolates are derived from OPV following replication in the host, OPV-like isolates and VDPVs. Most of the vaccine-related isolates are OPV-like and differ very little (<1 % of VP1 nts) from the respective parental Sabin strains. Vaccine-derived polioviruses occur less frequently and differ from the parental Sabin strains at 1-15 % of VP1 nts (i.e. they have ≥ 10 nt substitutions) (255). Vaccine-derived polioviruses biologically resemble wild-type PV isolates and have genetic properties consistent with prolonged replication or transmission (560). Vaccine-derived polioviruses are further classified into circulating VDPVs (cVDPVs), immunodeficient VDPVs (iVDPVs), and ambiguous VDPVs (aVDPVs). Circulating VDPVs are associated with sustained person-to-person transmission (255). Patients with primary B-cell immunodeficiencies who have prolonged VDPV infections following exposure to OPV can secrete iVDPVs (558). Clinical VDPV isolates from patients with no recognised immunodeficiency and not associated with a

PV outbreak, or environmental isolates whose ultimate source has not been identified are defined as aVDPVs (255).

The >1 % VP1 divergence demarcation between OPV-like isolates and VDPVs indicates that replication of a OPV, either within an individual or during person-to-person transmission has occurred for approximately 1 year or more, in contrast to the normal 4 to 8 weeks excretion of PV (11, 255). The definition of VDPVs is based on the view that VDPVs have a history of prolonged replication since the administration of the OPV. However the definition does not infer on the biological properties of VDPVs, i.e. the definition does not mean that isolates with <1 % VP1 divergence would lack the capacity to spread from person-to-person or cause paralytic disease in humans (255).

Circulating VDPVs were first identified in a PV outbreak of 21 reported cases on the islands of Hispaniola from 2000-2001 (253). The serotype 1 cVDPV isolates were found to be closely related to the Sabin 1 strain. Based on the degree of sequence drift they were judged to have been circulating for two years. Analysis of the cVDPV isolates determined that they were recombinants between the OPV strain and unidentified C type EVs (338). The strains were able to circulate on the islands as there was low OPV coverage and no NIDs had been conducted within the preceding five years (255). Under these conditions OPV can spread from person-to-person and recover the biological properties of wild-type PV through a series of mutational (and possibly recombination) events (103). These wild-type PV properties include the efficient transmission of the PV and the ability to cause paralytic disease in humans. In Egypt retrospective investigation found that serotype 2 cVDPV had re-established serotype endemicity from 1983 to 1993 (103, 570).

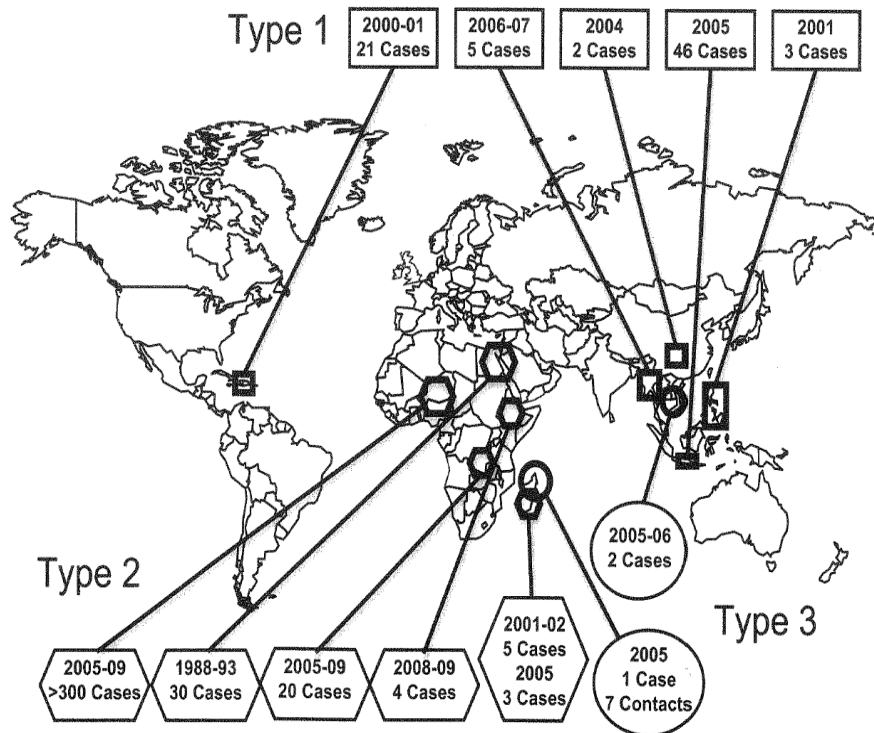


Figure 1.15. Location of poliovirus outbreaks associated with circulating vaccine-derived polioviruses

Serotypes of the cVDPV isolates, the year (s) of cVDPV isolation, and the number of reported cases associated with cVDPVs are shown (103).

Twelve cVDPV outbreaks, all in tropical and subtropical settings with gaps in OPV coverage, have been described (figure 1.15) (103). Although cVDPVs have been associated with all three serotypes, most cVDPV outbreaks have been due to serotype 2 strains (figure 1.15) (91, 255). In isolated communities with gaps in OPV coverage small cVDPV outbreaks have occurred (295, 420).

Insufficient population immunity is a critical risk factor for cVDPV outbreaks. Although PV excreted by OPV vaccinees can frequently recover the capacity to spread beyond immediate contacts, population immunity normally limits this spread. When the density of nonimmune susceptibles rises to the point at which the chains of cVDPV transmission can propagate outbreaks will occur (164, 255, 369). The size of the nonimmune population and the potential for transport of the outbreak PV to susceptible communities elsewhere determined the size of a cVDPV outbreak (255). The risk of a cVDPV outbreak is raised when indigenous wild-type PV circulation is eliminated as nonimmune susceptibles will

accumulate in the absence of high rates of PV vaccine coverage and naturally acquired immunity. Insensitive surveillance is an additional risk factor for the spread of cVDPV (255).

Vaccine-derived polioviruses are of particular risk to people with primary B-cell deficiencies, including, hypogammaglobulinemia, agammaglobulinemia, severe combined immunodeficiency and most frequently common variable immunodeficiency (90, 91, 485, 558). Approximately 50 people with B-cell immunodeficiencies have been found to be excreting iVDPVs since the introduction of OPV in 1961 (560). Most of the iVDPV infections (70 %) detected to date have spontaneously ceased within three years or the patients have died from complications of their immunodeficiency. A small number of patients (17 %) have excreted PV for three to eight years, and fewer still (10 %) have excreted the virus beyond nine years. Serotype 2 PV has been responsible for most iVDPV infections. Few iVDPV infections are associated with serotype 1 PV, and fewer still with serotype 3 PV (558).

B-cell immunodeficient patients in upper- and middle-income countries are sustained by regular intravenous administrations of gamma globulin. Although this treatment protects the patient from poliomyelitis or other infections, it does not prevent them from shedding the PV. Therefore as chronic excretors can act as a source of pathogenic PV capable of restarting PV if the population immunity level falls, they can pose a significant risk to their contacts and to the communities they live in (103). At least two antiviral drugs are being developed to clear iVDPV infections (371).

Ambiguous VDPVs are VDPVs that cannot be assigned as either a cVDPV or an iVDPV. Many aVDPVs are isolated from the environment during ES and have similar genetic properties to iVDPVs. In Israel, Estonia, Slovakia, and Finland some significantly divergent aVDPVs have been isolated (42, 91, 93, 468). Analysis of the sequence divergence of some of these isolates indicates that they have been replicating for more than 15 years since the initiating OPV dose (91, 103). Immunodeficient patients with asymptomatic symptoms could be the source of these isolates. Other aVDPVs may show similar properties to cVDPV, i.e. be able to transmit from person-to-person in communities with low vaccination coverage (103).

1.5.3 The End-game of poliovirus eradication

When the GPEI was launched in 1988, it was assumed the eradication of PV would be similar to the successful smallpox model (158), and a few years after the eradication of wild-type PV had been certified the OPV immunisations could cease. The identification of iVDPVs, from immunodeficient patients chronically infected with PV; and the finding that cVDPVs can, like wild-type PV, cause large outbreaks of paralytic disease, re-establishing endemic circulation have prompted a reassessment of WHO End-game and post-eradication strategy (145, 549). Continued use of OPV during the End-game and post-eradication phase would lead to more VAPP cases, more immunodeficient patients chronically infected with PV; potential outbreaks by cVDPVs and public health “fatigue” leading to reduced OPV coverage and its attendant dangers (364). Clearly the use of OPV must stop in a coordinated manner as soon as safely possible (137).

A strategic plan for the cessation of all routine use of OPV has been outlined by the WHO (547, 555). This plan has several components, one of which is the globally coordinated cessation of routine OPV immunisation two to three years after the last detection of wild-type PV. Another is that not all countries will routinely immunise with IPV, although this might change as research is currently being carried out to assess whether a global switch from OPV to IPV would be feasible, see below. For at least three years after the detection of the last VDPV AFP and other forms of PV surveillance will be maintained. Following the discontinuation of OPV all laboratory stocks of PV will be contained. To forestall against any potential PV transmission that may occur after the cessation of OPV a global mOPV stockpile and response capacity will be established (255).

A formal process for the certification of wild-type PV eradication has been established by the WHO (478). For the certification to be made there must be no wild-type PV isolation from patients with AFP, healthy individuals, or the environment for at least three years in the presence of high quality surveillance (255). At present, three of the six WHO regions have met this criteria and subsequently been certified PV-free. These include the Americas, the Western Pacific and European regions (80-82). Eradication is still progressing in the African, Eastern Mediterranean and Southeast Asia regions. After a series of Global Immunisation Days in countries using OPV, the use of OPV should cease in a coordinated fashion (255).

A Global Action Plan for PV containment in the pre-eradication, post-eradication and post-OPV phases has been developed by the WHO (561). Currently (pre-eradication) biomedical laboratories are being surveyed worldwide to identify those storing wild-type PV infectious or potentially infectious materials. Certification Commissions of each WHO region will receive national inventories of laboratories retaining such materials. In order to safely handle wild-type PV these laboratories now must work under biosafety level 2 (BSL-2) / polio measures (255). A year after the isolation of the last wild-type PV, all but the essential laboratories on the national inventories will be required to destroy stocks of wild-type PV (103). The essential laboratories will need to implement appropriate BSL-2 / polio or BSL-3 / polio measures (255). These laboratories will be involved in vaccine production, vaccine quality assurance, virus reference activities, and key research (103). After the use of OPV ceases, OPV Sabin strains will need to be contained with wild-type strains as any individual exposed to either could potentially transmit the virus to non-immune susceptible people in the post-OPV era (255).

In order to be able to generate a serotype specific response to any potential PV outbreak in the post-eradication phase the WHO, in coordination with national governments, is establishing a global stockpile of mOPV. This stock pile is being produced prior to the cessation of OPV immunisation as OPV production is likely to cease at the same time (255). This mOPV stockpile could also be used as a counter measure against bioterrorism. Research has shown that it is possible to generate PV through chemical synthesis of the PV genome (78). As the complete genetic sequences of many PV strains are detailed in scientific records, such research could be used to intentionally release PV in the post-eradication phase. Disastrous PV outbreaks could be caused by the intentional release or introduction of PV into populations in the post-eradication phase who have little or no immunity (103). Poliovirus surveillance must be maintained for the foreseeable future as it is essential to detect any PV that has been re-introduced into a population (e.g. by an accidental breach of containment in a laboratory or vaccine manufacturer, or through intentional release by terrorists) before it is able to cause large outbreaks (255).

1.5.4 Inactivated poliovirus vaccine in the End-game and post-eradication phases

There is a growing consensus that IPV must replace OPV for an indeterminate period of time until it can be reliably established that there is minimal risk of PV reintroduction and circulation during the End-game and post-eradication phase (103). Many high-income countries, including the USA, Japan and the UK, have already switched from using OPV to using IPV (146). However there are several barriers which inhibit a worldwide switch to IPV. One of these barriers is that IPV needs to be administered by injection. There are several problems with administering the IPV by injection. These include pain at the site of administration, logistical difficulties and safety and disposal concerns and the fact that injected administration requires trained medical staff (202, 546). An additional barrier is the cost of IPV. Currently the per-dose price and production costs of IPV are greater than OPV (562). To overcome these barriers a needle-free device for intradermal injection has been developed, which can be manually reset and used by volunteers. Intradermal injections of fractional doses of IPV have been trialled in Cuba and Oman (347, 425). The results of both studies indicated that when given at the correct interval, the fractional dose strategy with use of intradermal injection could reduce the cost and increase the ease of administration of IPV (347, 372, 425).

Another barrier to the worldwide switch to IPV is concerns over the efficacy of IPV to induce sufficient intestinal immunity. The mucosal intestinal immunity is essential to stop the faecal-oral transmission of PV which predominates in developing countries which have low hygiene and sanitation standards (163, 202). The findings of a series of vaccination-challenge studies indicate that IPV induces less mucosal immunity than OPV (282, 381, 498, 536). Vaccination with IPV can reduce the prevalence, duration and titres of PV shedding as compared to no vaccination, but it is not clear whether such reduction would be sufficient to stop an outbreak of PV (202, 498). As the dermis is a mucosal surface and intradermal injection may stimulate IgA mucosal immunity it has been hypothesised that administering IPV by an intradermal injection could improve the protection against infection in the gut (202, 548).

The final barrier to the worldwide switch to IPV is that the current cIPV is produced by inactivating large quantities of wild-type PV. As described above, facilities involved in IPV production will require higher containment during the End-game and post-eradication phase.

This is likely to raise the cost of IPV during these phases when the demand is likely to be high as populations will require protection from PV after the cessation of OPV. The supply of IPV could be significantly increased by shifting production to developing countries. This could also lower the production cost as a result of increasing competition among producers (27, 202). However there are concerns as to whether sufficient biosafety containment measures would be adhered to in developing countries. Manufacturing IPVs from wild-type PV strains has in the past resulted in the unintended re-introduction of wild-type PV from manufacturers into the community (356). Such an event in the post-eradication phase would have dire consequences, particularly in developing countries with high populations and poor hygiene and sanitation. A potential solution is to inactivate the attenuated Sabin strains, used in OPV, to develop Sabin-IPV (sIPV).

The Sabin strains were primarily selected for the development of a new IPV as they have been studied in depth and have been used in the production of OPV for decades (142, 255, 524). Previous research has also determined the molecular biology of the Sabin strains (255). The Sabin strains are considered safer to use than wild-type PV strains as the IPV seeds as the potential for the spread of the Sabin strains has been estimated to be two to ten times less than the wild-type PV strains (166, 495, 524). New vaccine producers have been urged by the WHO to develop sIPV as a safer alternative to introducing large-scale production of wild-type PV (202, 276). Several manufacturers are involved in the development of sIPV, including, the Japanese Polio Research Institute, the Chinese Academy of Medical Sciences, and the Netherlands Vaccine Institute (524).

In recent years much of the pharmaceutical development of sIPV has been completed, the clinical development will become the focus for the next 3-5 years (524, 557). In Japan and India clinical trials for sIPV are currently taking place (548). However there are concerns as preliminary research carried out during this development and by other laboratories has found discrepancies between the immunogenicity of cIPV and sIPV. The immunogenicity of sIPV and cIPV has been assessed in rat models and Tg mice expressing the PVR. Both the Tg mice and rat models showed that the serotype 2 sIPV 2 induced lower levels of antibodies than the serotype 2 cIPV (141, 276, 310, 532). However, the serotype 1 sIPV was found to raise at least the same, if not more antibodies than those induced by the serotype 1 cIPV (140, 276, 310, 312, 472, 532). The immunogenicity of the serotype 3 sIPV in rats varied between studies, with some finding it two times lower than the serotype 3 cIPV (310, 472), while

others found equivalent immunogenic responses elicited by the serotype 3 sIPV and cIPV (276, 532).

In comparison to the cIPVs the lower immunogenicity of the serotype 2 sIPV is particularly striking. This may have been due to the lower stability of the Sabin strains, which would have resulted in its D-Ag being destroyed during HCHO treatment (100, 160). A potential solution to this could be to use alternative inactivation agents which do not damage the viral antigens as much as HCHO (101).

1.6 INTRODUCTION TO THIS THESIS

Sabin-IPV offers a safer alternative to the large scale inactivation of wild-type PV strains. However, as discussed above, the immunogenicity of sIPV and cIPV differ, particularly for serotype 2 sIPV which is significantly less immunogenic than its cIPV counterpart. It is not clear why the two preparations differ so greatly in immunogenicity as very little is known about the molecular mechanisms which lead to the elimination of virus infectivity during the HCHO inactivation process.

This thesis explored the process of PV inactivation and its consequences and contributes to better understanding of the differences between sIPV and cIPV. As the serotype 2 sIPV and cIPV showed particularly significant differences this thesis focused on serotype 2 PV strains. Following inactivation with HCHO, the molecular, antigenic and immunogenic properties of a wide range of serotype 2 strains of different origins was assessed to gain a greater understanding of why serotype 2 sIPV and cIPV differ. The effect of alternative inactivation chemicals to HCHO on the antigenic and immunogenic properties of a series of serotype 2 strains was determined with a view to generate an IPV with improved immunogenicity. The molecular mechanisms which underlie the loss of PV infectivity during inactivation were characterised by assessing the effect of inactivation on viral entry into a host cell and the viral RNA.

This thesis aims to improve understanding of the inactivation of PV and contribute to the development of improved IPVs for the End-game and post-eradication phase of the GPEI.

This aim will be met by completing the following objectives:

- Identify and characterise a range of serotype 2 PV strains based on their antigenic properties.
- Assess the effect of conventional HCHO inactivation on the antigenic and immunogenic properties of a range of serotype 2 PV strains.
- Examine the effect of alternative inactivation chemicals, to HCHO, on the viral infectivity, antigenicity and immunogenicity.
- Assess the thermal stability of inactivated PV preparations generated with different inactivation chemicals.
- Characterise the molecular mechanisms which underlie the loss of PV infectivity during inactivation by assessing the effect of inactivation on viral entry into the host cells and the viral RNA.

This thesis is based on the hypothesis that the inactivation process alters the antigenic epitopes of PV resulting in changes in their immunogenicity. The extent of these changes is different depending on the strain of PV and / or the inactivation chemical used.

CHAPTER 2

MATERIALS AND METHODS

2.1 MATERIALS

2.1.1 Primers

Standard M-13-tagged primers with Sabin 2, MEF-1 and selected VDPV sequences from the collection at the National Institute for Biological Standards and Control (NIBSC), were used to sequence the viral capsid coding region of a series of serotype 2 PV strains. The primers, detailed in table 2.1, were of a similar length.

Sense	Code (Strain sequence)	Primer sequence	Position
Antisense	M-056 Sabin 2	TCA TTG CAA GCT GAC ACA	2405-2424
Sense	M-057 Sabin 2	CAG AGG GTG GTG GTG GAA	1179-1196
Antisense	M-071 Sabin 2	TTA CAC TGC ACG TGC AC	1276-1292
Antisense	M-087 Sabin 2	GCG AGCTCC ATC ATG TT	1891-1907
Sense	M-088 Sabin 2	AACACTCCT GGTAGT AACC	1783-1801
Sense	M-090 Sabin 2	AGCATG TTC TAC CAA AC	2338-2354
Sense	M-115 Sabin 2	GCG TGTGGG TAT AGT G	970-985
Antisense	M-117 Sabin 2	TTA CCA CGC GAA CTG CCA	3200-3217
Sense	M-202 Sabin 2	GTTGTT GTC CCG TTG TCC	2359-2376
Antisense	M-204 Sabin 2	CTG GAT GAC ATG GCG CGT	2668-2685
Sense	M-213 Sabin 2 VDPV	GGCGGA ACCGAC TAC TTT	530-547
Antisense	M-215 Sabin 2 VDPV	GATGATGTA TTC AGG CCA	1066-1080
Sense	M-221 Sabin 2	GTTTGA TGT CAC TCC ACC	1848-1865
Antisense	M-223 Sabin 2	TAA TGTGTG TTG TRT CTC	2444-2461
Sense	M-249 MEF 1	ATG TGCTGC GAG TTC AA	1717-1733
Sense	M-256 Sabin 2	TTTGTR TCR GCN TGY AAY GA	2404-2423
Sense	M-257 Sabin 2	CAG GTN TAY CAR ATN ATG TA	2938-2952
Antisense	M-259 Sabin 2	GAN GTT TGC CAN GTG TAA TC	2995-3014
Antisense	M-261 Sabin 2	AGG TCTCTG NYC CAC ATA	3483-3500
Antisense	M-263 Sabin 2	GTTNGCTTC CAT GTA TTG	3625-3642
Sense	M-448 Sabin 2	ACTAGA AATGCA TTG GTT CC	2521-2540

Table 2.1. M-13-tagged primers used to sequence serotype 2 poliovirus strains.

M-13-tagged primers with Sabin 2, MEF-1 and selected VDPV sequences from the collection at the NIBSC were used to sequence the viral capsid coding region of a series of serotype 2 strains.

Other primers were designed to yield different sized reverse transcription-PCR (RT-PCR) products at the region encoding VP1, and at the 5' and 3' end of the genome of the MEF-1 PV strain. The primers, detailed in table 2.2, were designed to have a similar melting point and length. The complete genomic sequence of the MEF-1 strain was obtained from the National Centre for Biotechnology Information database and used in conjunction with the online program, "Primer3 Input version 0.4.0" (442) to design these primers. These oligonucleotide primers were synthesised by Eurofins MWG Operon, an international provider of genomic services.

Region	Sense	Code	Primer sequence	Position
5'end of the genomic region	Sense	5NCR-44	GCG GCC AGT ACA CTG GTA TT	44-63
	Antisense	5NCR-153	ACT GGT TTG TAC CCC CTC CT	134-153
		5NCR-252	TCT CGA AGT ACA TGA GCG GAT A	231-252
		5NCR-455	GCC GGA GGA CTC TCA GGT A	437-455
		5NCR-654	ATC AAA TTC TCA CCG GAT GG	635-654
		5NCR-861	GCT CGC AGA ATC CCT GTA ATA A	840-861
VP1	Sense	VP1-2521	ACG AGA AAT GCC TTG ACA CC	2521-2540
	Antisense	VP1-2737	AAG CTC CTC TTG CGA AGA AA	2718-2737
		VP1-2937	ATT TAG TGC GTG CCC ATT GT	2918-2937
		VP1-3125	ACT TTG GCA AAC CCA TCG TA	3106-3125
		VP1-3338	TAG TCA ACC CCT GGT CCG TA	3319-3338
3'end of the genomic region	Antisense	3NCR-7412	ACA ACA GTA TGA CCC AAT CCA A	7391-7412
	Sense	3NCR-7288	AAG ATT AGA AGT GTG CCA ATC G	7288-7309
		3NCR-7201	AGA TCC CAG AAA CAC TCA GGA T	7201-7221
		3NCR-7011	CTA GCC CAA TCA GGA AAA GAC T	7011-7033
		3NCR-6782	ATT ATC TGA ATC ACT CGC ACC A	6782-6803
		3NCR-6583	AAG AAC CCA GGT GTA GTG ACA G	6583-6604

Table 2.2. Sequences of oligonucleotide primers used in real-time reverse transcription-polymerase chain reaction.

Primers were designed using a complete sequence of the MEF-1 strain in conjunction with the online program, "Primer3 Input version 0.4.0" (442).

2.1.2 Cell lines

Four cell lines were used throughout this research, HEp-2C, L20B, Ltk- and 293-CD155-AP.

2.1.2.1 HEp-2C cells

Human Caucasian larynx carcinoma epithelial (Hep-2C) cells were derived from neoplasms which were grown initially in an irradiated and cortisone-treated rat (351, 506). These cells are highly susceptible to PVs, many Coxsackie B viruses, and some other EVs, all resulting in characteristic EV CPE (309). These cells were available from the stock at the NIBSC.

	Growth	Maintenance
Eagle's minimum essential medium (MEM)	1x	1x
Foetal calf serum (FCS)	5 %	2 %
L-glutamine (L-glu)	1 %	1 %
Penicillin-Streptomycin (P-S)	1 %	1 %
Amphotercin B (AmpB)	1 %	1 %

2.1.2.2 L20B cells

L20B cells originate from a cloned cell line that was derived by transforming murine Ltk⁻ apt⁻ cells with HeLa cell (human) DNA (328, 329, 408). This cell line expresses the human PVR and consequently is highly selective for PVs. A small number of non-PV EVs (e.g. Coxsackie A) are able to infect L20B cells resulting in the characteristic EV CPE. A number of non-PVs (e.g. reoviruses and adenoviruses) which are able to infect Ltk cells, can infect L20B cells. However the resulting CPE is often different to that produced by a PV infection (309). These cells were available from the stock at the NIBSC.

	Growth	Maintenance
MEM	1x	1x
FCS	10 %	2 %
L-glu	1 %	1 %
P-S	1 %	1 %
AmpB	1 %	1 %

2.1.2.3 *Ltk-* cells

Ltk- cells are a sub-line of a BUdR resistant strain of the L-M mouse line, which in turn was derived from the L929 cells. The *Ltk-* cells lack TK and cannot grow in HAT medium (144, 226, 537). As they do not express the PVR they are not susceptible to infection by PV. These cells were available from the stock at the NIBSC.

	Growth	Maintenance
MEM	1x	1x
FCS	10 %	2 %
L-glu	1 %	1 %
P-S	1 %	1 %
AmpB	1 %	1 %

2.1.2.4 293-CD155-AP cells

293-CD155-AP cells express soluble PVR (sPVR, or CD155) tagged with alkaline phosphatase (AP). The plasmid pAPtag2 (167) has been used to fuse the coding region of the 337 N-terminal codons of CD155 to the N-terminal coding region of human placental AP. The resulting plasmid (pCD155-AP) was used as a vector with 293 cells (human embryonic kidney cells transformed with adenovirus E1A, B genes). Subsequently the 293 cells expressed the CD155-AP fusion protein (201). These cells were kindly provided by Dr Mueller (Stony Brook University, New York, USA).

	Growth	Maintenance
Dulbecco's modified Eagle's medium (DMEM)	1x	1x
FCS	10 %	2 %
L-glu	1 %	1 %
P-S	1 %	1 %
AmpB	1 %	1 %

2.1.3 Virus stocks

As discussed in the Introduction, the work detailed in this thesis focussed on serotype 2 PV strains. A number of serotype 2 PV strains were analysed including vaccine seeds; a cVDPV strain; a number of isolates from immunodeficient patients and wild-type strains from paralytic cases across the world isolated over many decades. These viruses were sourced from the large collection at the NIBSC. Many of these viruses, in particular the iVDPV strains, are unique to the NIBSC. The selected strains are shown in table 2.3. The characteristics of the strains are discussed in Chapter 3.

Serotype 2 poliovirus strain	Origin	Date / Place of isolation
Sabin 2	Sabin vaccine seed (OPV)	1956, USA
MAD029	cVDPV strain	2002, Madagascar
04-44140261	iVDPV strain	06/10/2004, UK
102050	iVDPV strain	16/01/1998, UK
071108	iVDPV strain	07/11/2008, UK
118/78	Wild-type strain	1978, Morocco
II-215	Wild-type strain	1959, Venezuela
II-316	Wild-type strain	1952, Egypt
MEF-1	Wild-type strain (IPV seed)	1942, Egypt

Table 2.3. Serotype 2 poliovirus strains analysed throughout this project.

A range of serotype 2 PV strains of different origins (vaccine seed, VDPV, wild-type) were sourced from the collection at the NIBSC.

2.2 METHODS

2.2.1 Virus characterisation

2.2.1.1 Growth, concentration and titration

The selected serotype 2 PV strains were propagated in HEp-2C cells as described previously (309). The Sabin 2, MAD029, 04-44140261, 102050, and MEF-1 strains were propagated on a larger scale as a greater quantity of these strains was required for additional study beyond the initial characterisation. This involved propagating the strains in 850 cm² roller bottles (Corning Incorporated) instead of 75 cm² tissue culture flasks (BD Biosciences). At later date the selected serotype 2 PV strains were inactivated with HCHO. To improve the yield of inactivated PV each strain was concentrated by ultracentrifugation on a 30 % sucrose cushion as described previously (309). Virus concentrates were resuspended in M199 medium (kindly provided by Dr Tano, Japan Poliomyelitis Research Institute, Tokyo, Japan). The increase in the yield of PV was assessed by determining the infectious titre both before and after concentrating the strains. The infectious titre was determined by assessing the tissue culture 50 % infectious dose (TCID₅₀) as described previously (309) with the alteration that strains were diluted either 10⁻⁶ to 10⁻¹⁰ or 10⁻⁷ to 10⁻¹¹ (before or after being concentrated, respectively) with maintenance medium (MEM with 2 % FCS and 1 % L-glu, P-S, AmpB). An additional alteration was that plates were incubated for five days and then stained with naphthalene black solution.

2.2.1.2 Characterisation of the molecular properties of poliovirus strains

To characterise the molecular properties of the PV strains the viral RNA was extracted and RT-PCR was used to isolate the capsid coding region of the genome, which was later sequenced. The MagNA Pure LC Total Nucleic Acid Isolation Kit (Roche) was used in conjunction with the Kingfisher ml particle processor (Thermo Electron Corporation) to extract the viral RNA from the propagated strains. The viral RNA was extracted according to the manufacturer's instructions. Briefly, using a strip of 5-tubes for the KingFisher ml particle processor, 600 µl of the propagated PV was added to 150 µl Proteinase K, while the remaining tubes were filled with wash buffers I-III and elution buffer. Lysis buffer and well

mixed magnetic glass beads were added to tube 1 containing the PV and Proteinase K. Following extraction the contents of tube 5 were transferred to a labelled microtube (Sarstedt). The Proteinase K and lysis buffer digest and denature the proteins, releasing the viral RNA. The chaotropic salt conditions and the high ionic strength of the lysis buffer encourage the PV RNA to bind to the silica surface of the magnetic glass particles. Wash buffers I-III remove unbound salts, proteins, cellular membranes and other impurities before the RNA is extracted (434).

Complementary viral DNA was synthesised by RT-PCR to analyse the capsid coding region of the PV genome using the Qiagen One-Step RT-PCR kit (309, 411). An alteration was that the annealing step of the PCR was carried out at 40 °C rather than 50 °C. Standard M-13 tagged primers with Sabin 2, MEF-1 and selected VDPV sequences from the collection at the NIBSC were used (section 2.1.1). Reverse transcription-polymerase chain reaction products were analysed by gel electrophoresis on a 1% agarose gel. The Qiagen QIAquick PCR Purification Kit was used to purify the RT-PCR products (412). Sequencing was performed in both directions by Eurofins MWG Operon (Germany). Sequence data were stored as standard chromatogram format (*.scf) files, analysed, and edited using the AlignIR Version 2.0 software (LI-COR).

Phylogenetic relationships between strains were established by comparing the sequences determined and aligning them using the alignment program CLUSTAL W (286, 501). Default scoring matrices were used to determine the degree of nt sequence identity and of protein similarity. The phylogenetic relationships between sequences were determined using a variety of phylogenetic based programs as described previously (376).

2.2.2 Inactivation

2.2.2.1 Inactivation with formaldehyde

Sucrose cushion-purified virus preparations were inactivated with HCHO (Sigma-Aldrich) as previously described (312). Briefly, the virus preparations were resuspended in HCHO inactivation medium (10.60 g M199 medium, 5.0 g glycine, 1.86 g EDTA.2H₂O, 0.35

g sodium hydrogen carbonate, 0.93 ml Tween 80 [5 %], made up to 1000 ml with sterile distilled water) to a final concentration of 1×10^9 TCID₅₀/ ml. To remove viral aggregates and facilitate HCHO access to all virus particles PV preparations were filtered through a 0.2 µm filter (PALL) prior to inactivation. Formaldehyde was added to the purified virus solutions to give a final dilution of 1:4000 of the concentrated stock. Inactivation was carried out for 12 days at 37 °C in a constant-temperature water bath. At day 6 viruses were again filtered through a 0.2 µm filter. At day 12 a 1:8 dilution of sodium bisulphite (35 % w/v) (Sigma-Aldrich) was added to the inactivated PV preparations at a 1:100 ratio to neutralise any remaining HCHO.

To monitor for the presence of infectious virus, aliquots of 200 - 500 µl were taken at days 6 and 12 of inactivation. Aliquots were added to HEp-2C cells and passaged three successive times over three weeks. The effect of HCHO inactivation on the antigenicity was assessed by determining the D-Ag/ml of the inactivated serotype 2 strains. In addition the antigenic structure of the serotype 2 strains was characterised both before and after inactivation with HCHO. Both of these measures of the effect of inactivation on the antigenicity of PV are described in section 2.2.3. The effect of HCHO inactivation on the immunogenicity of PV was assessed by a rat potency assay, as described in section 2.2.4.1.

2.2.2.2 Inactivation with alternative chemicals: Iodoacetamide

To determine whether the immunogenic properties of IPV could be improved, the effect of alternative inactivation chemicals to HCHO on PV was assessed. One of the chemicals assessed was iodoacetamide (IAN) (Sigma-Aldrich). To assess the efficacy of IAN as an inactivant of PV, the MEF-1 strain was inactivated with a broad range of concentrations of IAN. The infectivity of the inactivated preparations was assessed by determining the TCID₅₀. Briefly, the IAN inactivation medium (containing 0.05 g EDTA.2H₂O, 0.81 g Tris-base, 15.6 g sodium chloride, 16.0 g urea, made up to 100 ml with sterile distilled water) was made up 24 hours (h) before the inactivation assay. Preparations of the MEF-1 strain were resuspended in MEM to a final concentration of 1×10^9 TCID₅₀/ ml before being filtered through a 0.2 µm filter. The relevant amount of IAN was added to 10 ml aliquots of the IAN inactivation medium to create a range of buffers of different IAN concentrations, including, 2, 20, 100,

200 and 400 mM. The MEF-1 preparations were added to the different IAN buffers at a 3:1 ratio. The inactivation was carried out in darkness for 24 h at 37 °C.

As IAN is cytotoxic and no neutralising chemical could be identified it was necessary to remove the IAN from the samples after the inactivation by dialysis. This involved transferring the inactivated virus samples into Slide-A-Lyzer® G2 dialysis cassettes (10, 000 K, 0.5-3 ml, Thermo Scientific) using a 5 ml monoject syringe and needle. The inactivated samples were dialysed for four cycles by immersing the dialysis cassette (with an appropriate size buoy) in MEM using 500 ml beakers, magnetic stirrers and a multiple stirrer tray. All four cycles (each lasting 1 h) were carried out room temperature (18-20 °C). The dialysis buffer was changed at each cycle. The presence of infectious virus in the inactivated samples was assessed by determining the TCID₅₀ (section 2.2.1.1) and by addition to HEp-2C cells for three successive passages over three weeks.

To determine the kinetics of inactivation with IAN the MEF-1 strain was inactivated with 100 mM IAN over a 24 h time-course with aliquots (1 ml) being taken at 1, 4, 8 and 24 h. The method was as described above with alterations that only the 100 mM concentration of IAN was used to inactivate the PV, and that aliquots were taken at set times. As described above, the infectivity of these aliquots was assessed by titration and passaging onto HEp-2C cells for up to three weeks. To assess the effect of IAN on the antigenic structure of PV the D-Ag/ml of each aliquot was determined by an ELISA using antigenic site 2a, 2b and 3b specific MAbs as described in section 2.2.3.1.

2.2.2.3 Initial inactivation with alternative chemicals

In addition to IAN the effect of inactivation of PV with beta-propiolactone (BPL) (Ferak Berlin) and binary ethyleneimine (BEI) (Sigma-Aldrich) was determined alongside HCHO. However as a number of factors can affect the potency of the inactivated PV preparation it was necessary to carry out an initial series of inactivation assays with variable conditions. The range of concentrations of the inactivation chemicals, duration of inactivation, and the temperature at which it was carried out were set for each chemical on the basis of previous experience with influenza virus at the NIBSC and / or an extensive literature search. For all

the chemicals the pH during inactivation was maintained at 7.5 by adding HEPES (pH 7.5) (Sigma-Aldrich) to buffer the MEM inactivation media. These initial inactivation assays were carried out with the MEF-1 strain. As described above, preparations of the MEF-1 strain were filtered before being inactivated. An equivalent amount of the MEF-1 strain (1×10^9 TCID₅₀/ml) was inactivated with each chemical over a time-course. On the basis of previous research, time-points were set during these time-courses. At each time-point an aliquot of MEF-1 (1 ml) was taken for each concentration of the inactivation chemical. The time-points and inactivation conditions for each chemical are detailed in table 2.4.

Variable	Inactivation chemical		
	BPL	BEI	HCHO
Concentration of inactivation chemical	1:500, 1:1000, 1:2000	0.4 mM, 0.8 mM, 1.6 mM	1:2000, 1:4000, 1:8000
Temperature of inactivation (°C)	+4	37	37
Duration of inactivation time-course (h)	24	24	288
Time-points of aliquots (h)	2, 4, 8, 18, 24	2, 4, 6, 8, 18, 24	2, 12, 24, 36, 60, 288
Neutralisation of inactivation chemical	Sodium sulphite (Sigma-Aldrich) - equal volume of the aliquot	Sodium thiosulphate (Sigma-Aldrich) - 10 % the volume of the aliquot	1:8 dilution of 35 % (w/v) sodium bisulphite (Sigma-Aldrich) - 1 v : 100 v aliquot)

Table 2.4. Inactivation conditions of each chemical.

The MEF-1 strain was inactivated with a range of concentrations of each chemical at specific temperatures for set durations. Aliquots of MEF-1 were taken at time-points during each inactivation. Any remaining chemical was neutralised by the addition of a neutralising agent.

The infectivity of each aliquot was assessed by titration (section 2.2.1.1) and by addition to HEp-2C cells for three successive passages over three weeks. In addition the antigenic content of the aliquots was assessed by an ELISA with a MAb (MAb 1050) used for batch

releases at the NIBSC (section 2.2.3.1). As all the inactivation chemicals are cytotoxic and can cause vaccine-cell mutations it was necessary to remove any remaining chemical before the infectivity of the aliquots could be assessed (21). A literature search identified a series of sulphite solutions which could neutralise the inactivation chemicals, as detailed in table 2.4. Two live MEF-1 time 0 h controls (0i and 0ii) were included for each inactivation time-course. The 0i control was immediately stored at -20 °C following the initiation of the inactivation time-course. The 0ii control was incubated in the same conditions as the other samples during inactivation, but in the absence of the inactivating chemicals. Similar to the sample aliquots, the relevant neutralisation chemical was applied to it. To assess whether the inactivation conditions alone had an effect on the infectious titre and D-Ag of MEF-1 the two controls were compared.

2.2.2.4 Optimised inactivation with alternative chemicals

The findings of the initial inactivation experiments were used to select the concentration of each chemical for further inactivations of MEF-1 and other PV strains (table 2.5). As table 2.5 shows, the duration of inactivation and the time-point aliquots were also optimised as a result of the initial inactivation findings.

Variable	Inactivation chemical		
	BPL	BEI	HCHO
Concentration of inactivation chemical	1:500	1.6 mM	1:4000, 1:8000
Duration of inactivation time-course (h)	16	24	288
Time-points of aliquots (h)	2, 4, 8, 16	4, 8, 18, 24	12, 36, 72, 120, 180, 288

Table 2.5. Optimised inactivation conditions of each chemical.

Poliovirus was inactivated with optimised concentrations of the inactivation chemicals for set durations. Aliquots of PV were taken at time-points during inactivation.

Two dilutions were selected for HCHO inactivations to allow comparison to the 1:4000 HCHO inactivation currently used to generate cIPVs. In addition to the MEF-1 strain, the Sabin 2 strain and an iVDPV strain (04-44140261) were inactivated. An equivalent amount (5×10^9 TCID₅₀/ ml) of each PV strain was inactivated with the three chemicals. As with the initial inactivation experiments, aliquots (2-5 ml) were taken at set time-points in the inactivation time-courses (table 2.5). The temperature and pH for inactivation with each chemical remained identical to that described previously for the initial inactivation experiments (section 2.2.2.3). As with the initial inactivation experiments the viral infectivity of the aliquots was assessed by determining the infectious titre (section 2.2.1.1) and by addition to HEp-2C cells for three successive passages over three weeks. The antigenic content of the aliquots was assessed by an ELISA with MAb 1050 (section 2.2.3.1). In addition the antigenic structure of the inactivated PV strains was characterised (section

2.2.3.3). As with the initial inactivation experiments the Oi and Oii controls were included for each inactivation time-course with each PV strain.

2.2.3 Effect of inactivation on the viral antigenicity

The effect of inactivation on the viral antigenic content was primarily assessed by ELISA. However a surface plasmon resonance (SPR) based biosensor protocol was also developed to assess the antigenic content of IPV preparations.

2.2.3.1 Enzyme-linked immunosorbent assay

The enzyme-linked immunosorbent assay (ELISA) was performed as previously described (474) with some modifications. Microlon high-binding flat-bottomed plates (Greiner-Bio-one) were coated with 50 µl per well of serotype 2-specific sheep capture anti-PV antibody diluted in carbonate coating buffer (6.36 g sodium carbonate and 11.72 g sodium hydrogen carbonate made up to 4 l). Plates were incubated with the capture antibody overnight at 2-8 °C, and then washed four times using a Multidrop Combi (Thermo Scientific) with wash buffer (Phosphate buffered saline, [PBS], containing 2.0 % dried milk and 0.5 % Tween 20). The inactivated PV preparations were diluted two-fold in assay diluent (PBS containing 2.0 % dried milk) and added to the plate. Each dilution was tested in duplicate. Following 2 h incubation at 37 °C, plates were washed three times with wash buffer. An appropriate dilution of a serotype 2-specific MAb was added to each well and plates were incubated for 1 h at 37 °C. Plates were washed three times with wash buffer and peroxidase conjugated anti-mouse IgG whole molecule (Sigma-Aldrich) diluted with assay diluent was added to all wells. Following 1 h incubation at 37 °C, plates were washed three times with PBS before the o-Phenylenediamine dihydrochloride substrate (Sigma-Aldrich) was added to all wells. Plates were incubated in darkness at room temperature for 30 minutes (min) before the reaction was stopped by the addition of the 1 M sulphuric acid. The absorbance (Optical density, OD, at 492 nm) was read using a Multiskan Ascent spectrophotometer (Thermo labsystems). The Combistats program was used to carry out a sigmoid curves (In dose) analysis on the assay data to calculate the potency of the inactivated

PV preparations relative to a concurrently tested reference IPV (BRP batch 2, (176)). The dilutions and corresponding OD values were used to calculate the D-Ag content of each inactivated virus sample relative to the reference IPV.

2.2.3.2 Surface plasmon resonance based biosensor protocol

A SPR based biosensor protocol to determine the D-Ag/ml content of a range of IPV preparations was designed and carried out using the Biacore 2000 and T100 (GE Healthcare) biosensor instruments. This biosensor protocol involved initially immobilising rabbit anti-mouse Ig to a CM3 sensor chip (GE Healthcare). The immobilisation wizard program of the Biacore 2000 / T100 control software (GE Healthcare) was used to set the immobilisation for this protocol at a flow rate of 2 μl / min for 3600 s. The rabbit anti-mouse Ig was immobilised to a CM3 sensor chip using an amine coupling kit with sodium acetate (pH 5.0) (GE Healthcare).

After the rabbit anti-mouse Ig was successfully immobilised the concentration analysis wizard program of the Biacore 2000 / T100 control software was used to set up the remaining steps of the biosensor protocol. This involved injecting an appropriately diluted 'capture' MAb 1050 over the surface of the sensor chip at a flow rate of 2 μl / min for 600 s with a 150 s stabilization period. A two-fold dilution of an IPV preparation was subsequently injected over the surface of the sensor chip at a flow rate of 2 μl / min for 600 s. Binding was monitored at each of these steps by the Biacore instrument using SPR. The surface of the sensor chip was then regenerated in two steps. For each step, glycine-HCl (pH 1.5) (GE Healthcare) was injected over the surface of the chip at a flow rate of 30 μl / min for 120 s. A 240 s stabilisation period followed the second step. After regeneration the biosensor protocol could begin again with the injection of the 'capture' MAb 1050.

Immobilisation and regeneration conditions were optimised using the immobilisation and regeneration scouting programs of the Biacore 2000 / T100 control software. A variety of reagents and buffers at varying pH were used in these scoutings (including sodium acetate between pH 4.0-5.5, and glycine-HCl between pH 1.5-pH 3.0). The biosensor protocol was used to estimate the D-Ag of a reference IPV preparation; a range of commercial IPV's of

varying origins (including Sabin and wild-type monovalent or trivalent preparations); and a range of BPL-, BEI- and HCHO-inactivated MEF-1 preparations which were prepared “in-house” at the NIBSC (section 2.2.2.4).

2.2.3.3 Characterisation of antigenic structure

The antigenic structure of live and inactivated PV preparations was characterised by a series of ELISAs which incorporated a range of antigenic site-specific MAbs, shown in table 2.6.

Antigenic site specificity of MAb			
Antigenic site 1	Antigenic site 2a	Antigenic site 2b	Antigenic site 3b
969	1231	1037	1050
433	1247		1102
434	1269		1103
435			1121
436			1051

Table 2.6. Antigenic site-specific serotype 2 poliovirus monoclonal antibodies.

A range of antigenic site-specific serotype 2 MAbs were used to characterise the antigenic structure of live and inactivated PV preparations.

The ELISAs determined whether the live and inactivated PV could bind to antigenic site-specific MAbs. The resulting OD readings of the ELISAs were used as a measure of the interaction between a PV preparation and an antigenic site-specific MAb. When the antigenic structure of BPL-, BEI- and HCHO-inactivated preparations of the Sabin 2, MEF-1 and 04-44140261 strains was characterised, the D-Ag of the inactivated preparation was calculated relative to live preparations. The result was related to that determined using the MAb 1050. The ELISAs used to characterise the antigenic structure were carried out in an identical manner to that described above (section 2.2.3.1).

2.2.4 Effect of inactivation on viral immunogenicity

2.2.4.1 Rat potency test

Used for batch releases at the NIBSC the rat potency test assessed the immunogenicity of live and HCHO-inactivated serotype 2 PV strains. In addition the potency test was also used to assess the immunogenicity of PV preparations inactivated with different chemicals. Female Wistar (exCRL) rats are used in this test. Equal sized groups of these rats were immunised once intramuscularly in each hind leg with 0.25 ml of PV preparations at set doses (ranging from 0.0125-32 D-Ag). D-Antigen/ml doses were calculated from the D-Ag content of each of the PV preparations which was estimated by ELISA (section 2.2.3.1). Rats were exsanguinated 20 – 22 days post inoculation.

The harvested sera were challenged with three PV strains, (Sabin 2, MEF-1 and 04-44140261), in a cell culture neutralisation assay. In this assay the neutralising antibody titre for the sera was determined by a micro-method using HEp-2C cells as previously described (550) with modifications. Assay diluent (MEM with 4 % FCS and 1 % L-glu, P-S, AmpB) was added to all wells of the serum test plates, “in-house” control plates (50 µl) and the cell control plate (100 µl). Neat serum was added to row A with two wells per sample (50 µl) (figure 2.1). Serial two-fold dilutions of the test sera were made by using multichannel pipettes with disposable tips to mix and transfer 50µl from row A to row B. This was continued through to row H where the last 50 µl was discarded.

	Test serum 1		Test serum 2		Test serum 3		Test serum 4		Test serum 5		Test serum 6	
	1	2	3	4	5	6	7	8	9	10	11	12
1/2	A											
1/4	B											
1/8	C											
1/16	D											
1/32	E											
1/64	F											
1/128	G											
1/256	H											

Figure 2.1. Layout of serum test plates for neutralisation assay.

Serial two-fold dilutions of each test serum were made on the test plates.

At the end of the test sera or on a separate control plate an “in-house” negative sera was added to two wells (50 µl). The “in-house” positive sera (1000 µl aliquot) was diluted 1:1 with assay diluent before being added to wells A1-H1 (50 µl). Serial two-fold dilutions in an 8-12 orientation of the “in-house” positive sera were made in a similar manner to the test sera.

Each challenge virus strain was diluted to 100 TCID₅₀ before being added to a sufficient volume of assay diluent for the number of sera to be tested. The virus challenge was added to the wells of all the plates before the plates were sealed and incubated at +4 °C overnight. A 1:1 dilution of the virus challenge with assay diluent was also stored overnight. This virus challenge was then serially diluted ten-fold a further three times to create the back titration which was transferred to a plate. HEp-2C cells were added to the plates (1-2 x 10⁵ / ml) before the plates were sealed. The plates were incubated at 37 °C for five days and subsequently stained with naphthalene black. In some cases it was necessary to raise the initial dilution of the test sera from 1:2 to either 1:8 or 1:16.

2.2.4.2 Immunisation-challenge experiments

Immunisation-challenge experiments were used to assess the level of protection conferred by inactivated PV preparations to Tg mice which express the human PVR (TgPVR mice). The immunisation-challenge experiments were set up with the Tg21-Bx mouse line at the NIBSC as this mouse line had already been used to develop an immunisation-challenge model at the institute (312). The experiments were as described previously (312) with modifications. Groups of eight Tg21-Bx mice of equivalent age and gender were immunised by the intra-peritoneal route at 6-8 weeks with 0.2 ml 2x2 D-Ag/ml doses of inactivated PV preparations. Following 14 days the mice received a booster of the same dose. After a further 21 days the mice were inoculated by the intramuscular route with a paralysing dose (50 PD₅₀) of either the MEF-1 or 04-44140261 strain, at day 35 (50 µl). Mice were monitored for signs of paralysis for 14 days.

Blood samples were obtained before the first and booster inoculations of the inactivated preparation, before the challenge PV inoculation and at the end of the test. For each group of mice the blood samples obtained before the challenge PV inoculation were pooled. The neutralising antibody titre of these sera was determined as described previously (section 2.2.4.1).

2.2.5 Thermostability of inactivated preparations

The thermostability of BPL-, BEI- and HCHO-inactivated preparations of the MEF-1 serotype 2 strain was assessed by determining the degradation of the viral antigenicity and immunogenicity following heat-treatment at 45 °C for 24 h. The D-Ag of the heat-treated inactivated MEF-1 preparations was determined alongside untreated inactivated MEF-1 preparations by an ELISA as described previously (section 2.2.3.1). The viral immunogenicity of the heat-treated and untreated MEF-1 preparations was determined by a rat potency test. Briefly, Wistar rats were immunised with a 2 D-Ag/ml dose of the untreated inactivated MEF-1 preparations or an equivalent volume of the heat-treated MEF-1 preparations. After 22 days the rats were exsanguinated and their harvested blood sera were challenged with 100 TCID₅₀ of the Sabin 2, MEF-1 and 04-44140261 strains in a cell culture neutralisation assay as described previously (section 2.2.4.1). The viral immunogenicity of heat-treated and untreated HCHO-inactivated PV preparation was also assessed in a series of immunisation-challenge experiments with Tg21-Bx mice as described previously (section 2.2.4.2) with the alteration that an equivalent volume of the heat-treated preparations to the 2x2 D-Ag/ml dose of the untreated preparations was administered to the Tg21-Bx mice.

2.2.6 Effect of inactivation on interaction between poliovirus and the poliovirus receptor

2.2.6.1 Assessment of poliovirus – poliovirus receptor interaction using CD155-AP

The soluble CD155-AP fusion protein, expressed by 293-CD155-AP cells, was used to assess the effect of inactivation on the interaction between PV and the PVR.

Optimisation and quantification of CD155-AP expression by 293-CD155-AP cells

Three 75 cm² flasks of 293-CD155-AP cells were grown to 90-100% confluence using the growth medium described above (section 2.1.2.4). Growth medium was removed and 30 ml of either Optimem (Gibco), DMEM or DMEM (with 5 % FCS) was added to the cells. A one ml aliquot of the supernatant of the cells was immediately taken. Cells were incubated at

35 °C for six days with one ml aliquots being taken each day. Aliquots were stored at +4 °C. The amount of CD155-AP in each supernatant aliquot was quantified by an AP assay as described previously (354) with the modification that only the colorimetric AP determination steps were adopted for this research.

Neutralisation of poliovirus by secreted CD155-AP

Ten-fold serial dilutions from 10^2 - 10^9 of the Sabin 2 and MEF-1 serotype 2 PV strains were prepared with maintenance medium (MEM with 2 % FCS and 1 % L-glu, P-S, AmpB). For each of the two PV strains these dilutions were applied to six 96-well tissue culture plates (BD Biosciences). Expressed CD155-AP (50 µg / 50 µl) was diluted 1:5, 1:25, 1:125, 1:625 and 1:3125 with maintenance medium, each of which was transferred to one of the six plates. Maintenance medium was added to the sixth plate. Plates were incubated for one h at room temperature and then 37 °C for another hour. HEp-2C cells were added and the plates were incubated at 35 °C for three days. Cells were observed daily for signs of CPE and were stained with naphthalene black following three days. The virus TCID₅₀ was determined.

A plaque assay was also used to assess the neutralisation of PV by secreted CD155-AP. The Sabin 2 and MEF-1 strains were diluted with maintenance medium to make a PV challenge containing 100 plaque forming units (PFU) / well. Five-fold serial dilutions from 1:5 to 1:3125 of the CD155-AP (50 µg / 50 µl) were prepared with maintenance medium. The 100 PFU virus challenge was mixed in microtubes with the five-fold dilutions of CD155-AP at a 1:1 ratio and incubated for one h at room temperature and then 37 °C for another hour. Receptor negative PV controls were also included. All samples were transferred to 6-well plates (BD Biosciences) confluent with HEp-2C cells. A 2X complete solution overlay (1:1 2x MEM and bactoagar) was applied before the plates were incubated at 35 °C for three days. The overlay was removed, plates were stained and the plaques were counted.

Use of CD155-AP to assess the interaction between poliovirus and the poliovirus receptor

An AP assay which incorporated a sucrose cushion was devised to quantitatively determine the effect of inactivation on the interaction between PV and the PVR. The conditions for this assay were established using live preparations of the Sabin 2 serotype 2 strain. A live preparation of the Sabin 2 strain (4×10^8 TCID₅₀ / 100 μ l) was incubated with increasing concentrations of CD155-AP (100, 500, 1000, 2000, and 4000 μ g / 50 μ l) for 120 m at +4 °C. Poliovirus-CD155-AP samples were made up to 5 ml with DMEM before being ultracentrifuged through a 30 % sucrose cushion (SW 50 Beckman rotor, 40 000 rpm, 4 h, +4 °C). The resulting pellets were resuspended in Tris-HCl (0.01 M) and the amount of bound CD155-AP was quantified by a colorimetric AP determination assay as described above. This assay was repeated with a similar infectious titre of the MEF-1 strain. However this preparation was only incubated with two dilutions of CD155-AP (1000 and 2000 μ g / 50 μ l).

The interaction between live or HCHO-inactivated PV preparations and CD155-AP was analysed using this AP assay. Live and inactivated Sabin 2 and MEF-1 (17 D-Ag / 50 μ l) were incubated with CD155-AP for 120 m at +4 °C. Sabin 2 preparations were incubated with 1000 μ g / 50 μ l CD155-AP, while MEF-1 preparations were incubated with 2000 μ g / 50 μ l CD155-AP. Poliovirus-CD155-AP samples were pelleted through a 30 % sucrose cushion and analysed as described above.

Determination of poliovirus-poliovirus receptor interaction by surface plasmon resonance

The Biacore 2000 biosensor instrument was used to determine whether SPR could detect the interaction between PV and the PVR. The immobilisation wizard program of the Biacore 2000 control software was used to set the immobilisation for this protocol at a flow rate of 1 μ l / min for 126.33 min. A wild-type trivalent IPV was immobilised to a CM3 sensor chip using an amine coupling kit with sodium acetate (pH 5.0). The binding analysis program of the Biacore 2000 control software was used to set up the remaining steps of this protocol. A series of two-fold serial dilutions of CD155-AP, ranging from 1:4 to 1:32, were prepared with

HBS-EP running buffer. The diluted CD155-AP samples were injected over the surface of the sensor chip at a flow rate of 2 μ l / min for 10 min. Binding was monitored in real-time by SPR. Regeneration was performed between the CD155-AP dilutions and involved the injection of 10 mM glycine-HCl (pH 2.0) over the surface of the chip at a flow rate of 10 μ l / min for 90 s. As described above (section 2.2.3.2), immobilisation and regeneration scouting programs of the Biacore 2000 control software were used to optimise the immobilisation and regeneration conditions.

2.2.6.2 Assessment of poliovirus-poliovirus receptor interaction using fluorescence-activated cell sorting flow cytometry

Fluorescence-activated cell sorting (FACS) flow cytometry was used to assess the interaction between live or inactivated PV preparations and susceptible L20B cells or non-susceptible Ltk- cells. L20B and Ltk- cells (1×10^6 cells / ml) were incubated with increasing concentrations of live and HCHO-inactivated preparations of the Sabin 2 strain (1, 10, and 100 D-Ag / 100 μ l) for 120 min at room temperature. Cells were pelleted (2000 rpm, 5 min, room temperature) and washed twice with PBS flow buffer (PBS with 5 % FCS and 1 % sodium azide) (PFB) before being transferred to a 96-well plate (Corning incorporated). Cells were pelleted and resuspended with a serotype 2-specific MAb (MAb 267, (345)). For 30 min cells were incubated at room temperature on a shaker. Then cells were pelleted and washed twice with PFB before being resuspended with anti-mouse IgG antibodies conjugated to fluorescein isothiocyanate (FITC) (Sigma-Aldrich). After 20 min incubation in the dark at room temperature cells were pelleted and washed twice more with PFB before FACS FIX (150 ml PBS, 325 ml sterile distilled water and 25 ml HCHO) was added. Cells were analysed using a BD FACSCanto II flow cytometer (BD Sciences). Both the mean fluorescence intensity and percentage of cells with PV bound could be estimated.

Another assay was carried out, in which live and HCHO-inactivated preparations of the Sabin 2 strain (1, 10, and 100 D-Ag / 50 μ l) were incubated with CD155-AP (2 μ g / 50 μ l) or MEM at a 1:1 ratio for 60 min at room temperature before being incubated with L20B cells (1×10^6 cells / ml) for 120 min at room temperature. Binding was detected by FACS flow cytometry as described above.

The binding of BPL-, BEI- and 1:8000 HCHO-inactivated PV was assessed. Live and inactivated preparations of the Sabin 2 strain (1, 10, 100 D-Ag / 50 µl) were incubated with L20B cells (1×10^6 cells / ml) for 120 min at room temperature. Binding was detected by FACS flow cytometry as described above.

2.2.6.3 Assessment of poliovirus-poliovirus receptor interaction using real-time reverse transcription-polymerase chain reaction

An assay which incorporated real-time RT-PCR was used to assess the effect of inactivation on the interaction between PV and the PVR. This real-time RT-PCR binding assay was as previously described (243) with the some modifications. L20B and Ltk- cells were detached with trypsin, pelleted and washed twice in binding buffer (MEM with 2 % FCS and 1 % L-glu, P-S, AmpB). The cells (2.5×10^5 cells / ml) were then incubated with live preparations of the MEF-1 serotype 2 strain (0.004, 0.04, 0.4 D-Ag / 100 µl) at either +4 °C or room temperature for 120 min. Cells were pelleted (2000 rpm, 10 min) and washed twice with binding buffer before resuspension in MEM. Between each wash the supernatant was harvested and pooled. The viral RNA was extracted from both the pelleted cells and the pooled supernatant using the MagNA Pure LC Total Nucleic Acid Isolation Kit with the Kingfisher ml particle processor (section 2.2.1.2). Assay conditions for quantification of the extracted viral RNA were optimised using the QuantiTect SYBR Green RT-PCR kit (Qiagen) with the Rotor-Gene 3000 thermal cycler (Qiagen) (section 2.2.8.2).

In a second real-time RT-PCR binding assay live MEF-1 (0.04 D-Ag / 25 µl) was incubated with equal concentrations of CD155-AP, AP, a serotype 2-specific MAb (MAb 1050), a serotype 1-specific MAb (MAb 234) or MEM at a 1:1 ratio for 60 min at 37 °C. L20B and Ltk- cells (2.5×10^5 cells / 500 µl) were then incubated with the pre-treated MEF-1 at room temperature for 120 min. The amount of live MEF-1 bound to the cell lines was determined as described above.

For another real-time RT-PCR binding assay live and HCHO-inactivated preparations of the MEF-1 strain (0.02, 0.2, and 2 D-Ag / 50 µl) were incubated with L20B and Ltk- cells

(2.5×10^5 cells / 500 μ l) for 120 min at room temperature. The amount of PV bound to the murine cells was determined as described above.

In an additional assay live and HCHO-inactivated preparations of the MEF-1 strain (0.2 D-Ag / 25 μ l) were incubated with either CD155-AP (1 μ g / 25 μ l), a serotype 3-specific MAb (MAb 520), MEM or a range of antigenic site specific serotype 2 MAbs at a 1:1 ratio for 60 min at room temperature. The serotype 2 MAbs included MAbs 433 and 436 which bind to antigenic site 1; MAb 1269 which binds to antigenic site 2a; MAb 1037 which binds to antigenic site 2b; and MAbs 1050 and 1102 which bind to antigenic site 3b. The pre-treated MEF-1 preparations were then incubated with L20B cells (2.5×10^5 cells / 500 μ l) at room temperature for 120 min. The amount of PV bound to the L20B cells was determined as described above.

For another real-time RT-PCR binding assay live and HCHO-, BPL- and BEI-inactivated MEF-1 preparations (0.2 D-Ag / 25 μ l) were incubated with either CD155-AP (1 μ g / 25 μ l), a serotype 2-specific MAb (MAb 1050), a serotype 3-specific MAb (MAb 520) or MEM at a 1:1 ratio for 60 min at room temperature. The pre-treated MEF-1 preparations were incubated with L20B cells (2.5×10^5 cells / 500 μ l) at room temperature for 120 min. The amount of PV bound to the L20B cells was determined as described above.

2.2.7 Effect of inactivation on poliovirus entry

2.2.7.1 Effect of inactivation on conversion of poliovirus virions to 135S and 80S particles

To enter a host cell and release the viral RNA PV virions must undergo a series of conformational changes to form 135S and 80S particles. It is possible to trigger these conformational changes *in vitro* in the absence of the PVR by incubating PV at super-physiological temperatures in a hypotonic medium (50, 113). This approach was adopted to determine whether inactivated PV particles can form 135S and 80S particles. Live and BPL-, BEI- and HCHO-inactivated preparations of equivalent concentrations (0.2 D-Ag / 50 μ l) of the MEF-1 serotype 2 strain were incubated in hypotonic medium (1.21 g Tris, 0.147 g $\text{CaCl}_2 \cdot 2\text{H}_2\text{O}$, 0.50 ml Tween 20, made up to 500 ml with sterile distilled water) at 50 and 60

°C for 3 and 20 min to induce a conformational change to form 135S and 80S particles (respectively). Live and inactivated MEF-1 preparations were also incubated at room temperature as a control. As 135S and 80S particles differ in a number of characteristics to mature PV virions a range of assays were carried out to assess whether the inactivated samples had undergone the conformational changes.

The degree of conversion of the treated live and inactivated MEF-1 preparations to 135S and 80S particles was measured by characterising their antigenic properties in ELISAs (as described in section 2.2.3.1), assessing their ability to bind to L20B cells in real-time RT-PCR assays (as described in section 2.2.6.3), and by determining the presence of viral RNA by sensitivity to RNase A. A real-time RT-PCR was carried out to assess the sensitivity of the preparations to RNase A. In this assay live and inactivated MEF-1 preparations were incubated with RNase A (0.001 µg / µl) (Sigma-Aldrich) before being incubated at room temperature, 60 °C and 50 °C for 20 and 3 min, respectively. Poliovirus preparations were placed on ice and RNase inhibitor (Roche) was added. The viral RNA was extracted using the MagNA Pure LC Total Nucleic Acid Isolation Kit with the Kingfisher ml particle processor and a real-time RT-PCR was used to detect the presence of RNA (section 2.2.8.2).

2.2.7.2 Use of fluorescence-activated cell sorting flow cytometry to assess the effect of inactivation on poliovirus viral entry

To assess whether inactivated PV could undergo the necessary conformational changes FACS flow cytometry was used to track viral entry process of live and HCHO-inactivated PV preparations. L20B cells were detached with trypsin, pelleted and washed twice in binding buffer (MEM with 2 % FCS and 1 % L-glu, P-S, AmpB). The cells (1×10^6 cells / ml) were mixed with live and 1:4000 HCHO-inactivated preparations of the Sabin 2 strain (10 D-Ag / 100 µl). Preparations were incubated at either 20 or 37 °C for 11 h. During this time identical preparations were mixed and incubated with L20B cells for 1, 2, 4, 6 and 8 h. Incubations were arranged so that they would all finish at 11 h. In addition a 0 h control was set up for both the live and inactivated preparations. For each of the incubations a cell control was included to assess background fluorescence. Two temperatures were used as it was known that at 20 °C PV can only bind to cells, while at 37 °C the virus can bind and enter the cells.

Following 11 h incubation the binding (20 °C) and internalisation (37 °C) preparations were pelleted and washed twice with PFB before being transferred to 96-well plates (Corning incorporated). Binding preparations were pelleted and resuspended with the serotype 2-specific MAb 267. Internalisation preparations were pelleted and resuspended with a fixation medium (Invitrogen). Binding and internalisation preparations were incubated on a shaker at room temperature for 30 min. Both the binding and internalisation preparations were pelleted and washed twice with PFB. Pelleted binding preparations were resuspended with anti-mouse IgG (whole molecule)-FITC. The pelleted internalisation preparations were resuspended in a 1:1 mixture of a permeabilization medium (Invitrogen) and the serotype 2-specific MAb 267. Binding preparations were incubated on a shaker at room temperature for 20 min in the dark. Internalisation preparations were incubated on a shaker at room temperature for 30 min. Both sets of preparations were pelleted and washed twice with PFB. Pelleted binding preparations were resuspended in FACS FIX before being stored on a shaker at +4 °C. The pelleted internalisation preparations were resuspended in a 1:1 mixture of a permeabilization medium and the anti-mouse IgG (whole molecule)-FITC. Internalisation preparations were incubated on a shaker at room temperature for 20 min in the dark before being pelleted and washed twice with PFB. Pelleted internalisation preparations were resuspended in FACS FIX. Both sets of preparations were analysed using a BD FACSCanto II flow cytometer. In order to estimate the amount of PV that was internalised the fluorescence readings of the 20 °C incubated preparations were subtracted from those of the 37 °C incubated preparations.

2.2.8 Effect of inactivation on viral RNA

The effect of inactivation on the viral RNA was determined by assessing the biological activity and functionality of the RNA extracted from PV during inactivation time-courses. The MagNA Pure LC Total Nucleic Acid Isolation Kit was used with the Kingfisher ml particle processor to extract the viral RNA from aliquots taken during the BPL-, BEI- and HCHO-inactivation time-courses (section 2.2.2.4).

2.2.8.1 Effect of inactivation on biological activity of viral RNA

The biological activity of the extracted viral RNA was determined by its ability to produce infectious virus after transfection into HEp-2C cells. Both DEAE-dextran and electroporation were used to transfect the viral RNA. The DEAE-dextran-mediated transfection protocol was as previously described (453) with modifications. One day prior to the transfection HEp-2C cells were trypsinised and replated to 25 cm² flasks (BD Biosciences) (1 x 10⁵ cells / flask) or 35 mm dishes (BD Biosciences) (5 x 10⁴ cells / dish). Cells were incubated at 37 °C until they were 80 % confluent. A 1 x HBSS/glucose/DEAE-dextran solution was mixed and incubated with the extracted RNA on ice for 20-30 min (245 µl to 5 µl RNA). Medium was removed by aspiration and cell sheets were washed three times with PBS. RNA-1x HBSS/glucose/DEAE-dextran solutions were added to cells. Cells were incubated at room temperature for 20-30 min before the RNA-1x HBSS/glucose/DEAE-dextran solutions were removed by aspiration. Pre-warmed maintenance medium (MEM with 2 % FCS and 1 % L-glu, P-S, AmpB) was added and cells were incubated at 35 °C in a CO₂ incubator for seven days. Cells were observed daily for signs of CPE.

The electroporation protocol was as previously described (188) with modifications. One day prior to the transfection HEp-2C cells were trypsinised and replated to 25 cm² flasks (1 x 10⁵ cells / flask). Cells were incubated at 37 °C until they were 80 - 90 % confluent. Cells were trypsinised and resuspended in growth medium (MEM with 5 % FCS and 1 % L-glu, P-S, AmpB) before being pooled. Pooled cells were pelleted and washed twice with HeBS solution (HBSS [x1] and glucose [0.1 %]) before being transferred to 0.4 cm electroporation cuvettes (Invitrogen). Viral RNA (between 0.105 – 0.180 µg) was added to cuvettes and electroporated once at 250 V, 360 Ω, and 250 µF using an Electro Cell Manipulator 600 (BTX Harvard Apparatus). After being allowed to recover at room temperature for 5-10 min, cells were resuspended in growth medium and plated in 25 cm² flasks. Cells were incubated at 35 °C for seven days and observed for CPE.

2.2.8.2 Effect of inactivation on functionality of viral RNA

A series of RT-PCRs were carried out to determine whether inactivation affected the ability of the viral RNA to replicate. Viral RNA was extracted from live MEF-1 in addition to

that extracted from the inactivation time-course aliquots (section 2.2.2.4). A series of primers of equal length and melting point which yielded 200, 400, 600 and 800 bp RT-PCR products of the region encoding the VP1 were designed (section 2.1.1). The extracted viral RNA preparations were run in four RT-PCRs using the Qiagen One-Step RT-PCR kit (309, 411) with the respective primers. The resulting RT-PCR products were examined by gel electrophoresis on a 1 % agarose gel.

The results of these RT-PCRs were quantified by a real-time RT-PCR which incorporated the same primers described above. The relevant primers and viral RNA extracted from live MEF-1 were used to generate an 800 bp RT-PCR product of the VP1 coding region. The concentration of the extracted viral RNA samples and this RT-PCR product was determined using a nanodrop spectrophotometer at 230 nm (NanoDrop® ND-1000 spectrophotometer, NanoDrop Technologies). The RT-PCR product was diluted with RNase-free water to ensure that the gene copy number / 5 µl was approximately 10^9 log 10s. The diluted RT-PCR product was further diluted ten-fold from 10^{-1} to 10^{-7} . This serial dilution series was used to establish a calibration curve to calculate the genome copy of extracted RNA. Results were expressed relative to the D-Ag concentration of the PV preparations from which the RNA was extracted. A QuantiTect® SYBR® Green RT-PCR kit (Qiagen) was used for the real-time RT-PCR. This reaction was carried out using the Rotor-Gene 3000 thermal cycler (Qiagen). The conditions used are detailed in figure 2.2.

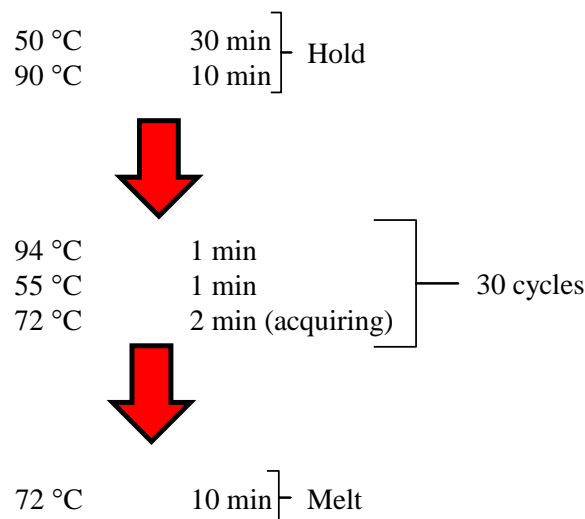


Figure 2.2. Real-time reverse transcription-polymerase chain reaction assay conditions.

Real-time RT-PCR was used to: quantify the effect of inactivation on the viral RNA; determine how much PV was bound to cells; detect viral RNA following RNase A treatment of heated PV preparations.

In addition to the region encoding the VP1 this real-time RT-PCR was also carried out at the 5' and the 3' ends (figure 2.3) of the genomic region with respective primers (section 2.1.1) and a diluted RT-PCR product.

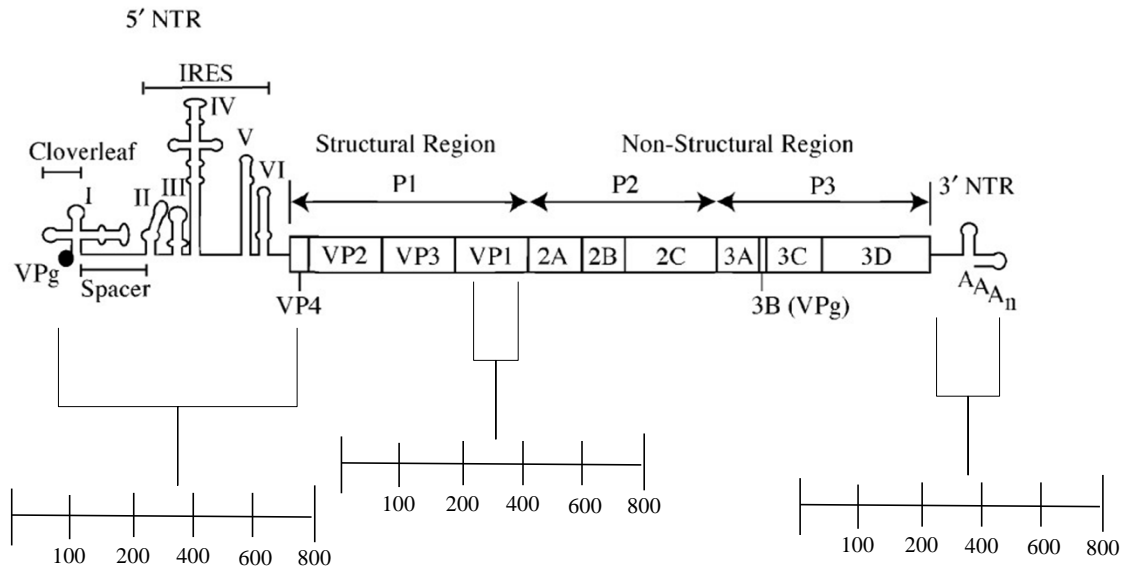


Figure 2.3. Regions of poliovirus genome analysed by real-time reverse transcription-polymerase chain reactions.

Real-time RT-PCRs quantified the effect of inactivation on three regions of the viral RNA genome of PV.

A bioanalyser was used to analyse the quality and size of the extracted viral RNA. Viral RNA extracted from a series of commercial IPV_s was analysed using the Agilent 2100 Expert Bioanalyser (Agilent technologies).

CHAPTER 3

CHARACTERISATION OF SEROTYPE 2 POLIOVIRUS STRAINS INACTIVATED WITH FORMALDEHYDE

3.1 INTRODUCTION

As the GPEI approaches its End-game there is a growing consensus that in order to avoid further cases of VAPP and VDPVs, OPV vaccination must cease alongside a transition to worldwide IPV vaccination (102, 145, 165, 166, 502). However as noted in the Introduction (section 1.5.4) there are several issues concerning this transition, in particular the biosecurity of manufacturing plants post eradication. This has led to the WHO promoting the development of sIPV (276). Several studies have found differences in the antigenic and immunogenic properties of sIPV and cIPV preparations (133, 140, 141, 252, 276, 312, 426, 472, 493). Studies using Tg mice expressing PVR and rat models have shown that the serotype 2 sIPV induces lower levels of antibodies than serotype 2 cIPV (141, 276, 310, 472).

Inactivation with HCHO has previously been found to modify some antigenic sites of PV (160, 426). It could be argued that due to genomic differences between sIPV and cIPV seeds the antigenic epitopes presented differ and that the sensitivity of these epitopes to HCHO also varies. This variable sensitivity might result in the antigenic epitopes of sIPV and cIPV being modified to different extents which would have a direct effect on the immunogenicity. The research detailed here aims to confirm whether this hypothesis could account for the difference in immunogenicity to serotype 2 sIPV and cIPV.

The serotype 2 cIPV was first developed by Salk *et al.* (451) by treating the MEF-1 strain with HCHO. The MEF-1 strain was isolated in 1942 from the CNS of poliomyelitis cases occurring among the Middle East Forces of the British Army, Cairo, Egypt (456, 519). Although a number of antigenically related strains were isolated from the same location and time (194) MEF-1 has remained the chosen strain for serotype 2 cIPV (409). A naturally occurring serotype 2 strain, P712, was isolated from the faeces of healthy children by Sabin. This strain possessed low neurovirulence for cynomolgus monkeys by the intraspinal route and was selected to generate the serotype 2 OPV seed. The strain was passaged four times (three terminal dilutions) in cynomolgus MKTC before being purified by three serial passages of plaque isolates. The least neurovirulent plaque progeny was fed to chimpanzees and the stool with the least residual neurotropism (P712, Ch) was further purified by three single-plaque passages in cynomolgus MKTC. The resulting strain (P712, Ch, 2ab) was used to prepare the Sabin 2 strain by passaging twice in cynomolgus MKTC (P712, Ch, 2ab/KP₂). At Merck, Sharp and Dohme Research Laboratories this SO was passaged once in rhesus

MKTC to create the current vaccine strain (P712, Ch, 2ab/KP3 or SO+1) (448). Two nt substitutions (G481A in the 5'NCR and C2909U encoding a threonine to isoleucine substitution at position 143 of VP1) are responsible for the attenuated phenotype of Sabin 2 (305, 424). As described previously (Introduction, section 1.3.2) the substitution at G481A in the stem-loop region V of the 5'NCR is the principal determinant of attenuation however its precise contribution is not clear (305, 424, 427). The capsid mutation (C2909U at 143 VP1) can influence the attenuated phenotype in various ways (52, 162, 304). In addition an alanine to serine substitution at position 41 of VP4 may contribute to the attenuated phenotype (305, 336).

The OPV serotype 2 monovalent lot can be mixed with the serotype 1 and 3 lots to form a trivalent preparation. However tOPV preparations with similar potency for each serotype have shown predominance for serotype 2 excretion and higher serotype 2 antibody titres than for serotypes 1 and 3 (151, 260, 277, 397, 505, 528, 575). The Sabin 2 strain has been argued to be more robust than the other OPV serotypes as it was a primary isolate rather than a product of laboratory selection from “wild” strains (164, 447). This might allow it to interfere with the Sabin 1 and 3 immunogenic responses. Initially the administration of three or more doses of the tOPV was sufficient to overcome this interference effect (485). However a later study (433) found that a single dose of a ‘balanced’ formulation of tOPV could induce sufficient seroconversion. This has been adopted and used for worldwide trivalent formulations. The WHO requires the following minimum TCID₅₀ values for each vaccine PV serotype: $10^{6.0} \pm 0.5$ TCID₅₀ for serotype 1, $10^{5.0} \pm 0.5$ TCID₅₀ for serotype 2 and $10^{5.8} \pm 0.5$ TCID₅₀ for serotype 3 (111, 485).

Before the use of PV vaccines four major wild-type PV serotype 2 genotypes had worldwide distribution and caused a number of outbreaks (for example (231, 257)). However little is known of these wild-type isolates and only a selection have been partially sequenced (570). Following the introduction of PV vaccines the transmission of these strains fell sharply (79). This disappearance of infectious serotype 2 strains occurred at a faster rate than for other serotypes, possibly due to the high immunogenicity and more efficient seroconversion of the Sabin 2 component of the tOPV and the tendency of this strain to spread from vaccinated persons to close contacts (390, 485). Between 1989 and 1999 all four known wild-type PV serotype 2 genotypes had disappeared.

Several serotype 2 isolates were obtained from the last known reservoirs: Bihar, Uttar Pradesh, and West Bengal in northern India. These isolates represented the final phase of wild-type PV serotype 2 transmission as their genetic diversity had rapidly declined. In October 1999 in West Bihar the last wild-type PV serotype 2 was isolated from a child reported as an AFP case (79). Only vaccine derived serotype 2 strains have been isolated since this date, which along with the declining genetic diversity of the last wild isolates indicated that wild-type PV serotype 2 had been eliminated (79). However in 2000 wild-type PV serotype 2 was isolated from three AFP cases in eastern Uttar Pradesh and Bihar. While sequencing found no relation of these isolates to the wild-type PV serotype strains previously circulating in India in 1999, a virtual identity to the laboratory reference serotype 2 reference strain MEF-1 was found (554). Between 2002 and 2003 wild-type PV serotype 2 was isolated from seven AFP cases, a healthy contact child and an environmental sewage sample (126). Sequencing determined that all isolates belong to one of two closely related strains of MEF-1. However no mutational evidence of circulation was detected. A later investigation found the source of these isolates to be batches of tOPV which had been contaminated with MEF-1 (554).

While tOPV remains in use vaccine derived serotype 2 strains are still emerging and causing cases of VAPP and VDPVs. As noted in the Introduction (section 1.3.2) due to the intense selection against attenuating mutations during replication within the intestinal tract OPV strains can undergo reversion to a neurovirulent state and cause VAPP. As attenuation of the Sabin 2 strain is primarily determined by only two highly unstable mutations, reversion can be very rapid (305, 341, 424, 572). The reverted phenotype of serotype 2 VAPP strains can be attributed to a reversion of the attenuation mutations G481A in the 5'NCR and C2909U at 143 VP1(336). Individuals with immunodeficiency disorders are at most risk to developing VAPP (485). The serotype 2 strains are the most common PV isolated from immunodeficient cases with VAPP (484).

OPV strains can circulate and evolve over a period of time by undergoing recombinations and other mechanisms of reversion and this can contribute to the development of VDPVs. There have been a large number of poliomyelitis outbreaks associated with serotype 2 cVDPV strains in Madagascar (420, 439); Nigeria (238, 531, 560); Niger ; Afghanistan; Chad; Democratic Republic of the Congo; India and Somalia (560). Also serotype 2 cVDPVs have been retrospectively identified in Egypt between 1983 and 1993 (570). Since

2010 the GPLN has redefined serotype 2 VDPVs to include isolates with >0.6% (rather than 1%) divergence to allow the detection of numerous pre-VDPV2 (0.5-1.0 % divergence) isolates from Nigeria. In Nigeria between 2005 and 2010 21 cases of pre-VDPV2 were detected alongside the 315 cases of serotype 2 cVDPV. The pre-VDPV2s were identified as outbreak intermediates as large numbers (16/21 cases) of them were ancestral to subsequently observed cVDPV2 lineages (531). This recognition of the early role of pre-VDPVs in the outbreaks has prompted the redefinition of serotype 2 VDPVs. This redefinition has partly led to the recent increase in frequency of detected VDPVs. It is thought that the increasing gaps in serotype specific immunity have contributed to the increase in serotype 2 cVDPV. The intensive use of mOPV1 and bOPV in supplementary immunisation activities and the inadequate coverage with routine immunisation of tOPV has resulted in conditions favouring multiple independent emergences of serotype 2 cVDPVs (560). Other factors contributing to these emergences include the rapid spread of Sabin 2 amongst unimmunised people, as seen in contact cases of VAPP (175), and the higher seroprevalence to PV serotype 2 in unvaccinated individuals in the USA and Europe (164, 485). Due to the low paralytic rate of serotype 2 PV infections (364), serotype 2 cVDPVs are difficult to detect by AFP surveillance and, thus, they are able to spread and cause further outbreaks.

Serotype 2 strains are prevalent in immunodeficient cases and have been associated with a large number of the 50 iVDPV reported infections (558, 560). In addition, the longest known excreted iVDPV is a serotype 2 strain (311, 558). Long-term excreted iVDPVs can show high divergence from the parental Sabin strain (311) and accumulate a number of mutations in various viral regions, including the viral capsid. Capsid mutations have been shown to involve amino acids in the canyon, the drug/lipid binding pocket, monomeric and pentameric interfaces and antigenic sites (33, 256, 313, 567).

In addition to cVDPVs and iVDPVs, a number of serotype 2 aVDPVs have been isolated, in particular from sampling of sewage. Highly divergent serotype 2 strains have been isolated from sewage in Estonia (559, 560), Finland (437) and Israel (468). These isolates had multiple lineages, many amino acid substitutions in antigenic sites and minimal recombinations which suggests they were probably iVDPVs (437, 468, 469, 560). Following a challenge with OPV, serotype 2 PV has replicated and been excreted by highly immune children, for up to three weeks. There is concern that highly divergent aVDPV strains could

be transmitted between immune individuals, in particular older individuals with less humoral protection (469).

The research described within this chapter aims to characterise the Sabin 2 and MEF-1 strains of serotype 2 sIPV and cIPV, respectively, to determine why the two strains differ in viral immunogenicity following inactivation with HCHO. In addition in order to gain a full understanding of the differences, the effect of HCHO inactivation on a number of other serotype 2 strains including VDPVs and wild-types was also investigated. The molecular characteristics of a range of serotype 2 strains are described within this chapter. Whether the genomic differences between them resulted in antigenic structures with different immunogenicity following inactivation with HCHO was determined. The results shown here represent the first study to explore the relationship between the sequence of a PV strain and the immunogenicity of inactivated PVs. Antigenic sites modified by inactivation with HCHO were identified and the effect of this inactivation on viral immunogenicity was explored

3.2 RESULTS

3.2.1 Molecular characterisation of serotype 2 poliovirus strains

In order to gain a better understanding of the difference in viral immunogenicity between serotype 2 sIPV and cIPV, the molecular and antigenic characteristics of a wide range of serotype 2 strains from different origins was determined. These strains included VDPV isolates from immunodeficient individuals (cases 4 and 5 described in (311)), a cVDPV strain from a PV outbreak (419) and wild-type strains from paralytic cases from various regions of the world, isolated over a large period of time (table 3.1).

Poliovirus serotype 2 strain	Origin	Date / Place of isolation
Sabin 2	Sabin vaccine seed (OPV)	1956, USA
MAD029	cVDPV strain	2002, Madagascar
04-44140261	iVDPV strain	06/10/2004, UK
102050	iVDPV strain	16/01/1998, UK
071108	iVDPV strain	07/11/2008, UK
118/78	Wild-type strain	1978, Morocco
II-215	Wild-type strain	1959, Venezuela
II-316	Wild-type strain	1952, Egypt
MEF-1	Wild-type strain (IPV seed)	1942, Egypt

Table 3.1. A representative collection of serotype 2 poliovirus strains.

A range of serotype 2 PV strains of different origins (vaccine seed, VDPV, wild-type) were sourced from the collection at the NIBSC.

Virus stocks of the selected serotype 2 PV strains were prepared in tissue culture and purified by ultracentrifugation through a 30 % sucrose cushion, as described in Materials and Methods (section 2.2.1.1). Purified PV preparations were titrated using a microtitre plate system and expressed as log₁₀ TCID₅₀/100 µl (Materials and Methods, section 2.2.1.1). Virus titre varied between 8.5 to 10.2 log₁₀ TCID₅₀/100 µl. The Sabin 2, MAD029, 04-44140261, 102050 and MEF-1 strains were grown to larger volumes using roller bottles (850 cm²) and, thus, showed a greater log₁₀ TCID₅₀ than other strains. The viral RNA of each strain was extracted, as described in Materials and Methods (section 2.2.1.2). Complementary viral DNA was synthesised by RT-PCR to analyse the region of the genome encoding the viral capsid. Standard M-13-tagged primers with Sabin 2, MEF-1 and selected VDPV sequences from the collection of the NIBSC were used (Materials and Methods, section 2.1.1). The RT-PCR products were analysed by gel electrophoresis and purified using a commercial kit (Materials and Methods, section 2.2.1.2). Sequencing was performed, as described in Materials and Methods (section 2.2.1.2).

The phylogenetic relationship between strains was established using the alignment program CLUSTAL W (286, 501). The degree of nt sequence identity and of protein similarity was determined using the default scoring matrices. The phylogenetic relationship between sequences was determined using the maximum likelihood method, with DNADIST/NEIGHBOR of PHYLIP (Phylogeny Inference Package) to analyse the respective sequences of the relevant strains (157). The robustness of the phylogenies was estimated by bootstrap analysis with 1000 pseudoreplicate data sets. In addition to the selected serotype 2 strains, the sequence of a serotype 1 strain (Mahoney) was introduced to allow correct rooting of the tree. The results of sequence comparisons are shown in table 3.2 and figure 3.1.

Strain	% difference from strain*								
	SAB 2	MAD	04-44	102050	071108	118/78	II-215	II-316	MEF-1
SAB 2		1.0	5.3	13.6	17.3	21.2	21.8	20.0	20.3
MAD	0.3		6.1	13.8	17.7	21.4	22.1	20.2	20.8
04-44	2.5	2.4		15.5	18.8	22.4	22.3	20.7	20.5
102050	5.5	5.4	6.0		14.5	24.2	24.3	23.0	23.8
071108	5.7	5.6	6.2	2.9		24.6	25.2	23.5	24.5
118/78	2.8	2.9	4.5	5.9	6.0		18.7	13.8	15.9
II-215	3.0	3.1	4.7	6.8	6.2	2.3		13.9	13.0
II-316	2.7	2.8	4.3	6.2	5.8	1.3	1.7		9.8
MEF-1	3.0	3.1	4.5	6.6	6.2	1.7	2.1	1.5	

Table 3.2. Nucleotide and amino acid differences between serotype 2 strains.

Following extraction, the region of the RNA encoding the viral capsid of the strains was sequenced using the relevant primers. The sequenced capsid of the strains was analysed using the AlignIR V2.0 and Pairwise deletion. * The lower left and upper right portions of the table show amino acid and nt differences (shown as %), respectively. Serotype 2 PV strains are abbreviated as follows: SAB 2, Sabin 2; MAD, MAD029; 04-44, 04-44140261.

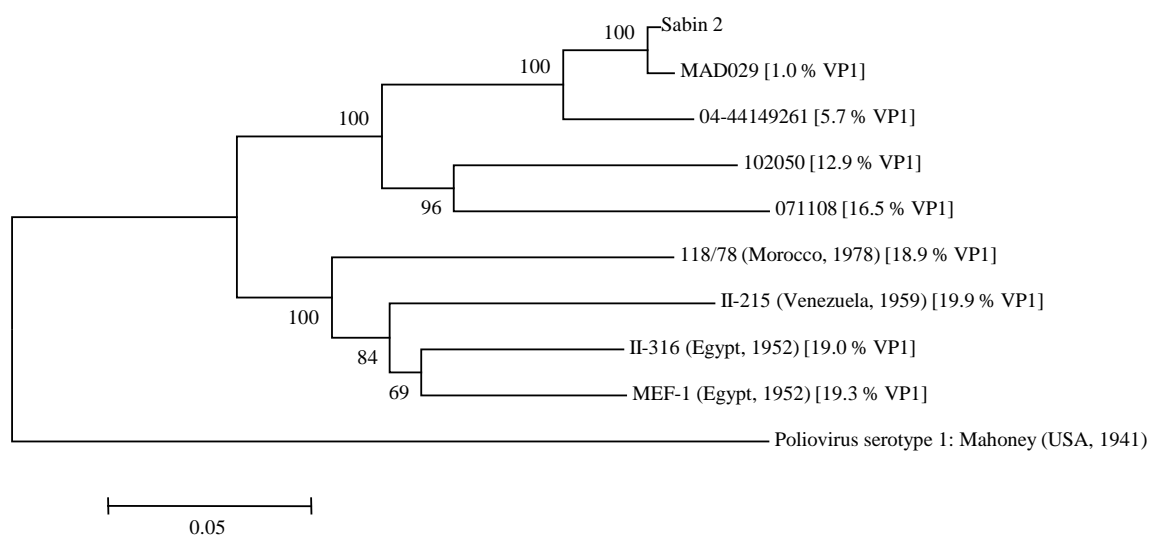


Figure 3.1. Neighbour-joining tree showing phylogenetic relationships between the serotype 2 strains and Mahoney of poliovirus serotype 1.

Following extraction, the region of the RNA encoding the viral capsid of the strains was sequenced using a variety of primers. The sequenced capsid region was analysed using the bootstrap analysis. The numbers at the

nodes indicate the percentages of 1,000 bootstrap pseudoreplicate data sets supporting the cluster. Percentage VP1 sequence divergence from Sabin 2 is bracketed.

As shown in figure 3.1, the phylogenetic tree confirmed the expected differences between strains. The cVDPV strain MAD029 showed less nt and amino acid differences to Sabin 2 than the iVDPV strains (table 3.2). This was confirmed by the closer relationship of MAD029 to Sabin 2 (figure 3.1). The iVDPV strains 102050 and 071108 showed a high percentage of VP1 sequence divergence from the parental Sabin 2. Previous research has found a PV capsid evolution of 1 % nt substitutions per year (544). Consequently, it is possible to establish a molecular clock of PV evolution which can be used to determine the age of these iVDPV isolates (544). Based on this molecular clock, one can conclude from the percentage VP1 sequence divergence of these strains that the individual who shed these two isolates has been excreting PV continuously since he was last immunised, approximately 12 and 22 years, respectively. As shown in figure 3.1, the wild-type strains (118/78, II-215, II-316 and MEF-1) were genetically distant to Sabin 2 and showed the greatest divergence in nt sequence to other strains (table 3.2). Although the nt sequence varied between the strains, the amino acid sequence was conserved to a greater extent. As table 3.2 shows, the iVDPV strains 071108 and 102050 had the greatest divergence in amino acid sequence in comparison to other strains. The proportion of non-synonymous nt changes was determined for some of strains described above and others for which sequences are available in public databases, as shown in figure 3.2.

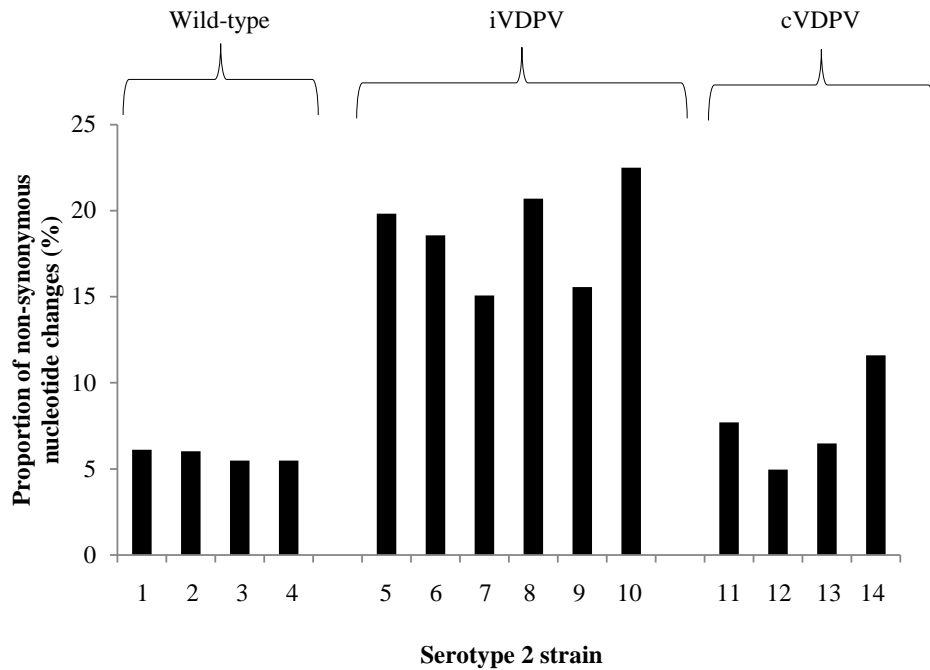


Figure 3.2. Proportion of non-synonymous nucleotide changes in serotype 2 poliovirus strains.

The proportion of non-synonymous nt changes of a range of serotype 2 strains was calculated determining the ratio of nt change and amino acid changes. 1= MEF-1; 2 = II-215; 3 = II-316; 4 = 118/78; 5 = 04-44140261; 6 = 102050; 7 = 071108; 8 = strain USA0911201 (GenBank: GU390707.1); 9 = strain USA9810768 (GenBank: DQ890387.1, (4)); 10 = strain USA9211202 (GenBank: GU390704.1); 11 = strain EGY88-074 (GenBank: AF448782.1, (94)); 12 = strain EGY93-034 (GenBank: AF448783.1, (94)); 13 = strain NIE0811204 (GenBank: GU390705.1); 14 = strain NIE0811203 (GenBank: GU390706.1)

As figure 3.2 shows, the iVDPV strains had a greater proportion of non-synonymous nt changes than the wild-type and cVDPV strains.

The amino acid sequence within the antigenic sites was analysed (table 3.3).

Virus Strain	Antigenic Site																																		
	Site 1								Site 2a								Site 2b				Site 3a						Site 3b								
	VP1 98-105, 175, 252								VP1 217-224								VP2 164, 168, 170, 172				VP2 72, 157, 158, 239, 240, 244						VP3 56, 58, 59, 61, 62, 66								
Sabin 2	T	K	R	A	S	R	L	F	A	R	L	A	G	Q	A	S	T	E	T	N	A	N	R	K	G	Y	T	K	N	T	S	R	K	D	
MAD.	-	-	-	-	-	-	-	-	-	-	-	T	-	-	-	-	-	-	-	-	-	-	-	-	-	-	-	-	-	-	-	-	-	-	
04-44.	-	R	-	T	-	K	-	-	-	-	-	-	-	-	-	-	-	-	-	S	S	-	-	-	-	-	-	-	-	-	-	-	-	-	
102050	-	N	-	T	-	K	-	-	-	-	-	S	H	-	A	-	D	-	-	-	E	N	E	R	-	-	-	-	-	-	-	H	R	-	
071108	-	N	-	-	-	K	-	-	S	-	-	-	-	H	-	A	A	D	N	-	-	K	N	-	-	-	A	-	-	-	-	H	R	-	
118/78	-	-	-	-	-	K	-	-	-	K	-	-	-	-	-	-	-	-	-	-	-	-	-	-	-	-	-	-	-	-	-	-	-	-	E
II-215	A	-	-	-	-	K	-	-	-	K	-	-	-	-	T	-	-	-	-	-	-	-	-	-	-	-	-	-	-	S	-	-	-	-	
II-316	-	-	-	-	-	K	-	-	-	K	-	-	-	-	-	-	S	-	-	S	-	-	-	-	-	-	-	-	-	S	-	-	-	-	
MEF-1	-	-	-	-	-	K	-	-	-	K	-	-	-	-	-	-	-	-	-	-	-	-	-	-	-	-	-	-	-	N	-	-	-	-	

Table 3.3. Amino acid difference between the serotype 2 poliovirus strains at antigenic sites 1, 2a, 2b, 3a and 3b.

Following extraction, the region of the RNA genome encoding the viral capsid of the strains was sequenced using a variety of primers. The sequenced capsid region was analysed using the Clustal W alignment program. - indicates that there was no change in sequence in comparison to Sabin 2 sequence. Serotype 2 PV strains are abbreviated as follows: MAD., MAD029; 04-44., 04-44140261.

As shown in table 3.3, the expected difference of only one substitution was found between the amino acid sequences of Sabin 2 and MAD029. While the cVDPV MAD029 strain only showed a single substitution (VP2 A₂₁₈-T) the iVDPV strains (in particular strains 102050 and 071108) showed the largest range of substitutions (table 3.3). The wild-type strains showed a range of substitutions across the antigenic sites, with some common amongst the strains (VP1 R₂₅₂-K) and others common with iVDPV strains (VP1 R₁₀₃-K).

3.2.2 Inactivation of serotype 2 poliovirus strains

3.2.2.1 Effect of inactivation on viral antigenicity

The effect of inactivation on the antigenic structure of the selected serotype 2 strains was assessed by a panel of site-specific MAbs after the strains had been inactivated with HCHO. Viral solutions containing 1×10^9 TCID₅₀ / 100 μ l of each of the purified virus strains were inactivated by incubation with HCHO, as detailed in Materials and Methods (section 2.2.2.1). The destruction of viral infectivity during the inactivation process was monitored by infecting HEp-2C cell cultures at days +6 and +12 of inactivation in three successive passages for three weeks. No infectivity was detected in any of the strains at days +6 or +12.

To determine the effect of inactivation on viral antigenicity, the antigenic structure of live and HCHO-inactivated serotype 2 PV strains was characterised by ELISA (Materials and Methods, section 2.2.3.3). This assay determined whether live and inactivated serotype 2 strains were able to bind to antigenic site-specific MAbs (389). The antigenic structure of live serotype 2 PV strains is shown in figure 3.3.

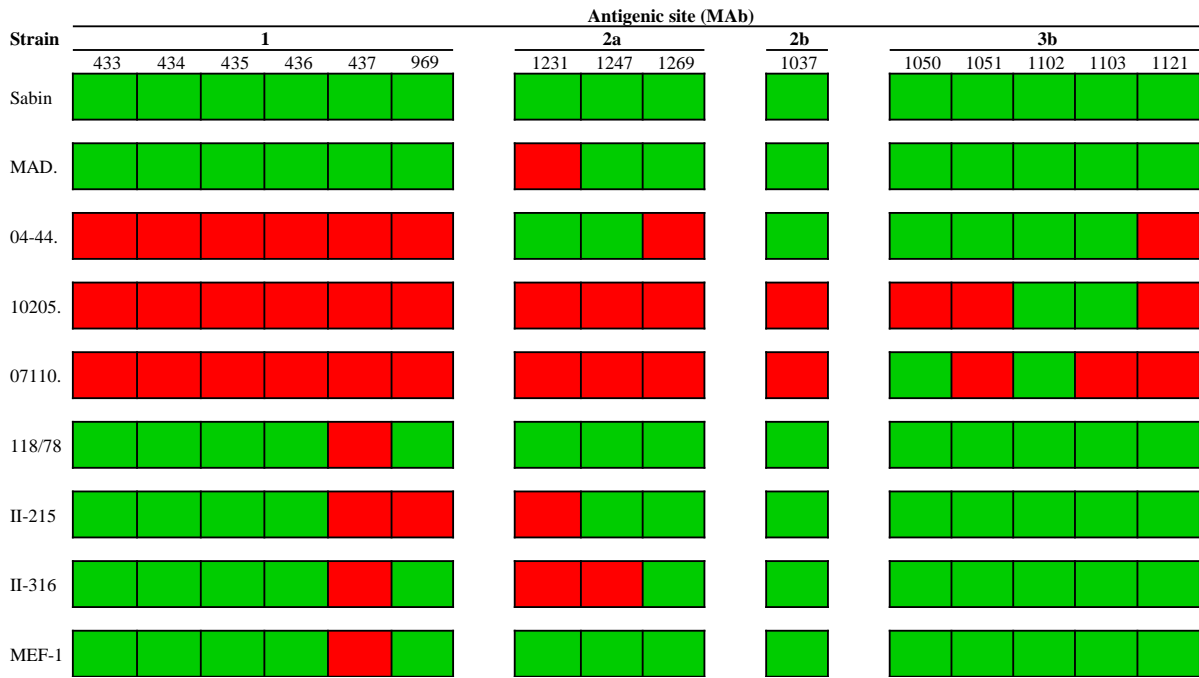


Figure 3.3. Antigenic structure of live serotype 2 poliovirus strains.

Antigenic structure of live serotype 2 PV strains was characterised by ELISA. Optical density readings were used to assess the binding of MAbs to live serotype 2 strains over four dilutions of virus. Average OD readings from two ELISAs are shown. Green, MAb reacts with live serotype 2 strain (≥ 0.4 OD above background); red, MAb does not react with live serotype 2 strain. Serotype 2 PV strains are abbreviated as follows: Sabin, Sabin 2; MAD., MAD029; 04-44., 04-44140261; 10205., 102050; 07110., 071108.

The previously determined variations in the amino acid sequence within the antigenic sites (table 3.3) largely correlated with the antigenic structure of live serotype 2 strains. The single substitution VP1 A₂₁₈-T of the MAD029 strain accounted for the lack of reaction between this strain and the site 2a-specific MAb 1231. Sabin 2 strains with point mutations at VP1_{97, 98, or 99} have been noted to have resistance to reacting with site 1-specific MAbs 433, 434, 435 and 969 (389). As the 04-44140261, 102050 and 071108 strains all possess the substitution VP1 K₉₉-R, N, it is possible that this could account for the lack of reactivity between these strains and the previously noted site 1-specific MAbs. The strain II-215 possesses the substitution VP1 T₉₈-A which could account for its lack of reaction with the site 1-specific MAb 969. Previous research with Sabin 2 point mutants has found that resistance to reacting with the antigenic site 1-specific MAb 436 might be due to the substitution VP1 K₁₇₄-E (389). A comparison of the sequenced antigenic sites and the mapped antigenic structure found that the strain 071108 has a similar substitution (VP1 A₁₇₅-S) and did not

react with MAb 436. However, the strains 04-44140261 and 102050 also failed to react with MAb 436, but they do not have an amino acid substitution at VP1₁₇₄, indicating that another substitution might confer resistance to this MAb. The effect of an amino acid substitution at VP1₁₀₁ on the antigenic structure has not been determined. Both the 04-44140261 and 102050 strains have the substitution VP1 A₁₀₁-T which could confer the resistance to MAb 436. With the exception of Sabin 2 and MAD029, all of the serotype 2 strains failed to interact with MAb 437. These serotype 2 strains share an amino acid substitution, VP1 R₁₀₃-K, which may confer resistance to this MAb.

The strains II-215 and II-316 did not react with the antigenic site 2a-specific MAbs 1231 and 1247. This might have been due to the amino acid substitutions VP1 A₂₂₁-T and VP1 T₂₂₃-S of II-215 and II-316, respectively. The iVDPV strains 04-44140261, 102050 and 071108 did not react with MAbs 1269 and 1121 which specifically bind to antigenic sites 2a and 3b, respectively. While the strains 102050 and 071108 showed a number of substitutions in the amino acid sequence which could account for the absence of reaction with these MAbs (table 3.3), the 04-44140261 strain lacked any such substitution within the amino acid sequence coding for these sites. The reason for this inconsistency is not clear.

Both the 04-44140261 and II-316 strains had substitutions within the region of the amino acid sequence coding for antigenic site 2b (VP2 N₁₆₈-S). However, both strains reacted with MAb 1037 which specifically binds to this antigenic site. This was also apparent with the strains II-316 and MEF-1 strains which reacted with the 3b-specific MAbs, despite possessing substitutions in the region of the amino acid sequence which encodes this antigenic site (VP3 T₅₈-S and VP3 S₅₉-N, respectively). It is possible that these substitutions were neutral and had no effect on this specific antigenic site. Although the VDPV strains did interact with some MAbs, these interactions were judged to be weaker than those of Sabin 2 and wild-type strains as the OD readings were lower.

Following inactivation with HCHO, almost all of the serotype 2 strains showed modifications to their antigenic structure. As figure 3.4 shows, the site 1-specific MAbs 436, 437 and 969 were unable to bind to the inactivated serotype 2 strains.



Figure 3.4. Antigenic structure of formaldehyde-inactivated serotype 2 poliovirus

strains. Serotype 2 PV strains were concentrated to 1×10^9 TCID₅₀/ 100 µl and inactivated with 1:4000 HCHO for 12 days at 37 °C. Antigenic structure of HCHO-inactivated serotype 2 strains was characterised by ELISA. The OD readings were used to assess the binding of MAbs to HCHO-inactivated serotype 2 strains over four dilutions of virus. Average OD readings from two ELISAs are shown. Green indicates that the MAb reacts with HCHO-inactivated serotype 2 strain (≥ 0.4 OD above background); red indicates that the MAb does not react with HCHO-inactivated serotype 2 strain. Serotype 2 PV strains are abbreviated as follows: Sabin, Sabin 2; MAD., MAD029; 04-44., 04-44140261; 10205., 102050; 07110., 071108.

This suggests that inactivation modified at least some of the epitopes of antigenic site 1 to the point that they were no longer recognised by these MAbs. This result confirmed previous observations (160). For some serotype 2 strains inactivation modified other antigenic sites in addition to site 1. The site 2a-specific MAb 1247 was unable to bind to inactivated MAD029, while the inactivated II-215 preparation was unable to interact with the site 3b-specific MAb 1051. Interestingly, MAb 1269 was able to bind to inactivated 04-44140261 despite being unable to bind to the live preparation of this strain. The modification to the antigenic structure

of this strain following inactivation appeared to allow this MAb to bind. Due to the weak or lack of reactivity between MAb 437 and live or inactivated serotype 2 PV, this MAb was not used beyond Chapter 3.

To determine the D-Ag content of inactivated serotype 2 PV strains and to assess whether inactivation with HCHO had caused a loss of antigenicity, a series of ELISAs were carried out (Materials and Methods, section 2.2.3.1). The D-Ag / ml of the serotype 2 strains was determined using an international reference standard (176) and a number of site-specific MAbs, as shown in table 3.4.

Sample	Live / Inactivated	MAb (antigenic site specificity)				
		433 (1)	1247 (2a)	1037 (2b)	1050 (3b)	1102 (3b)
Sabin 2	Live	45 ± 2.1	52 ± 1.3	52 ± 2.9	59 ± 1.7	64 ± 1.6
	Inactivated	43 ± 1.7	53 ± 4.7	60 ± 0.8	65 ± 0.1	60 ± 4.4
MAD029	Live	25 ± 1.8	5 ± 0.0	38 ± 1.2	40 ± 1.0	45 ± 0.4
	Inactivated	25 ± 2.1	1 ± 0.7	32 ± 0.0	34 ± 0.0	27 ± 0.0
04-44140261	Live	0 ± 0.0	40 ± 0.2	42 ± 7.9	31 ± 4.5	35 ± 5.6
	Inactivated	0 ± 0.0	29 ± 0.3	43 ± 0.0	31 ± 0.8	30 ± 0.0
102050	Live	0 ± 0.0	0 ± 0.0	0 ± 0.0	0 ± 0.0	66 ± 7.3
	Inactivated	0 ± 0.0	0 ± 0.0	0 ± 0.0	0 ± 0.0	22 ± 0.0
071108	Live	0 ± 0.0	0 ± 0.0	0 ± 0.0	1 ± 0.6	1 ± 0.6
	Inactivated	0 ± 0.0	0 ± 0.0	0 ± 0.0	3 ± 1.0	3 ± 0.2
118/78	Live	16 ± 0.0	20 ± 0.5	20 ± 0.3	22 ± 0.4	22 ± 0.9
	Inactivated	14 ± 1.0	17 ± 0.5	17 ± 0.0	22 ± 0.0	15 ± 0.0
II-215	Live	15 ± 0.9	22 ± 0.0	20 ± 1.9	18 ± 0.8	25 ± 2.0
	Inactivated	16 ± 5.8	12 ± 4.0	25 ± 0.0	20 ± 2.2	26 ± 0.0
II-316	Live	29 ± 3.6	0 ± 0.0	48 ± 2.9	40 ± 0.1	39 ± 2.2
	Inactivated	26 ± 1.8	1 ± 0.5	41 ± 0.0	34 ± 0.0	34 ± 0.0
MEF-1	Live	47 ± 12.1	53 ± 13.8	51 ± 3.4	53 ± 3.4	58 ± 1.9
	Inactivated	40 ± 7.8	38 ± 0.3	45 ± 0.0	47 ± 1.2	45 ± 0.0

Table 3.4. The D-Antigen content of live and inactivated poliovirus.

Serotype 2 PV strains were concentrated to 1×10^9 TCID₅₀/ 100 µl and inactivated with 1:4000 HCHO for 12 days at 37 °C. D-Antigen / ml was determined by an ELISA. The potency of the live and inactivated serotype 2

strains was calculated relative to a concurrently tested standard. The average of two ELISAs is shown with the standard error.

Measurement of all strains by ELISA with site 1 (MAb 433), 2a (MAb 1247), 2b (MAb 1037), and 3b (MAbs 1050 and 1102)-specific detection MAbs showed that there was little reduction in antigenic content following inactivation, indicating that inactivation did not result in a significant loss of these antigenic epitopes. D-Antigen / ml estimates of inactivated PVs obtained with the site 1-specific MAb 433 were slightly inconsistent with those obtained with the other MAbs. This may have been due to the modifications to antigenic site 1 following inactivation. Comparable D-Ag / ml estimates were found using site 2a, 2b and 3b-specific MAbs, indicating that the antigenic site did not influence the D-Ag / ml estimate obtained.

The D-Ag / ml of the strain 102050 could only be determined by the MAb 1102 due to the large number of mutations throughout its antigenic sites. In comparison to the other strains, the inactivated preparation of the strain 071108 showed a lower D-Ag content, despite the fact that the same amount of infectious virus was inactivated (Materials and Methods, section 2.2.2.1). This is likely to be due to the poor reactivity between this VDPV strain and the MAbs. Due to this low D-Ag content, the strain 071108 was not studied any further.

The potency of an IPV is expressed in D-Ag units as these are considered the protective immunogens as they induce neutralising antibodies following immunisation (289). The total number of infectious particles is represented by the infectious titre (TCID₅₀) of a PV strain. The ratio of infectious titre and D-Ag amongst viral strains gives an estimate of the proportion of infectious particles amongst total virions. This ratio was determined for the serotype 2 PV strains (table 3.5).

Strain	Log ₁₀ TCID ₅₀ / D-Ag / ml (antigenic site specificity of MAb)					
	MAb 433 (1)	MAb 434 (1)	MAb 1231 (2a)	MAb 1269 (2a)	MAb 1050 (3b)	MAb 1102 (3b)
Sabin 2	7.5	7.2	7.3	7.1	7.2	7.2
MAD029	7.7	7.5	-	7.3	7.4	7.3
04-44.	-	-	7.4	-	7.5	7.5
102050	-	-	-	-	-	7.2
118/78	7.7	7.6	7.7	7.6	7.7	7.7
II-215	7.8	7.5	7.7	7.8	7.7	7.6
II-316	7.5	7.3	-	7.4	7.4	7.4
MEF-1	7.1	7.1	7.4	7.3	7.4	7.3

Table 3.5. Infectious titre / D-Antigen ratio of serotype 2 poliovirus strains.

Infectious titre (TCID₅₀) and D-Ag/ml of the serotype 2 PV strains was determined and the TCID₅₀ / D-Ag ratio was calculated. The infectious titre was determined by incubating susceptible HEp-2C cells with ten-fold dilutions of each strain. After five days incubation at 35 °C, the cells were stained. The D-Ag /ml was determined by ELISA with a series of MAbs. - indicates that there was no interaction between the MAb and the serotype 2 strain during ELISA. 04-44140261 is abbreviated as 04-44.

As shown in table 3.5, the serotype 2 strains showed a similar infectious titre / D-Ag ratio. The use of different MAbs in the ELISA did not affect this ratio.

3.2.2.2 Effect of inactivation on viral immunogenicity

The viral immunogenicity of the HCHO-inactivated serotype 2 PV strains was assessed by a rat potency test in which equal sized groups of Wistar rats were immunised with set

doses (8 and 2 D-Ag/ml) of each of the inactivated serotype 2 strains. After 22 days, the rats were exsanguinated and their blood serum harvested. The sera were challenged with three serotype 2 PV strains, Sabin 2, MEF-1 and 04-44140261, in a cell culture neutralisation assay (Materials and Methods, section 2.2.4.1). These strains were selected as they were not closely genetically related (table 3.2 and figure 3.1) and their antigenic structure differed (figure 3.3) which enabled the specificity of the immune response to be assessed. As figure 3.5 shows, the log₂ neutralisation titre of the sera from rats immunised with different inactivated serotype 2 PVs varied between the strains and across the doses.

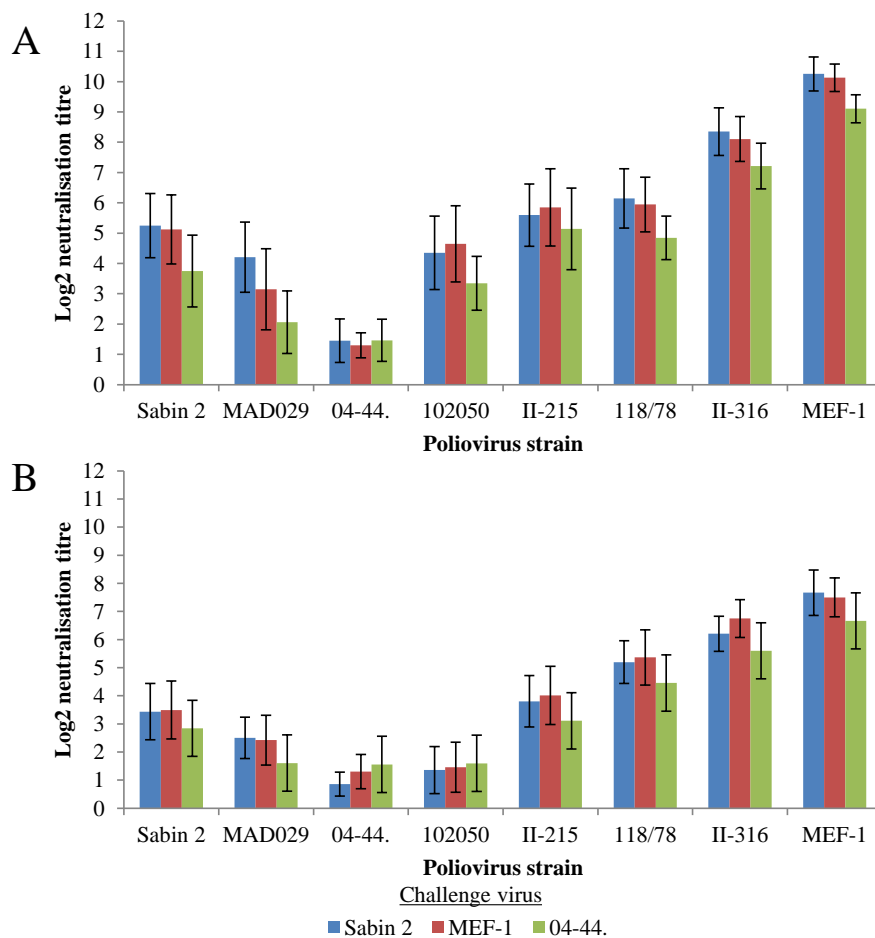


Figure 3.5. Immunogenicity of inactivated serotype 2 polioviruses against challenge virus strains.

Rats were immunised with 8 (A) and 2 (B) D-Ag/ml doses of the HCHO-inactivated serotype 2 PV preparations. After 22 days rats were exsanguinated and the sera were assayed to measure neutralising antibody to 100 TCID₅₀ of the relevant challenge virus using a fixed virus varying serum 50% end-point technique in a microtitre system. Sera were challenged with Sabin 2, MEF-1 and 04-44140261 strains. The average of two sets of rats per dose is shown with error bars. 04-44140261 is abbreviated as 04-44.

Analysis by balanced ANOVA (Minitab v.16, <http://www.minitab.com/en-GB/>) found that this variation was significant between the strains ($P < 0.001$) across both doses ($P < 0.001$) for all three challenges ($P < 0.005$). The sera of rats immunised with the Sabin 2 strain and the related VDPV strains showed low log₂ neutralisation titres against all three challenges (figure 3.5). The sera from rats immunised with the iVDPV strains showed the lowest log₂ neutralisation titres, while sera from rats immunised with the wild-type strains showed high log₂ neutralisation titres against all three challenge viruses, with an increasing neutralisation titre with II-215, 118/78, II-316 and MEF-1. This was confirmed by multiple comparison using the Tukey method (Minitab v.16, <http://www.minitab.com/en-GB/>). This analysis found that the mean immune responses of rats immunised with Sabin 2 and related VDPV strains were significantly different from those immunised with MEF-1 and other wild-type strains ($P < 0.05$).

Some degree of specificity in the rats' immune response to the challenge virus was noted (figure 3.5) and was examined further by determining the log₂ neutralisation titre of sera from rats immunised with HCHO-inactivated Sabin 2 and MEF-1 preparations against challenge viruses of different antigenic structures. The specificity of the immune response was determined across two doses of inactivated Sabin 2 and MEF-1 preparations, as shown in figure 3.6.

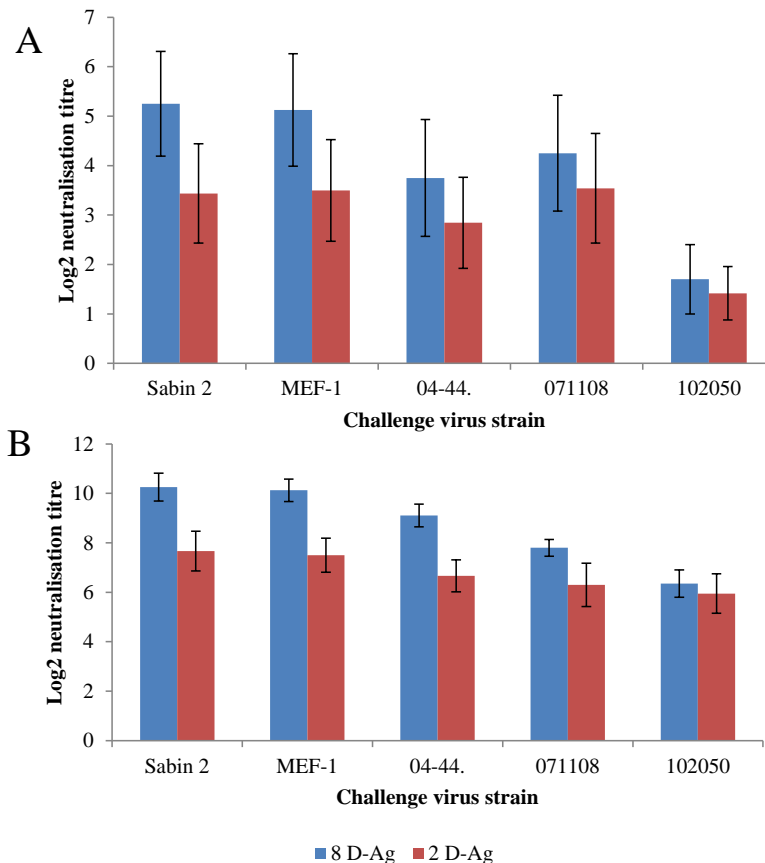


Figure 3.6. Specificity of immune response of rats immunised with inactivated poliovirus.

Rats were immunised with 8 and 2 D-Ag/ml doses of HCHO-inactivated Sabin 2 (A) and MEF-1 (B) preparations. After 22 days rats were exsanguinated and the sera were assayed to measure neutralising antibody to 100 TCID₅₀ of the relevant challenge virus using a fixed virus varying serum 50% end-point technique in a microtitre system. Sera were challenged with Sabin 2, MEF-1, 04-44140261, 071108 and 102050 strains. The average of two sets of rats per dose is shown with error bars. 04-44140261 is abbreviated as 04-44.

Similar log₂ neutralisation titres were found when rat sera were challenged with Sabin 2 and MEF-1. The iVDPV challenges (04-44140261, 071108, 102050) resulted in lower log₂

neutralisation titres, compared to those of sera from rats challenged with the Sabin 2 and MEF-1 strains. Analysis by balanced ANOVA (Minitab v.16, <http://www.minitab.com/en-GB/>) found that this variation in immune response to the different challenge virus strains was significant for rats immunised with HCHO-inactivated Sabin 2 ($P<0.005$) or MEF-1 ($P<0.001$). The Tukey method (Minitab v.16, <http://www.minitab.com/en-GB/>) found a significant difference between the immune responses to the iVDPV challenges to the responses to Sabin 2 and MEF-1 challenges ($P<0.05$). This difference was particularly apparent when the sera were challenged with the iVDPV strain 102050, which showed extensive antigenic changes (figure 3.3). The scale of this fall in log₂ neutralisation titre differed between VDPV challenge strains and between the strains of the HCHO-inactivated PV preparations.

The effect of inactivation on viral immunogenicity was further characterised by immunising Wistar rats with set doses of live and HCHO-inactivated Sabin 2 and MEF-1 preparations (varying from 0.125-32 D-Ag/ml). The resulting sera were harvested and challenged with three serotype 2 PV strains, Sabin 2, MEF-1 and 04-44140261 in a cell culture neutralisation assay. As figure 3.7 shows, the log₂ neutralisation titre of sera from rats immunised with live and inactivated Sabin 2/MEF-1 preparations differed between the nature (live or HCHO-inactivated) and strain (Sabin 2 or MEF-1) of the preparation.

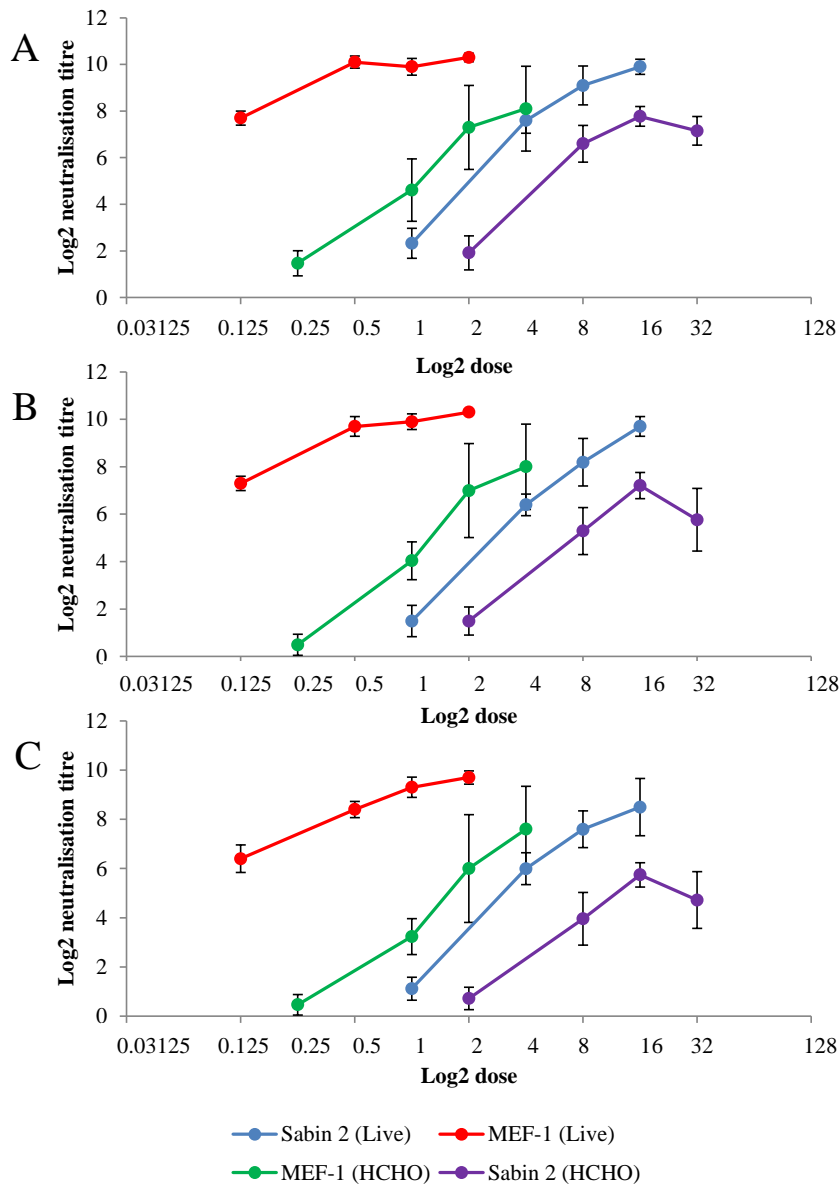


Figure 3.7. Immunogenicity of live and inactivated poliovirus strains against challenge viruses.

Rats were immunised with doses varying from 0.125-32 D-Ag/ml of each of the live and HCHO-inactivated Sabin 2 and MEF-1 preparations. After 22 days rats were exsanguinated and the sera were assayed to measure neutralising antibody to 100 TCID₅₀ of the relevant challenge virus, using a fixed virus varying serum 50% end-point technique in a microtitre system. The rat sera were challenged with Sabin 2 (A), MEF-1 (B) and 04-44140261 (C) strains. The average of two sets of rats/dose is shown with error bars.

The log₂ neutralisation titres of sera from rats immunised with HCHO-inactivated Sabin 2 / MEF-1 were lower than those obtained from rats immunised with live preparations of these strains (figure 3.7), indicating that inactivation resulted in a reduction in the

immunogenicity. Potencies calculated relative to a standard curve using a parallel line sigmoid curve model in EDQM Combistats (v.4, <http://combistats.edqm.eu/>) confirmed this. Potencies were calculated relative to that obtained with inactivated MEF-1 or Sabin 2. This analysis found that the potency of live MEF-1 was 21-24 times higher than that of inactivated MEF-1 with a confidence interval between 12 and 54 for the three challenge strains, while the potency of live Sabin 2 was 3-4 times greater than that of its inactivated counterpart with a confidence interval between 2 and 8. The scale of the reduction in immunogenicity following inactivation seemed to vary between the two PV strains.

As previously determined (figure 3.5), the immunogenicity of the PV preparations varied between strains. Inactivated MEF-1 showed a higher immunogenicity than inactivated Sabin 2. Calculated potencies confirmed this, finding that the potency of inactivated MEF-1 was 5-10 times greater than that of inactivated Sabin 2 with a confidence interval between 3 and 11. Interestingly the sera from rats immunised with live Sabin 2 also showed a lower log₂ neutralisation titre against all challenge strains than sera from rats immunised with MEF-1 indicating that HCHO inactivation was not responsible for the poor immunogenicity of the serotype 2 sIPV on its own. This was confirmed by calculated potencies which found that live MEF-1 generated potencies 41-52 times higher than that of live Sabin 2 with confidence intervals between 22 and 114 for the three challenge strains. The MEF-1 preparations were far more immunogenic than the Sabin 2 preparations.

3.3 DISCUSSION

The current drive to develop sIPV as a safer alternative to cIPV is hindered by the differences between the two, in particular the difference in the immunogenicity of sIPV2 and cIPV2. The molecular / biological reasons for the differences between sIPV and cIPV are not well understood. To understand these differences a range of serotype 2 strains, including VDPV and wild-type strains were characterised and inactivated alongside Sabin 2 and MEF-1 in this chapter. The effect of both inactivation and the genetic properties of each strain on the viral antigenicity and immunogenicity of inactivated PV preparations were determined. Nucleotide sequence analysis through the capsid coding region confirmed the expected differences between the selected PV strains (table 3.2 and figure 3.1). The iVDPV strains

showed a greater number of non-synonymous mutations in the sequenced capsid region with respect to the Sabin 2 strain than those shown by the other strains (table 3.2 and figure 3.2). Many of these changes were found within antigenic sites (table 3.3) and this in turn resulted in extensive changes to the antigenic structure of the strains (figure 3.3) when analysed by assessing reactivity with site-specific MAbs. Such changes to the antigenic epitopes of long term excreted iVDPVs have been seen previously (199, 256, 313).

Remarkably, the wild-type strains showed a lower proportion of non-synonymous mutations than the iVDPV strains (figure 3.2) despite being genetically distant from Sabin 2 (figure 3.1) as they were isolated in different parts of the world over a 36-year period. This may be due to differences in the evolution of wild-type and iVDPV strains. Circulation of wild-type strains is associated with permanent changes in the nt sequence of their genomes. These changes occur at a constant rate of $\sim 3 \times 10^{-2}$ substitutions per synonymous site per year and are characterised by the predominant accumulation of synonymous, mostly neutral mutations (183, 564). Evolution of wild-type strains is based on stochastic drift caused by bottlenecking events during person-to-person transmission of small sets of variants picked from intrinsically heterogeneous PV populations (7, 8, 564).

The evolution of OPV strains to VDPVs occurs in the gastrointestinal tract of the vaccinee and their contact (either single person or person-to-person transmission) and is driven by replication with the error prone RNA-dependent RNA polymerase and a selective pressure to improve the strain's fitness. This typically results in the reversion of attenuation point mutations and the appearance of non-synonymous mutations in the coding and non-coding regions of the genome. These adaptive mutations reduce the adverse effect of the fitness-decreasing mutations accumulated during the development of OPV strains (338). Previous research has suggested that mutations within antigenic site regions of OPV strains are also the result of the selective pressure to eliminate fitness-decreasing attenuation point mutations (564). This may account for the large number of mutations across the antigenic site regions of the iVDPV strains. It is not clear why wild-type strains do not accumulate as many non-synonymous mutations as iVDPV strains during replication in the host. It may be that, as wild-type strains are biologically fit and able to replicate and transmit from one individual to another, they do not have the drive to accumulate such mutations.

Interestingly, the cVDPV strain from Madagascar showed a lower proportion of non-synonymous mutations with respect to the Sabin 2 strain than those shown by the iVDPV strains (figure 3.2). This suggests that the Sabin 2 OPV strain accumulates non-synonymous changes more rapidly during evolution in a single patient than when it is transmitted from person-to-person. As described above OPV strains accumulate a number of fitness-increasing mutations during their evolution. The selection of these mutations is likely to be due to a combination of factors, including the ability to bind to the PVR, evasion of immune pressure and improvement of fitness to replicate in the gut. These factors might differ between immunocompetent and immunodeficient patients, leading to differences in mutation profiles of viruses.

The variation in the number of mutations and their location within the viral capsid (table 3.3) largely correlated to the different antigenic structure (figure 3.3) of the serotype 2 strains. Characterisation of the antigenic structure of live and inactivated PV found that following inactivation, all strains showed partial modification to antigenic site 1 (figure 3.4). This confirmed published findings which examined the antigenic structure of the MEF-1 and Sabin 2 strains (160, 426). To assess what effect this partial modification has on the immunogenicity of PV, a rat potency test was carried out. Analysis of the sera from rats immunised with live or inactivated PV strains found that inactivation resulted in a reduction in the immunogenicity of PV (figure 3.7). Given the scale of this reduction in immunogenicity, it is unlikely that partial modification of antigenic epitopes by crosslinks or other reactions alone account for this.

In addition to the inactivation process reducing the immunogenicity of inactivated PV preparation, the large disparity in immunogenicity of live and inactivated PV preparations could also be due to the live preparations replicating in the rat. Although PV in theory only replicates in humans and some subhuman primate species (as they possess cells which express the PVR) (355, 413), previous research using photosensitised PV has found some multiplication in non-primate species, including newborn and adult cotton rats (271-273). The pattern of infection in these rats resembled the one-cycle infection produced by PV RNA in that the newly formed virus had a low titre, which failed to increase after first 24 hours and there was a lack of clinical signs in the rats (211, 215, 216). From this research one could infer that PV maybe replicating on a small scale in the rats which could be increasing the yield and consequently the immune response elicited. As inactivated PV preparations cannot

replicate, their yield would not increase resulting in a lower immune response than the live preparations. This potential explanation for the disparity in immunogenicity between live and inactivated PV could be assessed by monitoring the rat immune response to PV non-structural viral proteins which are involved in PV multiplication. As a negative control to this analysis, rats could be infected with temperature sensitive PV strains.

A comparison of the sera from rats immunised with inactivated preparations of different serotype 2 strains found that Sabin 2 and related VDPV strains had low immunogenicity against challenge viruses. MEF-1 and other wild-type strains were more immunogenic against the challenge viruses. These results show that the effect of inactivation on the viral immunogenicity differs between strains. Strain-specific differences in the antigenic epitopes which trigger the immune response, may contribute to this.

There was some degree of specificity in the immune responses induced by all inactivated serotype 2 PV strains against the different challenge viruses. Inactivated PVs had a lower immunogenicity against the iVDPV strain 04-44140261 compared to challenges with the Sabin 2 and MEF-1 strains. The scale of this fall in immunogenicity differed between the inactivated serotype 2 strains. Whether these differences would lead to differences in protection against disease will be investigated using an immunisation-challenge model in Tg mice that express the human PVR (Chapter 5).

A comparison of the immunogenicity of live preparations of the Sabin 2 and MEF-1 strains found that the wild-type strain to be significantly more immunogenic (figure 3.7). This suggests that inactivation was not the only factor responsible for the disparity in immunogenicity between the serotype 2 sIPV and cIPV. Analysis of the sequenced viral capsid proteins of Sabin 2 and MEF-1 found a total of 26 amino acid differences between the two strains. Of these, only three were within the known antigenic sites: VP1 R, K₁₀₃; R, K₂₅₂; and VP3 S, N₅₉. Moreover, as both showed similar antigenic structures (figures 3.3 and 3.4), it is not clear why they differ in immunogenicity both as live and inactivated preparations. It may be that the manner in which the antigen of each strain is processed by the immune system differs resulting in a different response, but further work will be required to explore this.

CHAPTER 4

INACTIVATION OF POLIOVIRUS WITH ALTERNATIVE INACTIVATION CHEMICALS

4.1 INTRODUCTION

The previous chapter described how inactivation of PV with HCHO resulted in a significant loss of immunogenicity, possibly due to modification of the antigenic sites. The main objective of inactivation is to irreversibly eliminate the infectivity of the original live virus-containing material to an extent that ensures the safety of the vaccine and, at the same time, retains maximum immunogenicity of the virion (68). Since the development of the IPV by Salk *et al.* in the 1950s (451), HCHO has been used to inactivate PV. Preparation of IPV has been fine-tuned with the introduction of a filtration step and the development of improved high-density cell culture systems (142, 349, 350). However, inactivation with HCHO has been found to result in a loss of immunogenicity of PV.

One approach to avoid this loss of immunogenicity following inactivation is to use alternative inactivation agents which selectively inactivate the viral genome. Two such inactivation chemicals have been identified: BPL and BEI. Beta-propiolactone is a four membered ring (figure 4.1A) which can undergo ring opening at the alkyl and acyl bonds, making it a highly reactive alkylating agent (400). Due to its highly electrophilic alkylating moiety, BPL readily reacts with many nucleophilic agents (including proteins and nucleic acids). Beta-propiolactone interacts in a pH-dependent manner with SH and SS groups and the amino acids methionine, cysteine and cysteine (63). In addition, BPL alkylates the N7 and N1 atoms of guanine bases and the N3 atom of adenine bases (57, 97, 432, 458, 459). These interactions can result in modified guanine being misread as adenine by polymerases, leading to transition mutations (400). When a high concentration of BPL is present, alkylation of purine bases can cause depurination following the break of the glycoside bond between the base and the deoxyribose/ribose moieties without disrupting the structural integrity of the phosphodiester backbone (297, 464). Neighbouring alkylated guanine bases are able to crosslink each other and protein to form complexes (400). While BPL does interact with viral capsid proteins (56), the preferential carboxyethylation of guanine and adenine (leading to extensive mispairing) is the basis of BPL inactivation (53, 57, 182). Beta-propiolactone has been extensively used to inactivate viruses for both human and veterinary vaccine production. Beta-propiolactone-inactivated whole influenza and rabies human vaccines have been developed and safely administered (69, 171, 244). Experimental inactivated vaccine candidates for severe acute respiratory syndrome, human immunodeficiency virus and infectious bovine rhinotracheitis are being developed using BPL (77, 245, 417, 431).

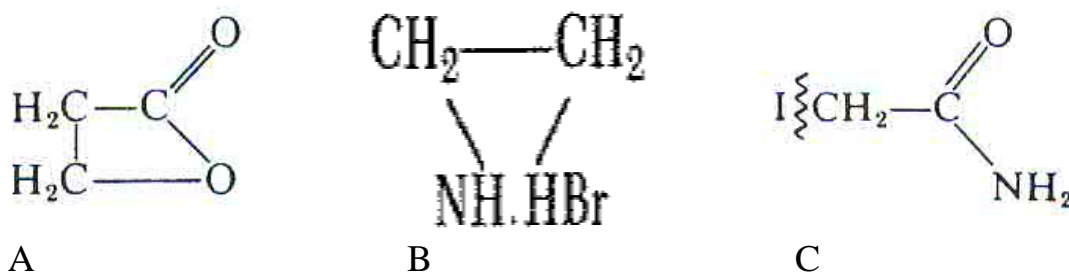


Figure 4.1. Chemical structure of beta-propiolactone (A), binary ethyleneimine (B), and iodoacetamide (C).

Both BPL and BEI have a ring structure. Adapted from (131, 169).

Binary ethyleneimine is an aziridine produced by cyclisation of haloethylamines under alkaline conditions (417). Binary ethyleneimine was developed as a safer and more stable alternative to N-acetyleneimine (AEI) for inactivating Foot-and-Mouth-Disease (FMD) virus (23). Aziridines possess a ring structure (figure 4.1B) which, similar to BPL, undergo ring opening reactions with nucleophiles, in particular adenine and guanine (56). Binary ethyleneimine alkylates nucleophilic positions N7, N3 and N1 in purine bases, and to a lesser extent N3 in pyrimidine bases (205, 206, 525). It is not clear whether BEI impairs the antigenicity and biological activity of viral capsid proteins. Some research has found that aziridines react with α and ϵ amino, imidazole, carboxyl, sulphhydryl and phenolic groups of proteins (124, 186), while other studies show that aziridines do not alter the viral capsid proteins (60, 61, 132, 190, 512). Binary ethyleneimine has been used to generate commercial vaccines, in particular for livestock. Due to concerns about the risk of live virus contamination with HCHO, the aziridine AEI was used to generate FMD vaccines. As a less carcinogenic and more stable aziridine, BEI has now become the inactivation reagent of choice to generate inactivated FMD vaccine (440). In addition, BEI has been used to generate bluetongue vaccines (40).

Previous research (73, 239, 512) has highlighted the possibility of using BPL or BEI to inactivate PV. This research found that inactivation with either chemical resulted in a greater retention of viral antigenicity than that achieved with HCHO inactivation. Such greater retention of antigenicity may result in inactivated PV preparations with improved immunogenicity. An alternative means of reducing the loss of immunogenicity following

inactivation is to reduce the concentration of HCHO used. This approach was adopted alongside the inactivation of PV with BPL and BEI.

Iodoacetamide is a novel inactivation chemical (figure 4.1C), which covalently modifies cysteine residues (to form s-carboxymethylcysteine), so that disulphide bonds can no longer form. It has recently been used to successfully inactivate toxins (botulinum) as a non-cross-linking chemical (203, 242). As IAN represented a novel non-cross-linking chemical which may result in less modification of the antigenic sites and potentially a lower loss of immunogenicity, it was selected to inactivate PV in addition to BPL, BEI and HCHO.

As detailed in the previous chapter the potency of inactivated PV preparations and IPV is expressed in D-Ag units (31). Currently, the D-Ag content is determined by ELISA using an international reference standard (176). The ELISA is variable, in particular with the use of specific reagents and antibodies; which leads to inconsistency when results are compared both within and between laboratories (22, 541). A recent collaborative study, organised by the NIBSC and involving many national control laboratories and manufacturers, underlined this problem. The study found that measuring the D-Ag of sIPV preparations by ELISA was problematic with high variation between laboratories and reagents (310). An alternative approach to the current ELISA is the biosensor-based analytical system.

The biosensor-based analytical system is based on the SPR technique. This an optical method which measures the refractive index of very thin layers of material adsorbed on a metal (such as gold). The Kretschmann configuration is the most common geometrical setup of SPR (figure 4.2).

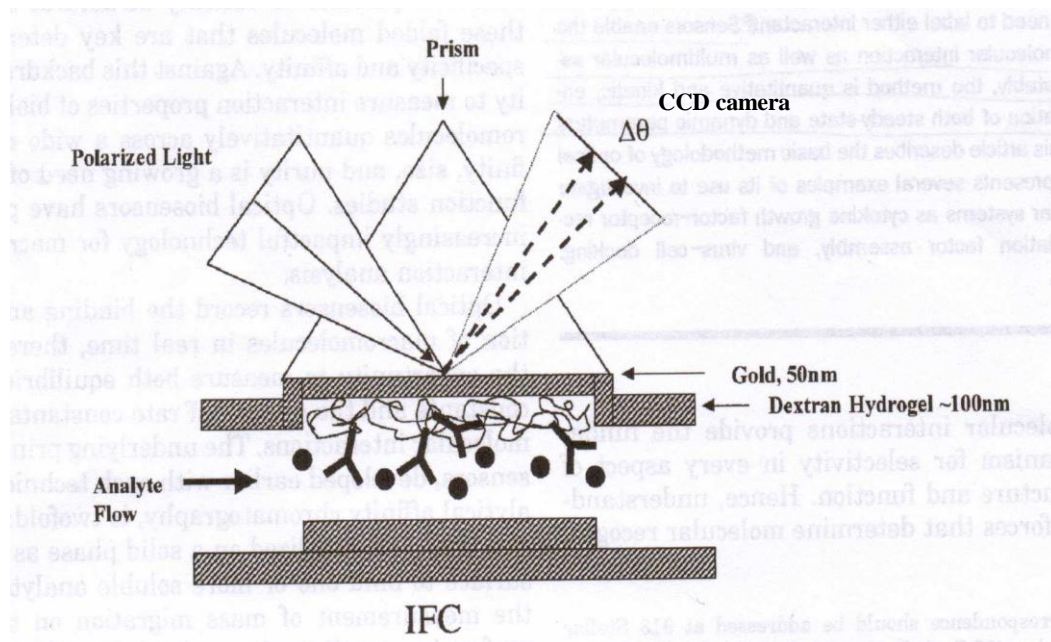


Figure 4.2. Schematic of the Kretschmann configuration of surface plasmon resonance.

Light is shone onto the gold film forming an evanescent wave. At a certain angle of incident light, this evanescent wave field excites electrons triggering the formation of surface plasmons on the adsorbate side of the metallic film (237). As surface plasmons form, photons of light disappear, resulting in a dip in reflected light at that angle (SPR angle) (391). For the pictured Biacore biosensor the principle determinant of this angle is the refractive index of the adsorbate located on the backside of the gold film. Binding to this region leads to a shift in the local refractive index which leads to a change in the SPR angle. A charged couple device chip measures this angle. Charged couple device is abbreviated as CCD (76).

The incoming light is positioned on opposite side of the metallic film than the adsorbate (391). When light is shone onto the metallic film it leaks an electromagnetic component, the evanescent wave, across the film. At a certain angle of incident light, this evanescent wave field excites electrons triggering the formation of surface plasmons (electron charge density waves) on the adsorbate side of the metallic film (237). As surface plasmons form, photons of light disappear, resulting in a dip in reflected light at that angle (SPR angle) (391). A charged couple device chip measures the angle.

For the Biacore biosensor instrument described in this chapter, the principle determinant of this angle is the refractive index of the adsorbate. This angle is located close to the backside of the metal film, to which ligands are immobilised and addressed by analytes injected alongside the flow cell. Binding leads to a shift in the local refractive index which leads to a change in the SPR angle. This is monitored in real-time by the detection of changes in the intensity of the reflected light and is used to produce a sensorgram (391). Responses are measured in resonance units (RU), where one RU corresponds to 0.0001° shift in the SPR angle (237). The rate constants for the association and disassociation phases of the interaction can be determined by analysing the rate of change of the SPR signal. The affinity (equilibrium constant) can be determined by calculating the ratio of the association and disassociation phases. The stoichiometry of the interaction can be determined as the size of the change in the SPR signal is directly proportional to the mass being immobilised (391).

SPR-based biosensors are able to analyse biomolecular interactions, such as antibody-antigen and ligand-receptor. This property has several qualitative and quantitative applications. Qualitative applications include epitope mapping and orphan ligand fishing. Quantitative applications include determining the reaction kinetics and affinity constants for molecular interactions (391). The biosensor described in this chapter is the Biacore (GE Healthcare). The Biacore instrument consists of an optical detector system, exchangeable sensor chips, a processing unit and a personal computer for control and evaluation (518). The exchangeable sensor chips are glass slides with a gold film coated on one side which is coated with a nonderivatized or derivatized dextran matrix (518). One of the interacting molecules (ligand) is either covalently immobilised to the surface of the chip or captured (237). The other interacting molecule (analyte) is passed over the surface of the sensor chip via an integrated microfluidic system (360). The biomolecular interaction occurs across the surface of the chip and the optical detector system monitors changes in the SPR signal in real-time (237). The processing unit carries both the optical detector system and an integrated microfluidic cartridge in addition to an autosampler for dispensing samples automatically (518). Preliminary work by Kersten *et al.* (252) indicates that the biosensor approach could be used to determine the D-Ag content of IPV. This biosensor-based approach was explored further in this chapter.

This chapter describes the first study to explore in detail the use of alternative chemicals to inactivate PV. The efficacy of IAN to inactivate PV was determined. The data presented here identified the optimal concentration of BPL, BEI and HCHO needed to inactivate PV and determined the effect of each on the viral infectivity and antigenic content. A biosensor-based approach was used to determine the D-Ag/ml of inactivated PV preparations. These estimates were compared to those obtained by the conventional ELISA and the implications on the assessment of the potency of IPV were discussed.

4.2 RESULTS

4.2.1 Inactivation of poliovirus with Iodoacetamide

Iodoacetamide is a sulfhydryl reactive reagent which inactivates via a non-cross-linking mechanism. Previous research found that IAN can reduce or abolish the infectivity of a range of viruses, however PV was not among these (13). To assess the efficacy of IAN as an inactivation chemical for PV, a broad range of concentrations of IAN (2, 20, 100, 200, 400 mM) were selected to inactivate the MEF-1 PV strain (Materials and Methods, section 2.2.2.2). The infectivity of the inactivated MEF-1 preparations was assessed by determining the infectious titre (Materials and Methods, section 2.2.1.1), shown in figure 4.3, and by addition onto susceptible HEP-2C cells. Cultures which showed no CPE were passaged twice more for periods of up to three weeks to ensure that infectivity had been eliminated.

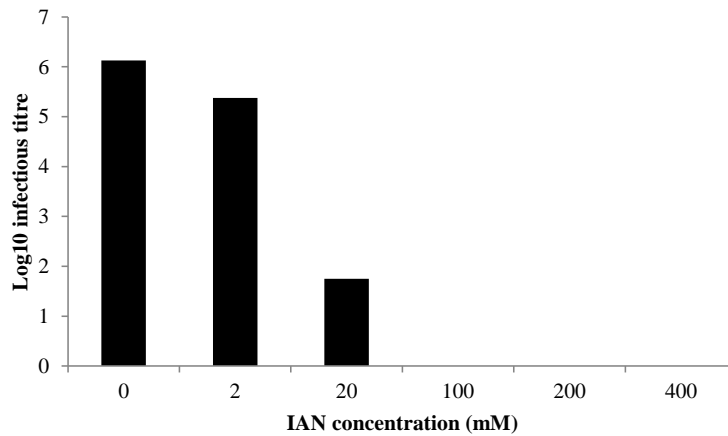


Figure 4.3. Inactivation of viral infectivity with iodoacetamide.

The MEF-1 strain was incubated with the relevant concentration of IAN for 24 h at 37 °C. Effect of inactivation on viral infectivity was determined by incubating susceptible cells with a range of ten-fold dilutions of each inactivated MEF-1 preparation. After five days, incubation cells were stained and the infectious titre was determined. One determination is shown as bars.

Both assays found that viral infectivity was eliminated following treatment with 100, 200 and 400 mM IAN. To establish the kinetics of inactivation with IAN the MEF-1 strain was inactivated with 100 mM IAN over a 24 h time-course, with aliquots (1 ml) taken at 1, 4, 8 and 24 h (Materials and Methods, section 2.2.2.2). The infectivity of the virus within these aliquots was assessed by titration and by adding onto HEp 2C cells, as described above. As figure 4.4 shows, viral infectivity was eliminated by 8 h.

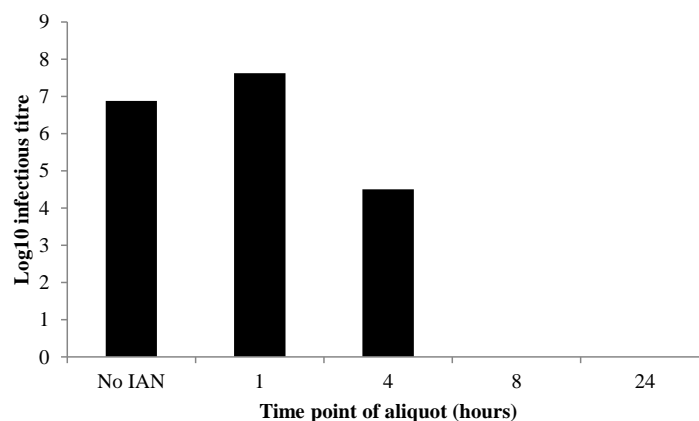


Figure 4.4. Loss of viral infectivity during inactivation with iodoacetamide.

The MEF-1 strain was incubated with 100 mM IAN for 24 h at 37 °C. At 1, 4, 8 and 24 h aliquots were taken. The infectious titre of the virus within each aliquot was determined by incubating susceptible cells with a range

of ten-fold dilutions of each aliquot. After five days, incubation cells were stained and the infectious titre was determined. One determination is shown as bars.

While the elimination of viral infectivity was confirmed, it was not clear whether inactivation with IAN modified the antigenic structure of PV. To assess this and to determine whether inactivation with IAN resulted in a loss of antigenicity, the D-Ag/ml of each aliquot from the 24 h time-course inactivation of MEF-1 was determined by ELISA. A range of site-specific MAbs were used to ensure that any modification to specific antigenic sites was detected. As figure 4.5 shows, following 4 h incubation with IAN, the D-Ag of the MEF-1 preparation was much reduced and by 8 h was no longer detectable by any of the MAbs.

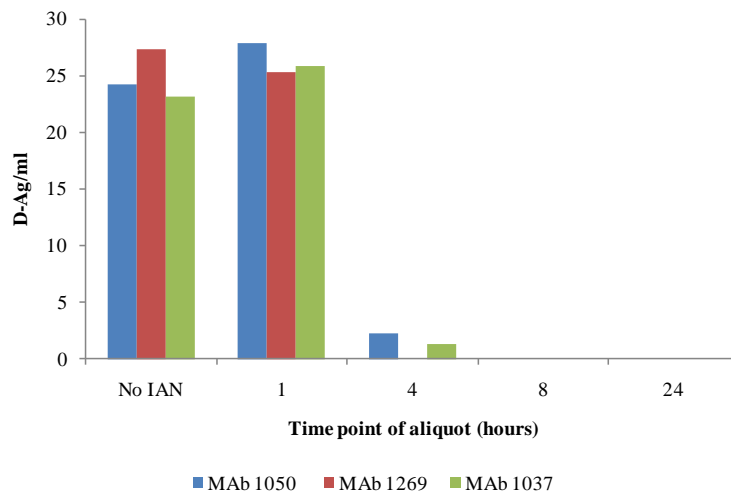


Figure 4.5. Effect of inactivation with iodoacetamide on viral antigenicity.

The MEF-1 strain was incubated with 100 mM IAN for 24 h at 37 °C. At 1, 4, 8 and 24 h aliquots were taken. The effect of inactivation on viral antigenicity was determined by ELISA to assay the D-Ag/ml of each virus aliquot. One determination is shown as bars.

The decline in D-Ag suggests that IAN may have modified or destroyed the antigenic epitopes on the surface of the virus. Unlike HCHO (Chapter 3, section 3.2.2.1), this decline was detected by a range of antigenic site-specific MAbs, indicating that this modification affected more than one antigenic site. The inactivation of MEF-1 with 100 mM IAN over 24 h was repeated at +4 °C to determine whether a lower temperature would slow down or reduce these modifications. However, the resulting inactivated MEF-1 preparations remained

infectious (full CPE within a day), indicating that IAN cannot inactivate PV within such a period of time at this low temperature.

It has been postulated that the regular surface subunits of PV are held together by disulfide bonds formed between cysteine residues. Each subunit has approximately five cysteine residues which may be involved with binding subunits together (12). Iodoacetamide is argued to covalently modify cysteine residues so that disulfide bonds cannot form. This reaction may prevent capsid subunits separating, a key step in the emergence of viral RNA during viral replication (12). This mechanism of action may have resulted in extensive modifications, causing a reduction in the physical stability of the virion and eventually its spontaneous destruction (68).

Another difficulty encountered when inactivating PV with IAN was the inability to neutralise the chemical. Unlike for HCHO, BPL and BEI, previous research did not identify a chemical which could neutralise IAN. Due to the cytotoxic nature of IAN, it was necessary to remove it before determining the infectivity of the IAN-inactivated MEF-1. A series of methods were used to remove the IAN, including dialysis and passage through a 30 % sucrose cushion. However, each method also resulted in a large loss of virus. Consequently, this loss of virus may have contributed to the reduction in D-Ag of the aliquots as inactivation progressed. It is possible that both this loss of virus and the modification / destruction of viral epitopes by IAN contributed to the loss of D-Ag as the time-course progressed. This loss of D-Ag meant that IAN was an unsuitable chemical for inactivation.

4.2.2 Optimisation of inactivation with beta-propiolactone, binary ethyleneimine and formaldehyde

An excessive duration of inactivation and / or concentration of the inactivation chemical can result in a fall in the stability and immunogenic properties of virions (68). Therefore, the optimal concentration of the chemical and the minimum and maximum duration of inactivation must be determined for each inactivating agent. Additional factors to be considered include the temperature and pH during the inactivation process. During the development of IPV, research was carried out to determine the optimal conditions for the inactivation of PV with HCHO (301, 450, 503). This led to the adoption of the current inactivation conditions: 1:4000 HCHO, 37 °C, neutral pH, for 12 days (409).

Little is known about the optimal inactivation conditions required to inactivate PV or similar viruses with BPL and BEI (1, 239). The research presented within this chapter represents the first optimisation of conditions for inactivation of PV with these chemicals (Materials and Methods, section 2.2.2.3). The duration of inactivation and a range of concentrations of each chemical were selected from previous experience at the NIBSC with influenza virus and / or an extensive literature search. While a neutral pH was maintained for all inactivations, the temperature was dependent on the chemical. Due to its instability at higher than ambient temperatures (288), BPL-based inactivations were carried out at +4 °C, instead of 37 °C as with BEI and HCHO.

To determine the optimal inactivation conditions which eliminated infectivity with the least impact on antigenicity, the effect of inactivation on the viral infectivity and antigenicity of the MEF-1 strain was determined for each concentration of the inactivation chemicals. An equivalent amount of MEF-1 (1×10^9 TCID₅₀/ ml) was inactivated with each chemical over a time-course with aliquots (1 ml) being taken at pre-determined points throughout. These points were determined for each chemical by the findings of previous studies (1, 239, 245). The MEF-1 strain was inactivated with BPL and BEI for 24 h. Aliquots were taken at 2, 4, 8, 18 and 24 h for both chemicals. During inactivation with BEI an additional aliquot was taken at 6 h. The WHO recommends that the inactivation period with HCHO should exceed the time required to reduce the titre of live virus to undetectable amounts by a factor of at least two (545). Therefore, MEF-1 was inactivated for 288h with aliquots being taken at 2, 12, 24, 36, 60 and 288 h.

All three inactivation chemicals are cytotoxic and can cause vaccine-cell mutations (21). In order to assess the infectivity of MEF-1 preparations inactivated with each chemical it is necessary to neutralise the chemicals. Beta-propiolactone was neutralised with sodium sulphite; BEI with sodium thiosulphite; and HCHO with sodium bisulfite (23, 239, 312). Two live MEF-1 time 0 h controls (0i and 0ii) were included for each inactivation. The 0i control was immediately stored at -20 °C following the initiation of the inactivation time-course. The 0ii control was incubated in the same conditions as the other samples during inactivation, but in the absence of the inactivating chemicals. Similar to the sample aliquots, the relevant neutralising chemical was applied to it. To assess whether the inactivation conditions alone had an effect on the infectious titre and D-Ag of MEF-1, the two controls were compared.

4.2.2.1 Effect of inactivation on viral infectivity of MEF-1

As described above (section 4.2.2), to determine the optimal concentration of each of the chemicals which would eliminate viral infectivity, inactivation time-courses were carried out. During each time-course, a series of aliquots were taken at pre-determined times (section 4.2.2). The point at which viral infectivity was eliminated by each concentration of the relevant chemical was determined by adding the virus aliquots onto HEP-2C cells. Cultures not showing CPE were passaged two further times for up to three weeks to ensure infectivity had been eliminated. With the exception of 0.4 mM BEI and 1:2000 BPL, viral infectivity was destroyed by the final time-point for all of the concentrations of BPL, BEI and HCHO. The loss of infectivity during the course of inactivation was assessed by determining the infectious titre at each time point. As figure 4.6 shows, with the exception of 0.4 mM BEI and 1:2000 BPL, all other concentrations of each of the chemicals eliminated viral infectivity by the final time-point.

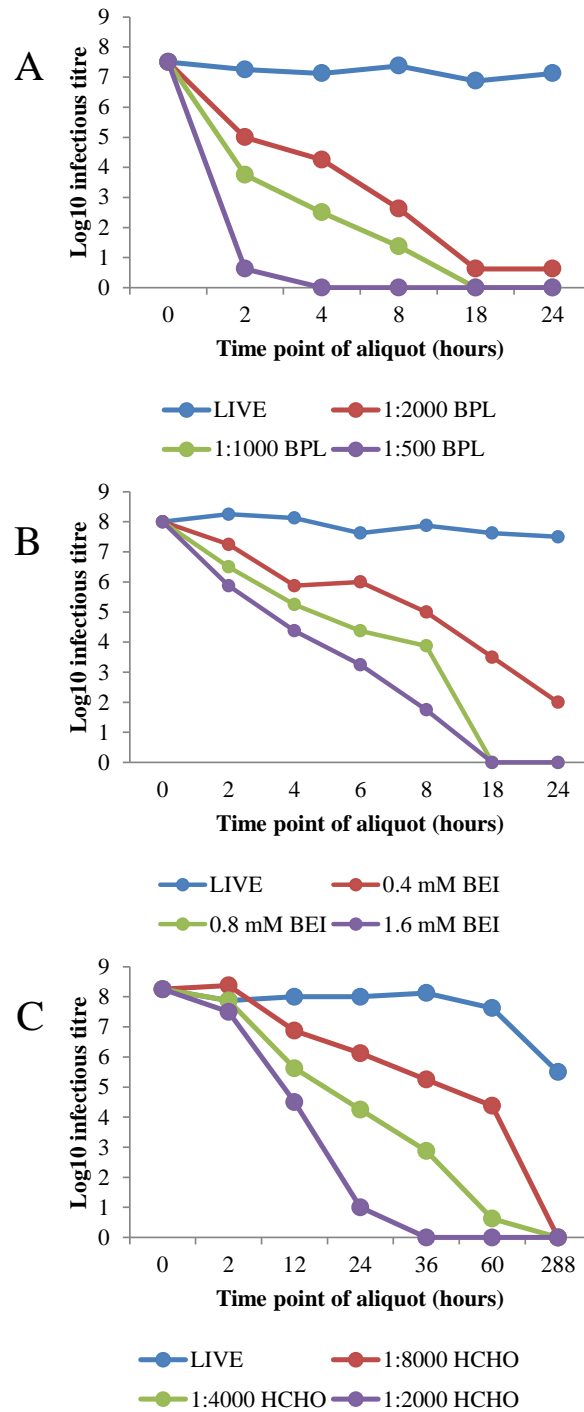


Figure 4.6. Effect of inactivation with beta-propiolactone, binary ethyleneimine, and formaldehyde on viral infectivity of MEF-1 strain.

The MEF-1 strain was incubated with the relevant concentration of BPL (A), BEI (B) or HCHO (C) for specific time-courses. Aliquots were taken at pre-determined times, denoted on the log scale X axis. The live Oii control is included at 0 h for the LIVE MEF-1 samples. Effect of inactivation on viral infectivity was determined by incubating susceptible cells with a range of ten-fold dilutions of each virus aliquot. Following five days incubation cells were stained and the infectious titre was determined. One determination is shown as a line graph.

As figure 4.6 shows, the rate of elimination of viral infectivity differed between the inactivation chemicals. Beta-propiolactone and BEI eliminated viral infectivity by 18 h, while HCHO required 288 h. As with the LIVE MEF-1 samples, the infectious titre of the live 0ii control remained consistent for the BPL and BEI inactivation time-courses (data not shown). This indicated that the inactivation conditions during these time-courses did not have a significant effect on the titre of the MEF-1 samples. However, the infectious titre of LIVE MEF-1 samples dropped by almost three logs during the HCHO inactivation. This fall in titre was found for the 0ii control but not the 0i control (data not shown), indicating that it was caused by the inactivation conditions. While the pH remained neutral (pH 6.5-7.0) throughout each inactivation with HCHO the prolonged incubation at 37 °C for 288 h may have caused this reduction as previous research has found that PV is thermolabile and can lose infectious titre when dissociated by heat-treatment (95, 325). The amount of MEF-1 used for inactivation by each chemical was determined against the infectious titre of the strain. Although an effort was made to ensure the same amount of MEF-1 was inactivated with each chemical, the actual amount inactivated may have varied slightly as inactivations were carried out separately and consequently repeated freeze-thawing of the live MEF-1 stock was required.

4.2.2.2 Effect of inactivation on viral antigenicity of MEF-1

It has been shown that inactivation with HCHO did not result in a significant reduction in antigenic content (Chapter 3, section 3.2.2.1). To confirm this and to assess whether the antigenic content was reduced following inactivation with BPL and BEI, the antigenicity of the virus aliquots from previously described inactivation time-courses (section 4.2.2) were determined by ELISAs using the detection MAb 1050. As tables 4.1A, B and C show, each inactivation chemical reduced the antigenic content of the MEF-1 preparation. The extent of this reduction varied between the chemicals.

Time-point of aliquot (h)	D-Ag / ml		
	1:500 BPL	1:1000 BPL	1:2000 BPL
0	18	18	18
2	10	12	11
4	10	9	9
8	9	9	7
18	9	9	6
24	10	12	7

Table 4.1A. Effect of inactivation with beta-propiolactone on viral antigenicity of MEF-1 strain.

Time-point of aliquot (h)	D-Ag / ml		
	0.4 mM BEI	0.8 mM BEI	1.6 mM BEI
0	25	25	25
2	15	16	22
4	17	15	19
6	14	20	12
8	16	18	19
18	19	24	19
24	19	20	20

Table 4.1B. Effect of inactivation with binary ethyleneimine on viral antigenicity of MEF-1 strain.

Time-point of aliquot (h)	D-Ag / ml		
	1:2000 HCHO	1:4000 HCHO	1:8000 HCHO
0	51	51	51
2	35	46	36
12	34	43	30
24	39	34	35
36	35	46	34
60	24	34	36
288	45	45	39

Table 4.1C. Effect of inactivation with formaldehyde on viral antigenicity of MEF-1 strain.

Table 4.1. Effect of inactivation with beta-propiolactone, binary ethyleneimine, and formaldehyde on viral antigenicity of MEF-1 strain.

The MEF-1 strain was incubated with the relevant concentration of BPL (A), BEI (B) or HCHO (C) for specific time-courses. Aliquots were taken at pre-determined times. Effect of inactivation on viral antigenicity was determined by ELISAs using the detection MAb 1050. One determination is shown.

As tables 4.1B and C show, inactivation with BEI or HCHO only resulted in a minor reduction of the antigenic content of the MEF-1 strain, confirming the finding in Chapter 3 that inactivation with HCHO did not result in a significant loss of antigenic content. However, as table 4.1A shows, inactivation with BPL appears to have resulted in a greater loss of the antigenic content of the MEF-1 strain than that shown following inactivation with BEI or HCHO. Inactivation with all three chemicals resulted in an initial drop in the antigenic content of MEF-1 within the first two hours. The scale of this drop seemed to vary randomly between the different concentrations of each chemical. The D-Ag remained the same for both live controls. While the titre of the live Oii control fell during inactivation with HCHO, the D-Ag remained the same throughout. The antigenic content did not differ significantly between the different concentrations of each chemical.

4.2.3 Inactivation of poliovirus with beta-propiolactone, binary ethyleneimine and formaldehyde

The data derived from the initial optimisation inactivation experiments described in section 4.2.2 were used to select the concentration of each chemical for further inactivations of MEF-1 and other PV strains (Materials and Methods, section 2.2.2.4). The concentration which gave the most efficient loss of infectivity with minimal loss of D-Ag / ml was selected. Therefore, 1:500 and 1.6 mM were selected for BPL and BEI inactivations, respectively. Two dilutions (1:4000 and 1:8000) were selected for HCHO inactivation to allow comparison to the 1:4000 HCHO inactivation currently used to generate cIPVs. In addition to the MEF-1 strain, the Sabin 2 strain and an iVDPV strain (04-44140261) were inactivated. These strains were selected because they differ in their antigenic structure and immunogenicity (Chapter 3). Inactivation time-courses were set up for each chemical and the three virus strains. Aliquots (2-5 ml) were taken during each time-course to assess the effect of each chemical on viral properties. The length of the time-courses and the choice of time-points at which aliquots were taken were chosen on the basis of the initial experiments (section 4.2.2). Strains were inactivated with BPL for 16 h with aliquots being taken at 2, 4, 8 and 16 h. Binary ethyleneimine was used to inactivate strains over a 24 h period, with aliquots being taken at 4, 8, 18 and 24 h. Strains were inactivated with two concentrations of HCHO for 288 h with aliquots being taken at 12, 36, 72, 120, 180 and 288 h.

An equivalent amount (5×10^9 TCID₅₀ / ml) of each PV strain was inactivated with the three chemicals. The amount of PV inactivated was greater than that previously used for the optimisation of each chemical to ensure the D-Ag of the resulting inactivated PV preparation was sufficiently large (between 100 – 200 D-Ag/ml) to be used for *in vivo* immunogenicity assays. The temperature and pH for inactivation with each chemical remained identical to that described previously for the initial experiments (section 4.2.2). The resulting inactivated PV preparations were used to determine the effect of inactivation with each chemical on the viral infectivity and antigenicity. As before, two live time 0 h controls (0i and 0ii) were included for each strain with each chemical. These controls were treated as described above (section 4.2.2).

4.2.3.1 Effect of inactivation with beta-propiolactone, binary ethyleneimine and formaldehyde on viral infectivity

All three chemicals previously fully eliminated the infectivity of the MEF-1 strain (section 4.2.2.1). To assess whether the rate of loss of infectivity differed between strains, the infectivity of different PV strains inactivated with BPL, BEI or HCHO over a range of time-courses was determined. Aliquots of the treated viruses were taken during these time-courses, as detailed above (section 4.2.3). The point during the time-courses at which viral infectivity was eliminated was determined by adding each virus aliquot onto HEp-2C cells. Cultures not showing CPE were passaged two further times for up to three weeks to ensure infectivity had been eliminated. All inactivation chemicals destroyed viral infectivity by the last two time-points (section 4.2.3), irrespective of PV strain.

The effect of inactivation on the viral infectivity was assessed further by determining the infectious titre of each virus aliquot. As figure 4.7 shows, the kinetics of inactivation with each chemical was similar for all three strains.

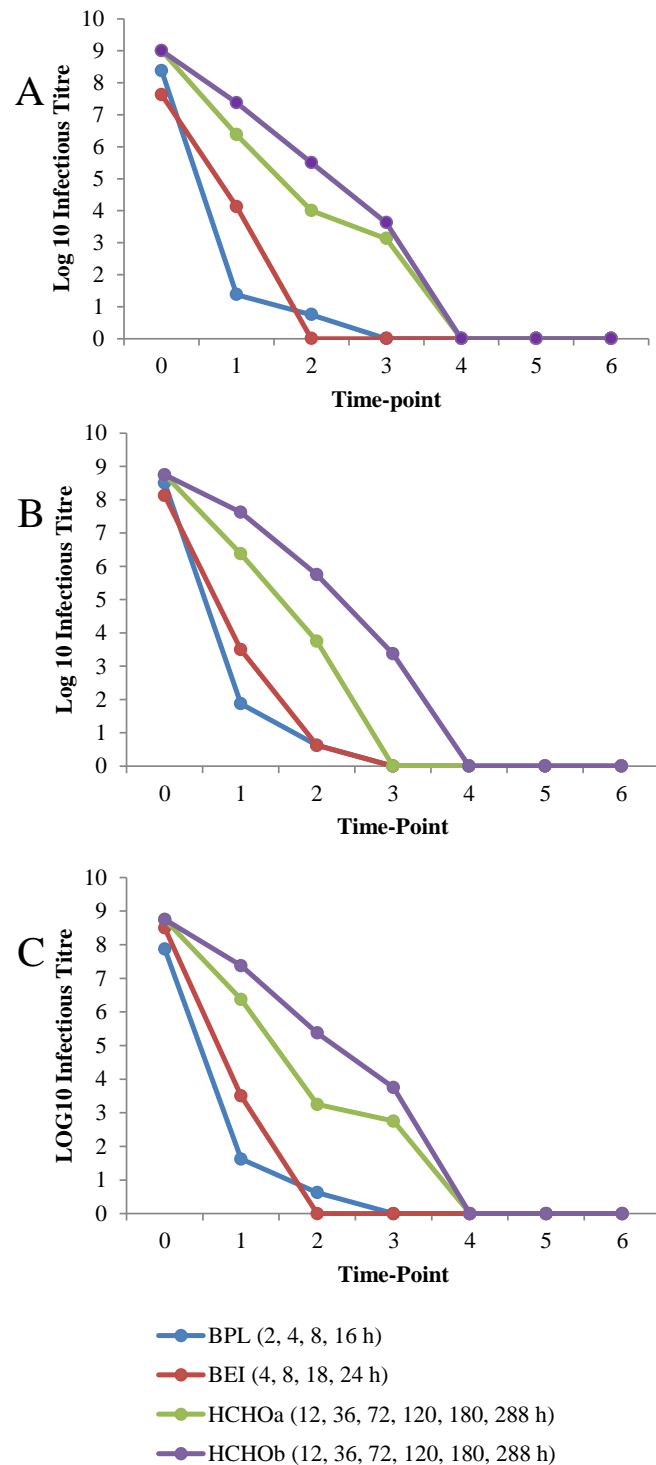


Figure 4.7. Effect of inactivation with beta-propiolactone, binary ethyleneimine, and formaldehyde on viral infectivity.

Sabin 2 (A), MEF-1 (B) and 04-44140261 (C) PV strains were incubated with BPL, BEI and 1:4000 or 1:8000 HCHO for set time-courses. Aliquots of the treated viruses were taken at pre-determined times (noted in the legend). Effect of inactivation on viral infectivity was determined by incubating susceptible cells with a range of ten-fold dilutions of each virus aliquot. Following five days incubation cells were stained and the infectious titre

was determined. One determination is shown as a line graph. 1:4000 HCHO is abbreviated as HCHOa; 1:8000 HCHO is abbreviated as HCHOb.

All inactivation chemicals fully eliminated infectivity of the three PV strains. The rate of this loss of infectivity differed between the chemicals. Beta-propiolactone and BEI completely eliminated infectivity within 24 h, while the two concentrations of HCHO required 72-288 h, confirming the findings obtained with the MEF-1 strain (section 4.2.2.1). Although the kinetics of inactivation with each chemical was similar for all three strains, some minor differences were apparent. The infectivity of the MEF-1 strain took a further 10 h than the other strains to be eliminated by BEI inactivation, while Sabin 2 and 04-44140261 required between 72-120 h incubation with 1:4000 HCHO before their infectivity was destroyed. As previously described for the initial inactivations (section 4.2.2.1) the infectious titre of the Oii control for the HCHO inactivations fell by three logs (data not shown). Again no significant fall in infectious titre was noted for the Oi control indicating that the inactivation temperature is likely to have caused this fall. As described above, the actual amount of the serotype 2 strains inactivated may have varied slightly as inactivations were carried out separately and consequently repeated freeze-thawing of the live PV stocks was required.

4.2.3.2 Effect of inactivation with beta-propiolactone, binary ethyleneimine and formaldehyde on viral antigenicity

To confirm the previous findings obtained with the initial inactivations of the MEF-1 strain and to assess whether the other serotype 2 strains showed similar results, the antigenicity of different PV strains inactivated with BPL, BEI and HCHO over a time-course was assessed. Aliquots of the treated viruses were taken during these time-courses as detailed above (section 4.2.3). The antigenicity of each virus aliquot was determined by ELISAs. As figure 4.8 shows, the retention of D-Ag following inactivation varied between serotype 2 strains and inactivation chemicals.

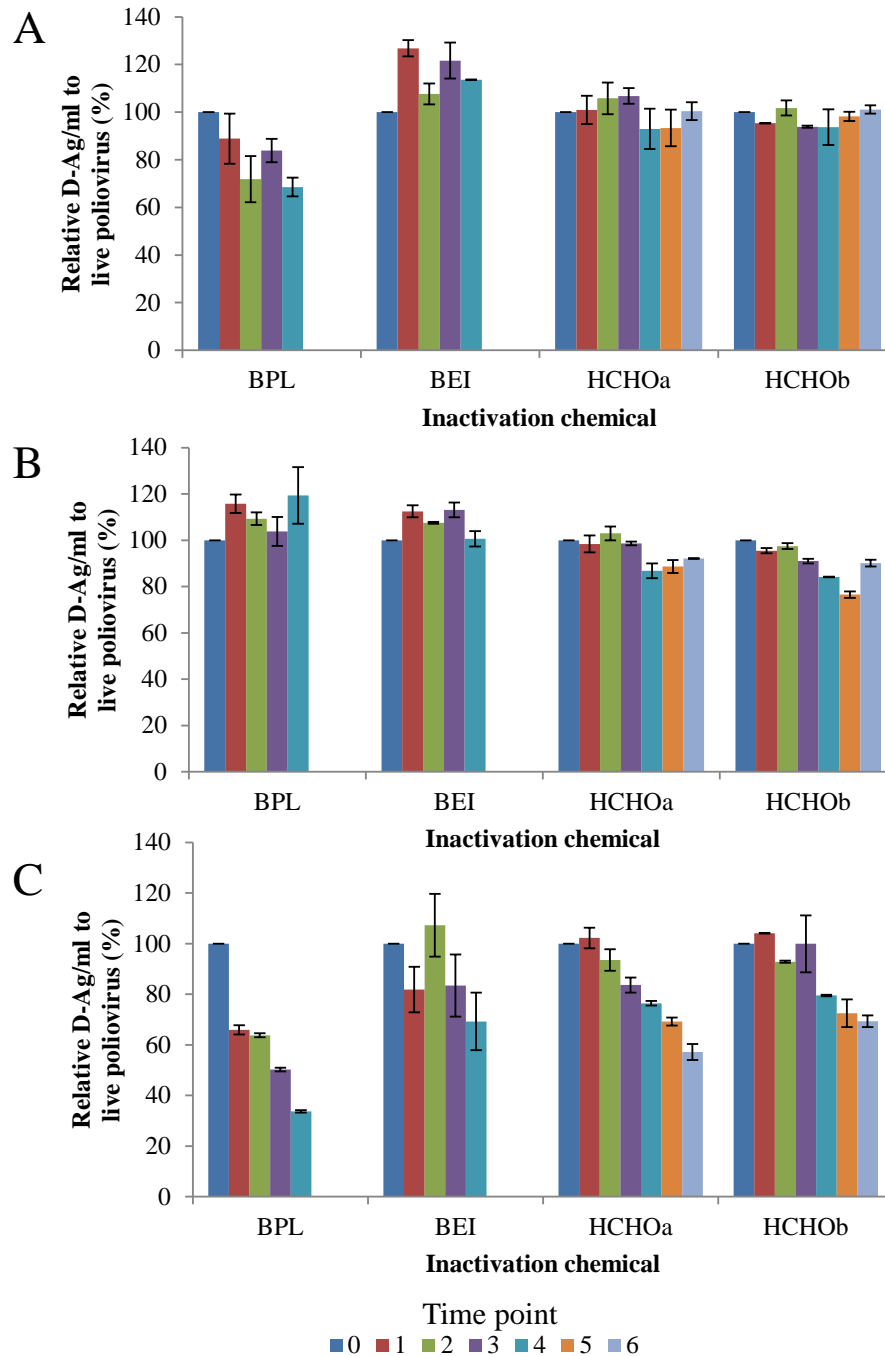


Figure 4.8. Effect of inactivation with beta-propiolactone, binary ethyleneimine and formaldehyde on viral antigenicity.

Sabin 2 (A), MEF-1 (B) and 04-44140261 (C) PV strains were incubated with BPL, BEI or HCHO for set time-courses. Aliquots of the treated viruses were taken at pre-determined times. For BPL at: 0, 2, 4, 8, 16 h; for BEI at: 0, 4, 8, 18, 24 h; for both 1:4000 and 1:8000 dilutions of HCHO at: 0, 12, 36, 72, 120, 180, 288 h. The effect of inactivation on viral antigenicity was determined by ELISA using the batch release detection MAb 1050. The percentage of live PV D-Ag retained following inactivation was calculated. The average of two determinations is shown as bar with standard error. 1:4000 HCHO is abbreviated as HCHOa; 1:8000 HCHO is abbreviated as HCHOb.

For the Sabin 2 and MEF-1 strains, inactivation with BEI and HCHO resulted in a minimal loss of D-Ag, confirming the findings obtained with the MEF-1 strain (section 4.2.2.2). With the exception of the MEF-1 strain, inactivation with BPL resulted in a greater loss of D-Ag than that seen following inactivation with BEI and HCHO. This result conflicted the previous finding obtained with the MEF-1 strain in section 4.2.2.2. For all of the chemicals, the 04-44140261 strain showed a greater loss of D-Ag than the Sabin 2 and MEF-1 strains, particularly when BPL was used. The D-Ag remained the same for both 0i and 0ii live controls for all three strains.

To further assess the effect of inactivation on the viral antigenicity, the antigenic structure of the three selected PV strains was characterised following inactivation with BPL, BEI and HCHO by ELISAs which determined whether antigenic site-specific MAbs would bind following inactivation (Materials and Methods, section 2.2.3.3). The binding of MAbs to the inactivated PV preparations was compared and related to the binding to live PV. As figure 4.9 shows, the structure of antigenic site 1 was modified following inactivation with all three chemicals.

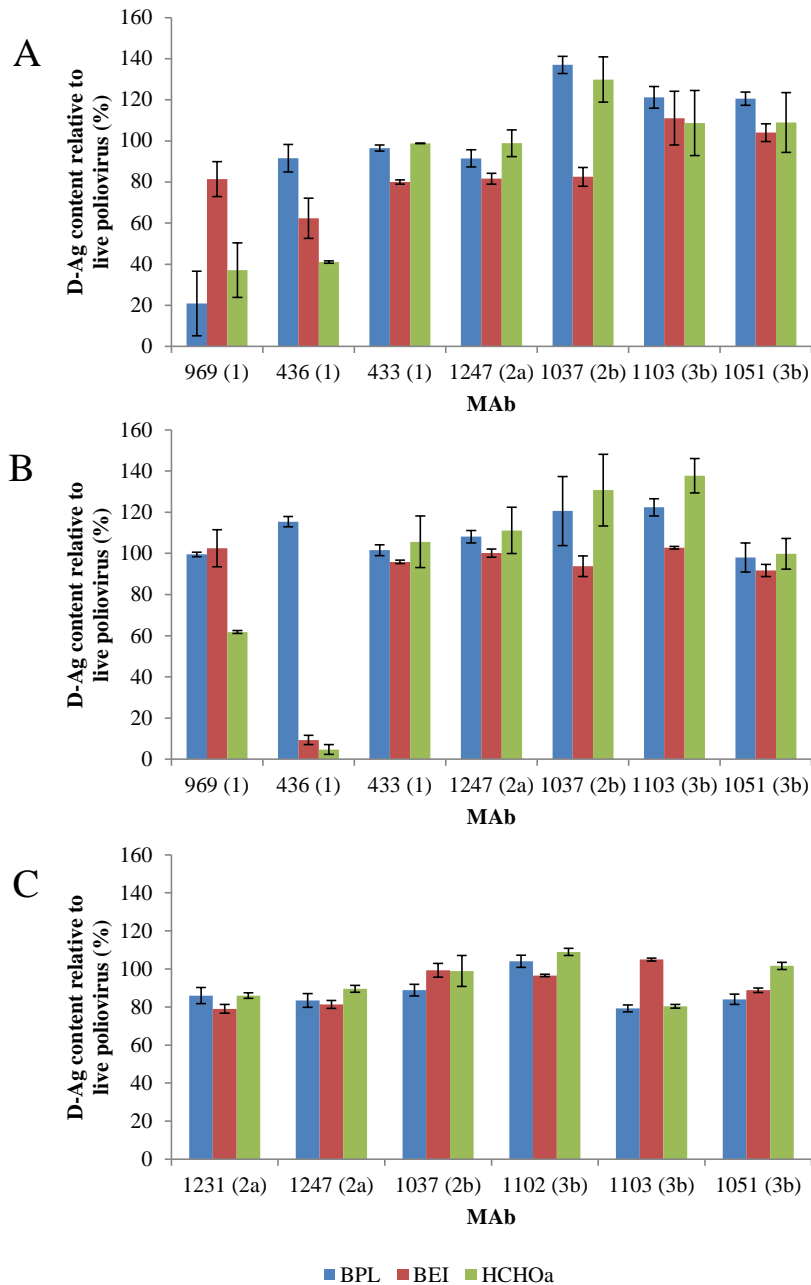


Figure 4.9. Antigenic structure of beta-propiolactone-, binary ethyleneimine- and formaldehyde-inactivated poliovirus strains.

Sabin 2 (A), MEF-1(B) and 04-44140261 (C) PV strains were inactivated by incubation with BPL, BEI and 1:4000 HCHO (HCHOa). Antigenic structure was characterised by an ELISA with site-specific MAbs in which the D-Ag of inactivated PV preparations was calculated relative to live PV. The result obtained was related to that determined using the batch release detection MAb 1050. Antigenic site-specificity of MAbs is bracketed. The average of two determinations is shown with standard error bars.

The results shown in figure 4.9 confirm those of Chapter 3, that inactivation with HCHO modifies antigenic site 1. Inactivation with BPL or BEI was also found to affect antigenic site 1 as shown by MAbs 436 and 969. Using these two MAbs showed that the extent to which each chemical modified this site seemed to vary between the chemicals and the PV strains. For example, analysis of inactivated Sabin 2 and MEF-1 preparations with MAb 436 found that while BPL had little effect, both BEI and HCHO reduced the antigenic content relative to live PV preparations. This reduction appeared to be more significant for the MEF-1 strain. Modification to antigenic site 1 of the 04-44140261 strain cannot be assessed, as site 1-specific MAbs do not react with its live form due to its inherent antigenic characteristics (Chapter 3). The remaining antigenic sites of the strains showed little modification following inactivation with the three chemicals. The lack of modification to antigenic sites 2a, 2b and 3b of HCHO-inactivated PV preparations confirms previous findings (Chapter 3).

4.2.4 Determination of D-Antigen/ml by surface plasmon resonance

Currently, the viral antigenic content (D-Ag) or potency of IPVs is determined by ELISA using an international reference standard (176). However, this test is variable both within and between laboratories, depending on the specific reagents and antibodies used (22, 541). It has been previously noted that the biosensor-based analytical system can determine the antigenic activity of a vaccine component by assessing its capacity to bind to a panel of MAbs (518). Preliminary work by Kersten *et al.* (252) has shown that this could be applied to assess the D-Ag content of IPVs.

To explore the use of this biosensor approach as an alternative method to determine the D-Ag / ml, a protocol was devised (Materials and Methods, section 2.2.3.2). This protocol used the Biacore 2000 and T100 (GE Healthcare) biosensor instruments to assess the D-Ag / ml content of IPV preparations. Both instruments have a fluidic system which creates four serially linked flow cell areas on one sensor chip, allowing a number of simultaneous measurements (237). The biosensor protocol began with the immobilisation of rabbit anti-mouse Ig (GE Healthcare) to the dextran layer of a sensor chip. This anti-mouse Ig was covalently immobilised to a single flow cell by primary amine coupling. Subsequently, a serotype-2 specific MAb and an IPV were injected separately over the surface of the sensor

chip for pre-determined periods and at set flow rates. The binding of this MAb and IPV caused differences in the refractive index which is, between limits, proportional to the concentration of the MAb-IPV complex (252). The surface of the sensor chip was regenerated with 10 mM glycine-HCl (pH 1.5) for a pre-determined period and flow rate. In comparison to ELISA, the catching antibodies are monoclonal rather than polyclonal. As detection is mass-dependent, no detecting antibodies or conjugates are required (252).

Several parameters of this protocol had to be optimised before it could be carried out. A ligand can be immobilised to the surface of a range of sensor chips which can be divided into non-derivatized and derivatized dextran-containing chips. Non-derivatized dextran-containing chips are coated with a hydrogel matrix of flexible, unbranched carboxymethylated dextran. The derivatized dextran-containing chips are coated with a dextran matrix to which either streptavidin or nitrilotriacetic acid has been immobilised. These are designed to capture biotinylated ligands and poly-histidine tagged ligands. In addition, a number of sensor chips have modifications to the surface which allows the capture of liposomes and lipid monolayers (237). As this protocol required the immobilisation of rabbit anti-mouse Ig rather than a tagged ligand, the non-derivatized dextran-containing chips were selected for immobilisation.

Three non-derivatized dextran-containing chips are available from Biacore; CM5, CM4 and CM3. The length of dextran and the level of carboxymethylation varied between the chips. A comparison of immobilisation of rabbit anti-mouse Ig to CM5 and CM3 sensor chips was carried out. The CM3 chip showed a larger amount of bound ligand than the CM5 chip following immobilisation (4189.2 RU and 2999.8 RU, respectively). This may have been due to the shorter dextran chains of the CM3 chip which would reduce the steric effects during immobilisation. An immobilisation wizard program was used to set up the immobilisation for this protocol. This software allows immobilisation to be set either to an RU target or for a set period of time at a set flow rate. A comparison of both methods found greater immobilisation when a set time period at a set flow rate, rather than a set RU target was applied (38939.3 and 2110.5, respectively). This may have been due to the slower rate of the set time/flow rate method, as this would allow more time for binding to the chip.

The biosensor protocol relies on the use of a MAb to catch the IPV. In order to determine the optimal MAb (s) to do this, a range of serotype 2 MAbs specific to different antigenic sites were screened in a binding assay. As table 4.2 shows, this binding assay determined the amount of MAb bound to the immobilised anti-mouse Ig and the subsequent amount of a trivalent IPV bound to the MAb at two dilutions of IPV.

Monoclonal antibody	Amount of analyte bound (RU)			
	1:4 IPV dilution		1:2 IPV dilution	
	MAb to AM Ig	IPV to MAb	MAb to AM Ig	IPV to MAb
433	483	388	701	617
1247	574	585	758	954
1037	293	193	301	364
1050	275	427	298	759
267	441	80	672	147
268	503	40	648	80
1118	474	54	685	98
1255	323	16	359	22

Table 4.2. Binding of serotype 2-specific monoclonal antibodies to immobilised rabbit anti-mouse immunoglobulins.

Rabbit anti-mouse Ig was immobilised to a CM3 sensor chip. Serotype 2-specific MAbs were injected over the surface of the chip, followed by injections of a 1:4 diluted trivalent IPV (23.8 D-Ag). Following a regeneration cycle, the process was repeated with a 1:2 diluted IPV (47.5 D-Ag). Binding of MAbs and IPV dilutions was monitored in real-time by SPR using the Biacore 2000. MAb indicates monoclonal antibody; rabbit anti-mouse Ig is abbreviated as AM Ig; inactivated poliovirus vaccine is referred to as IPV.

The optimal MAb selected for the biosensor D-Ag protocol was required to show a reliable binding to the anti-mouse Ig and to catch a consistent amount of IPV between regeneration cycles. The results of the binding assay, shown in table 4.2, found two MAbs to have consistent binding to the anti-mouse Ig between regeneration cycles, MAbs 1037 and 1050. The MAb 1050 was selected for the biosensor protocol, as it bound more of the IPV at the two dilutions. In addition, both MAbs 1050 and 1037 are currently used in batch release ELISA potency testing of IPV at the NIBSC and, therefore, the use of MAb 1050 in the biosensor protocol would allow direct comparison to the ELISA method.

In the biosensor protocol a regeneration step is required at the end of each MAb-IPV cycle. A regeneration scouting software was used to optimise the regeneration buffer. Both glycine-HCl and NaOH were assessed using this program. Glycine-HCl was found to give a better regeneration with an optimal pH of 1.5. Different durations and flow rates of regeneration were assessed before an optimal regeneration of 10 mM glycine-HCl (pH1.5) for 120 s at a flow rate of 30 μ l/m was reached. As this regeneration removed the bound MAb-IPV without causing significant loss of immobilised anti-mouse Ig, two runs in succession were included in the biosensor protocol.

The biosensor protocol was carried out using the Biacore 2000 and T100 instruments to estimate the D-Ag of a reference IPV preparation and a range of commercial IPV of varying origins (including Sabin and wild-type monovalent or trivalent preparations). In addition, the biosensor protocol was used to estimate the D-Ag of a range of BPL-, BEI- and HCHO-inactivated MEF-1 preparations which were prepared “in-house” at the NIBSC (as described in section 4.2.3). As figure 4.10 shows, for both commercial IPV and “in-house” inactivated MEF-1 preparations, the D-Ag estimates determined by the biosensor protocol and ELISA were comparable.

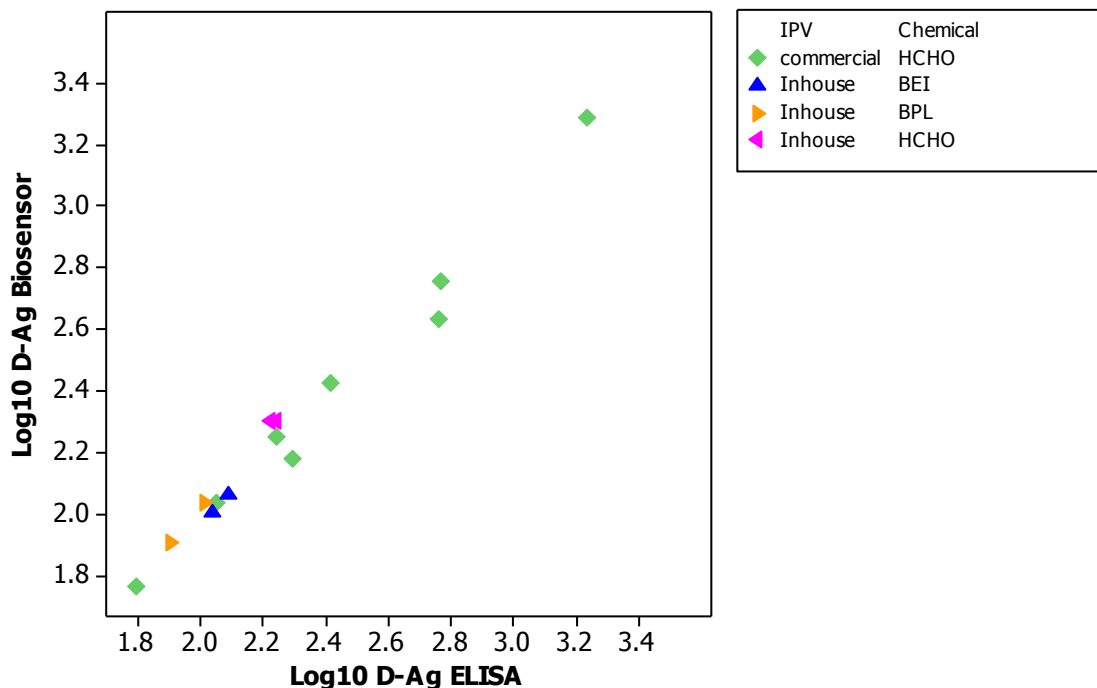


Figure 4.10. Correlation of D-Antigen estimates of inactivated poliovirus vaccines determined by biosensor and ELISA protocols.

For the biosensor protocol rabbit anti-mouse Ig was immobilised to a sensor chip. MAb 1050, followed by the relevant IPV / inactivated MEF-1 preparation were injected over the surface of the chip. The binding of each injection was monitored by SPR. For ELISA a serotype specific capture antiserum antibody was bound to a plate, followed by the relevant IPV / inactivated MEF-1 preparation. The IPV was detected by MAb 1050 and peroxidase conjugated anti-mouse IgG whole molecule. Plates were washed between the additions of reagents.

The linear relationship between the two methods, (figure 4.10), was confirmed by the Pearson product moment correlation coefficient (Minitab v.16, <http://www.minitab.com/en-GB/>) which found a correlation coefficient of 0.989 ($R^2 = 0.978121$). These findings indicate that

biosensor approach offers an alternative means to assess the antigenic content of an IPV preparation.

4.3 DISCUSSION

Inactivation with HCHO is known to lower the immunogenicity of PV and research within the previous chapter has found that the partial modification of the antigenic structure of PV may, at least in part, contribute to this. One approach to prepare IPVs with improved immunogenicity has been to use chemicals which inactivate by different mechanisms to that of HCHO. Beta-propiolactone and BEI were selected as they primarily inactivate by introducing nucleic acid adducts, principally 7-(2-carboxyethyl) guanine (97, 205, 206, 432, 459, 525). The optimal concentration of these chemicals to inactivate PV was determined alongside the conventional HCHO.

While both chemicals eliminated viral infectivity, the rate at which they did so differed from HCHO. Within 24 h (16-18 h), both fully inactivated PV strains while HCHO took at least 120 h. This rapid loss of viral infectivity was indicative of BPL and BEI inactivation involving the viral nucleic acids (169) and confirmed previous studies in which both BPL- and BEI-inactivated a range of viruses at a much faster rate than HCHO (73, 77, 229, 239, 245).

The antigenic content of the PV strains was assessed during the optimisation and final inactivations by ELISA. For the Sabin 2 and 04-44140261 strains, treatment with BPL resulted in a greater loss of antigenic content than when inactivated with BEI or HCHO. This loss of antigenic content was not expected, as previous research (57, 97, 432, 459) had indicated that the main mechanism of inactivation of BPL was the preferential carboxyethylation of guanine and adenine. However, it should be noted that BPL has been found to interact with viral capsid proteins (56) and at least part of this effect on the antigenic content of PV preparations could have been due to variables which can influence the activity of BPL during inactivation, for example the temperature at which the inactivation was carried out. While BEI and HCHO inactivations were carried out at 37 °C, BPL inactivations were carried out at +4 °C, due to its instability at higher than ambient temperatures (288).

Budowsky and Zaleskaya (70) argue that incubation at a lower temperature decelerates the hydrolysis of BPL to a greater extent than the reaction between BPL and the virion components. Therefore, incubating the BPL inactivation at +4 °C may have led to a prolonged interaction of BPL with the virion antigenic epitopes, as well as RNA resulting in a reduced D-Ag content.

The pH of the inactivation medium during inactivation influences the nature of the viral proteins which interact with BPL (169). During inactivation BPL is completely hydrolysed into a non-toxic degradation product, beta-hydroxypropionic acid. The accumulation of this product can decrease the pH which, in turn, can affect the BPL consumption (70). In addition, the nature of the proteins which BPL interacts with also shifts when the pH becomes more acidic (169). Although HEPES was added to buffer the inactivation medium, the pH fell from 7.5 to 6.5 following 16 h incubation with 1:500 BPL. This fall in pH may have resulted in a shift in the proteins which interacted with BPL and this, in turn, may have resulted in a greater interaction between BPL and the viral proteins.

The antigenic content of the MEF-1 strain fell during the optimisation inactivation with BPL. However, this was not apparent during the final inactivation. The less stable nature of BPL may account for this discrepancy between the two inactivations. Due to the less stable nature of BPL, variations in the temperature and pH of the inactivation medium may have led to the minor difference between the inactivated MEF-1 preparations from the optimisation and final inactivations. In addition, the concentration of serotype 2 strains also differed between the optimisation and final inactivations with BPL (1×10^9 and 5×10^9 TCID₅₀ / 100 µl, respectively). This difference in the amount of the PV being inactivated may have also contributed to the discrepancy between the BPL-inactivated MEF-1 preparations from the optimisation and final inactivations. Inactivated Sabin 2 and MEF-1 preparations showed little or no loss of antigenic content following inactivation with BEI or HCHO. The high retention of PV D-Ag (relative to that of live PV) following inactivation with BEI confirmed findings from a related study (529) examining the effect of BEI on Sabin 2 .

The PV strain of the inactivated preparations was indicated to contribute to the observed differences in the retention of live PV D-Ag. In comparison to Sabin 2 and MEF-1, the 04-44140261 strain showed a greater loss of D-Ag following inactivation, irrespective of the

chemical used. This may indicate that the 04-44140261 strain was less stable than the other strains during the inactivation process, resulting in a greater loss of D-Ag. Alternatively, due to difference between PV strains, the viral capsid of the 04-44140261 had a larger quantity of amino acid residues which interacted with the inactivation chemicals than the other strains. Recently, various amino acid derivatives and synthetic peptides were analysed using nuclear magnetic resonance spectroscopy and tandem reversed-phase liquid chromatography mass spectrometry to determine the reaction of BPL with proteins (514). This study has identified nine amino acid residues with which BPL interacts. The most reactive include cysteine, methionine and histidine. Beta-propiolactone reacts to a lesser degree with aspartic acid, glutamic acid, tyrosine, lysine, serine and threonine (514). An analysis of the previously sequenced antigenic sites of the Sabin 2, MEF-1 and 04-44140261 strains (Chapter 3, table 3.3) found that there were a larger number of amino acid residues which potentially reacted with BPL within the iVDPV strain than the other strains. This may have led to BPL reacting to a greater extent with the 04-44140261 strain than the other strains, possibly resulting in a greater loss of D-Ag.

The antigenic structure of inactivated PV preparations was characterised by a series of ELISAs which determined whether antigenic site-specific MAbs were able to bind following inactivation. The binding of MAbs to the inactivated PV preparations was compared and related to the binding to live strains. Inactivation with BEI and HCHO resulted in modification to the structure of antigenic site 1 of the Sabin 2 and MEF-1 strains. The extent of these modifications appeared to vary between PV strains. The remaining antigenic sites were not modified by inactivation with BEI or HCHO. Inactivation with BPL did not result in any significant modification to any of the antigenic sites.

The modification of antigenic site 1 by BEI conflicts with the findings of previous research that BEI does not alkylate the viral capsid proteins (56, 123, 131). However, there is evidence that BEI can modify proteins. An analysis of albumin samples by isoelectric focusing found that inactivation with BEI modified the albumin, altering its charge (66, 67). Previous research has found the reactivity of BEI with polynucleotides and viral proteins to be similar (71). This similar reactivity may have led to the inactivation of the viral proteins as well as the genome resulting in a modification to the antigenic structure. One way to increase the selective inactivation of the viral genome would be to inactivate with ethyleneimine oligomers, rather than the monomeric BEI (66, 67, 71, 509). The difference in the

modification of antigenic site 1 between BEI, HCHO and BPL may, at least in part, affect the immunogenicity of the inactivated PV preparations. This will be explored in Chapter 5 using a batch-release rat potency assay and an immunisation-challenge model. In addition to the approach described within this chapter there are alternative ELISA approaches which may give more detailed findings of epitope modification (426).

A biosensor-based protocol established comparable D-Ag/ml estimates to those obtained by the current ELISA, indicating that it could offer an alternative means to assess the potency of IPVs. Variation within assays and laboratories could be lessened by the automated nature of biosensors. The variability in polyclonal and monoclonal antibodies could be eliminated with the use of a biosensor system, as this would allow the rapid characterisation (within days) of antibodies, which would enable laboratories to rapidly screen and select the optimal antibodies. In addition to providing a less variable means to determine the D-Ag content, the biosensor approach offers additional tools for research that the ELISA cannot offer. As a biosensor system measures direct binding between a ligand and an analyte and it can analyse the kinetics of an interaction, it could be used to provide a more detailed analysis of the nature of the interaction between MAbs and antigens. In addition, the affinity-dissociation and competition of MAbs to bind to certain antigen could be determined.

The expression of the viral antigenicity of IPV as D-Ag unit/ml can be problematic, as D-Ag is a poorly defined measurement. The use of “in-house” antibodies and reagents by manufacturers and official medicines control laboratories can affect the obtained D-Ag and result in variation between laboratories (532). Recent research (532) has shown that biosensors can determine the antigenic (or active) content of IPVs by a calibration-free concentration assay. This assay determines the active concentration of IPVs without the use of a reference strain. The assay measures the observed binding rate of the IPV to a specific MAb during sample injection under partially or complete mass transport limited conditions (471, 532). Preliminary investigations have found that active concentration of a range of IPVs (Sabin and wild-type) was independent of MAbs used. For cIPVs the active particle concentration correlated with the virus concentration calculated from the absorbance at 260 nm of the purified monovalent bulk intermediate after ion exchange chromatography purification (532). This assay could be used instead of ELISA to assess the antigenic content of inactivated PV preparations. The assessment of the active content of IPVs offers the

advantages of not requiring a calibration curve and of being independent of variation between different MAb (532).

CHAPTER 5

IMMUNOGENICITY OF POLIOVIRUS INACTIVATED WITH BETA- PROPIOLACTONE, BINARY ETHYLENEIMINE OR FORMALDEHYDE

5.1 INTRODUCTION

The previous chapter detailed how an indirect ELISA was used to quantify the potency of IPV preparations. However, when the IPV was developed by Salk in the 1950s, the potency of IPVs was not assessed. Each dose of IPV was designed to be the equivalent of a specific volume of harvest fluid from PV-infected primary MKTC (170, 452). Inactivated poliovirus vaccines developed by this method showed variable immunogenicity in humans (170). In response to the Cutter incident (365) in which vaccine recipients were paralysed by the use of incompletely inactivated IPV, filtration steps were introduced to remove aggregates. While these steps led to increased safety, the antigenicity of the IPVs fell as a result (326) and this, in turn, lowered the immunogenicity of the vaccine (361). Consequently, potency assays for the final products were required.

Both *in vitro* and *in vivo* potency assays have been developed to assess the immunogenicity of IPV. Previously the *in vivo* assays were used as the official batch release tests carried out on the final IPV product, while the *in vitro* assays were principally used for in-process monitoring (150). This situation has since changed and due to the requirements of the European convention on the protection of vertebrate animals used for experimental and other scientific purposes, it is possible to waive the *in vivo* assay and assess the potency solely by *in vitro* assays, should certain conditions be met (153). *In vitro* assays measure the potency of IPV preparations by determining the D-Ag units. As noted previously (Chapter 4), the D-Ag unit is used as a measure of potency as it is largely expressed on native infectious virions and is the protective immunogen (31, 289). The most commonly used *in vitro* test is the indirect ELISA. This assay is used to assess the D-Ag content of IPVs and ensure consistency throughout production.

A range of *in vivo* assays have been developed in monkeys, chicks, guinea pigs, mice and rats. All have an advantage over *in vitro* assays in that they can measure the ability of the IPV to induce protective, neutralising antibodies (474). Initially the monkey potency test was the standard *in vivo* assay to determine the potency of IPV preparations (515). In this test at least 10 simians are inoculated, using a three dose schedule comparable to that used for human recipients (540). The geometric mean titre of neutralising antibodies for each of the three serotypes is compared with a reference trivalent antiserum (150). An IPV is deemed acceptable if the mean titre is above that of the reference antiserum (540).

While the monkey potency test can distinguish qualitatively between good and poor IPVs, it is not sufficient for obtaining quantitative data about vaccine potency, as it uses a reference serum rather than a reference vaccine. In addition, this test requires many expensive primates (39, 520). These concerns led to a search for another animal model to assess the potency of IPVs. Animals which are non-susceptible to PV are known to be capable of forming specific neutralising antibodies following parenteral administration of live or inactivated PV (181). Consequently, a range of non-susceptible animal models have been developed, one of which is the guinea pig model (181). Initially, this test involved single and booster inoculations of groups of guinea pigs with ten-fold dilutions of live and inactivated PV preparations (115). Following 6-7 weeks, the guinea pigs were bled and the antibody levels were determined at a low dilution by a neutralisation test, described previously (181). From this, the extinction end-point of the median effective dose (ED_{50}) after a single dose was calculated (150). The end-point of the ED_{50} is the logarithm of the reciprocal of the dilution which evokes neutralising antibodies in 50 % of the animals (320). The chick potency test follows a similar protocol and after a single dose calculates the ED_{50} (504).

Both the guinea pig and chick potency test have been adopted as a single test within the European Pharmacopeia (153). In this test, three or more dilutions of an IPV are used to immunise either guinea pigs or 3-week-old chicks (10 animals / dilution). After 5-6 days, animals are bled and sera are diluted to 1 in 4. Poliovirus (100 TCID₅₀) is mixed with the diluted serum and incubated at 37 °C for 4.5-6 h and then 5 ± 3 °C for 12-18 h. Mixtures are added to cell cultures for up to seven days, to detect unneutralised PV. For each group of animals, the number of sera which have neutralising antibodies is noted and the dilution of the IPV which gives an antibody response in 50 % of the animals (the end-point of the ED_{50}) is calculated. An IPV is acceptable if a dilution of 1 in 100 or more produces an antibody response for each of the three serotypes of PV in 50 % of the animals (153).

Although an accepted technique of the European Pharmacopoeia, the guinea pig / chick potency test is limited in that the calculated single dose ED_{50} can only provide a qualitative measure of the immunogenicity of an IPV. This test lacks the sensitivity and reproducibility to distinguish between IPVs which differ in antigenic content as much as four-fold to eight-fold (150). In addition, this test is a poor predictor of human immune response. In particular, this test can only measure IgM instead of IgG which is typically measured following vaccination in humans (334, 520). In response to these limitations the Rijks Instituut voor de

Volksgezondheid developed an alternative potency test in which the titre of the antibody response was measured rather than the extinction titre (end-point). The antibody response of guinea pigs and various strains of rats and mice were assessed to identify the animal which would produce a good dose-related titre response after a single injection, preferably in the IgG class. Rats were found to give the highest titres, a good dose-related titre response in the IgG class and were consistent across different strains. Consequently, a rat potency test was developed to assess the immunogenicity of a range of IPVs in relation to a reference IPV of proven efficacy in humans. Comparable distribution of antibody titres for reference and sample IPVs was found, allowing accurate assessment of potency. These quantitatively determined potencies were comparable to those obtained using an *in vitro* D-Ag test. Antibody patterns of rats and humans were similar, indicating that the rat maybe a suitable model to assess the immunogenicity of IPV in humans (520).

An international collaborative study compared the use of the chick / guinea pig and the rat potency tests to determine the immunogenicity of six trivalent IPVs. Wide variation was found between laboratories using the chick /guinea pig potency test. The rat potency test was found to be far less variable between laboratories (540). The results of this study led to the validation of the rat potency test by manufacturers (39) and national control laboratories (e.g. the NIBSC, (111)) as an alternative means of determining the immunogenicity of IPVs. The rat potency test is now included within the European Pharmacopeia (153). In this test, three or more dilutions of an IPV and a reference IPV are administered to groups of pathogen-free rats (10 / dilution). After 20-22 days, rats are bled and neutralising titres against the three PV serotypes are measured separately using 100 TCID₅₀ of the Sabin strains as challenge viruses. Neutralisation is carried out at 35-37 °C for 3 h followed by 18 h at 2-8 °C before Vero or HEp 2C cells are added. After seven days incubation at 35 °C the cells are fixed, stained and read by eye. For the assay to be valid the titre of each challenge virus must be between 10 – 1000 TCID₅₀ and the neutralising antibody titre of a control serum must be within 2 two-fold dilutions of the geometric mean titre of the test serum. The potency is calculated by comparing the proportion of responders (defined by a cut-off neutralising antibody titre) for the IPV sample and the reference IPV by the probit method (153). This is a statistical method for estimating the dilution which will give a 50 % neutralisation titre. Currently the European Pharmacopeia guidelines require that the potency of an IPV is assessed either *in vivo* by the chick / guinea pig or rat tests or by an *in vitro* method (following a waiving of *in vivo* tests)

(153). Due to its benefits, the rat potency test is considered the *in vivo* method of choice (153).

An immunisation-challenge test using Tg mice to further evaluate the immunogenicity and protective properties of IPVs has been developed independently by the US Food and Drug Administration (FDA) and the NIBSC (312, 491). The identification and isolation of genes which encode human and primate PVRs (265, 267, 329) has allowed Tg mice lines which express the human PVR (TgPVR mice) to be established (269, 423). Transgenic mice expressing the human PVR can be infected with PV serotypes by various routes and develop clinical signs of paralysis and morphological lesions in the CNS. Due to these properties TgPVR mice have been used to investigate the pathogenesis of poliomyelitis (416), and the neurovirulence of OPV preparations (2, 138, 139, 217). As the TgPVR mice can clinically manifest paralysis, it is possible to determine the 50 % end-points for paralysis (PD₅₀) or lethality (LD₅₀), if a suitable dose range of a PV is used (539). A number of TgPVR mouse lines have been developed which differ in genetic background, copy number, insertion site and expression of the transgene in the CNS. These factors influence the sensitivity of TgPVR mice to PV (268).

Previous research by the FDA and the NIBSC (140, 141, 312, 491) has identified suitable immunisation-challenge regimes with TgPVR mice for assessing the immunogenicity of IPV preparations. A single or booster vaccination (one week apart) followed by a challenge was sufficient to model protection (312, 490, 491). In Tg21PVR mice both protection and the level of neutralising antibody elicited by vaccination with IPV have been found to be dose-dependent (491). The strain of the immunogen used to immunise the Tg21PVR mice affected the protection conferred. A good correlation has been found between the neutralising antibody titres in blood samples from Tg21PVR mice and the immune protection conferred (312). Immunisation-challenge regimes with TgPVR mice allow a more direct analysis of the protection conferred by IPV preparations than other potency test which assess the immunogenicity on the basis of seroconversion. The immunisation-challenge test with TgPVR mice assesses the protection conferred by other aspects of the immune response (e.g. cellular immunity) in addition to the neutralising antibody response. Discrepancies between antibody response and protection conferred indicate that other aspects of the immune response contribute to protection against the PV challenge (490). As a consequence, the research detailed in this chapter will assess the immunogenicity of a range of inactivated PV

preparations using both the rat potency assay and a series of immunisation-challenge experiments with TgPVR mice.

In addition to immunogenicity, thermostability is one of the key measures to assess the quality of an IPV. The thermostability of an IPV is a measure of the stability of the vaccine for long-term storage. It is known that serotype 2 cIPV can be stored at +4 °C for 20 years and remain potent (353). It is not clear what effect inactivation with other chemicals may have on this thermostability. As a consequence, the thermostability of BPL- and BEI-inactivated PV preparations will be determined alongside HCHO-inactivated PV preparations. A small study detailed in this chapter will assess the thermostability of inactivated preparations of three serotype 2 strains prepared with different inactivation chemicals.

5.2 RESULTS

5.2.1 Immunogenicity of inactivated poliovirus preparations

5.2.1.1 Assessment of immunogenicity by rat potency test

It was described in Chapter 3 that inactivation with HCHO resulted in a reduction in the immunogenicity of a range of serotype 2 PV strains. To improve the immunogenicity (potency) of inactivated PV preparations, BPL and BEI were used to inactivate three strains. To assess the effect of these chemicals along with HCHO on the immunogenicity of serotype 2 PV strains, an *in vivo* rat potency test was carried out. Wistar rats were immunised with 2 D-Ag/ml doses of inactivated MEF-1 preparations. After 22 days, the rats were exsanguinated and their blood serum was harvested. The sera were challenged with 100 TCID₅₀ of three serotype 2 PV strains: Sabin 2, MEF-1 and 04-44140261 in a cell culture neutralisation assay.

As figure 5.1 shows, the immunogenicity of the inactivated MEF-1 preparations varied with the inactivation chemicals. Analysis by balanced ANOVA (Minitab v.16, <http://www.minitab.com/en-GB/>) found that this variation in the log₂ neutralisation titre of sera from rats immunised with the different inactivated MEF-1 preparations was significant between the three inactivation chemicals ($P < 0.005$). As there were concerns about the reliability of this finding with respect to the data obtained from this potency assay, a binary logistic regression analysis and a non-parametric Kruskal-Wallis test were carried out. After scoring the log₂ neutralisation titres, the binary logistic regression analysis (Minitab v.16, <http://www.minitab.com/en-GB/>) found that the chemical of the inactivated MEF-1 preparations had a significant effect on the neutralisation titre of the rat sera ($P < 0.01$). The Kruskal-Wallis test (Minitab v.16, <http://www.minitab.com/en-GB/>) confirmed this ($P < 0.005$).

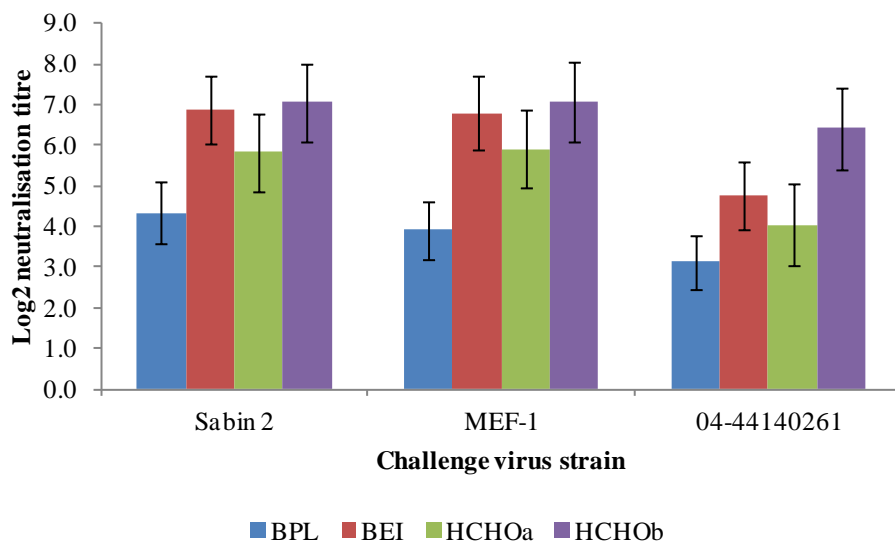


Figure 5.1. Immunogenicity of beta-propiolactone-, binary ethyleneimine- and formaldehyde-inactivated MEF-1 against challenge viruses.

Rats were immunised with a 2 D-Ag/ml dose of either BPL-, BEI- or HCHO-inactivated MEF-1. After 22 days, rats were exsanguinated and the sera were assayed to measure neutralising antibody to 100 TCID₅₀ of the relevant challenge virus using a fixed virus varying serum 50% end-point technique in a microtitre system. The average of five determinations is shown as a bar with the standard error. 1:4000 HCHO is abbreviated as HCHOa; 1:8000 HCHO is abbreviated as HCHO b.

Both the BEI- and HCHO-inactivated MEF-1 induced higher titres of neutralising antibodies than BPL-inactivated MEF-1, indicating that they were more immunogenic. Beta-

propiolactone-inactivated MEF-1 was found to be the least immunogenic. This grouping of the immune response was confirmed by multiple comparison, using the Tukey method (Minitab v.16, <http://www.minitab.com/en-GB/>) which found that the mean immune responses of rats immunised with BEI-inactivated MEF-1 were significantly higher than those immunised with BPL-inactivated MEF-1 ($P < 0.05$). The immune responses of rats immunised with HCHOa- and HCHO b-inactivated MEF-1 did not significantly differ from those of rats immunised with BPL- or BEI-inactivated MEF-1. There was some degree of specificity in the immune responses induced by each inactivated MEF-1 preparation against the different challenge viruses, with all preparations showing higher immunogenicity against Sabin 2 and MEF-1 strains than the iVDPV strain 04-44140261. However, analysis by balanced ANOVA (Minitab v.16, <http://www.minitab.com/en-GB/>) determined that this specificity was not significant.

5.2.1.2 Assessment of protection by transgenic mice immunisation-challenge experiments

The effect of inactivation with different chemicals on the viral immunogenicity of serotype 2 strains was further explored by assessing the level of protection conferred to TgPVR mice in a series of immunisation-challenge experiments (Materials and Methods, section 2.2.4.2). Following the development of an immunisation-challenge model with the Tg21-Bx mouse line at the NIBSC (312), a series of immunisation-challenge experiments were set up with this mouse line. This inbred strain of mice was derived at the NIBSC from a cross between normal BALB/c mice and ICR PVR Tg-1 mice (307). For these immunisation-challenge experiments, groups of eight Tg21-Bx mice were immunised at 6-8 weeks with 2x2 D-Ag/ml doses of an inactivated PV preparation and received a booster at day 14. After a further 21 days, the Tg21-Bx mice were challenged with a 50 PD₅₀ of either the MEF-1 strain or an iVDPV strain, 04-44140261, at day 35. Mice were then monitored for 14 days for any signs of paralysis. Blood samples were obtained before the challenge and the sera were then assayed to measure neutralising antibody against 100 TCID₅₀ of the relevant challenge virus using a fixed virus varying serum 50 % end-point technique in a microtitre system. Sera were challenged with Sabin 2, MEF-1 and 04-44140261 strains (Materials and Methods, section 2.2.4.1).

As figure 5.2 shows, the number of mice protected by an inactivated PV preparation varied between both the inactivation chemical used and the strain of the preparation. After scoring the number of mice on the basis of protection, the findings were analysed by binary logistic regression (Minitab v.16, <http://www.minitab.com/en-GB/>). It was found that both the strain and the inactivation chemical of the inactivated PV preparation had a significant effect on the protection conferred to the Tg21-Bx mice ($P < 0.001$). While the strain of the challenge PV had a significant effect on the protection conferred to the Tg21-Bx mice ($P < 0.01$), the gender of the mice did not.

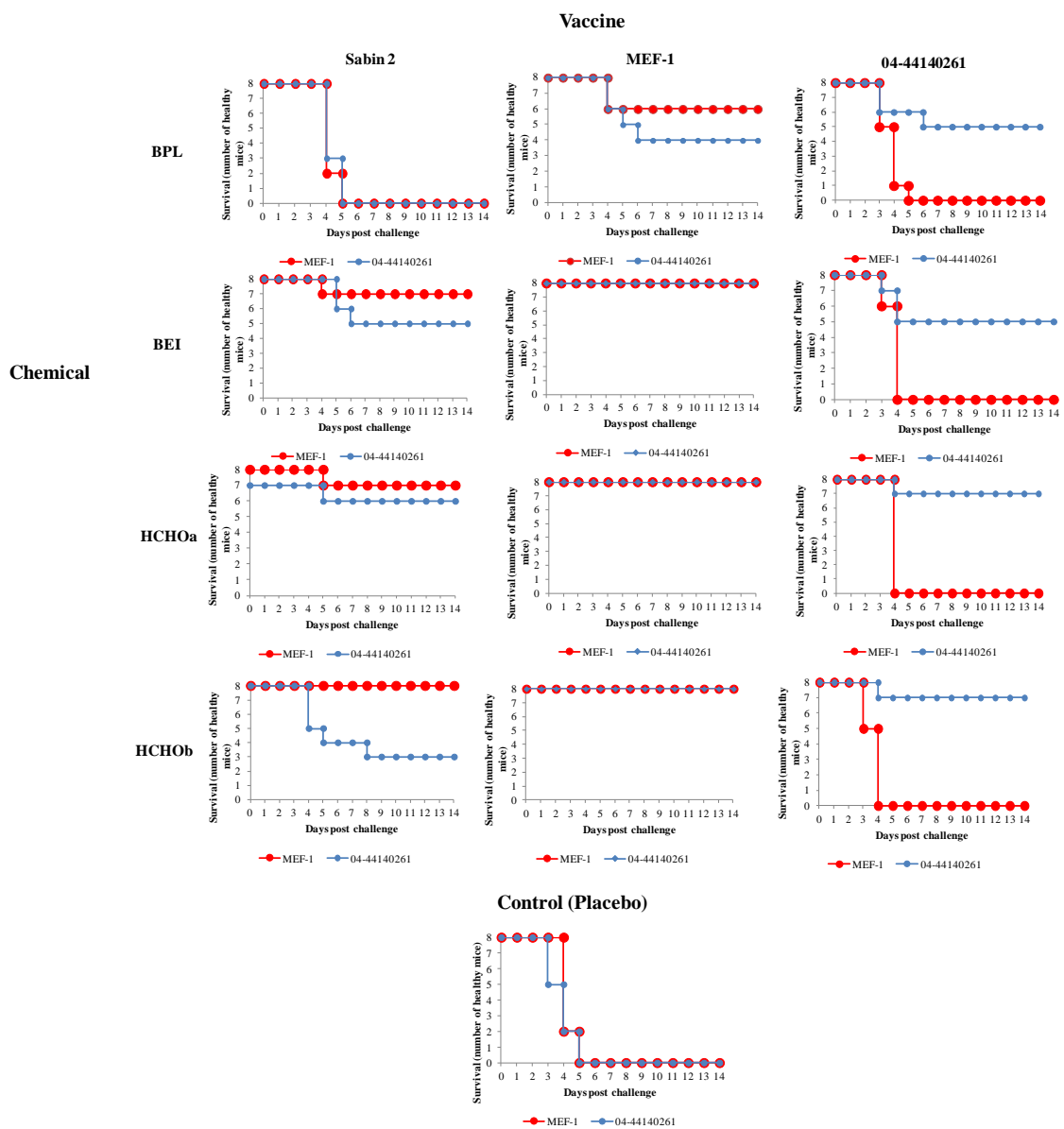


Figure 5.2. Protection conferred by inactivated poliovirus to transgenic mice.

Transgenic (Tg21-Bx) mice were immunised at 6-8 weeks with 2x2 D-Ag/ml doses of either BPL-, BEI-, or HCHO-inactivated preparations of three serotype 2 PV strains and were boosted at day 14. After a further 21

days, mice were challenged with a paralysing dose of either the MEF-1 strain or an iVDPV strain, 04-44140261. Mice were then monitored for any signs of paralysis for 14 days. Eagle's minimum essential medium was administered to mice as a placebo. For the HCHOa-inactivated Sabin 2 preparation one of the eight Tg21-Bx mice died before the test began. 1:4000 HCHO is abbreviated as HCHOa; 1:8000 HCHO is abbreviated as HCHOb.

Irrespective of the strain, the BPL-inactivated PV preparations conferred less protection against the challenge viruses than the HCHO- or BEI-inactivated preparations. The HCHO- and BEI-inactivated PV preparations conferred similar levels of protection to each other. Using the HCHOa-inactivated PV preparations as a reference, this was confirmed by a binary logistic regression analysis which found only the protection conferred by BPL-inactivated preparations to differ significantly from that conferred by the HCHOa-inactivated preparations ($P < 0.001$). The BPL-inactivated PV preparations were found to have low odds (5 %) of achieving a similar level of protection to the HCHOa-inactivated preparations. The BEI- and HCHOb-inactivated PV preparations had similar odds to the HCHOa-inactivated preparations of conferring protection (odds ratio of 0.58 and 0.67, respectively).

The MEF-1 preparations conferred the most protection to the mice against both challenges, while the number of mice protected following immunisation with the Sabin 2 preparations fell when challenged with the 04-44140261 strain. While the 04-44140261 preparations conferred protection to the mice when challenged with the 04-44140261 strain, no mice were protected when challenged with the MEF-1 strain. Using the MEF-1 preparations as a reference, this variation in protection conferred was confirmed by a binary logistic regression analysis which found that the protection conferred by Sabin 2 and 04-44140261 preparations was significantly different to the protection conferred by the MEF-1 preparations ($P < 0.001$). Both the Sabin 2 and the 04-44140261 preparations had low odds of achieving the level of protection conferred by the MEF-1 preparations (odds ratio of 0.06 and 0.02, respectively). This was most likely due to the specificity of protection conferred by the Sabin 2 and 04-44140261 preparations. As table 5.1 shows, the log₂ neutralisation titre of the sera from the immunised mice also showed specificity to the relevant challenge serotype 2 strain.

Inactivated preparation	Log 2 neutralisation titre		
	Sabin 2 challenge	MEF-1 challenge	04-44. challenge
HCHOa Sabin 2	11.0	9.5	5.0
HCHOb Sabin 2	10.5	9.2	<4.0
BEI Sabin 2	>11.5	10.0	4.5
BPL Sabin 2	9.2	6.5	<4.0
HCHOa MEF-1	10.7	10.7	6.7
HCHOb MEF-1	10.7	10.2	7.7
BEI MEF-1	11.0	11.2	5.2
BPL MEF-1	11.2	11.2	6.2
HCHOa 04-44.	4.7	<4.0	7.7
HCHOb 04-44.	5.2	5.0	8.5
BEI 04-44.	5.0	4.2	7.5
BPL 04-44.	<4.0	<4.0	<4.0

Table 5.1. Neutralisation titre of the sera from immunised transgenic mice against challenge viruses.

Transgenic (Tg21-Bx) mice were immunised at 6-8 weeks with 2x2 D-Ag/ml doses of either BPL-, BEI-, or HCHO-inactivated preparations of three serotype 2 PV strains and were boosted at day 14. After a further 21 days tail bleeds were obtained. The sera were challenged with 100 TCID₅₀ of three serotype 2 PV strains: Sabin 2, MEF-1 and 04-44140261 (04-44.) in a cell culture neutralisation assay. 1:4000 HCHO is abbreviated as HCHOa; 1:8000 HCHO is abbreviated as HCHOb.

The sera from mice immunised with MEF-1 and Sabin 2 preparations showed a lower log 2 neutralisation titre when challenged with the 04-44140261 strain, in comparison to when challenged with the Sabin 2 and MEF-1 strains. Conversely, sera from mice immunised with 04-44140261 preparations showed a higher log 2 neutralisation titre when challenged with the 04-44140261 strain, in comparison to when challenged with the Sabin 2 and MEF-1 strains. Analysis by balanced ANOVA (Minitab v.16, <http://www.minitab.com/en-GB/>) found that the log 2 neutralisation titre of sera from mice immunised with inactivated preparations of different PV strains and inactivation chemicals was significant between the strains for challenge viruses Sabin 2 and MEF-1 (P<0.001) and 04-44140261 (P<0.05). The specificity in protection conferred by the inactivated PV preparations (figure 5.2) suggested

that in both Wistar rats and Tg21-Bx mice, the low immune response induced by the inactivated preparations to the iVDPV strain (noted in section 3.2.2.2 of Chapter 3 and above in figure 5.1 and table 5.1) appeared to lead to less protection against disease.

For the BEI- and HCHO-inactivated PV preparations there was a good correlation between immune protection conferred on the Tg21-Bx mice and the neutralising antibody titres in the blood samples of the same mice. This confirms the previously documented significant contribution of the neutralising antibody response to the protection against paralytic poliomyelitis (486). However, for the BPL-inactivated PV preparations, there was a lack of correlation between the number of Tg21-Bx mice protected and the neutralising antibody titre in the blood samples taken from the same mice. For example, a high neutralising response did not correlate with full protection. Conversely, a low neutralising antibody titre was found in the sera of mice with near full protection. This result has been found previously in research with FMD vaccines (530)

5.2.2 Thermostability of inactivated poliovirus preparations

The thermostability of an IPV is a measure of its stability during long-term storage. Although the thermostability of the HCHO-inactivated serotype 2 cIPV has been determined, it is not clear whether inactivated PV preparations developed with BPL or BEI would have a similar thermostability. The thermostability of BPL-, BEI- and HCHO-inactivated preparations of the MEF-1 serotype 2 strain was assessed by determining the degradation of the viral antigenicity and immunogenicity of the preparations following treatment at 45 °C (Materials and Methods, section 2.2.5).

The thermostability of BPL-, BEI- and HCHO-inactivated MEF-1 preparations was assessed by heating the preparations at 45 °C for 24 h. The D-Ag of the heat-treated inactivated MEF-1 preparations was determined by an ELISA along with untreated inactivated MEF-1 preparations. All inactivated MEF-1 preparations showed a large reduction in D-Ag/ml following heat treatment. This reduction was most significant for the BPL-inactivated MEF-1 preparation (99 %), while the BEI-inactivated preparation showed the least reduction (81 %). The viral immunogenicity of the heat-treated and untreated MEF-1

preparations was determined by a rat potency test. This involved immunising Wistar rats with a 2 D-Ag/ml dose of untreated inactivated MEF-1 preparations and an equivalent volume of the heat-treated MEF-1 preparations. After 22 days, the rats were exsanguinated and their sera harvested. The sera were challenged with 100 TCID₅₀ of the serotype 2 PV strains; Sabin 2, MEF-1 and 04-44140261, in a cell culture neutralisation assay (Materials and Methods, section 2.2.4.1).

As table 5.2 shows, all inactivated MEF-1 preparations showed a reduction in immunogenicity following heat-treatment.

Inactivated MEF-1 preparation (chemical)	Log 2 neutralisation titre against challenge virus					
	Sabin 2		MEF-1		04-44140261	
	NT	HT	NT	HT	NT	HT
BPL	6.1	1.7	6.0	1.6	5.4	0.3
BEI	7.9	7.2	8.3	6.4	6.7	6.1
HCHO _a	8.4	5.7	8.5	5.2	7.5	4.2

Table 5.2. Reduction of viral immunogenicity of inactivated poliovirus following heat-treatment.

Beta-propiolactone-, BEI- and HCHO-inactivated MEF-1 preparations were incubated at 45 °C for 24 h. Viral immunogenicity of heated MEF-1 preparations was assessed along with untreated inactivated MEF-1 preparations by a rat potency test. Rats were immunised with 2 D-Ag/ml of untreated inactivated MEF-1 preparations and an equivalent volume of the heat-treated inactivated preparations. After 22 days, rats were exsanguinated and the sera were assayed for neutralising antibody to 100 TCID₅₀ of the relevant challenge virus using a fixed virus varying serum 50% end-point technique in a microtitre system. Challenge virus strains included: Sabin 2, MEF-1, and 04-44140261. NT indicates not heat-treated; HT indicates heat-treated; 1:4000 HCHO is abbreviated as HCHO_a.

Analysis by balanced ANOVA (Minitab v.16, <http://www.minitab.com/en-GB/>) found that the heat-treatment of inactivated MEF-1 preparations led to a significant difference in the immunogenicity of the MEF-1 preparations (P<0.001). This analysis also found that the variation in the immunogenicity of the heat-treated and untreated inactivated MEF-1 preparations was significant between the three inactivation chemicals (P<0.001). However,

grouping of these results by multiple comparison using the Tukey method (Minitab v.16, <http://www.minitab.com/en-GB/>) found that only the immune response of rats immunised with heat-treated and untreated BPL-inactivated MEF-1 preparations significantly differed to the immune responses elicited by the other inactivated preparations ($P < 0.05$). A comparison of the serum log₂ neutralisation titre of rats immunised with the untreated and heat-treated inactivated MEF-1 preparations found that BPL-inactivated preparations had the largest reduction in titre following heat-treatment. In comparison, the sera of rats immunised with BEI-inactivated MEF-1 preparations had the least loss in log₂ neutralisation titre following heat-treatment. Following heat-treatment, the reduction in the log₂ neutralisation titre of the sera of rats immunised with HCHO-inactivated MEF-1 preparations fell between that of the sera of rats immunised with BPL- and BEI-inactivated preparations. These findings suggest that the BEI-inactivated MEF-1 preparation had a greater thermostability than HCHO- and BPL-inactivated preparations.

To further assess the thermostability of inactivated PV preparations, the reduction of the viral immunogenicity following treatment at 45 °C was determined using Tg21-Bx mice. Formaldehyde-inactivated preparations (1:4000 HCHO) of the Sabin 2, MEF-1 and 04-44140261 strains were incubated at 45 °C for 24 h. Groups of eight Tg21-Bx mice were immunised at 6-8 weeks with 2x2 D-Ag/ml untreated HCHO-inactivated PV preparations and an equivalent volume of the heat-treated preparations and received a booster at day 14. After a further 21 days, the Tg21-Bx mice were challenged with 50 PD₅₀ of either the MEF-1 strain or an iVDPV strain, 04-44140261, at day 35. Mice were then monitored for any signs of paralysis for 14 days. Blood samples were obtained before the challenge and the sera were assayed to measure neutralising antibody to 100 TCID₅₀ of the relevant challenge virus using a fixed virus varying serum 50 % end-point technique in a microtitre system. Sera were challenged with Sabin 2, MEF-1 and 04-44140261 strains.

As table 5.3 shows, both the serum log 2 neutralisation titre of the mice and the protective properties of the inactivated PV preparations fell following heat-treatment.

HCHO preparation	Treatment	Challenge poliovirus strain (100 TCID ₅₀)				
		Sabin 2	MEF-1		04-44140261	
		Log 2 Neut. titre	Log 2 Neut. titre	Protect. (/8)	Log 2 Neut. titre	Protect. (/8)
Sabin 2	NT	11.0	9.5	7	5.0	6*
	HT	9.5	8.0	0	<4.0	0
MEF-1	NT	10.7	10.7	8	6.7	8
	HT	9.0	8.0	6	<4.0	5
04-44140.	NT	4.7	<4.0	0	7.7	7
	HT	<4.0	<4.0	0	<4.0	2

Table 5.3. Immunogenicity of untreated and heat-treated formaldehyde-inactivated poliovirus in transgenic mice.

Formaldehyde-inactivated preparations (1:4000 HCHO) of the Sabin 2, MEF-1 and 04-44140261 (04-44140.) strains were incubated at 45 °C for 24 h. Viral immunogenicity of heat-treated and untreated HCHO-inactivated PV preparations was assessed by a series of immunisation-challenge experiments and a neutralisation assay. Transgenic (Tg21-Bx) mice were immunised at 6-8 weeks with 2x2 D-Ag/ml doses of the untreated HCHO-inactivated PV preparations and an equivalent volume of heat-treated preparations. Mice were boosted at day 14. After a further 21 days mice were challenged with paralysing doses of either the MEF-1 strain or an iVDPV strain, 04-44140261. Mice were then monitored for 14 days for any signs of paralysis. Tail bleeds were obtained from the mice before they were challenged. The sera were challenged with 100 TCID₅₀ of three serotype 2 PV strains, Sabin 2, MEF-1 and 04-44140261, in a cell culture neutralisation assay. NT indicates not heat-treated; HT indicates heat-treated. *, One of the eight Tg21-Bx mice died before the test began.

The sera of mice immunised with the three HCHO-inactivated serotype 2 PV preparations showed a similar reduction in the log 2 neutralisation titre following heat-treatment. A grouping analysis of these results by multiple comparison using the Tukey method (Minitab v.16, <http://www.minitab.com/en-GB/>) found that only the immune response of mice immunised with 04-44140261 preparations was significantly lower than the immune response elicited by the other strains (P<0.05). For many of the HCHO-inactivated PV preparations, there was a good correlation between the drop in the protection conferred to the Tg21-Bx

mice and the drop in the neutralising antibody titres in the blood samples following heat-treatment, confirming the previous finding that the neutralisation antibody response contributes significantly to the protection against poliomyelitis (486). However there was not complete correlation between the levels of antibodies in the mice sera and the protection conferred against some challenge strains. For example mice immunised with the heat-treated HCHO-inactivated Sabin 2 preparation showed a good serum neutralisation titre when challenged with the MEF-1 strain, but none were protected against a direct challenge with this strain.

5.3 DISCUSSION

Research in Chapter 3 described how inactivation with HCHO resulted in a significant loss of immunogenicity, possibly due to a partial modification of antigenic site 1. To improve the immunogenicity of the IPVs, BPL and BEI were selected to inactivate PV, as they inactivate by alternative mechanisms to that of HCHO. Research in the previous chapter detailed that these two chemicals resulted in different modifications to the antigenic structure of PV from those inactivated with HCHO. The effect of the different modifications to the antigenic structure conferred by these three chemicals on the immunogenicity of PV was determined.

The immunogenicity of MEF-1 preparations inactivated with the three chemicals was assessed by a rat potency assay. Both the BEI- and HCHO-inactivated MEF-1 induced similar titres of neutralising antibodies which were higher than that induced by the BPL-inactivated MEF-1, indicating that they were more immunogenic. The BPL-inactivated MEF-1 showed the lowest immunogenicity of the inactivated MEF-1 preparations. This low immunogenicity, despite the lack of any significant modification to the antigenic sites (Chapter 4), indicates that changes to the antigenic structure of PV do not alone account for the immunogenicity of inactivated PV.

The immunogenicity of the inactivated serotype 2 PV preparations generated with different inactivation chemicals was further assessed by a series of immunisation-challenge experiments using Tg21-Bx mice. For all serotype 2 strains, BPL-inactivated PV preparations

conferred less protection than HCHO- and BEI-inactivated preparations which conferred similar levels of protection. This finding confirmed that of the rat potency assay, further indicating that modifications to the antigenic structure are not solely responsible for the immunogenicity of inactivated PV.

The findings of a series of immunisation-challenge experiments and neutralisation assays with Tg21-Bx mice indicated that for the BEI- and HCHO-inactivated PV preparations, there was a good correlation between number of mice protected and the titre of serum neutralising antibodies in the same mice. This indicated that the immune protection against PV is significantly mediated by neutralising antibodies. However, for the BPL-inactivated PV preparations, there was a lack of correlation between the number of mice protected and the neutralising antibody titre. In some cases, all mice were protected against challenge viruses, despite having low serum neutralising antibody titres. It is possible that the full protection conferred to the mice, in spite of the low neutralising antibodies in the sera was a result of other aspects of the immune response, such as the innate immune system and the T-cell response. The innate immune system acts as the earliest response to immunised IPV or PV and regulates the adaptive immune response. For example, following IPV or PV immunisation, the nuclear factor kappa B is activated which, in turn, activates interferon- β (IFN- β). This leads to the expression of a number of proinflammatory cytokines (383). In humans and in mouse models, CD4+ T cells responses are triggered following immunisation with IPV. These cells can recognise distinct T-cell epitopes in all four capsid proteins, in particular a T-cell epitope in VP1 which is located near a neutralising B-cell epitope (249, 306). It has been demonstrated that Th1 cells can mediate a protective immune response against PV infection *in vivo* through helper activity for humoral (antibody) immunity (307). As both the innate immune system and the T cells contribute to the immune response to IPV and PV immunisation, it may be necessary to introduce means to assess these aspects of the immune response. Both flow cytometry and the enzyme-linked immunosorbent spot assay could be used to characterise the cellular T-cell responses and the contributions of innate immunity, in addition to the antibody B-cell response (20, 47, 477).

The thermostability of inactivated MEF-1 preparations generated with BPL, BEI and HCHO was determined to vary significantly ($P < 0.001$). These findings indicated that inactivation with BEI resulted in a preparation with greater thermostability, a finding that could be further explored by carrying out a full-scale accelerated degradation study.

Inactivated PV preparations generated with different chemicals would be subjected to a range of elevated temperatures at which significant and detectable degradation is induced in a short time. The rate at which it occurs would be measured and extrapolations would be made to the lower temperature (i.e. +4 °C) at which the preparations are stored, in accordance with the Arrhenius equation (513).

The thermostability of HCHO-inactivated PV preparations was further assessed by determining the loss of immunogenicity of different inactivated serotype 2 strains following heat-treatment. A series of immunisation-challenge experiments and a neutralisation assay of Tg21-Bx mice found that loss in neutralising antibody titre and protective properties of the PV preparations was similar for the different strains. Against some challenge PV strains, the HCHO-inactivated Sabin 2 and MEF-1 preparations lacked correlation between the drop in the immune protection conferred to the Tg21-Bx mice and the drop in the serum neutralising antibody titres following heat-treatment. For some inactivated PV preparations, there was a lack of protection, despite high neutralising antibody titres remaining after heat-treatment. Although there is not a large drop in neutralising antibodies following heat-treatment, other aspects of the immune response in the mice are likely to have been affected by the heat-treatment. The heat-treatment may have resulted in an alteration or reduction in the innate and cell immune responses which would have a knock-on effect on the protection conferred to the mice. For some inactivated PV preparations, nearly full protection was conferred, despite the sera of immunised mice showing a large reduction in neutralising antibodies following heat-treatment. As discussed above this is likely to be due to other aspects of the immune response (innate and cell mediated immunity) contributing to the overall protective immune response.

CHAPTER 6

MOLECULAR PROPERTIES OF INACTIVATED POLIOVIRUS

6.1 INTRODUCTION

Research detailed within the previous chapters has shown that treatment of infectious PV containing material with inactivation chemicals irreversibly eliminates the infectivity and causes a reduction in the immunogenicity. However, it is not clear how treatment with inactivation chemicals achieves this. Although some hypotheses have been discussed (180), the molecular mechanisms that underlie the inactivation of PV have not been explored. Such research could help to explain the differences that have been found between serotype 2 cIPV and sIPV and, eventually, lead to the development of improved IPVs for the post-eradication era. In order to gain greater understanding of the molecular mechanisms that underlie the inactivation of PV, this chapter will focus on the effect of inactivation on essential biological properties of PV. The interaction between PV and its cellular receptor; the subsequent conformational changes which accompany or precede viral entry; and the functionality of the viral RNA are all essential properties which are integral to the cellular life cycle of PV (Introduction, section 1.1.4). The effect of inactivation on these properties of PV was analysed using a series of novel assays.

6.1.1 Interaction between poliovirus and the poliovirus receptor

Early PV research indicated that susceptible cells possess a receptor entity which allows PV attachment and mediates infection (213, 214). For example, it was shown that human tissue homogenates or cell lines infectable by PV harbour binding activity, while non-susceptible murine cells are unable to bind PV (479). Biochemical analyses determined that the receptor entity was protein in nature, as proteinases (e.g. trypsin) and denaturing agents could destroy its binding activity (213). Subsequent transformation-based research determined that sensitivity to PV was a genetic trait which could be transmitted to non-susceptible cells and was, therefore, an autosomal trait encoded by the human genome (328). The human PVR gene was isolated by transfer of human DNA into murine L cells, isolation of transfectants which bind an anti-receptor MAb and are infectable with PV, and subsequent rescue of human sequences linked to Alu repeats (329). All three PV serotypes bound to the receptor encoded by this gene (535). Analysis of this gene and human genomic DNA characterised PVR as CD155 (479) which is a glycosylated single-span cell surface molecule

belonging to the Ig super family (429). The CD155 protein is made up of three successive Ig-like domains (D1, D2 and D3), a transmembrane domain and a C-terminal cytoplasmic domain (37, 574) (figure 6.1).

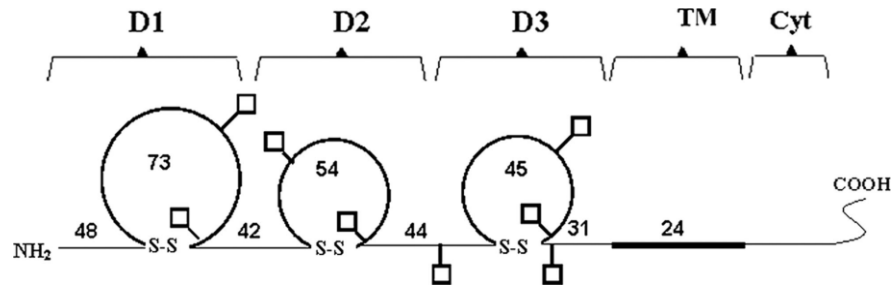


Figure 6.1. Schematic diagram of human CD155 α .

The CD155 protein is made up of three Ig-like domains (D1, D2 and D3), a transmembrane domain (TM) and a C-terminal cytoplasmic domain (Cyt) (37, 574). Adapted from Zhang *et al.* (574).

The expression of the human CD155 gene yields four splice variants (α , β , γ , and δ). All variants have identical extracellular domains, but isotypes β and γ lack a transmembrane domain and are secreted. Isotypes α and δ only differ in their cytoplasmic domain and can function as PVRs (265, 429). It is not clear what the cellular functions of CD155 are, but it is closely related to nectin, a component of intracellular junctions, and has been implicated in a range of cellular interactions and functions (36). These include cell-cell interactions (51, 463); interactions with extracellular matrix proteins (285); cell migration (177, 476) and natural killer cell function (36, 51). Mutational analysis of the cDNA of CD155 in murine cell lines has determined that the amino terminal domain, D1, is responsible for virus recognition (38, 266, 352, 460, 461).

Knowledge of the three-dimensional structure of the PV capsid (162, 209) and the availability of the cDNA of CD155 (or PVR) (329) has allowed the interaction of the PVR with PV to be studied in depth. A range of genetic approaches have been used to analyse this interaction. Poliovirus mutants which showed resistance to neutralisation with a sPVR or the ability to utilise mutant PVR were selected for (108, 109, 296). Other PV mutants were generated by site-directed mutagenesis (200). Analysis of these mutants indicated that the main contact site of the PVR on the PV capsid is the floor of the canyon, above the hydrocarbon-binding pocket, and on the outer (“south”) rim of the canyon (34) (Introduction, Figure 1.3). Cryo-electron microscopy (cryo-EM) and three dimensional image-

reconstruction techniques of the complex between PV and the ectodomain of its receptor at $\sim 22\text{-}\text{\AA}$ resolution confirmed this (34, 201, 563). As did the fitting of the crystal structure of an unglycosylated form of a two-domain construct of the PVR into $\approx 8.5\text{-}\text{\AA}$ resolution cryo-EM reconstructions of the PV-PVR complexes for the three PV serotypes (574). The complementarity between PV and PVR in the contact regions, indicated that the initial binding occurs without significant structural changes in the PV (292).

The interaction between PV and PVR is biphasic with two classes of binding sites (K_{D1} and K_{D2}) for the PVR on PV. At low temperatures the K_{D1} site dominates with a dissociation constant (K_d) of approximately 10^{-6} M. The fraction of K_{D2} sites, with a K_d of approximately 10^{-7} M, increases with temperature and constitutes 50 % of the sites at 20 °C (292, 317). Given that the K_{D2} binding sites require a higher temperature, it is possible that reversible conformational changes in the virus and / or receptor precede the formation of the higher-affinity PV-PVR complex (292). A receptor-decorated liposome model system was used with cryo-EM and cryo-electron tomography (cryo-ET) methods at $\sim 30\text{ }\text{\AA}$ resolution to solve the structure of a PV-PVR-membrane complex at room temperature (49, 65). The structure shows that five copies of membrane-bound receptor are bound by a PV, bringing one of the five-fold mesas in close proximity to the membrane (292).

With the advent of the cloning of cDNA of human PVR, it has become possible to express sPVR in cell systems. For example, Kaplan *et al.* (246) developed a recombinant *Autographa californica* nuclear polyhedrosis virus containing the PVR cDNA. This was used to infect *Spodoptera frugiperda* IPLB-SF-21 cells which were then solubilised to release the sPVR (246). A number of expression vectors have been designed to express PVR in mammalian cells (201, 317), one of which was designed by He *et al.* (201) who expressed CD155 in 293 cells. Briefly, the coding region of the 337 N-terminal codons of CD155 was fused to the N-terminal coding region of human placental AP and a recombinant plasmid, pCD155-AP, was generated. This recombinant plasmid was used to generate 293 cells expressing CD155-AP as a soluble fusion protein (201). As CD155-AP binds to infectious PV virions, it can be used to quantitatively study receptor binding (354). The CD155-AP fusion protein expressed using 293-CD155-AP cells was used in this chapter.

As noted above it is possible to render cell lines susceptible to PV by transfecting relevant regions of the DNA of cells sensitive to PV to non-susceptible cells. Non-susceptible mouse

Ltk⁻ aprt⁻ cells have been transformed with HeLa cell (human) DNA to generate a cloned cell line which was susceptible to infection with all three PV serotypes (328). This cloned line has been used to establish several cell lines (265, 408). Pipkin *et al.* (408) established and characterised one of these derived cell lines, L20B cells. The expression of the PVR on the cell surface renders L20B cells susceptible to infection by PV, with the development of typical CPEs. Being cells of murine origin, very few other human enteric viruses are able to produce a productive infection (408, 542). The use of L20B cells as a means to simplify the primary diagnosis of PV from clinical samples has been assessed and, as a result, L20B cells have been introduced for routine use by the WHO global PV network laboratories (542). Given the high sensitivity of this cell line to recognise and bind PV, L20B cells can be used to explore the interaction between PV and the PVR.

6.1.2 Entry of poliovirus into host cell

After binding to PVRs, PV virions must undergo a series of conformational changes (summarised in figure 6.2) to enter a host cell.

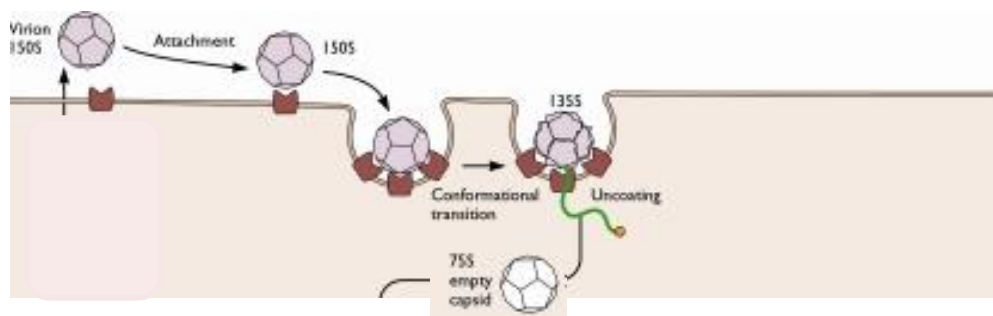


Figure 6.2. Schematic of poliovirus entry into a host cell.

On binding to the PVR at physiological temperature, PV virions (150/160S) undergo a conformational transition to 135S particles. Some or all of the normally internal VP4 and amino-terminal extension of VP1 are externalised in 135S particles. A second conformational change results in ejection of the viral RNA and in the production of an empty particle which sediments at 75/80S. Adapted from Hogle (208).

The binding of PV to the PVR at physiological temperature catalyses conformational changes which result in the formation of altered (or A) particles. These particles sediment in sucrose gradients more slowly (135S) than native PV virions (160S) and, thus, are sometimes called

135S particles (511). The 135S particles have externalised some or all of the normally internal VP4 and amino-terminal extension of VP1, but retain the full complement of genomic RNA (121, 173, 191). In contrast to mature virions, 135S particles are antigenically distinct and are susceptible to proteases (154, 174, 510). Although 135S particles lack the ability to bind to the PVR, they are still capable of infecting cells in a receptor-independent fashion (113). As they cannot bind to the PVR, 135S particles cannot concentrate at the surface of cells and, consequently, have a low infection efficiency. This efficiency can be brought within an order magnitude of that of PV virions by binding the 135S particles to non-neutralising antibodies and initiating infection in Fc expressing cells (227). This indicates that the 135S particles act as intermediates in the cell entry process (113, 227).

Even in the absence of a receptor, mature PV virions have been found to transiently and reversibly externalise VP4 and the N-terminus of VP1, when incubated at physiological temperatures by a “breathing” process (294). Kinetic studies which analysed the rate of virus to 135S particle conversion in PV as a function of temperature in the presence and absence of the PVR have found that a large energy barrier (enthalpy of activation) traps PV particles in their native state, and that receptor binding lowers this barrier (508). These studies indicate that it is a combination of both physiological temperature and receptor binding which releases the virus particle from its metastable state and catalyses irreversible conformational changes (511). Mature PV particles can be induced to form 135S particles by incubating them with membrane extracts (120), solubilised PVR (187, 246) and soluble ectodomains of the PVR (19).

Following the formation of the 135S particle, the PV undergoes a second conformational change where the viral RNA is ejected, resulting in the production of an empty particle which sediments at 80S (173, 510). This particle is antigenically distinct from the PV virion and the 135S particles (173, 510). High resolution cryo-EM reconstructions (~9.5 Å) have been produced for the 80S particles of PV (293). Two structures made up the 80S preparations, one of which contained more density, corresponding to RNA inside, than the other. In both preparations the inter-pentamer and inter-protomer interfaces had disruptions (293). A small number of the 80S particles were caught in the act of releasing RNA (50, 293). A contiguous RNA-like density on the inside and outside surfaces of the 80S particles was confirmed by asymmetric three-dimensional reconstructions using cryo-EM and cryo-ET. This analysis

found that the RNA exits from openings approximately 20 Å away from the two-fold axis (50).

While it is not clear how PV is able to breach the cell membrane, structural analyses of PV virions, 135S and 80S particles have highlighted several capsid structures that may be involved in membrane interaction and permeabilisation, including VP4 and the N-terminus of VP1. The hydrophobic N-terminus of VP1 that is externalised in 135S particles may be able to induce membrane permeability, as it can interact with membranes (173, 510). Both cellular and liposome membranes have been found to interact with PV VP4 released during the conversion to 135S particles (116, 510). Electrophysiology experiments with PV particles containing VP4 mutants have suggested that a proposed VP4 membrane channel may be critical for PV entry and infection. These mutations which alter or prevent channel formation in model membranes, delay or prevent the delivery of viral RNA into the cytoplasm of cells (116). Such research has led to the development of a membrane penetration model which is described in detail elsewhere (64, 511). Briefly, receptor binding results in conformational conversion to 135S particles with the externalisation of VP4 and the N-terminus of VP1. The 135S particles dissociate from the receptor and directly interact with the membrane via the externalised N-terminus of VP1. Released VP4 also interacts with the membrane at this time. A membrane pore is formed by VP1 and/or VP4, through which the genomic RNA is transported into the cytoplasm (511).

6.1.3 Viral RNA of poliovirus

After the PV particles have undergone conformational changes to enter a cell, the viral genome is essential for subsequent steps in the replication cycle (Introduction, section 1.1.4). As a positive-stranded RNA virus, the genome of PV is infectious as naked RNA (10, 385). Although HCHO, BPL and ethyleneimines have all been found to interact with RNA, it has not been determined whether these chemicals can even reach the viral RNA during inactivation, although some hypotheses have been discussed (61, 156, 180, 204). While previous research has found that treatment of tissue samples with HCHO reduces the amount of detectable RNA, there has been little research concerning the effect of inactivation on viral RNA (106, 122). The biological activity of viral RNA of inactivated PV was assessed in this

chapter. The functionality of the viral RNA following inactivation was analysed by RT-PCRs.

While a considerable amount of research has been carried out to explore the interaction between PV and the PVR and the entry of PV into cells, as of yet it is not known whether PV is still able to bind to the PVR and undergo the necessary conformational changes following inactivation. The minor modification to the antigenic structure of PV following inactivation (Chapters 3 and 4) suggests that inactivated PV may still be able to bind to the PVR. Even if this is the case, it is likely that inactivation will modify this interaction, particularly if capsid proteins are cross-linked or modified during the process. Such modification could also affect the subsequent conformational changes that virions undergo. This chapter describes the use of the soluble CD155-AP fusion protein to directly assess whether inactivated PV was able to bind to the PVR. The ability of inactivated PV to recognise and bind to susceptible L20B cells was determined by a novel FACS flow cytometry assay and a real-time RT-PCR binding assay. Previous research has shown that by incubating PV virions at high temperatures in hypotonic medium, it is possible to trigger conformational changes to 135S and 80S particles (50, 113). Assays which assess the presence of viral RNA and the antigenic and binding properties can be used to assess whether virions have undergone conformational changes. This approach was adopted to determine whether inactivated PV could undergo the conformational changes to form 135S and 80S particles. A series of RT-PCRs which were used to explore what effect the chemicals had on the functionality of the viral RNA are detailed.

6.2 RESULTS

6.2.1 Effect of inactivation on the interaction between poliovirus and soluble poliovirus receptor

6.2.1.1 Optimisation and quantification of CD155-AP secretion by 293-CD155-AP cells

As previous research has shown that soluble derivatives of CD155 are able to recognise and bind PV (201, 246, 317), a number of novel assays were carried out to assess whether PV

could still bind to expressed sPVR post-inactivation. These studies were done with 293-CD155-AP cells expressing a CD155-AP fusion protein. In order to ensure that sufficient quantities of CD155-AP were available, the secretion of this fusion protein by 293-CD155-AP cells was optimised by culturing 293-CD155-AP cells of 90 % confluence in different media over a six-day period, with aliquots being taken on a daily basis (Materials and Methods, section 2.2.6.1). As a control, 293-T cells which do not express CD155-AP, were cultured under the same conditions. The amount of CD155-AP secreted was quantified by a colorimetric AP determination assay (Materials and Methods, section 2.2.6.1)

As figure 6.3 shows, the secretion of the CD155-AP fusion protein varied with different culture media.

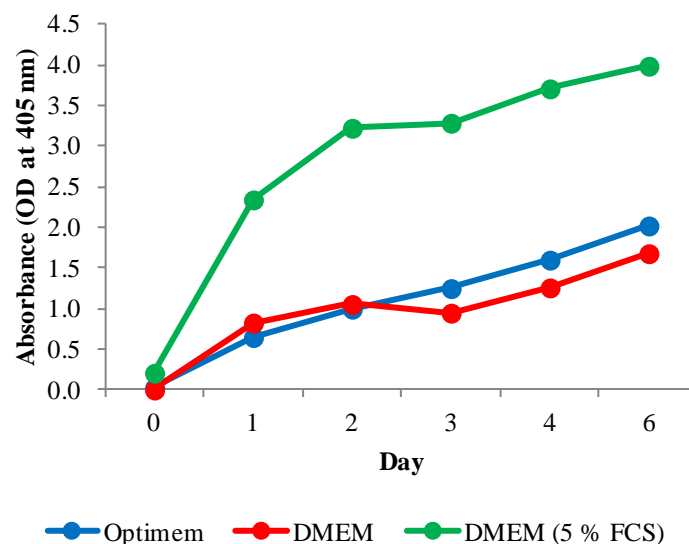


Figure 6.3. Optimisation of CD155-AP secretion by confluent 293-CD155-AP cells.

The 293-CD155-AP cells were grown to 90-100 % confluence on DMEM (with 5 % FCS, 1 % L-glu, 1 % P-S). Medium was replaced with either Optimem, DMEM or DMEM (with 5 % FCS) and cells were incubated at 35 °C for six days. Aliquots were taken on a daily basis and were analysed by a colorimetric AP determination assay.

The incubation of confluent 293-CD155-AP cells in DMEM supplemented with 5 % FCS resulted in a greater quantity of CD155-AP being expressed than when 293-CD155-AP cells were incubated in OPTIMEM or DMEM. Day six of the time-course was the optimal time to

harvest the supernatant containing the CD155-AP, when secretion of CD155-AP peaked. The lack of any increase in secreted CD155-AP for 293-T cells confirmed these results.

6.2.1.2 Neutralisation of poliovirus by secreted CD155-AP

To determine whether the expressed CD155-AP was biologically active, the ability of the secreted receptor to bind and neutralise PV was assessed by TCID₅₀ and plaque assays (Materials and Methods, section 2.2.6.1). Ten-fold serial dilutions (TCID₅₀) or 100 PFU (plaque assay) of the Sabin 2 and MEF-1 serotype 2 strains were incubated with increasing concentrations of CD155-AP in maintenance medium for 60 min at room temperature (18-20 °C), followed by 60 min at 37 °C. The virus titre was then determined on HEp-2C cell monolayers. The supernatant of 293-T cells was used as a negative control. The results of both assays are shown in table 6.1 and figure 6.4.

CD155-AP (µg / 50 µl)	Log10 titre reduction of virus (TCID ₅₀ / 50 µl Log10)	
	Sabin 2	MEF-1
No CD155-AP	0.0 ± 0.0	0.0 ± 0.0
0.02	0.6 ± 0.2	0.0 ± 0.0
0.08	1.1 ± 0.0	1.0 ± 0.3
0.40	3.3 ± 0.2	2.0 ± 0.1
2.00	3.8 ± 0.1	3.5 ± 0.1
10.00	5.1 ± 0.3	4.5 ± 0.1

Table 6.1. Neutralisation of infectious poliovirus by expressed CD155-AP.

Serial dilutions of live Sabin 2 and MEF-1 strains were incubated with increasing concentrations of CD155-AP at room temperature for 60 min and then at 37°C for 60 min. Virus titre was determined by a TCID₅₀ assay on a HEp-2C cell monolayer. The supernatant of 293-T cells, which lack the ability to express CD155-AP, were used as a negative control. The average of two assays is shown with the standard error.

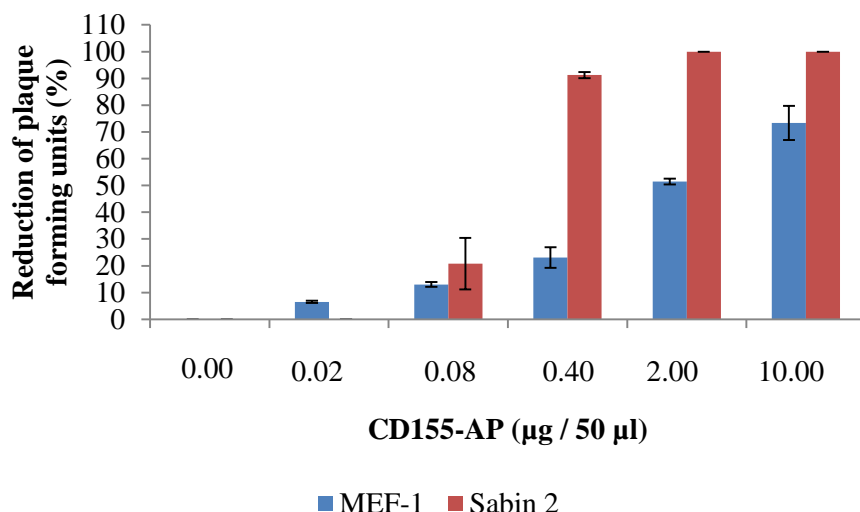


Figure 6.4. Reduction of plaque forming units by neutralisation with CD155-AP.

One hundred PFU of live Sabin 2 and MEF-1 strains were incubated with increasing concentrations of CD155-AP at room temperature for 60 min and then at 37°C for 60 min. Virus titre was determined by a plaque assay on a HEp-2C cell monolayer. The average of two assays is shown with the standard error.

As table 6.1 and figure 6.4 show, both PV strains were neutralised by CD155-AP. The Sabin 2 strain was more readily neutralised than the MEF-1 strain. For example, the TCID₅₀ assay found that the Sabin 2 strain showed up to five log₁₀s of neutralisation, while the MEF-1 showed 4.5 log₁₀s. This might indicate that the Sabin 2 and MEF-1 strains differed in their affinity to bind to CD155-AP. Alternatively, the ability of CD155-AP to neutralise a PV strain might have been related to an effect on the virus-cell entry.

6.2.1.3 Use of CD155-AP to assess the interaction between poliovirus and the poliovirus receptor

An AP assay which incorporated a sucrose cushion was devised to quantitatively determine the interaction of the Sabin 2 and MEF-1 serotype 2 strains with CD155-AP (Materials and Methods, section 2.2.6.1). The conditions for this assay were established using a live preparation of the Sabin 2 serotype 2 strain. Increasing concentrations of CD155-AP were incubated with the live Sabin 2 strain (4×10^8 TCID₅₀ / 100 µl) for 120 min at +4 °C. The PV-CD155-AP preparation was then ultracentrifuged through a 30 % sucrose cushion in conditions that are known to allow PV virions to pass through the cushion, while other

proteins do not. The resulting pellets were resuspended in Tris-HCl (0.01 M) and the amount of bound CD155-AP quantified by a colorimetric AP determination assay (Materials and Methods, section 2.2.6.1).

As figure 6.5 shows, using this assay it was possible to measure the interaction between the Sabin 2 strain and CD155-AP. This interaction increased as the concentration of CD155-AP rose. Control preparations of either Sabin 2 or CD155-AP alone were also ultracentrifuged. These preparations showed no absorbance (data not shown), confirming the interaction between the PV strain and the CD155-AP.

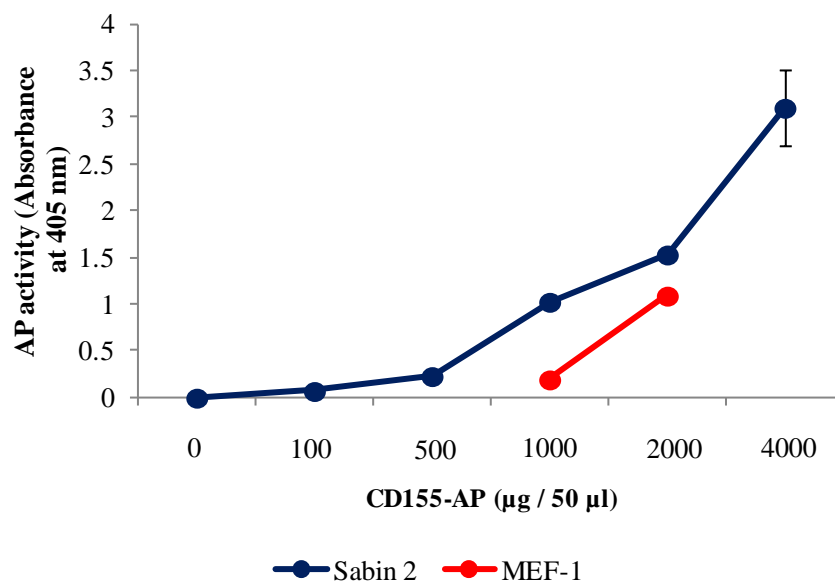


Figure 6.5. Analysis of the interaction between poliovirus and poliovirus receptor by an alkaline phosphatase assay.

Increasing concentrations of CD155-AP were incubated with live preparations of the Sabin 2 and MEF-1 strains for 120 min at +4 °C, before being ultracentrifuged through a 30 % sucrose cushion. The resulting pellets were resuspended in Tris-HCl and the amount of bound CD155-AP was quantified by an AP colorimetric assay. Only two concentrations of CD155-AP were incubated with the MEF-1 strain. Average of two preparations is shown with error bars.

The conditions for this assay were further optimised using the MEF-1 serotype 2 strain (Materials and Methods, section 2.2.6.1). As figure 6.5 shows, the AP assay measured a positive interaction between MEF-1 and CD155-AP. As with the findings of the

neutralisation assays described above, the MEF-1 strain was found to have a lower affinity than the Sabin 2 strain to bind to CD155-AP.

The interaction between HCHO-inactivated Sabin 2 or MEF-1 and CD155-AP was analysed in the same manner (Materials and Methods, section 2.2.6.1). A single concentration of live and HCHO-inactivated Sabin 2 and MEF-1 was incubated with different concentrations of CD155-AP (1000 and 2000 $\mu\text{g} / 50 \mu\text{l}$, respectively) for 120 min at +4 °C. A greater concentration of CD155-AP was incubated with the MEF-1 preparations to compensate for the lower binding affinity of this strain (figure 6.4). The PV-CD155-AP preparations were then ultracentrifuged through a 30 % sucrose cushion. The resulting pellets were resuspended in Tris-HCl (0.01 M) before the amount of bound CD155-AP was quantified by a colorimetric AP determination assay (Materials and Methods, section 2.2.6.1).

As figure 6.6 shows, both live and HCHO-inactivated Sabin 2 and MEF-1 bound to the secreted CD155-AP.

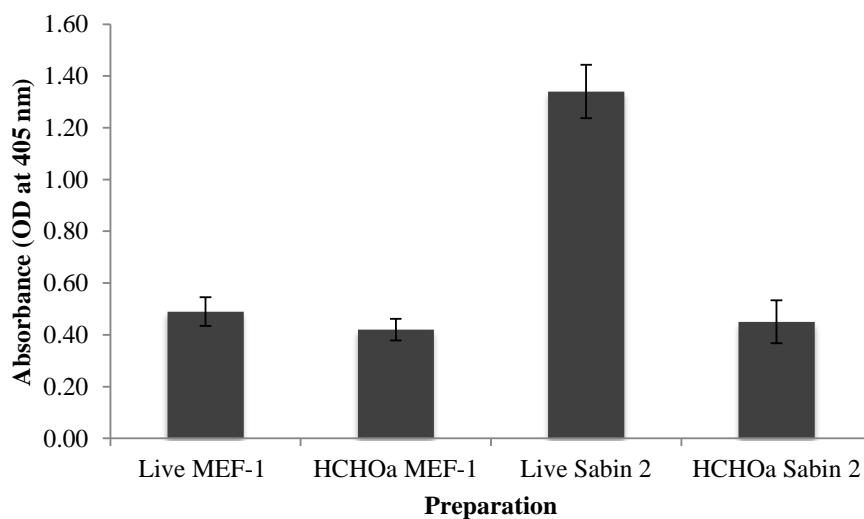


Figure 6.6. Analysis of the interaction between live or inactivated poliovirus and poliovirus receptor.

Either 1000 or 2000 $\mu\text{g} / 50 \mu\text{l}$ of CD155-AP were incubated with live or HCHO-inactivated Sabin 2 or MEF-1 preparations (respectively), for 120 min at +4 °C, before being ultracentrifuged through a 30 % sucrose cushion. The resulting pellets were resuspended in Tris-HCl and the amount of bound CD155-AP was quantified by a colorimetric AP assay. The average of three determinations is shown as bar with the standard error. 1:4000 HCHO is abbreviated as HCHOa.

Compared to the live preparations of each strain, a lower quantity of the inactivated preparations was bound to the CD155-AP. Analysis by balanced ANOVA (Minitab v.16, <http://www.minitab.com/en-GB/>) found that this reduction in the amount of bound PV following inactivation was significant ($P < 0.001$). The reduction in the amount of PV bound to CD155-AP following inactivation differed between the two strains. The MEF-1 strain showed a 14 % reduction in bound PV, while the Sabin 2 strain showed a 66 % reduction.

6.2.1.4 Determination of poliovirus-poliovirus receptor interaction by surface plasmon resonance

A biosensor-based analytical system could be used to examine the effect of inactivation on the interaction between PV and its cellular receptor. This technique directly analyses an interaction between a ligand and an analyte in real-time. A protocol was devised to determine whether the biosensor system could be used to detect the binding between HCHO-inactivated PV and its cellular receptor (Materials and Methods, section 2.2.6.1). This protocol used the Biacore 2000 biosensor instrument (GE Healthcare). Similar to the biosensor protocol developed to assess the potency of commercial IPVs (Chapter 4, section 4.2.4), the immobilisation and regenerations steps of this protocol were optimised using the relevant scouting programs. A wild-type trivalent IPV was immobilised to a CM3 sensor chip by amine coupling, before two-fold serial dilutions of CD155-AP were injected over the surface of the chip. The interaction between these dilutions and the immobilised IPV was monitored in real-time by SPR. As figure 6.7 A and B shows, the biosensor system detected the interaction between the trivalent IPV and the diluted CD155-AP in a dose-dependent manner, confirming that inactivated PV was still able to bind to the PVR.

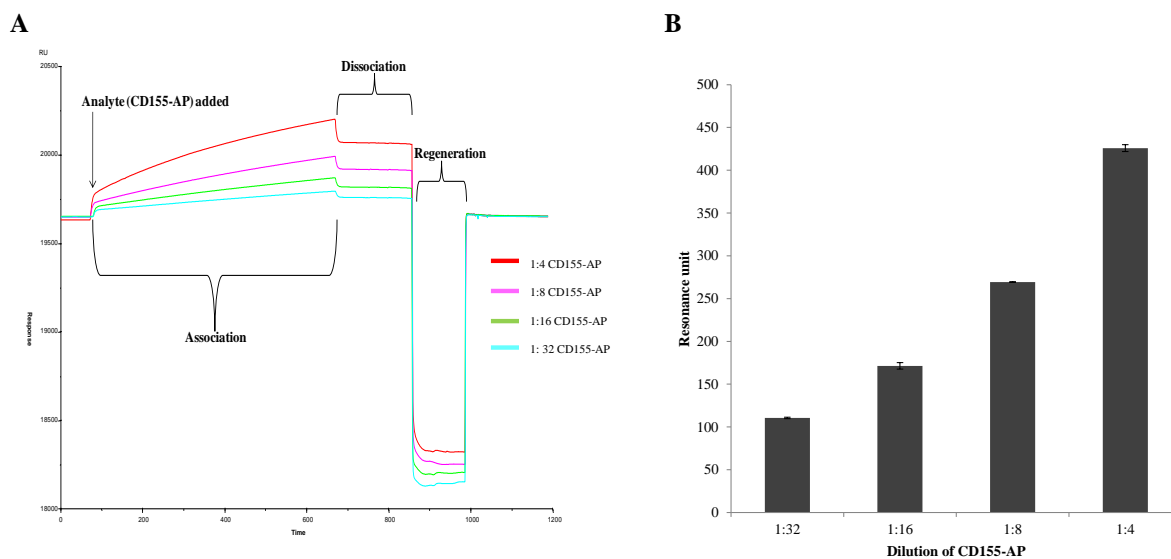


Figure 6.7. Determination of virus-receptor binding by surface plasmon resonance.

A wild-type trivalent IPV was immobilised to a Biacore sensor chip. CD155-AP diluted to various serial dilutions in running buffer was injected over the surface of the chip. Binding was monitored in real-time using SPR. The key stages of the biosensor approach are denoted on the sensorgram (A). Dose-dependent binding interaction of CD155-AP to immobilised IPV is also shown as a bar chart (B).

A biosensor approach to analyse the kinetics of this interaction between PV and CD155-AP was devised. This assay would involve immobilising CD155-AP to a sensor chip before assessing binding during injections of PV under partially or complete mass transport limited conditions. However despite several attempts, it was not possible to immobilise the CD155-AP to a sensor chip.

6.2.2 Effect of inactivation on the interaction between poliovirus and L20B cells

As described in previous sections, inactivated PV can still bind to sPVR although at an apparent reduced rate with respect to live PV. The next step was to assess whether inactivated PV is able to bind to cells susceptible to PV infection. L20B cells, transformed mouse Ltk cells that express the human PVR (329), were used for this purpose. Expression of the receptor at the cell surface, otherwise only present in primate cells, renders L20B cells susceptible to infection with PV. As the cells are of murine origin, very few other human enteric viruses produce cytopathic infection which means L20B cells are commonly used in PV diagnostic laboratories (408, 542). Ltk- cells were used as control for this research. The ability of inactivated PV to bind to L20B cells was analysed using FACS flow cytometry analysis and real-time RT-PCR.

6.2.2.1 Fluorescence-activated cell sorting flow cytometry

Flow cytometry is a technology which simultaneously measures and analyses multiple physical characteristics of single particles (usually cells), as they flow in a fluid stream through a beam of light (30). Fluorescence-activated cell sorting flow cytometry is a specialised type of flow cytometry which is able to sort single particles based on the specific light scattering and fluorescent characteristics of each particle. During FACS flow cytometry particles are carried in a rapidly flowing fluid stream to a laser intercept. As the particles pass through the laser intercept they scatter the laser light. Any fluorescent molecules present on the particle fluoresce. The scattered and fluorescent light is steered to detectors by beam splitters and filters. Electronic signals proportional to the optical signals are produced by the detectors. Fluorescence-activated cell sorting flow cytometry is based on the use of fluorochromes which are fluorescent compounds that absorb light over a range of wavelengths characteristic of the compounds. When the electrons of a fluorochrome absorb light they become excited and release the excess energy as a photon of light (i.e. they fluoresce). The amount of fluorescent signal detected is proportional to the number of fluorochrome molecules on a particle (30). It is possible to detect specific antigens on either the surface or the inside of a cell by conjugating fluorochromes to relevant antibodies.

This approach was adopted to measure the interaction between PV and L20B cells (Materials and Methods, section 2.2.6.2). The serotype 2 PV strain Sabin 2 was used for these experiments due to biosafety requirements. Briefly, L20B and Ltk- cells (1×10^6 cells / ml) were incubated with increasing concentrations of live and HCHO-inactivated Sabin 2 at room temperature for 120 min. Cells were then transferred to 96-well plates (Corning incorporated) and incubated with MAb 267 (specific for serotype 2 PV, (345)) at room temperature for 30 min. Cells were pelleted and washed with PFB before being incubated with anti-mouse IgG antibodies conjugated to FITC (Sigma-Aldrich). After this, cells were fixed with a FACS FIX solution and then analysed using a BD FACS Canto II flow cytometer (BD Sciences).

As presented in figure 6.8, L20B cells incubated with PV showed increased fluorescence in a virus dose-dependent manner which demonstrates that both live and HCHO-inactivated Sabin 2 were able to bind to these cells.

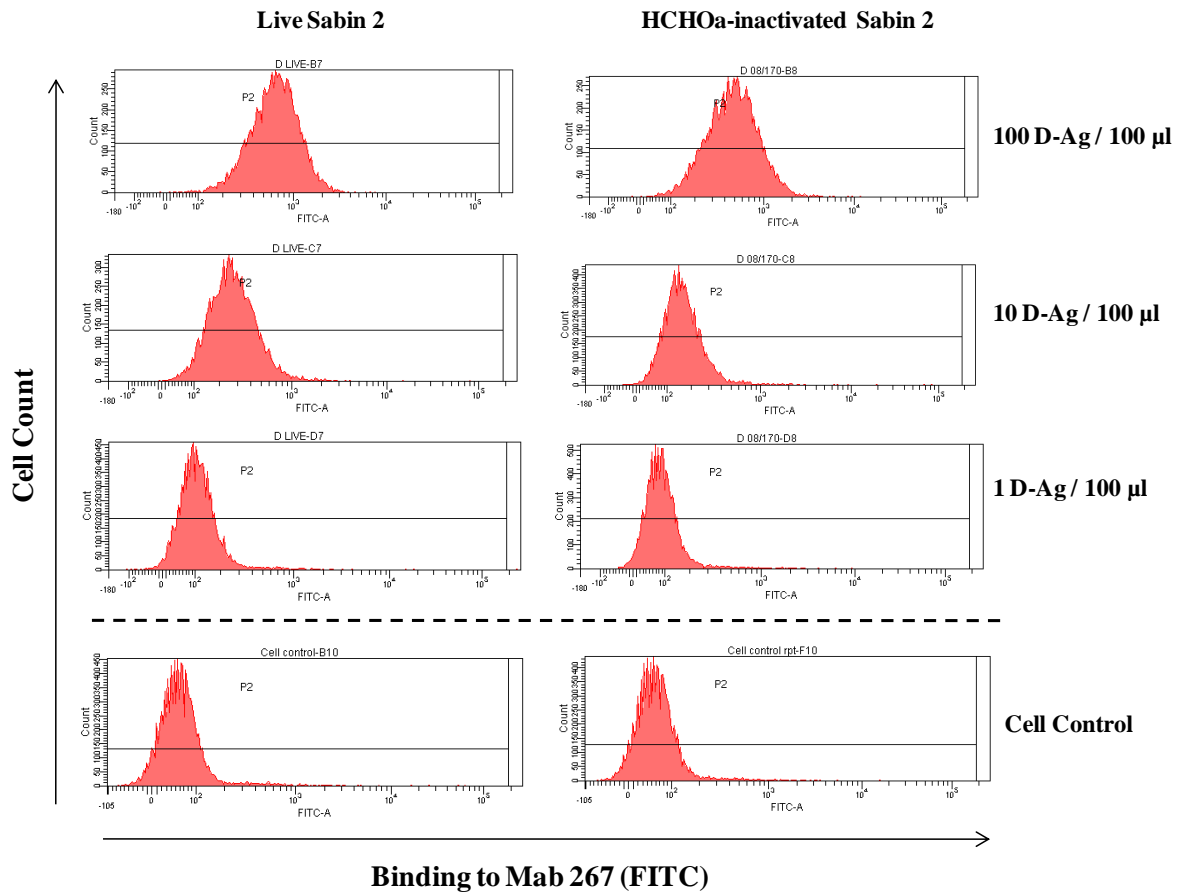


Figure 6.8. Binding of poliovirus to L20B cells analysed by fluorescence-activated cell sorting flow cytometry.

Live and HCHO-inactivated Sabin 2 was incubated with L20B cells, followed by incubation with anti-PV serotype 2-specific MA b 267 and FITC-labelled anti-mouse IgG. Histograms show mean fluorescence intensity on the surface of 10,000 L20B cells. 1:4000 HCHO is abbreviated as HCHOa.

No PV binding to Ltk- cells was observed at any virus concentration in the same conditions (data not shown). Ltk- cells in any combination with live or HCHO-inactivated Sabin 2 preparations showed fluorescence levels similar to those shown by Ltk- or L20B cells alone (≤ 70 mean fluorescence intensity).

The results were quantified and expressed both as the mean fluorescence intensity, shown by cells after incubation with PV, and the percentage of cells showing fluorescence above background levels (figure 6.9). Formaldehyde-inactivated Sabin 2 preparations showed less interaction to L20B cells with respect to live Sabin 2 preparations. For example, when L20B cells were incubated with 10 D-Ag of either virus preparation, the cells treated with HCHO-inactivated PV preparations showed reduced mean fluorescence intensity (31 %) and percentage of fluorescent cells (29 %) than those incubated with live PV preparations.

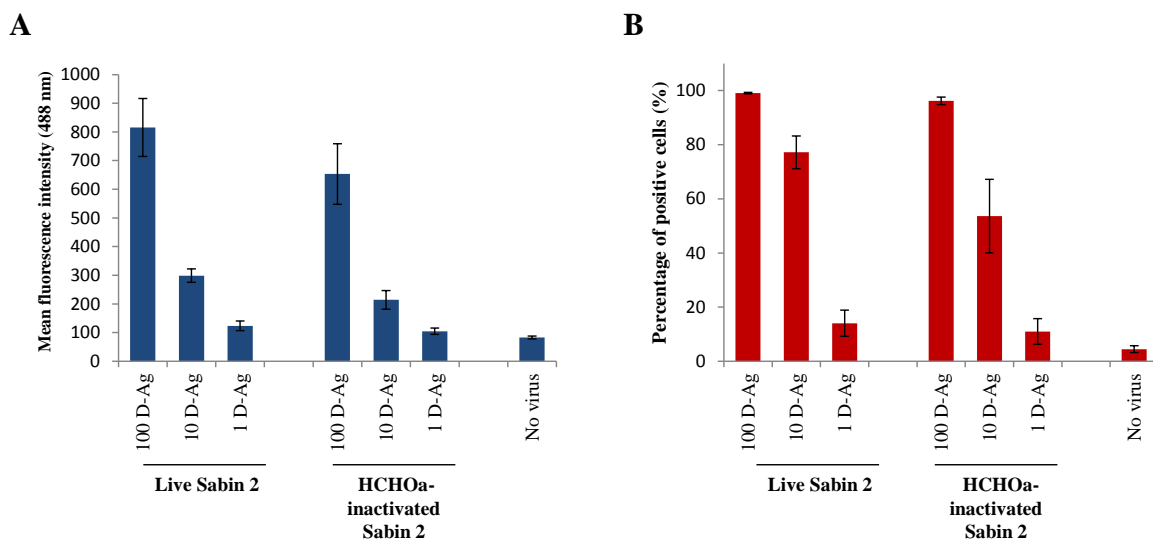


Figure 6.9. Quantification of the binding of poliovirus to L20B cells analysed by fluorescence-activated cell sorting flow cytometry.

Cells were analysed as described in figure 6.8. The mean fluorescence intensity (A) and the proportion of cells showing fluorescence levels above background (B) after incubation with PV, MAb 267 and FITC-labelled anti-mouse IgG are shown. The data are representative of three independent experiments. For each sample a total of 10,000 cells were analysed. The average values are shown as columns. Standard deviations are indicated as error bars. 1:4000 HCHO is abbreviated as HCHOa.

The interaction between inactivated PV and L20B cells was confirmed by second FACS flow cytometry assay (Materials and Methods, section 2.2.6.2). In this assay, increasing concentrations of live and HCHO-inactivated Sabin 2 were incubated with either CD155-AP or MEM for 60 min at room temperature. Following this, the incubated Sabin 2 preparations were mixed and incubated with L20B cells (1×10^6 cells / ml) for 120 min at room temperature. Binding was detected by FACS flow cytometry as described above. As shown in figure 6.10, pre-incubation of PV with CD155-AP prevented the virus binding to L20B cells,

as a reduction of 84 % and 93 % in fluorescence levels was observed for cells incubated with HCHO-inactivated and live PV, respectively. The reduction in the binding of live Sabin 2 was higher than that of the inactivated preparations, confirming previous results (figures 6.6 and 6.9) that the inactivated PV bound to CD155-AP at a lower affinity than the live PV.

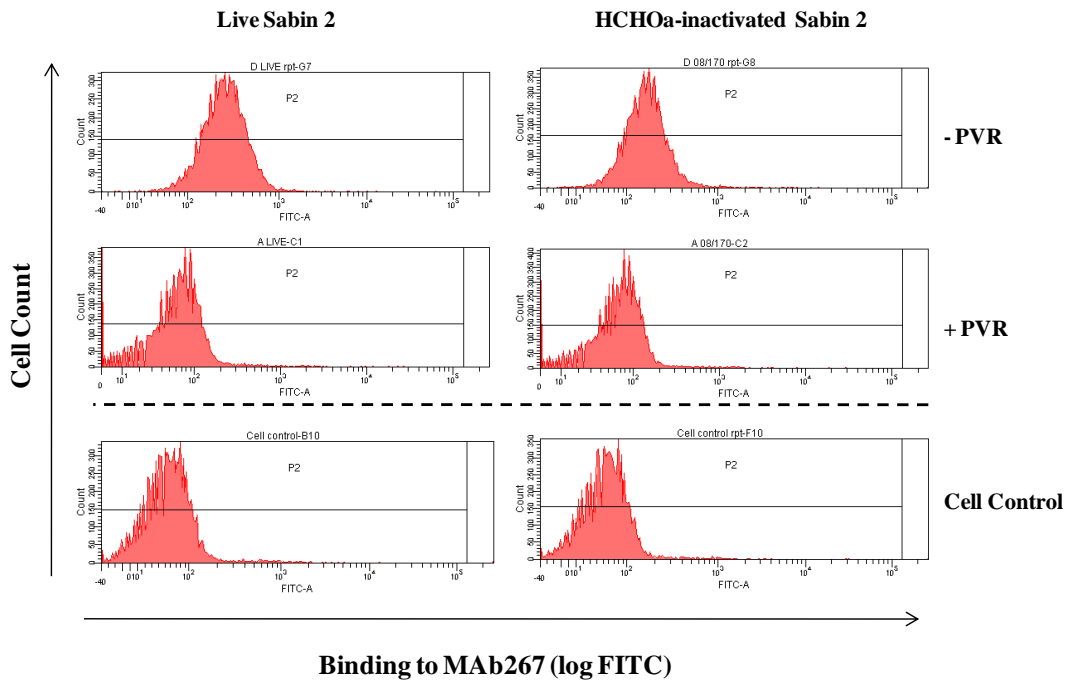


Figure 6.10. Inhibition of poliovirus binding to L20B cells by pre-incubation with soluble poliovirus receptor analysed by fluorescence-activated cell sorting flow cytometry.

Live and HCHO-inactivated Sabin 2 (10 D-Ag) were incubated with L20B cells after pre-incubation with CD155-AP (+PVR) or MEM (-PVR), followed by incubation with anti-PV serotype 2-specific MAb 267 and FITC-labelled anti-mouse IgG. Histograms show fluorescence intensity on the surface of 10,000 L20B cells. 1:4000 HCHO is abbreviated as HCHOa.

From these assays, it can be concluded that both live and HCHO-inactivated PV were able to bind to L20B cells by interacting with human PVR expressed on the cell surface.

The ability of PV inactivated with BPL, BEI and 1:8000 HCHO to bind to L20B cells was also assessed (Materials and Methods, section 2.2.6.2). As shown in figure 6.11, 1:8000 HCHO-, BEI- and BPL-inactivated PV preparations were also able to bind to L20B cells at an apparent reduced rate with respect to live PV preparations.

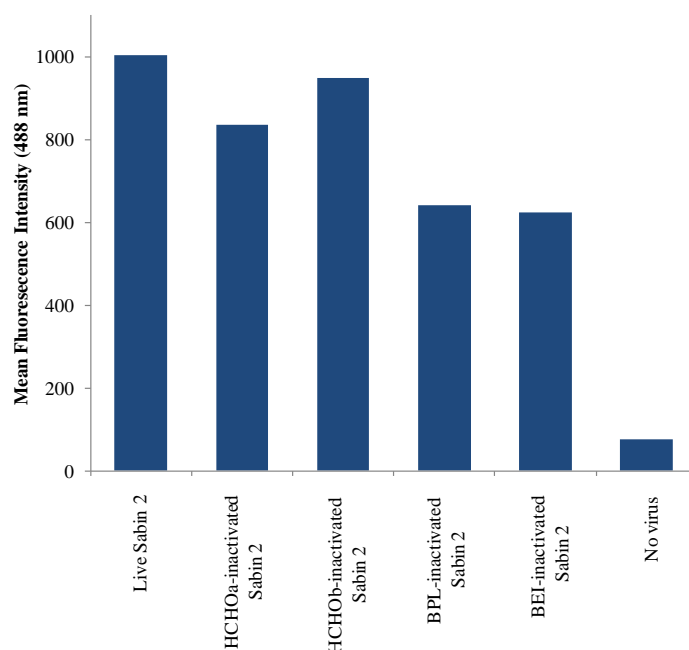


Figure 6.11. Binding of live and inactivated poliovirus to L20B cells analysed by fluorescence-activated cell sorting flow cytometry.

Live, BPL-, BEI-, and HCHO-inactivated Sabin 2 preparations were incubated with L20B cells followed by incubation with anti-PV serotype 2-specific MAb 267 and FITC-labelled anti-mouse IgG. The mean fluorescence intensity after incubation with PV, MAb-267 and FITC-labelled anti-mouse IgG are shown. For each sample, a total of 2,500 cells were analysed. Average values are shown. 1:4000 HCHO is abbreviated as HCHO_a; 1:8000 HCHO is abbreviated as HCHO_b.

6.2.2.2 Real-time reverse transcription polymerase chain reaction

The real-time RT-PCR binding assay to assess the interaction between inactivated PV and L20B cells was as previously described with some modifications (243) (Materials and Methods, section 2.2.6.3). Briefly, L20B and Ltk- cells were detached, pelleted and washed twice in binding buffer before being incubated with live preparations of the MEF-1 serotype 2 PV strain at either +4 °C or room temperature for 120 min. Cells were pelleted and washed twice with binding buffer before resuspension in MEM. Between each wash the supernatant

was harvested and pooled. The RNA was extracted from the pelleted cells using the MagNA Pure LC Total Nucleic Acid Isolation Kit (Roche) and the Kingfisher ml particle processor (Thermo Electron Corporation). Assay conditions for quantification of the extracted viral RNA were optimised using the QuantiTect SYBR Green RT-PCR kit (Qiagen) with the Rotor-Gene 3000 thermal cycler (Qiagen) (Materials and Methods, section 2.2.8.2). Briefly, a 200 bp fragment was amplified using a series of MEF-1 specific primers with the QuantiTect SYBR Green RT-PCR kit. To determine the optimal virus concentration, this initial assay assessed the interaction between the two murine cell lines and a range of different concentrations of a live preparation of the MEF-1 serotype 2 strain.

As figure 6.12 shows, the real-time RT-PCR binding assay detected an interaction between the live MEF-1 and the L20B cells.

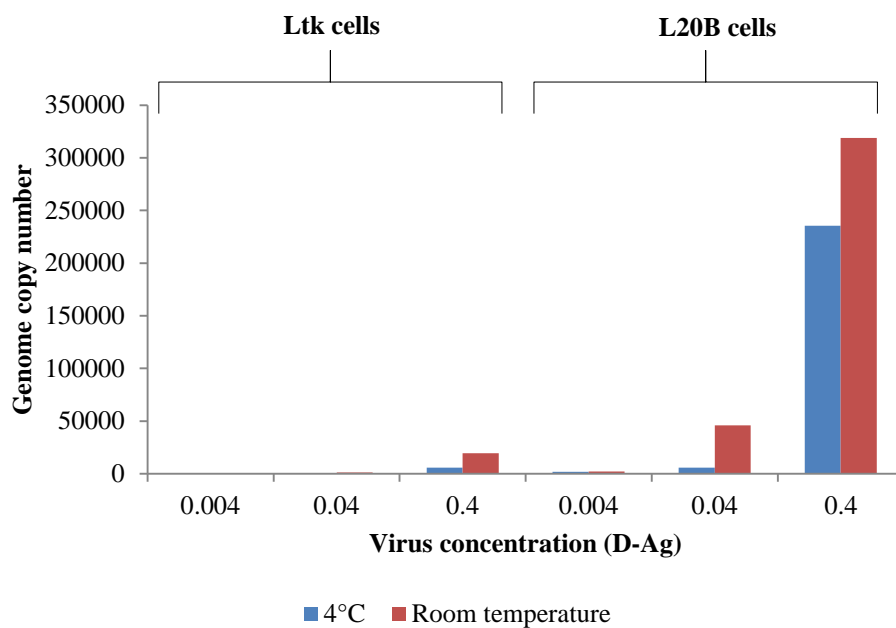


Figure 6.12. Real-time reverse transcription-polymerase chain reaction analysis of interaction between live poliovirus and murine cell lines.

Live MEF-1 was incubated with L20B and Ltk- cells for 120 min at either +4 °C or room temperature. Bound cells were pelleted and RNA was extracted. The amount of viral RNA associated with the cell pellet was quantified by a real-time RT-PCR.

The genome copy number of viral RNA extracted from pelleted cells increased in a dose-dependent manner, indicating that there was an interaction between the MEF-1 strain and the

L20B cells. The temperature at which the PV and the cells were incubated influenced the interaction between the two. A greater quantity of live MEF-1 was found to interact with the L20B cells when the two were incubated at room temperature, than when they were incubated at +4 °C. The detected binding of MEF-1 to L20B cells was supported by the lack of any significant interaction between the PV strain and the non-permissive Ltk- cells.

To confirm this interaction between PV and L20B cells, a second real-time RT-PCR binding assay was carried out (Materials and Methods, section 2.2.6.3). In this assay, live MEF-1 (0.04 D-Ag) was incubated with equal concentrations of CD155-AP, AP, a serotype 2-specific MAb (MAb 1050), a serotype 1-specific MAb (MAb 234) or MEM for 60 min at 37 °C. Subsequently, L20B and Ltk- cells (2.5×10^5 cells / 500 μ l) were incubated with this pre-treated MEF-1 for 120 min at room temperature. The amount of live MEF-1 bound to the cell lines was determined, as described above.

As table 6.2 shows, pre-incubation with CD155-AP and MAb 1050 prevented any significant interaction between live MEF-1 and L20B cells.

Pre-incubation agent	Reduction of poliovirus binding (%)
CD155-AP	98 \pm 0.2
MAb 1050	96 \pm 0.8
AP	2 \pm 0.3
MAb 234	2 \pm 0.3
MEM	2 \pm 0.3

Table 6.2. Reduction in poliovirus binding to L20B cells following pre-incubation with different agents.

Live MEF-1 was incubated with either CD155-AP, a serotype 2-specific MAb (MAb 1050), a serotype 1-specific MAb (MAb 234), AP or MEM for 60 min at 37 °C. Pre-treated MEF-1 was incubated with permissive L20B and non-permissive Ltk- cells for 120 min at room temperature. Bound cells were pelleted and RNA was extracted. The amount of viral RNA associated with the cell pellet was quantified by a real-time RT-PCR. Average of three determinations is shown with the standard error.

Neither AP (part of the CD155-AP fusion protein) or the serotype 1-specific MAb 234 prevented live MEF-1 from interacting with L20B cells. This was expected, as both agents

lacked the ability to bind to serotype 2 PV strains. The interaction between MEF-1 and L20B cells was confirmed by this assay.

A real-time RT-PCR binding assay was carried out to characterise the interaction between live or inactivated PV and L20B or Ltk- cells (Materials and Methods, section 2.2.6.3). In this assay, a range of concentrations of live and HCHO-inactivated MEF-1 were incubated with L20B and Ltk- cells (2.5×10^5 cells / 500 μ l) for 120 min at room temperature. The amount of PV bound to the murine cells was determined, as described above.

As figure 6.13 shows, both live and HCHO-inactivated MEF-1 bound to the permissive L20B cells over a range of concentrations.

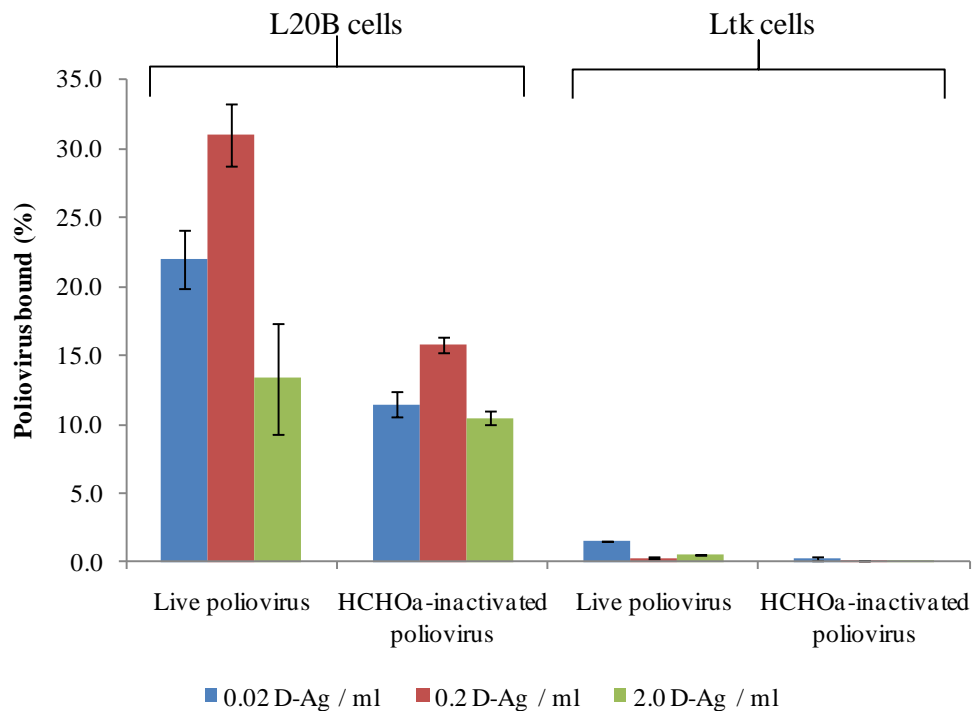


Figure 6.13. Real-time reverse transcription-polymerase chain reaction analysis of the interaction between live / inactivated poliovirus and L20B / Ltk- cells.

Live and HCHO-inactivated MEF-1 were incubated with permissive L20B and non-permissive Ltk- cells for 120 min at room temperature. Bound cells were pelleted and RNA was extracted. The amount of viral RNA associated with the cell pellet was quantified by a real-time RT-PCR. An average of two determinations is shown with the standard error. 1:4000 HCHO is abbreviated as HCHOa.

The lack of any significant interaction between live or inactivated MEF-1 and the non-permissive Ltk- cells supported this observation. The results of this analysis confirmed findings obtained with CD155-AP and FACS flow cytometry that inactivated PV was still able to bind to the PVR. In comparison to the live MEF-1, the inactivated preparations bound at a reduced affinity. In this assay, the inactivated MEF-1 showed a 78 % reduction in binding to L20B cells.

To further characterise the interaction between inactivated PV and L20B cells, another real-time RT-PCR binding assay was carried out (Materials and Methods, section 2.2.6.3). In this assay, live and HCHO-inactivated MEF-1 (0.2 D-Ag / 25 μ l) were incubated with either CD155-AP, a serotype 3-specific MAb (MAb 520), MEM or a range of serotype 2-specific MAbs for 60 min at room temperature. Following this, the pre-treated MEF-1 was incubated with L20B cells (2.5×10^5 cells / 500 μ l) for 120 min at room temperature. The amount of PV bound to the L20B cells was determined, as described above.

As figure 6.14 shows, the interaction between MEF-1 and the L20B cells was significantly reduced following pre-incubation with either CD155-AP or a range of serotype 2-specific MAbs.

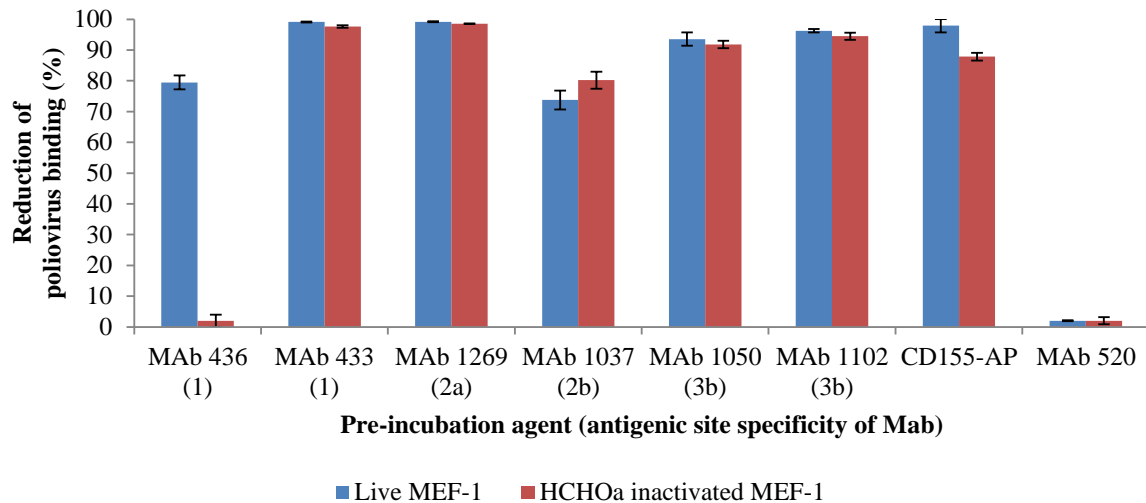


Figure 6.14. Reduction of poliovirus binding to L20B cells following incubation with monoclonal antibodies and CD155-AP.

Live and HCHO-inactivated MEF-1 were incubated with either CD155-AP, a serotype 3-specific MAb (MAb 520), MEM or a range of serotype 2-specific MAbs for 60 min at room temperature. Pre-treated MEF-1 was incubated with L20B cells for 120 min at room temperature. Bound cells were pelleted and RNA was extracted. The amount of viral RNA associated with the cell pellet was quantified by a real-time RT-PCR. The results are expressed as a percentage of reduction of PV binding to L20B cells with respect to the amount of untreated (incubated with MEM) PV bound. Antigenic sites to which serotype 2-specific MAbs bind to are bracketed. An average of two determinations is shown with the standard error. 1:4000 HCHO is abbreviated as HCHOa.

The level of inhibition of the interaction between MEF-1 and L20B cells varied slightly between the serotype 2-specific MAbs indicating that the location of the antigenic site to which the MAbs bound to (denoted in figure 6.14) could have influenced how much of the receptor binding site was blocked. Pre-incubation with MAb 436 resulted in an inhibition of binding between the live but not the HCHO-inactivated MEF-1 and the L20B cells. This was because the antigenic site 1 of the MEF-1 strain, which MAb 436 binds to, is modified by HCHO inactivation (Chapter 4, figure 4.9). This modification prevented MAb 436 from binding. This result alongside the lack of any significant reduction in the interaction between MEF-1 pre-incubated with the serotype 3-specific MAb 520 and L20B cells (figure 6.14) supports the previous findings that inactivated PV is still able to bind to L20B cells.

The effect of inactivation with BPL or BEI on the binding of PV to L20B cells was assessed in a further real-time RT-PCR binding assay (Materials and Methods, section 2.2.6.3). In this assay live and HCHO-, BPL- or BEI-inactivated MEF-1 (0.2 D-Ag / 25 µl) were incubated with either CD155-AP, a serotype 2-specific MAb (MAb 1050), a serotype 3-specific MAb (MAb 520) or MEM for 60 min at room temperature. Following this, the pre-treated MEF-1 was incubated with L20B cells (2.5×10^5 cells / 500 µl) for 120 min at room temperature. The amount of PV bound to the L20B cells was determined as described above.

As table 6.3 shows, pre-incubation with CD155-AP and MAb 1050 prevented any significant interaction between MEF-1 and L20B cells. Analysis by balanced ANOVA (Minitab v.16, <http://www.minitab.com/en-GB/>) found that this inhibition of the interaction between MEF-1 and the L20B cells was significant ($P < 0.001$). Pre-incubation with MAb 520 or Eagle's MEM did not reduce the interaction between the MEF-1 preparations and the L20B cells.

Pre-incubation agent	Reduction of poliovirus binding (%)			
	Live MEF-1	HCHOa-inactivated MEF-1	BPL-inactivated MEF-1	BEI-inactivated MEF-1
CD155-AP	98 ± 0.2	87 ± 2.5	92 ± 0.2	88 ± 2.8
MAb 1050	95 ± 0.1	93 ± 0.7	97 ± 1.6	92 ± 0.7
MAb 520	2 ± 0.4	2 ± 0.4	2 ± 0.4	2 ± 0.4
MEM	2 ± 0.4	2 ± 0.4	2 ± 0.4	2 ± 0.4

Table 6.3. Effect of pre-incubation with CD155-AP and monoclonal antibodies on the interaction between poliovirus and L20B cells.

Live and inactivated MEF-1 were incubated with either CD155-AP, a serotype 2-specific MAb (MAb 1050), a serotype 3-specific MAb (MAb 520) or MEM for 60 min at room temperature. Pre-treated MEF-1 was incubated with L20B cells for 120 min at room temperature. Bound cells were pelleted and RNA was extracted. The amount of viral RNA associated with the cell pellet was quantified by a real-time RT-PCR. An average of two determinations is shown with the standard error. 1:4000 HCHO is abbreviated as HCHOa.

6.2.3 Effect of inactivation on poliovirus entry

6.2.3.1 Effect of inactivation on conversion of poliovirus virions to 135S and 80S particles

As mentioned in the introduction to this chapter, the ability of PV particles to undergo conformational changes to form 135S and 80S particles is essential for PV to enter cells and to release the viral genome. Previous research has shown that it is possible to induce PV virions to form 135S and 80S particles by heating PV particles to super-physiological temperatures (50 and 56 °C, respectively) in hypotonic medium (50, 113). The 135S and 80S particles obtained *in vitro* by this approach have been found to be indistinguishable to those obtained at physiological temperature in the presence of receptor (55, 113). This approach was adopted to determine whether inactivated PV particles can form 135S and 80S particles (Materials and Methods, section 2.2.7.1). Live and BPL-, BEI- and HCHO-inactivated preparations of equivalent concentrations of the MEF-1 serotype 2 PV strain were incubated at 50 and 60 °C for 3 and 20 min to induce a conformational change to form 135S and 80S particles, respectively. Live and inactivated MEF-1 were also incubated at 18-20 °C (room temperature) as a control.

As described above, 135S and 80S particles differ in a number of characteristics from mature PV virions. Both are antigenically distinct from virus particles, are more sensitive to proteases (173) and are unable to bind to cells (55, 159, 241). The 135S and 80S particles differ in sensitivity to RNase (55, 113). The viral RNA is still present and protected within 135S particles, while 80S particles either lack RNA or it is exiting from them, which exposes it to RNase. To determine whether live and inactivated PV showed similar characteristics to 135S and 80S particles following heating, three of these characteristics were analysed. These included, antigenicity, ability to bind to the PVR and sensitivity to RNase A which was used as a measure of the presence of viral RNA.

The antigenicity of the heated MEF-1 preparations was assessed by an ELISA using the serotype 2-specific MAb 1050 as the detection antibody. The ability of the heated MEF-1 preparations to bind to L20B cells was assessed by a real-time RT-PCR binding assay as described above (section 6.2.2.2). A real-time RT-PCR was carried out to assess the sensitivity of the MEF-1 preparations to RNase A. Sensitivity to RNase A was used as an

indirect measure for the presence of viral RNA in the MEF-1 preparations. MEF-1 preparations were incubated with RNase A (0.001 µg / µl) at the relevant temperature. The presence of RNA was detected by a real-time RT-PCR (Materials and Methods, section 2.2.8.2). Table 6.4 shows the results of these three assays. The results of MEF-1 preparations heated to super-physiological temperature were expressed relative to those obtained with native viral samples (which were incubated at 18-20 °C).

Poliovirus preparation	Relative activity to that of 20 °C control (%)					
	Antigenic		Binding		Presence of RNA	
	50 °C	60 °C	50 °C	60 °C	50 °C	60 °C
Live	0	0	0	0	71	0
HCHO	87	0	67	0	85	6
BPL	0	0	3	1	75	0
BEI	80	0	57	0	69	0

Table 6.4. Antigenic and binding ability and presence of viral RNA of heated poliovirus.

Live and HCHO-, BPL- and BEI-inactivated preparations of the MEF-1 strain were heated at 50 °C and 60 °C and at room temperature as a control. Antigenic activity of heated MEF-1 preparations was assessed by an ELISA. Real-time RT-PCRs were carried out to assess binding to L20B cells and sensitivity to RNase A. Sensitivity to RNase A was used as a measure for the presence of viral RNA in the MEF-1 preparations.

Following incubation at 50 °C, live MEF-1 did not interact with MAb 1050 and showed no antigenic activity. Live MEF-1 was also unable to bind to L20B cells following incubation at 50 °C. Viral RNA was detected in live MEF-1 incubated at 50 °C. Beta-propiolactone-inactivated MEF-1 showed similar results to live MEF-1 following incubation at 50 °C. Post-incubation at 50 °C, the properties of HCHO- and BEI-inactivated MEF-1 differed from those of live MEF-1. Unlike live MEF-1, HCHO- and BEI-inactivated MEF-1 incubated at 50 °C were still able to interact with MAb 1050 and bind to L20B cells. Viral RNA could be detected in HCHO- and BEI-inactivated MEF-1 following incubation at 50 °C. Following incubation at 60 °C none of the MEF-1 preparations recognised the MAb, showing no antigenic activity. A similar result was found with the binding activity of the MEF-1 preparations incubated at 60 °C. No viral RNA could be detected in any of the MEF-1 preparations following incubation at 60 °C.

The findings described above were used to assess whether live and inactivated preparations of the MEF-1 strain showed similar properties to those of 135S and 80S particles. The lack of antigenic activity and ability to bind to L20B cells of live and BPL-inactivated MEF-1 following incubation at 50 °C was compatible with the properties of 135S particles, indicating that these MEF-1 preparations had undergone the conformational change. The presence of viral RNA in these MEF-1 preparations following incubation with RNase A supported this, as it is known that 135S particles are resistant to RNase A. The HCHO- and BEI-inactivated MEF-1 still showed antigenic activity and the ability to bind to L20B cells following incubation at 50 °C. These properties are not compatible with those of 135S or 80S particles, indicating that these MEF-1 preparations had remained in the mature virion conformation. Viral RNA could be detected from these MEF-1 preparations following RNase A treatment. Although this is a property of 135S particles, it is also one of mature virions. Following incubation at 60 °C, none of the MEF-1 preparations showed antigenic or binding activity and no viral RNA could be detected. These properties are similar to those of 80S particles, suggesting that the MEF-1 preparations had undergone the conformational changes to reach this state.

6.2.3.2 Use of fluorescence-activated cell sorting flow cytometry to assess the effect of inactivation on poliovirus viral entry

The aforementioned results suggest that inactivation with BEI and HCHO prevents the conformational change of mature virions to 135S particles. This would be assumed to prevent the entry of the inactivated PV into a susceptible cell, as the 135S particle is an essential intermediate structure of the entry process (511). To investigate this further, FACS flow cytometry was used to track viral entry process of live and HCHO-inactivated PV (Materials and Methods, section 2.2.7.2). L20B cells (1×10^6 cells / ml) were incubated with live and HCHO-inactivated Sabin 2 preparations of equivalent concentrations at either 20 or 37 °C for 1, 2, 4, 6, 8, 11 h. In addition a 0 h control was set up for both the live and inactivated Sabin 2 preparations. For each of these incubations a cell control was included to assess background fluorescence. Two temperatures were used as it was known that at 20 °C PV can only bind to cells, while at 37 °C the virus can bind and enter the cells. The amount of PV inside and outside of cells was assessed by FACS flow cytometry using permeabilisation agents as

described in Materials and Methods (section 2.2.7.2). To obtain an accurate measure of the amount of PV within the cells the fluorescence readings of the 20 °C incubated Sabin 2 preparations were subtracted from those of the 37 °C incubated preparations.

As figure 6.15 shows, the amount of live Sabin 2 increased after 4 h incubation, indicating that it had entered the cells and was replicating resulting in an increased virus yield.

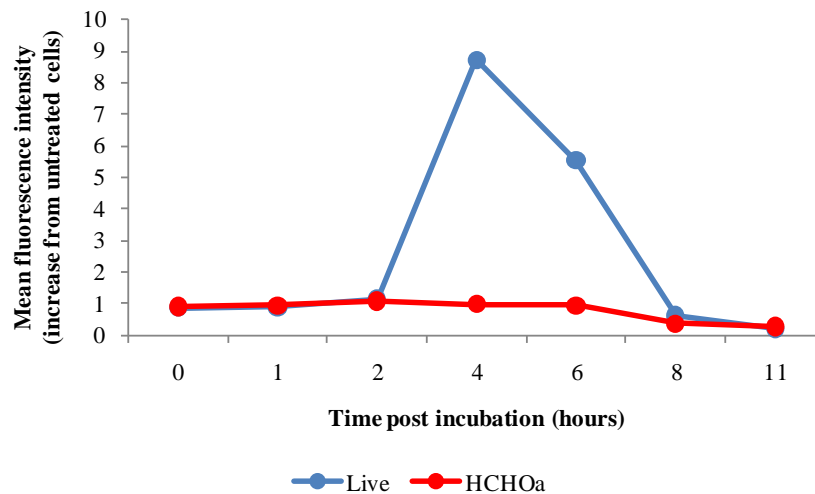


Figure 6.15. Amount of live and formaldehyde-inactivated poliovirus within cells post incubation.

Live and HCHO-inactivated Sabin 2 preparations were incubated with L20B cells at either 20 or 37 °C for 0, 1, 2, 4, 6, 8 and 11 h. The amount of PV inside and outside of cells was assessed by FACS flow cytometry using permeabilisation agents. The amount of PV detected within the L20B cells was adjusted to factor in the amount of PV bound to PVR on the surface of L20B cells. 1:4000 HCHO is abbreviated as HCHOa.

The increase in the amount of live PV within the L20B cells after 4 h incubation confirmed the results of previous studies which found that following a 3-4 h eclipse period the intracellular PV progeny increased exponentially (179, 225). Following 6 h incubation the increased PV yield fell and by 8 h the amount of PV within the cell was similar to the background levels determined at 0 h. This could be due to the release of PV from the cells. For HCHO-inactivated Sabin 2 no virus was detected within the L20B cells. This may have been because either the inactivated PV could not enter the cells and / or its viral RNA was defective and could not replicate. This finding was expected as it is known that inactivated

PV is not infectious. The findings of this assay did not determine whether inactivated PV could or could not enter L20B cells, only that the yield of the inactivated virus did not increase. An alternative assay was set up in which L20B cells (1.5×10^4 L20B cells/400 μ l) were incubated with live or 1:4000 HCHO-inactivated PV (0.5 D-Ag multiplicity of infection) in 8-well glass slides (NUNC Lab-Tek 8 well chamber slide system) at 35 °C for between 1, 2, 6 and 16 h. Cells were washed with PBS before being fixed with either methanol or acetone (internalised PV) or HCHO (3.5 %) and NH_4Cl (50 mM) (externally bound PV). Following washing with PBS, cells were incubated with the serotype 2-specific MAb 267 and subsequently anti-mouse IgG (whole molecule)-FITC. After further washing with PBS, slides were viewed using an immunofluorescence microscope (Olympus IX71). Unfortunately the presence of live or 1:4000 HCHO-inactivated PV within L20B cells could not be visualised by this technique.

6.2.4 Effect of inactivation on viral RNA

The replication of the viral RNA of PV is an essential step in the virus replication cycle. Following HCHO treatment the viral infectivity of PV is eliminated. However it is not clear whether the viral RNA in the inactivated virus particle maintains its integrity and ability to replicate and produce virus. Previous research has found that following 60 h inactivation with HCHO PV RNA cannot be detected from phenol/SDS extracts, implying that during inactivation HCHO is able to interact with the viral RNA (312). However it is not clear what effect it has on the viral RNA. No biological activity was detected for these phenol/SDS extract following transfection into HEp-2C cells (312). The effect of inactivation on the viral RNA was explored further by assessing the biological activity and RNA functionality of aliquots taken during inactivation time-courses.

The biological activity of viral RNA isolated during inactivation was determined by its ability to produce infectious virus after transfection into HEp-2C cells. Viral RNA of the MEF-1 strain was extracted from aliquots taken during inactivation time-courses with BPL, BEI and HCHO (detailed in Chapter 4, section 4.2.3) using the MagNA Pure LC Total Nucleic Acid Isolation Kit and the Kingfisher ml particle processor. The extracted RNA was transfected into susceptible HEp-2C cells by DEAE-dextran-mediated transfection or electroporation. To assess the sensitivity of the transfection techniques, viral RNA extracted from a serial dilution series of live MEF-1 was also transfected into HEp-2C cells. DEAE-dextran was originally used as a facilitator to introduce PV RNA into cells (516). The DEAE-dextran-mediated transfection protocol was as previously described with modifications as described in the Materials and Methods (section 2.2.8.1) (453).

As table 6.5 shows, DEAE-dextran transfected viral RNA from live MEF-1 PV was able to infect HEp-2C cells. However the DEAE-dextran transfection protocol was found to have low sensitivity. Viral RNA equivalent to PV of an infectious titre of 6.2×10^4 TCID₅₀ (0.1 ng viral RNA) or lower failed to generate any CPE in transfected cells.

Prep.	Inac. aliquot	Equivalent titre (TCID ₅₀ /5 µl)	Cytopathic effect (day post transfection)						
			1	2	3	4	5	6	7
Live MEF-1	Neat	6.2 x 10 ⁷	O	CPE	CPE	CPE	CPE	CPE	CPE
	1:10	6.2 x 10 ⁶	O	CPE	CPE	CPE	CPE	CPE	CPE
	1:100	6.2 x 10 ⁵	O	O	CPE	CPE	CPE	CPE	CPE
	1:1000	6.2 x 10 ⁴	O	O	O	O	O	O	O
	1:10000	6.2 x 10 ³	O	O	O	O	O	O	O
BPL (1:500)	2	7.4 x 10	O	O	O	O	O	O	O
	4	<1.0	O	O	O	O	O	O	O
	8	<1.0	O	O	O	O	O	O	O
	12	<1.0	O	O	O	O	O	O	O
	16	<1.0	O	O	O	O	O	O	O
BEI (1.6 mM)	4	3.2 x 10 ²	O	O	O	O	O	O	O
	8	<1.0	O	O	O	O	O	O	O
	18	<1.0	O	O	O	O	O	O	O
	24	<1.0	O	O	O	O	O	O	O
HCHO (1:4000)	12	5.6 x 10 ⁵	O	O	CPE	CPE	CPE	CPE	CPE
	36	5.6 x 10 ²	O	O	O	O	O	O	O
	71	<1.0	O	O	O	O	O	O	O
	120	<1.0	O	O	O	O	O	O	O
	180	<1.0	O	O	O	O	O	O	O
	288	<1.0	O	O	O	O	O	O	O
HCHO (1:8000)	12	4.2 x 10 ⁶	O	CPE	CPE	CPE	CPE	CPE	CPE
	36	5.6 x 10 ⁴	O	O	O	O	O	O	O
	71	2.4 x 10 ²	O	O	O	O	O	O	O
	120	<1.0	O	O	O	O	O	O	O
	180	<1.0	O	O	O	O	O	O	O
	288	<1.0	O	O	O	O	O	O	O

Table 6.5. Biological activity of poliovirus RNA transfected using DEAE-dextran.

RNA was extracted from serial dilutions of live PV and virus aliquots taken during inactivation time-courses with BPL, BEI and two concentration of HCHO. Extracted viral RNA preparations were transfected into HEp-2C cells by a DEAE-dextran transfection protocol. Cells were incubated at 35 °C for seven days and observed for signs of CPE. CPE indicates cytopathic effect present; O indicates no cytopathic effect present.

With the exception of viral RNA extracted before 36 h of inactivation with HCHO, RNA extracted from virus aliquots taken during inactivation time-courses with BPL, BEI and two concentrations of HCHO did not show any biological activity.

The electroporation protocol was as previously described with modifications as described in the Materials and Methods (section 2.2.8.1) (188). As table 6.6 shows, the electroporation protocol showed greater sensitivity than the DEAE-dextran protocol. Viral RNA equivalent to live PV of an infectious titre lower than 6.2×10^2 TCID₅₀ failed to generate any CPE in electroporated cells. It is not clear why viral RNA equivalent to PV of an infectious titre of 6.2×10^4 TCID₅₀ failed to generate any CPE in electroporated cells. However, as viral RNA equivalent to PV of a lower infectious titre generated CPE when electroporated into cells it is possible this was due to limitations inherent to the electroporation technique. For example electroporation can result in significant cell death resulting in a lower yield of cells in the electroporated samples (188). This would reduce the number of cells viable for the transfection of the viral RNA.

Prep.	Inac. aliquot	Equivalent titre (TCID ₅₀ /5 µl)	Cytopathic effect (day post transfection)						
			1	2	3	4	5	6	7
Live MEF-1	1:10	6.2 x 10 ⁶	O	CPE	CPE	CPE	CPE	CPE	CPE
	1:100	6.2 x 10 ⁵	O	CPE	CPE	CPE	CPE	CPE	CPE
	1:1000	6.2 x 10 ⁴	O	O	O	O	O	O	O
	1:10000	6.2 x 10 ³	O	O	CPE	CPE	CPE	CPE	CPE
	1:100000	6.2 x 10 ²	O	O	O	O	O	O	O
	1:1000000	6.2 x 10	O	O	O	O	O	O	O
HCHO (1:4000)	12	5.6 x 10 ⁵	O	CPE	CPE	CPE	CPE	CPE	CPE
	36	5.6 x 10 ²	O	O	O	O	O	O	O
	71	<1.0	O	O	O	O	O	O	O
	120	<1.0	O	O	O	O	O	O	O
	180	<1.0	O	O	O	O	O	O	O
	288	<1.0	O	O	O	O	O	O	O
BEI (1.6 mM)	4	3.2 x 10 ²	O	O	O	O	O	O	O
	8	<1.0	O	O	O	O	O	O	O
	18	<1.0	O	O	O	O	O	O	O
	24	<1.0	O	O	O	O	O	O	O

Table 6.6. Biological activity of poliovirus RNA transfected using electroporation.

RNA was extracted from serial dilutions of live PV and virus aliquots taken during inactivation time-courses with HCHO and BEI. Extracted viral RNA preparations were transfected into HEp-2C cells by electroporation. Cells were incubated at 35 °C for seven days and observed for signs of CPE. CPE indicates cytopathic effect present; O indicates no cytopathic effect present.

As with the DEAE-dextran transfection technique, only the viral RNA extracted before 36 h of inactivation with HCHO showed biological activity during the inactivation time-courses.

To determine whether inactivation affected the functionality of the viral RNA a series of RT-PCRs were carried out (Materials and Methods, section 2.2.8.2). The viral RNA of the MEF-1 strain was extracted from aliquots taken during inactivation time-courses with BPL, BEI and HCHO, as described in Chapter 4, section 4.2.3. Viral RNA was also extracted from live MEF-1 as a control. A series of primers of equal length and melting point which yielded 200, 400, 600 and 800 bp RT-PCR products of the region encoding the VP1 protein were designed (Materials and Methods, section 2.1.1). The extracted viral RNA preparations were run in four RT-PCRs with the respective primer. The resulting RT-PCR products were examined by gel electrophoresis on a 1 % agarose gel.

As figure 6.16 A and B show, for RNA extracted from the final aliquots of each time-course, RT-PCR products of low size (200 and 400 bp) were successfully amplified. However, as figure 6.16 C and D show, RT-PCR products of 600 and 800 bp of the final two aliquots of the time-course of BPL, HCHO and to a lesser extent BEI inactivations either produced narrower fainter bands or failed to produce any bands indicating that either less or no RT-PCR product was amplified. Reverse transcription-polymerase chain reaction products of 600 and 800 bp of aliquots taken earlier in the inactivation time-courses were successfully amplified. This suggests that the inactivation chemicals affected the functionality of the viral RNA, with an increasing effect as the time-courses proceeded. Inactivation with BPL prevented the successful amplification of the 800 bp RT-PCR products from the final two aliquots of the time-course. The viral RNA extracted from the final aliquots of inactivation time-courses with the other chemicals were all able to generate 800 bp RT-PCR products, although the bands were small and less clear. This suggests that inactivation with BPL results in greater damage to the viral RNA than the other inactivation chemicals.

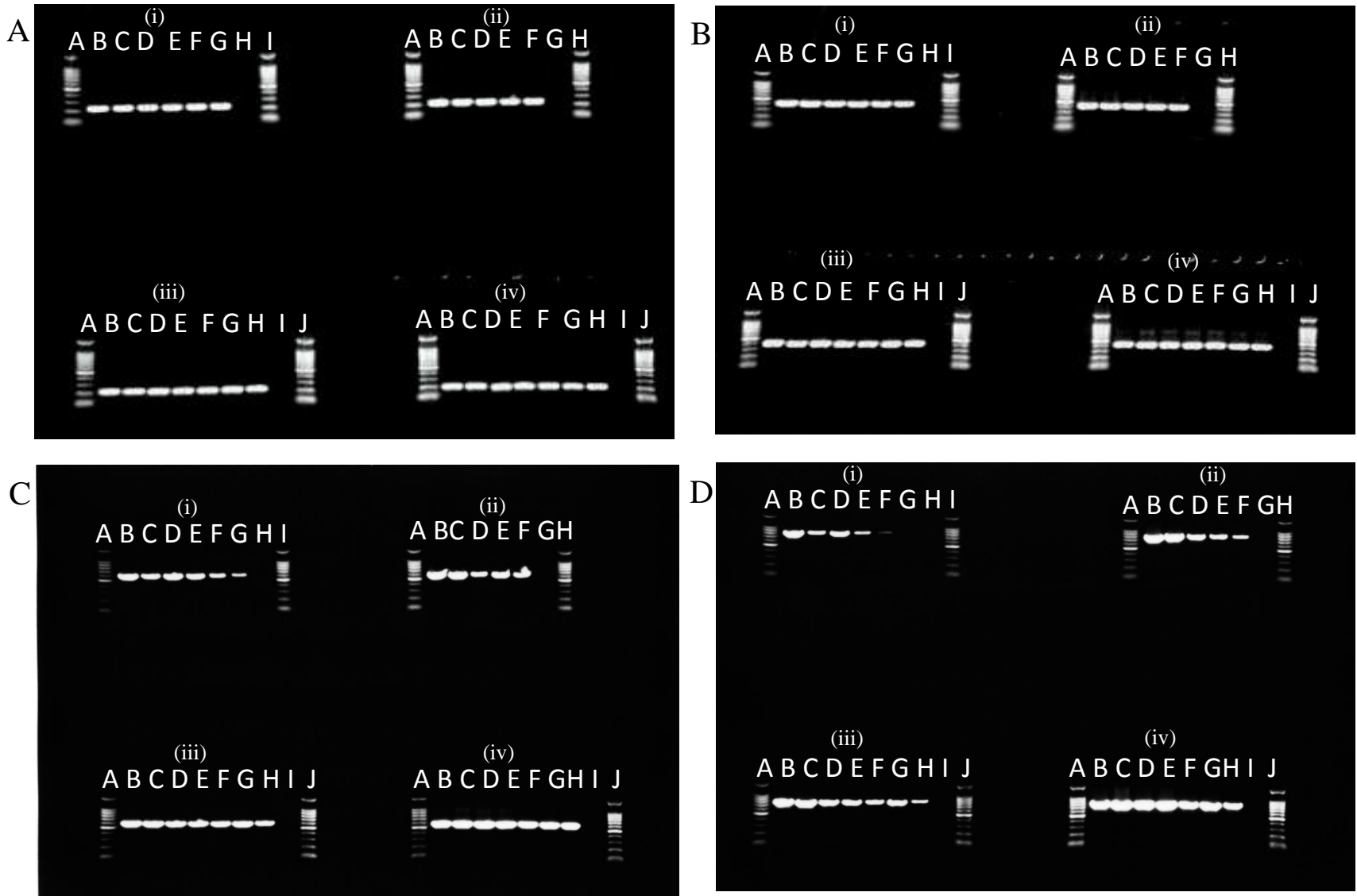


Figure 6.16. See next page for legend.

Figure 6.16. Reverse transcription-polymerase chain reaction products of viral RNA extracted from live and inactivated poliovirus.

The serotype 2 PV strain MEF-1, was inactivated with BPL, BEI and two concentrations of HCHO (1:4000 and 1:8000). During the inactivation time-courses, aliquots were taken at predetermined time- points. Viral RNA was extracted from these aliquots along with an aliquot of live MEF-1. A series of primers which yielded 200, 400, 600 and 800 bp RT-PCR products of the region encoding the VP1 protein were designed. The extracted viral RNA was run in four RT-PCRs with the respective primers. The resulting RT-PCR products of 200 (A), 400 (B), 600 (C) and 800 (D) bp were run on 1% agarose gels. Position of samples is as follows for gels A, B, C and D:

BPL inactivation (i): Ladder (A, I), Live (B), 2 h (C), 4 h (D), 8 h (E), 12 h (F), 16 h (G), RNase-free water (H).

BEI inactivation (ii): Ladder (A,H), Live (B), 4 h (C), 8 h (D), 18 h (E), 24 h (F), RNase-free water (G).

1:4000 HCHO (iii): Ladder (A, J), Live (B), 12 h (C), 36 h (D), 72 h (E), 120 h (F) 180 h (G), 288 h (H) RNase-free water (I).

1:8000 HCHO (iv): Ladder (A,J), Live (B), 12h (C), 36h (D), 72h (E), 120h (F), 180h (G), 288h (H) RNase-free water (I).

A real-time RT-PCR was developed to quantify the results of previous assay. This calculated the genome copy number / D-Ag by real-time RT-PCR using primers which amplified RT-PCR products of increasing size, as described in Materials and Methods, section 2.2.8.2. For this assay, a QuantiTect[®] SYBR[®] Green RT-PCR kit (Qiagen) was used with the primers and extracted viral RNA from the previous RT-PCR. A serial dilution series to establish a calibration curve (figure 6.17) was created as described in the Materials and Methods (section 2.2.8.2). This calibration curve was used to calculate the genome copy number of 5 µl of the extracted RNA. The results were expressed as log₁₀ genome copy number / D-Ag of the original inactivation time-point aliquots. In addition, to the region encoding the VP1 this real-time RT-PCR was also carried out with respective primers at the 5' and 3' ends of the genomic region.

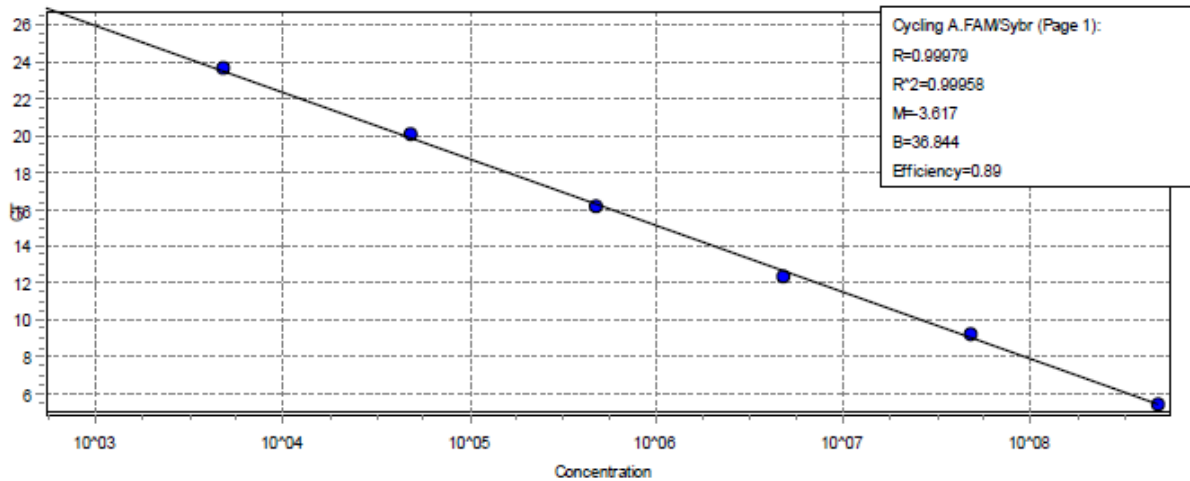


Figure 6.17. Calibration curve used to assess the genome copy number of extracted viral RNA.

The relevant primers and viral RNA extracted from live MEF-1 were used to generate an 800 bp RT-PCR product of the VP1 coding region. The concentration of this RT-PCR product was determined using a nanodrop spectrophotometer at 230 nm. The RT-PCR product was diluted with RNase-free water to ensure that the gene copy number/ 5 µl was approximately 10⁹. The diluted RT-PCR product was further diluted ten-fold from 10⁻¹ to 10⁻⁷. This serial dilution series was used to establish a calibration curve to calculate the genome copy of extracted RNA.

The results for all three regions in the PV genome supported the previous finding (figure 6.16) that inactivation reduced the functionality of the viral RNA. As the RT-PCR product increased in size, the genome copy number fell significantly for RNA extracted from MEF-1 treated with an inactivation chemical. For RNA extracted from live MEF-1 there was very little decrease in the genome copy number as the RT-PCR product increased in size. These results are represented in figure 6.18 which shows the log 10 genome copy number of RNA extracted from live and inactivated MEF-1 as the RT-PCR products increased in size.

Analysis by General Linear Model ANOVA (Minitab v.16, <http://www.minitab.com/en-GB/>) found that the difference in log 10 genome copy number, as the RT-PCR products increased in size was significant between RNA extracted from live and inactivated PV (P<0.001). The limits of detection for this assay corresponded to between 2-3 log 10s of genome copy number.

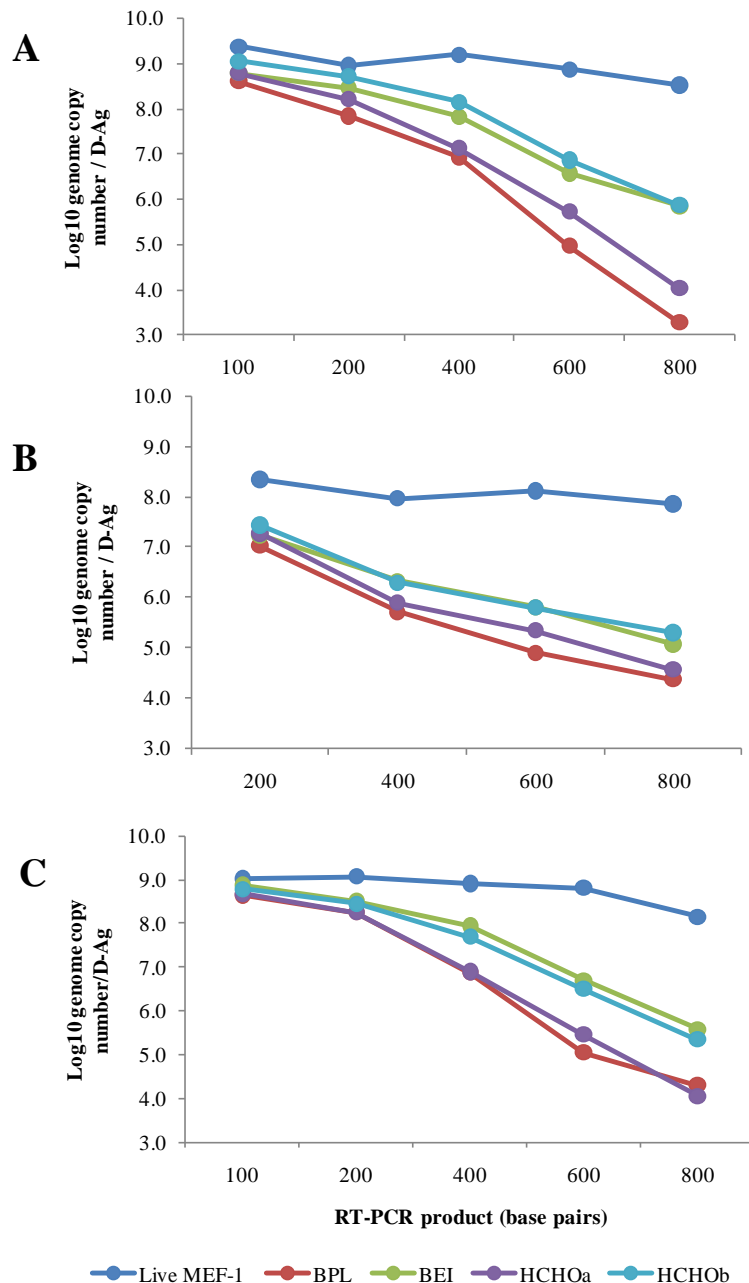


Figure 6.18. Effect of inactivation on functionality of viral RNA extracted from live MEF-1 and beta-propiolactone-, binary ethyleneimine- and formaldehyde-inactivated MEF-1.

Viral RNA was extracted from live MEF-1 and the final aliquot of the BPL, BEI and HCHO inactivation time-courses. A range of primers which yielded RT-PCR products of 100, 200, 400, 600 and 800 bp of the VP1 coding region (B) and the 5' (A) and 3' (C) ends of the genomic region were designed. A series of real-time RT-PCRs, which incorporated these primers, were carried out with a calibration curve. The results of these assays were expressed as log₁₀ genome copy number / D-Ag of the original inactivation time-point aliquots. The real-time RT-PCR of the VP1 coding region with primers which yielded a 100 bp RT-PCR product was not included due to discrepancies with the data. 1:4000 HCHO is abbreviated as HCHOa; 1:8000 HCHO is abbreviated as HCHOOb.

The concentration of the extracted RNA samples was determined using a nanodrop spectrophotometer at 230 nm (NanoDrop[®] ND-1000 spectrophotometer, NanoDrop Technologies). As table 6.7 shows, the total amount of viral RNA did not show any significant reduction during the inactivation time-courses indicating that there was no degradation of the viral RNA.

Sam.	Aliqt. (h)	RNA conc. (ng / µl)	Log10 genome copy number / D-Ag (RT-PCR, bp)														
			5'end of genomic region					VP1				3'end of genomic region					
			100	200	400	600	800	200	400	600	800	100	200	400	600	800	
Live	Live	36	9.4	9	9.2	8.9	8.5	8.6	8.8	8.2	8.1	9	9.1	8.9	8.8	8.2	
BPL	2	30	8.7	8.4	7.9	6.9	5.8	8.8	8.9	7.8	7.3	9.1	8.8	8.5	7.6	6.9	
	4	30	8.8	8.5	8	7.1	5.9	8.8	8.8	7.5	6.8	9	8.7	8.3	7.2	6.3	
	8	30	8.8	8.4	7.8	6.3	5.1	8.6	8.5	6.9	5.9	9	8.6	8	6.6	5.3	
	16	25	8.6	7.9	6.9	5	3.3	7.8	7.5	5.3	4.4	8.7	8.2	6.9	5	4.3	
BEI	4	28	8.4	8.1	7.6	7	6.2	8.8	8.8	8.0	7.7	8.9	8.7	8.6	8.2	7.6	
	8	27	9	8.6	8.2	7.5	7.5	8.8	8.9	8.0	7.3	9	8.8	8.3	7.8	7.2	
	18	29	8.9	8.3	7.7	6.7	6.2	8.5	8.5	7.0	6.3	8.9	8.7	8	7	6	
	24	34	8.8	8.5	7.8	6.6	5.8	8.3	8.4	6.6	5.8	8.9	8.5	7.9	6.7	5.6	
HCHOa	12	21	9	8.8	8.6	8.2	7.6	9.0	9.0	8.4	8.2	9.1	9.1	8.6	8.4	8	
	36	25	9.1	8.8	8.4	7.8	7.3	8.6	8.8	7.9	7.5	9.1	8.9	8.5	8	7	
	72	21	8.8	8.6	8	7.4	6.6	8.5	8.5	7.4	7.4	9	8.8	8.1	7.6	6.6	
	120	25	9.1	8.8	8.1	6.8	5.5	8.8	8.4	7.1	6.3	9	8.5	7.9	6.8	5.8	
	180	28	8.7	8.4	7.5	6.1	4.7	8.2	7.9	6.3	5.3	8.9	8.6	7.4	6.1	4.8	
	288	26	8.8	8.2	7.1	5.7	4	7.9	7.4	5.4	4.4	8.7	8.2	6.9	5.5	4	
HCHO b	12	25	8.9	8.8	8.7	8.2	7.8	8.8	8.9	8.4	8.3	8.6	8.9	8.6	8.3	7.8	
	36	25	9.1	8.9	8.7	8.1	7.8	8.8	8.9	8.2	7.9	9	8.8	8.5	8.1	7.7	
	72	22	9	8.8	8.6	8.1	7.4	8.7	8.7	8.0	7.7	9.1	8.8	8.5	8	7.3	
	120	17	9.2	8.9	8.6	7.7	6.8	8.6	8.6	7.5	6.9	8.9	8.7	8.2	7.3	6.6	
	180	19	9.1	8.8	8.2	7.4	6.4	8.8	8.5	7.3	6.8	9.1	8.7	8.1	7.1	6.2	
	288	25	9.1	8.7	8.2	6.9	5.9	8.5	8.1	6.7	6.0	8.8	8.4	7.7	6.5	5.3	

Table 6.7. Effect of inactivation on concentration and functionality of viral RNA extracted from live and inactivated MEF-1.

Viral RNA was extracted from live MEF-1 and virus aliquots from BPL, BEI and HCHO inactivation time-courses. The concentration of the extracted viral RNA samples was determined using a nanodrop spectrophotometer at 230 nm. Primers which yielded RT-PCR products of 100, 200, 400, 600 and 800 bp of the VP1 coding region and the 5' and the 3' ends of the genomic region were designed. A series of real-time RT-PCRs, which incorporated these primers, were carried out with a calibration curve. The results of these assays

were expressed as log₁₀ genome copy number / D-Ag of the original inactivation time-point aliquots. The real-time RT-PCR of the VP1 coding region with primers which yielded a 100 bp RT-PCR product was not included due to discrepancies with the data. Log₁₀ genome copy number / D-Ag values are coloured from high (green) to mid (yellow) to low (red). 1:4000 HCHO is abbreviated as HCHOa; 1:8000 HCHO is abbreviated as HCHO_b. Sam. indicates sample; Aliqt. indicates aliquot.

The reduction in the functionality of the viral genome during inactivation was confirmed by the fall in the genome copy number, but not concentration of the viral RNA. The inactivation chemicals could be reducing the functionality of the viral RNA by fragmenting it or by inducing chemical modifications. As table 6.7 shows, this effect is seen throughout the three regions tested, indicating that inactivation reduces the functionality of the whole genome rather than a specific area. Analysis by General Linear Model ANOVA (Minitab v.16, <http://www.minitab.com/en-GB/>) of the log₁₀ genome copy number of the regions found that they did not differ significantly. A comparison of the fall in log₁₀ genome copy number of the RNA extracted from inactivation time-courses found that inactivation with BPL produced a larger reduction in log₁₀ genome copy number than inactivation with BEI or HCHO. Analysis by General Linear Model ANOVA (Minitab v.16, <http://www.minitab.com/en-GB/>) found that this difference in the reduction of log₁₀ genome copy number was significant (P<0.001). For all inactivation chemicals the reduction in the genome copy number of the extracted RNA became progressively greater as the inactivation time-courses progressed. As table 6.7 shows, this effect was particularly prominent when the 600 and 800 bp RT-PCR products were amplified.

In order to discard nonspecific damage to the viral RNA caused by the inactivation conditions, RNA extracted from the A0i and A0ii live MEF-1 controls (Chapter 4) was analysed in a series of real-time RT-PCRs of the three genomic regions which amplified 800 bp RT-PCR products. The viral RNA extracted from the A0i and A0ii controls of the BPL and BEI inactivation time-courses showed a similar genome copy number to RNA extracted from live MEF-1 (data not shown). This was also apparent for the A0i control of the HCHO inactivation time-courses. However, viral RNA extracted from the A0ii HCHO control showed a reduction in genome copy number in comparison to the A0i control. The scale of this reduction varied for the VP1 coding region and the 5' and 3' ends of the genomic region

(1.0, 0.7 and 1.2 log 10s, respectively). This finding correlates with the reduction in the infectious titre of the A0ii control of the HCHO inactivation time-courses (Chapter 4).

As discussed above the viral RNA used in these RT-PCRs was extracted using the MagNA Pure LC Total Nucleic Acid Isolation Kit and the Kingfisher ml particle processor. In order to verify that the amount of RNA detected did not significantly differ between extraction kits a real-time RT-PCR was used. The genome copy number of viral RNA extracted from a commercial IPV by the QIAamp viral RNA mini (Qiagen) and the MagNA Pure LC Total Nucleic Acid Isolation extraction kits was assessed by a real-time RT-PCR. This assay incorporated the primers described above which yielded RT-PCR products of 200, 600 and 800 bp of the VP1 encoding region. The log 10 genome copy number of the extracted RNA was calculated relative to a calibration curve as described above.

As table 6.8 shows, there was little difference between the two extraction kits as the resulting RNA showed similar log 10 genome copy number across three RT-PCR products. In addition the MagNA Pure LC Total Nucleic Acid Isolation kit had an advantage of being largely automated and therefore it could be practical when a large number of samples need to be processed.

Extraction technique	Log 10 genome copy number (RT-PCR product)		
	200	600	800
Qiagen	5.4	3.6	3.4
MagNA Pure	5.4	3.4	3.5

Table 6.8. Genome copy number of RNA extracted using different techniques.

Viral RNA of a commercial IPV was extracted using the QIAamp viral RNA mini kit and the MagNA Pure LC Total Nucleic Acid Isolation Kit. The genome copy number of the resulting viral RNA was determined by a real-time RT-PCR which incorporated primers which yielded RT-PCR products of 200, 600 and 800 bp of the VP1 coding region. The genome copy number of the extracted RNA was calculated relative to a calibration curve. Values were logged.

The effect of inactivation on the viral RNA was explored further using a bioanalyser which could analyse the quality and size of the extracted viral RNA using an electrophoresis system. Viral RNA extracted from a series of commercial IPVs was analysed using the Agilent 2100 Expert Bioanalyser (Agilent technologies). As figure 6.19 shows, the viral RNA from the IPVs were all of approximately 7400 nts in size. This is equivalent to the size of the whole PV genome which suggests that inactivation with HCHO does not fragment the viral RNA.

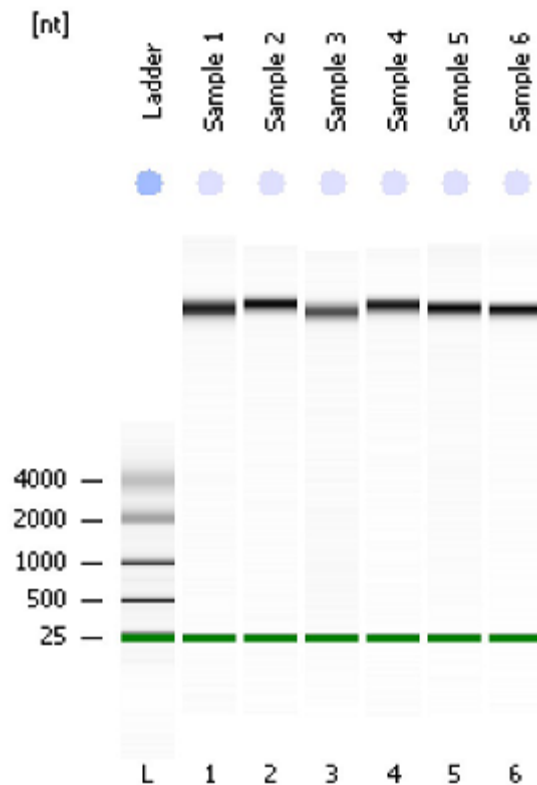


Figure 6.19. Visualisation of RNA extracted from inactivated poliovirus vaccine preparations using an electrophoresis system.

Viral RNA was extracted from six commercial IPV preparations and analysed using the Agilent 2100 Expert Bioanalyser.

6.3 DISCUSSION

A range of assays have been carried out to analyse the effect of inactivation on three properties of PV: the ability to bind to the PVR; the ability to undergo conformational changes necessary to enter a cell; and the functionality of the viral RNA. Alkaline phosphatase, FACS flow cytometry and real-time RT-PCR assays found that inactivated PV was able to bind to the PVR expressed as a soluble fusion protein or on the surface of L20B cells, although at an apparent reduced rate. The scale of this reduction varied slightly between the PV strain and the type of assay used to assess the PV:PVR interaction. For example, analysis of the binding of live and inactivated PV to CD155-AP by the AP assay found that the Sabin 2 strain showed a 66 % reduction, while the MEF-1 strain showed a 14 % reduction. In comparison to the AP assay the real-time RT-PCR binding assay found that inactivated MEF-1 showed a 78 % reduction in binding. This difference could be due to the amount and accessibility of binding surface of the soluble CD155-AP and the PVR expressed on L20B cells. The reduction in binding between inactivated PV and the PVR could have been due to the inactivation chemicals altering the capsid protein coat of the PV virions in such a manner that their receptor binding site (canyon) was chemically changed resulting in the virus being less able to bind to the receptor (180, 450). For example, previous research has suggested that inactivation of PV with HCHO results in capsid proteins being cross-linked (512). This cross-linking may result in the canyon being partially blocked which would lead to a reduction in the probability of effective contact between the PV and its cellular receptor.

In addition to HCHO both BPL and BEI were found to reduce but not prevent the interaction between PV and the PVR. Recently published research has used ellipsometry to analyse the effect of BPL treatment on the adsorption of two H1N1 influenza strains on a mixed phospholipids DMPC/GM3 monolayer at the air-water interface. This research found that BPL reduced the viral affinity for the mixed monolayer, possibly through a modification of the hemagglutinin (125). The results detailed in this chapter indicate that BPL has a similar effect on the interaction between PV and its cellular receptor. This was not unexpected as it has been previously noted that BPL interacts with viral capsid proteins (56). In addition it was described in Chapter 4 how inactivation with BPL resulted in a loss of antigenic material, indicating that the viral capsid was affected by BPL treatment. Finally it should be noted that despite previous literature indicating that main mechanism of inactivation of BPL was the

preferential carboxyethylation of guanine and adenine (57, 97, 432, 459) a recent study has determined that proteins are more extensively modified than nucleic acids during inactivation with BPL (514). Thus BPL could have modified the viral capsid proteins resulting in the observed reduction in affinity for the PVR.

Binary ethyleneimine-inactivated PV also showed a reduced affinity to interact with the PVR, indicating that viral capsid proteins were modified by BEI treatment. This was expected as findings detailed in Chapter 4 showed that inactivation with BEI resulted in minor modifications to the antigenic structure of PV virions. Previous research has also confirmed that BEI can modify viral proteins as well as viral nucleic acid (66, 67, 71, 247).

The effect of inactivation on the entry of PV into target cells has been determined by a number of assays which assessed whether inactivated PV particles could undergo the necessary conformational changes to enter the cells. These assays suggested that PV inactivated with either BEI or HCHO was unable to undergo the conformational change to form 135S particles, an essential intermediate structure of the entry process (511). An explanation for this is that both chemicals induce modifications to the PV virions which prevent the conformational change. Inactivation with HCHO is known to result in the formation of cross-links which have been previously indicated to improve the stability of FMD virus preparations (28, 441). Such cross-links could have prevented the inactivated PV virions from undergoing the conformational change to 135S particles when heated to 50 °C. In addition, as a tanning agent HCHO may harden viral proteins (156, 316). This tanning of the surface of the inactivated PV virions could further prevent them from undergoing a conformational change.

As an aziridine, BEI has been previously noted to lack the cross-linking and fixation activity of HCHO (28). However, BEI has been shown to interact with capsid proteins (Chapters 4 and 6) and has been previously noted to modify viral proteins (66, 67, 71, 247). The findings of this chapter suggest that HCHO and BEI mediated modifications to the viral proteins of the inactivated PV virions prevent them from shifting conformation to 135S particles when heated to 50 °C.

Like live (untreated) PV, BPL-inactivated PV virions appeared to undergo the conformational change to 135S particles when heated to 50 °C. The results detailed in this chapter show that if BPL modifies the viral proteins, such modifications do not appear to

prevent a conformational change to 135S particles. A possible explanation for this is that BPL induced chemical modifications are of a different nature to those of HCHO and BEI and do not increase the stability of PV virions allowing them to undergo the conformational change at the relevant temperature.

Both live and inactivated PV were indicated to have undergone a conformational change to 80S particles following heat-treatment at 60 °C. Modification conferred to PV virions by HCHO and BEI inactivation, which seemed to prevent the conformational change to 135S particles, did not prevent the conformational change at 60 °C. An explanation for this could be that the inactivation modifications formed by these chemicals were not stable at 60 °C and broke down allowing the virus to undergo the conformational change to 80S particles. It has been previously found that HCHO cross-links are reversed when heated to 65 °C (418). Thus it is possible that heating the PV preparations to 60 °C was sufficient to break down the inactivation modifications to PV virions. While the results of this chapter suggest that inactivation with HCHO and BEI prevents PV from undergoing the conformational changes, it will be necessary to verify this using a sucrose gradient following a similar approach to Arita *et al.* (19). The sucrose gradient would allow the structural properties of inactivated PV bound to the PVR to be assessed.

Analysis of the biological activity of viral RNA extracted from inactivated PV using two transfection techniques found that inactivation with the three chemicals eliminated the biological activity of the RNA. Only the viral RNA extracted before 36 h of inactivation with HCHO showed biological activity during the inactivation time-courses. This supports Martin *et al.* (312) who found that viral RNA was no longer infectious following partial inactivation with HCHO. This suggests that inactivation with the three chemicals rapidly alters the viral RNA molecules. However the sensitivity of the DEAE-dextran transfection technique was limited.

Previous research using phenol / SDS could only detect viral RNA extracted from PV partially inactivated with HCHO (312). However research described in this chapter has shown that it is possible to extract viral RNA from fully inactivated PV using the magnetic bead-based MagNA Pure LC Total Nucleic Acid Isolation kit. When the extracted viral RNA was analysed by RT-PCRs with PV-specific primers it was found that for RNA extracted from the final aliquots of each inactivation time-course only RT-PCR products of low size

(200 and 400 bp) were successfully amplified. Reverse transcription-polymerase chain reaction products of high size (600 and 800 bp) either produced narrower fainter bands or failed to produce any bands indicating that either less or no RT-PCR product was amplified. Similar results have been obtained following the analysis of DNA extracted from formalin-fixed paraffin-embedded tissues (122). The successful amplification of RT-PCR products of 600 and 800 bp of aliquots taken earlier in the inactivation time-courses indicates that the inactivation chemicals affected the functionality of the viral RNA, with an increasing effect as the time-courses proceeded.

The findings of the RT-PCRs were confirmed following quantification. Viral RNA extracted from each inactivation time-course showed lower genome copy number / D-Ag as the time-courses progressed and larger RT-PCR products were amplified. This was found for all of the three sequenced regions of the PV genome, with no significant difference in the genome copy number / D-Ag between the three regions. The RT-PCRs suggest that as the inactivation time-courses progress that the functionality of the viral RNA is reduced. This could be due to the inactivation chemicals either fragmenting the viral genome or modifying the nt bases which make up the viral genome. Analysis of the viral RNA extracted from commercial IPV found that inactivation with HCHO did not appear to fragment the RNA. So modifications to nt bases may be responsible for the reduction in the functionality of the viral RNA of HCHO-inactivated PV. Formaldehyde interacts with nt bases in two steps. The first reaction involves the addition of the HCHO group to NH-group of bases resulting in the formation of labile methylol-derivatives. The secondary electrophilic reaction with N-methylol on an amino base forms a methylene bridge between two amino groups (21, 156). Beta-propiolactone and BEI can modify the viral RNA by alkylation which can result in the formation of covalent adducts on adenosine (N-1), cytidine (N-3) and guanosine (N-7) (204, 205). These modifications could have a negative effect on RT-PCR and other enzymatic procedures (527). For example following HCHO inactivation, the addition of monomethylol groups to nt bases which modify the poly A tail could inhibit oligo primer annealing to the poly A tail and consequently the reverse transcription reaction (74). In addition these chemical modifications can reduce or block the base pairing necessary for molecular analysis by hybridization techniques (155, 156, 193). Thus the amplification of reverse transcriptase products during the RT-PCR assays might have been restricted if the nt bases were modified during inactivation.

It is not clear how BPL or BEI reduced the functionality of the viral RNA during inactivation. While both can modify the viral RNA, BPL has been previously found to fragment nucleic acids (48, 122, 417) by inducing cross-linking reactions between nucleic acid bases and proteins. This can restrict the extraction of nucleic acids and can inhibit polymerase during PCR-based molecular assays (106, 155). Therefore if BPL or BEI did fragment the viral genome they could have reduced the efficiency of the RT-PCR resulting in a reduced amplification of the template. Fragmentation of the viral RNA or modification of the nt bases could have had a negative effect on the biological activity of the RNA. This could explain why RNA extracted from fully inactivated PV did not cause CPE in transfected cells.

Poliovirus inactivated with BPL showed a larger reduction in genome copy number than PV inactivated with BEI or HCHO. A grouping analysis using the Tukey method (Minitab v.16, <http://www.minitab.com/en-GB/>) confirmed that this difference was significant ($P < 0.05$). The experimental conditions (in particular the pH) could have contributed to the large reduction in genome copy number of the viral RNA extracted from the BPL-inactivated aliquots. It has been previously found that the reaction between BPL and DNA was of greater efficacy when carried out at weakly basic pH (7.4-8.0) (193). As described in Chapter 4 the pH of the BPL inactivation was around 7.5, which might have led a more efficacious reaction between the viral RNA and BPL, resulting in more modifications to the RNA. Despite both BPL and BEI inactivating viruses by interacting with similar nucleophilic positions in nucleic bases (205, 206, 400, 526) the BEI induced modification seemed to have less effect than BPL modifications on the viral RNA functionality. This may be due to differences between how each chemical interacts with the nucleic acid targets. One difference is that BPL is capable of cross-linking to RNA to other macromolecules, while BEI has not shown this property.

The results detailed here indicate that PV inactivated with HCHO or BEI is unable to undergo the necessary conformational changes to enter a target cell and initiate an infection. All three chemicals were able to modify the viral RNA during inactivation, eliminating its infectivity and reducing its functionality. The real-time RT-PCR successfully assessed the effect of inactivation on the functionality of the viral RNA. This assay could be used as a quality control test for IPV production. As this assay involves the extraction and amplification of viral RNA using strain specific primers, it could be used as an identity test to monitor for any contaminating strains in the IPV. In addition if the fall in genome copy

number of viral RNA following inactivation is reproducible then this assay could be used as a measure of consistency of IPV production. The effect of inactivation with BPL or BEI on the viral RNA could be further explored using a Bioanalyser or mass spectrometry (106, 315).

CHAPTER 7

GENERAL DISCUSSION

As explained in the introduction, the use of safer improved IPV products will be required for the End-game of the GPEI. One of the main objectives of this PhD thesis was to characterise and understand the differences between current IPV preparations made from wild-type PV strains and those produced from live-attenuated Sabin virus seeds currently used for OPV production. Analyses of inactivated PV preparations developed with the use of alternative chemicals for virus inactivation, such as BEI and BPL, were also carried out. In addition the molecular mechanisms underlying virus inactivation with HCHO, BEI and BPL were investigated.

To gain full understanding of why Sabin 2 and MEF-1 differ in immunogenicity following inactivation with HCHO, the molecular, antigenic and immunogenic properties of inactivated PV preparations made from a wide range of serotype 2 strains were determined. They included four wild-type strains from different years and regions, three iVDPV strains from two different patients and one cVDPV strain from an outbreak in Madagascar. The nt sequence covering the entire capsid coding region (2637 nts) was first determined for all serotype 2 strains in the study. Remarkably, the iVDPV strains showed a much higher proportion of non-synonymous changes with respect to the Sabin 2 strain than those shown by the wild-type serotype 2 strains, despite the latter being genetically distant from Sabin 2 as they span 40 years and were isolated in very distant geographical areas.

Interestingly, the cVDPV strain from Madagascar and other cVDPV strains for which sequences are available in public databases, showed a low proportion of non-synonymous nt changes compared to the Sabin 2 virus, like wild-type viruses. The conclusion is that Sabin 2 vaccine virus appears to accumulate amino acid changes more rapidly during evolution in a single patient than when it is transmitted from person to person. It is likely that the combination of a number of factors, such as evasion to immune pressure, ability to bind the cell receptor and improvement of fitness to grow in the gut contribute to the selection of mutations during the evolution of Sabin vaccine strains in humans. These factors might be different in individuals with immunodeficiency, resulting in viruses with different mutation profiles. This observation could be useful when identifying VDPV strains found in environmental samples, as analysis of their mutation profile could help to determine whether any particular strain is likely to be a cVDPV or an iVDPV, which would help deciding public health interventions. Many of these mutations affected capsid regions corresponding to known antigenic sites or their flanking amino acid residues. Analysis by ELISA confirmed

that these specific amino acid alterations correlated with changes in reactivity with MAbs directed against different antigenic sites.

The serotype 2 PV strains were then inactivated with HCHO following the conventional technique used to generate commercial IPV. The D-Ag content of HCHO-inactivated serotype 2 PV preparations was determined by ELISA using various anti-serotype 2 PV MAbs. All serotype 2 strains showed similar ratios of D-Ag content and infectious titre (TCID₅₀), suggesting the presence of similar proportions of infectious virus in the original preparations. A new technique, based on the use of SPR mediated technology (Biacore), was developed and validated. This method could result in more accurate and consistent measurement of the potency of IPV products, which would benefit the process of quality control of such vaccines. Analysis of the antigenic properties of the inactivated serotype 2 strains found that while inactivation with HCHO did not result in a significant loss of antigenicity, it did modify the structure of antigenic site 1. It is not clear what impact the modifications to antigenic site 1 has on the immunogenicity of inactivated PV, but as this site, with site 3, has been found for serotype 3 PV strains to be immunogenic in humans, it is likely to have some effect (207).

Analysis of sera from rats immunised with the inactivated serotype 2 PV strains found that wild-type strains showed high neutralisation titres against challenge viruses, with the highest neutralisation shown with inactivated MEF-1. The inactivated Sabin 2 strain showed significantly lower immunogenicity than MEF-1 and other wild-type strains, and inactivated iVDPV strains showed the lowest levels of immunogenicity of all the inactivated serotype 2 strains. Research with model peptides has determined the structures of HCHO-induced modifications in proteins and the intrinsic reactivity of each amino acid residue (331, 332). The initial reaction of HCHO with a peptide or protein results in the formation of methylol adducts on the amino and thiol groups of arginine, cysteine, histidine, lysine and tryptophan residues. On the lysine and tryptophan residues the methylol groups partially dehydrate resulting in the formation of Schiff bases (Scheme 1) which can form stable crosslinks (methylene bridges) with a range of amino acid residues, including arginine, asparagine, glutamine, histidine, tryptophan and tyrosine (331, 332). Sequence analysis of the viral capsid confirmed the presence of some of these amino acids within the antigenic sites. The variation in the presence and location of these HCHO “targets” within the antigenic sites may

at least in part, explain why the immunogenicity differed between strains, although the extent of this is not easy to predict.

Sera from rats immunised with the inactivated serotype 2 PV strains showed lower neutralisation titres when challenged with an iVDPV strain that had extensive amino acid changes in antigenic sites. These extensive amino acid changes may have contributed to the reduced capacity of these strains to be neutralised by sera from immunised rats. This finding could have ramifications for communities with low PV immunity if the reduced capacity of these strains to be neutralised leads to less protection against PV.

A comparison of live and inactivated serotype 2 PV preparations showed that inactivation with HCHO resulted in a significant reduction in the overall immunogenicity. Given the scale of this reduction in immunogenicity it is unlikely that the modification of antigenic site 1 alone accounts for such difference. It cannot be dismissed that changes in epitopes undetected by the panel of MAbs occur as a consequence of inactivation. However, as the MAb panel covers all known antigenic sites, the explanation is likely to be of a more general phenomenon, such as inactivation affecting processing and presentation of viral peptides by the immune system.

Inactivated poliovirus vaccine induces a neutralising antibody response which controls infection (251). This immune response is initiated following recognition of peptides displayed by major histocompatibility complex (MHC) class II molecules at the surfaces of antigen-presenting cells (APCs) (497). Antigen-presenting cells (including dendritic cells, macrophages and B cells) take up the IPV antigen by endocytosis (29). As the early endosomes mature into lysosomes and undergo progressive acidification, the antigen is processed into peptide fragments by endosomal proteases (e.g. asparaginyl endopeptidase) (436). Nascent MHC class II $\alpha\beta$ heterodimers assemble with the invariant chain (Ii) and enter the endocytic pathway (497) where vacuoles containing this complex fuse with late endosomes carrying the antigen peptides (436). Within the late endosomes the Ii is digested by proteases to leave the class II-associated invariant chain peptide (CLIP) within the peptide binding groove of the MHC class II. The protein chaperone HLA-DM catalyses the exchange of CLIP for endosomal antigen peptides (198, 482). The MHC-peptide complexes then traffic to the cell surface where they can bind to receptors of T_H1 or T_H2 T-helper cells and B cells (TCR and BCR, respectively) within the draining lymph node. Binding of specific antigenic

peptides to these receptors and additional binding between co-stimulatory molecules on APCs and T-helper cells activates the T-helper and B cells. Activated T_H1 cells enhance IFN- γ production, while T_H2 release interleukin 2, 4, 5 and 6 which induce further B-cell activation, differentiation and proliferation with isotype switch (IgM to IgG) and memory cell formation (29, 444).

Given that it has been shown previously that HCHO can interact with amino acid residues, it is possible that it could alter antigen processing; peptide-MHC association or; TCR recognition of the peptide-MHC complex (331, 332). For example HCHO could induce cross-linking or tanning reactions to viral proteins which would confer resistance to proteolytic processing. This would, in turn, reduce the presentation of viral peptides to TCR and BCR and, consequently, the immune response. Indeed, previous research has found that HCHO treatment can constrain antigen presentation to T cells by altering proteolytic processing of the treated proteins (129).

In order to investigate the development of inactivated PV with higher immunogenicity, BPL and BEI were used to inactivate selected serotype 2 strains. These chemicals were chosen as previous research indicated that they selectively inactivate the viral genome. They primarily inactivate by introducing nucleic acid adducts, principally 7-(2-carboxyethyl) guanine (97, 205, 206, 432, 459, 525). Iodoacetamide was also chosen as an alternative inactivation chemical as it inactivates in a non-cross-linking manner which might result in less modification to the antigenic structure of PV. However, IAN was found to be an unsuitable alternative chemical as it modified or destroyed antigenic epitopes and there was difficulty in removing it following inactivation. Optimal conditions for inactivation were established using different concentrations of the chemicals in time-course experiments. Both BPL and BEI eliminated viral infectivity at a much faster rate than HCHO. Like HCHO, inactivation with BPL or BEI resulted in modification to antigenic site 1, although the extent varied between the chemicals and the PV strains. Inactivation of the MEF-1 strain with BEI or HCHO modified antigenic site 1. Beta-propiolactone-inactivated MEF-1 showed no evidence of modification to any of the antigenic sites.

The immunogenicity of PV strains inactivated with HCHO, BEI or BPL was assessed with a rat potency assay, commonly used for the batch release of IPV (153), and a series of immunisation-challenge experiments with TgPVR mice, developed at the NIBSC (312). The

results of the rat potency assay showed that BEI- and HCHO-inactivated MEF-1 generated similar immune responses. Beta-propiolactone-inactivated MEF-1 was less immunogenic than BEI- and HCHO-inactivated MEF-1. The low immunogenicity of BPL-inactivated MEF-1, despite lacking any detectable modification to the antigenic sites indicates that changes to the antigenic structure do not alone account for the immunogenicity of inactivated PV. As discussed above it is more likely that inactivation affected the processing and presentation of viral peptides. A potential explanation for the low immunogenicity of BPL-inactivated MEF-1 could be that the acylation and alkylation reactions that BPL induces in viral proteins could result in viral peptides of low stability (514). Previous research has indicated that MHC class II complexes with unstable peptides can lead to aberrant pathways of T cell differentiation and potentially a poor immune response (455).

The results of the rat potency assay showed that the sera from rats immunised with BPL-, BEI- or HCHO-inactivated MEF-1 had lower neutralisation titres against an iVDPV strain in comparison to when challenged with the Sabin 2 and MEF-1 strains. A series of immunisation-challenge experiments using TgPVR mice showed that this selective immunogenicity resulted in selective protection against different challenge strains. The low protection conferred by inactivated Sabin 2 and MEF-1 preparations against the iVDPV strain could mean that such strains may pose a greater risk of spread in populations with low herd immunity to PV and a real threat for the re-introduction of PV into the community in the post-eradication era. However it is not clear how transmissible these strains are and there are no current techniques to measure this. A potential solution would be to use adjuvants to improve the immunogenicity of IPV preparations. The addition of adjuvants may also allow antigen sparing of IPV (25, 524). Adjuvants could also boost the immunogenicity of inactivated Sabin 2 which, as described above, was found to have a lower immunogenicity than inactivated MEF-1. One such adjuvant under development is aluminium hydroxide, Al(OH)₃. This has been found to increase the immunogenicity two-fold for all three sIPV strains in rats (524). In mice, the humoral and cellular immune response to sIPV is enhanced by Al(OH)₃ with or without CpG (566). Sabin-IPV preparations admixed with either chitosan glutamate or chitosan sulfate micro/nanoparticles showed improved immunogenicity when administered to mice (185). The 1,25-Dihydroxyvitamin D₃ could also be used as an adjuvant for sIPV preparations (232).

While the rat potency assay measured the antibody response induced by the inactivated PV preparations, the immunisation-challenge experiments with TgPVR mice assessed the protection conferred by such PV preparations. This encompasses the innate immune response in addition to the antibody response. Modifications to PV virions following inactivation may affect both immune responses. Innate immune recognition is mediated by germ line-encoded pattern recognition receptors (PRRs) which bind to conserved molecular patterns characteristic of microorganisms termed pathogen associated molecular patterns (PAMPs) (274, 457). The binding of PAMPs by PRRs (including toll-like receptors, TLRs) triggers the release of cytokines and chemokines which activate APCs and initiate the adaptive immune response (457, 470). Previous research has determined that the viral genomic RNA acts as a PAMP and that a number of TLRs (including TLR7 and TLR3) are able to recognise and bind to it and trigger an immune response (184, 274). Research within this thesis has shown that during inactivation with BPL, BEI or HCHO, the viral RNA is fragmented or modified. This could affect the ability of the TLRs to recognise, bind and trigger an immune response. Picornavirus RNA is also detected by the cytoplasmic melanoma differentiation-associated gene 5 (MDA5) which is a retinoic acid-inducible gene I-like receptor (26, 248, 300). After detecting double stranded RNA, MDA5 associates with mitochondrial IFN- β promoter stimulator-1 which triggers a signalling pathway to activate type 1 IFN genes (26, 492). Fragmentation or modification of the viral RNA by inactivation may affect the ability of MDA5 to recognise and trigger the signalling pathway that results in a type 1 IFN response.

In addition to the immunogenicity, thermostability is a critical property of a vaccine. The thermostability of BPL, BEI or HCHO-inactivated MEF-1 preparations was assessed by determining the degradation of the viral antigenicity and immunogenicity of these preparations following treatment at 45 °C. This analysis found that the BEI-inactivated MEF-1 had a greater thermostability than HCHO- and BPL-inactivated MEF-1. The BPL-inactivated MEF-1 was found to have the lowest thermostability of all the MEF-1 preparations. Poliovirus inactivated with BEI showed similar antigenic and immunogenic characteristics to HCHO-inactivated PV. Both HCHO- and BEI-inactivated vaccines are well tolerated and considered safe (409, 421, 440). Binary ethyleneimine is considered to be less carcinogenic and toxic than HCHO (5, 440). In addition, elimination of infectivity is far more rapid with BEI and the resulting inactivated PV preparations show slightly better thermostability than HCHO-inactivated PV preparations. Such results indicate that BEI may

be a suitable alternative to HCHO for vaccine manufacturers. In particular, it may be of value to manufacturers looking to develop vaccines against other EVs, such as EV71.

Although it is known that inactivation of PV eliminates viral infectivity and causes a reduction in immunogenicity, the molecular mechanisms which underlie this process are not known. Knowledge of such mechanisms could help understanding the results above and fine-tuning the process of inactivation during vaccine production. It could also contribute to the development of alternative methods for the quality control of IPV products. To gain a better understanding of the effect of chemical inactivation on the biology of PV, some properties of inactivated viral particles and viral RNA were analysed. The ability of inactivated PV to bind to PVR was analysed in a series of binding assays using a sPVR (expressed as a PVR-AP recombinant fusion protein) and L20B cells susceptible for PV infection. Analysis of the PV-PVR interaction, using ultracentrifugation and SPR techniques (Biacore), showed that inactivated PV retained the ability to bind to sPVR.

As expected, inactivated PV was able to bind to L20B cells, as shown by a FACS flow cytometry method that detected virus particles on the cell surface, and a real-time RT-PCR binding assay that measured the amount of viral RNA associated with cells. In both cases, binding of PV to cells was inhibited by pre-incubation of the virus with sPVR and/or anti-serotype 2 PV MAbs which indicates that binding of PV to L20B cells was mediated by its interaction with the PVR on the cell surface. The alteration of antigenic site 1 in inactivated MEF-1 was further confirmed by these assays as the PV-cell interaction was not inhibited by pre-incubation with MAb 436 which had shown an inability to bind to inactivated MEF-1 in ELISAs and did block binding of live virus to cells. The binding experiments showed that although retaining the ability to bind to PVR, inactivated PV bound at a 60-80 % reduced rate in comparison to live PV. It has been previously noted that the interaction between PV and the PVR is biphasic with two classes of binding sites for the PVR on PV virions. The binding affinities of the two sites differ and current research suggests that reversible conformational changes in the virus / receptor precede the formation of the higher-affinity PV-PVR complex (292). The findings in this thesis indicate that inactivation may result in modifications to the viral capsid proteins which prevent these conformational changes and, therefore, the progression from low affinity to high affinity PV-PVR complexes.

The effect of inactivation on the ability of PV to enter permissive cells was assessed by establishing whether inactivated PV could still undergo the necessary conformational changes that follow virus-receptor binding and lead to virus-cell entry. These conformational changes result in sequential 160S, 135S and 80S virus particles that represent native virus, antigenically altered virus and empty viral capsids that lack viral RNA or show viral RNA in the process of release. Following incubation in hypotonic medium at 50 °C in conditions known to generate 135S particles *in vitro* (50, 113), both live and BPL-inactivated MEF-1 showed similar properties to 135S particles in that they had lost their antigenic activity and their ability to bind to L20B cells, but retained viral RNA inside the particle as shown by resistance to RNase A treatment. By contrast, the HCHO- and BEI-inactivated MEF-1 still showed antigenic activity and the ability to bind to L20B cells following incubation in hypotonic medium at 50 °C, indicating that these PV preparations had remained in the native virion conformation. Chemical modifications induced by HCHO and BEI during inactivation may have stabilized the viral particles, preventing the PV virions from shifting to the 135S particle conformation. This correlates with previous research showing covalent linking protein interaction (28, 441). However, inactivation with BPL does not appear to stabilize PV particles in the same manner, which agrees with the fact that heated BPL-inactivated PV showed the lowest immunogenicity in animal assays. It is not clear whether these results can explain what happens *in vivo* in that the HCHO- and BEI-inactivated PV particles lose their infectivity due, at least in part, to their inability to undergo conformational changes that precede virus cell-entry. Clarifying these issues would require further studies.

A series of transfection and RT-PCR assays were used to study changes in the biological activity and functionality of viral RNA during chemical inactivation. Infectious virus was not recovered from transfection of viral RNA extracted from samples taken at early stages of chemical inactivation indicating a rapid alteration of RNA molecules with all three chemicals employed. Similarly, reduced RT-PCR yields were obtained as inactivation progressed from viral RNA extracted from inactivated MEF-1 preparations as compared to RT-PCR products obtained from RNA of live PV, suggesting that all three chemicals interacted directly with viral RNA molecules, somehow modifying them and preventing amplification by PCR polymerases (527). This was true for all three genomic regions analysed and was more dramatic for the BPL-inactivated samples. These alterations might also be responsible, at least in part, for the destruction of virus infectivity as inactivation advanced.

These findings and those regarding the effect of inactivation on the ability of PV to bind and enter cells, allow a model for the mechanism of chemical inactivation to be proposed. When the inactivation chemical is added to the infectious PV virions it undergoes chemical reactions (including cross-linking and tanning) with the capsid proteins affecting both the antigenic structure and ability of PV to bind and enter permissive cells. During inactivation, the chemical somehow penetrates through the viral capsid proteins and interacts with viral RNA. Due to their small size, the chemical molecules may be able to diffuse through the hydrated protein (56, 180). Alternatively, the chemical molecules may penetrate in a step-wise fashion, from one reaction to another (180).

The hypothesis that inactivation alters the antigenic epitopes of PV resulting in changes in their immunogenicity can be accepted. However, research detailed in this thesis has shown that the effect of inactivation on PV is more complex. It is likely that other factors beyond modifications to the antigenic structure influence the immunogenicity of IPVs. A range of novel assays have been described in this thesis which could be used in the quality control of IPVs; including the use of a real-time RT-PCR to assess the loss of viral RNA functionality during inactivation. Research in this thesis has emphasised the importance of both the PV strain and the inactivation chemical used in the development of an improved IPV for the End-game of PV eradication and beyond.

CHAPTER 8

CONCLUSIONS AND RECOMMENDATIONS

The research detailed in this thesis has met its aim in improving understanding of the inactivation of PV which will contribute to the development of improved IPVs for the End-game and post-eradication phase of the GPEI. The objectives under this aim have been achieved and a series of conclusions can be found. To explore why the immunogenicity of serotype 2 sIPV and cIPV differed one of the objectives of this research was to assess the molecular, antigenic and immunogenic properties of a range of serotype 2 strains following conventional HCHO inactivation. The molecular, antigenic and immunogenic characteristics of the inactivated preparations varied between the PV strains suggesting that differences in genomic sequence may be responsible. This finding suggests that if the vaccine seed for IPV is to be changed for the End-game it is important to characterise the inactivated product in terms of its potency and immunogenicity. The immunogenicity of all inactivated serotype 2 PV preparations was lower when challenged with iVDPV strains. A recommendation from this finding would be that during the End-game all PV vaccines will need to be assessed as to whether they confer protection against iVDPVs in the same manner that they should be assessed against currently circulating wild-type strains (i.e. via vaccine potency assays or seroprevalence studies).

Inactivation with HCHO did not cause a significant loss of antigenicity, but it did cause a partial modification of antigenic site 1 in serotype 2 PV strains. The degree to which this partial modification contributed to the large reduction in viral immunogenicity following inactivation is not clear. In an effort to improve the immunogenicity of inactivated PV alternative inactivation chemicals, BPL and BEI, were used to inactivate selected serotype 2 strains. Neither of these chemicals generated inactivated PV preparations of higher immunogenicity than those generated with HCHO. However BEI inactivated PV preparations showed higher thermostability. Future research could be concentrated on generating an IPV of a higher immunogenicity than the cIPV by optimising the inactivation of PV with BEI, possibly through the use of the more selective ethyleneimine oligomers or by optimising the inactivation conditions. Optimisation of inactivation conditions, including pH and temperature, would also be beneficial in the potential use of BPL as an inactivation chemical for PV. The antigenic and immunogenic properties of inactivated PV preparations generated with BPL and BEI would need to be assessed. A biosensor based protocol established comparable D-Ag / ml estimates to those obtained by the current ELISA indicating that it could offer an alternative means to assess the potency of IPV. Further research will be required to validate this protocol, possibly through an international collaboration.

The molecular mechanisms which underlie the loss of viral infectivity during inactivation were characterised by assessing the effect of inactivation on the viral entry into the host cell and the viral RNA. Inactivation was found to affect both the viral protein and RNA. Inactivation was shown to affect the viral protein as it reduced the binding between PV and the PVR by 60-80% and appeared to prevent PV from undergoing the necessary conformational changes to enter the host cell. The biological activity and functionality of the viral RNA was reduced by inactivation. It is likely that inactivation causes a loss of viral infectivity through a combined effect on the protein and RNA of PV virions. The effect of inactivation on the viral protein and RNA could be used to optimise the inactivation of PV. As discussed previously (Chapter 6) the real-time RT-PCR assay used to assess the functionality of RNA from inactivated PV could be used as a quality control test for IPV. Future research could also determine whether inactivation disrupts additional stages in PV replication. For example research could assess whether the binding of PV to the PVR triggers a cellular signalling pathway and if so whether this action is disrupted or altered following inactivation. There should be further study of the structural changes (if any) induced to inactivated PV following receptor binding in comparison to live PV. It should be investigated as to whether the indicated prevention of PV conformation changes by inactivation actually results in the blockage of viral RNA release.

Finally research will need to be directed to assessing how inactivated PV preparations are processed and presented during the immune response as this may be affecting the overall immunogenicity of IPVs.

REFERENCES

1. **Aarathi, D., K. Ananda Rao, R. Robinson, and V. A. Srinivasan.** 2004. Validation of binary ethyleneimine (BEI) used as an inactivant for foot and mouth disease tissue culture vaccine. *Biologicals* **32**:153-6.
2. **Abe, S., Y. Ota, S. Koike, T. Kurata, H. Horie, T. Nomura, S. Hashizume, and A. Nomoto.** 1995. Neurovirulence test for oral live poliovaccines using poliovirus-sensitive transgenic mice. *Virology* **206**:1075-83.
3. **Abraham, R., P. Minor, G. Dunn, J. F. Modlin, and P. L. Ogra.** 1993. Shedding of virulent poliovirus revertants during immunization with oral poliovirus vaccine after prior immunization with inactivated polio vaccine. *J Infect Dis* **168**:1105-9.
4. **Adu, F., J. Iber, D. Bukbuk, N. Gumede, S. J. Yang, J. Jorba, R. Campagnoli, W. F. Sule, C. F. Yang, C. Burns, M. Pallansch, T. Harry, and O. Kew.** 2007. Isolation of recombinant type 2 vaccine-derived poliovirus (VDPV) from a Nigerian child. *Virus Res* **127**:17-25.
5. **Agency for Toxic Substances and Disease Registry** 2011, posting date. Medical management guidelines for formaldehyde (HCHO). [Online.]
6. **Agol, V. I.** 1991. The 5'-untranslated region of picornaviral genomes. *Adv Virus Res* **40**:103-80.
7. **Agol, V. I.** 2006. Molecular mechanisms of poliovirus variation and evolution. *Curr Top Microbiol Immunol* **299**:211-59.
8. **Agol, V. I.** 2002. Poliovirus genetics: an overview, p. 127-148. *In* B. L. Semler and E. Wimmer (ed.), *Molecular biology of picornaviruses*. American Society for Microbiology, Washington, D.C.
9. **Aldabe, R., A. Barco, and L. Carrasco.** 1996. Membrane permeabilization by poliovirus proteins 2B and 2BC. *J Biol Chem* **271**:231-237.
10. **Alexander, H. E., G. Koch, I. M. Mountain, and O. Van Damme.** 1958. Infectivity of ribonucleic acid from poliovirus in human cell monolayers. *J Exp Med* **108**:493-506.
11. **Alexander, J. P., Jr., H. E. Gary, Jr., and M. A. Pallansch.** 1997. Duration of poliovirus excretion and its implications for acute flaccid paralysis surveillance: a review of the literature. *J Infect Dis* **175 Suppl 1**:S176-82.
12. **Allison, A. C.** 1962. Observations on the inactivation of viruses by sulfhydryl reagents. *Virology* **17**:176-83.

13. **Allison, A. C., F. E. Buckland, and C. H. Andrewes.** 1962. Effects of sulfhydryl reagents on infectivity of some viruses. *Virology* **17**:171-5.
14. **Ambros, V., and D. Baltimore.** 1978. Protein is linked to the 5' end of poliovirus RNA by a phosphodiester linkage to tyrosine. *J Biol Chem* **253**:5263-6.
15. **Andino, R., G. E. Rieckhof, and D. Baltimore.** 1990. A functional ribonucleoprotein complex forms around the 5' end of poliovirus RNA. *Cell* **63**:369-80.
16. **Andrus, J. K., C. de Quadros, J. M. Olive, and H. F. Hull.** 1992. Screening of cases of acute flaccid paralysis for poliomyelitis eradication: ways to improve specificity. *Bull World Health Organ* **70**:591-6.
17. **Arita, I., and D. P. Francis.** 2011. Safe landing for global polio eradication: a perspective. *Vaccine* **29**:8827-34.
18. **Arita, I., M. Nakane, and F. Fenner.** 2006. Public health. Is polio eradication realistic? *Science* **312**:852-4.
19. **Arita, M., S. Koike, J. Aoki, H. Horie, and A. Nomoto.** 1998. Interaction of poliovirus with its purified receptor and conformational alteration in the virion. *J Virol* **72**:3578-86.
20. **Arvilommi, H.** 1996. ELISPOT for detecting antibody-secreting cells in response to infections and vaccination. *APMIS* **104**:401-10.
21. **Auerbach, C., M. Moutschen-Dahmen, and J. Moutschen.** 1977. Genetic and cytogenetical effects of formaldehyde and related compounds. *Mutat Res* **39**:317-61.
22. **Baca-Estrada, M., and E. Griffiths.** 2006. Regulation and standardization of IPV and IPV combination vaccines. *Biologicals* **34**:159-61.
23. **Bahnemann, H. G.** 1990. Inactivation of viral antigens for vaccine preparation with particular reference to the application of binary ethylenimine. *Vaccine* **8**:299-303.
24. **Balanant, J., S. Guillot, A. Candrea, F. Delpeyroux, and R. Crainic.** 1991. The natural genomic variability of poliovirus analyzed by a restriction fragment length polymorphism assay. *Virology* **184**:645-54.
25. **Baldwin, S. L., C. B. Fox, M. A. Pallansch, R. N. Coler, S. G. Reed, and M. Friede.** 2011. Increased potency of an inactivated trivalent polio vaccine with oil-in-water emulsions. *Vaccine* **29**:644-9.
26. **Barral, P. M., D. Sarkar, Z. Z. Su, G. N. Barber, R. DeSalle, V. R. Racaniello, and P. B. Fisher.** 2009. Functions of the cytoplasmic RNA sensors RIG-I and MDA-5: key regulators of innate immunity. *Pharmacol Ther* **124**:219-34.

27. **Barrett, S.** 2009. Polio eradication: strengthening the weakest links. *Health Aff (Millwood)* **28**:1079-90.
28. **Barteling, S. J., and N. I. Cassim.** 2000. Formaldehyde enhances BEI-inactivation rates of foot-and-mouth disease (FMD) virus by at least a ten-fold, p. 270-275, European Commission for the Control of Foot-and-Mouth Disease. Research Group of the Standing Technical Committee. FAO, animal production and health division, Borovets, Bulgaria.
29. **Baxter, D.** 2007. Active and passive immunity, vaccine types, excipients and licensing. *Occup Med (Lond)* **57**:552-6.
30. **BD Biosciences.** 2000. Introduction to Flow Cytometry: A Learning guide.
31. **Beale, A. J., and P. J. Mason.** 1962. The measurement of the D-antigen in poliovirus preparations. *J Hyg (Lond)* **60**:113-21.
32. **Beales, L. P., A. Holzenburg, and D. J. Rowlands.** 2003. Viral internal ribosome entry site structures segregate into two distinct morphologies. *J Virol* **77**:6574-9.
33. **Bellmunt, A., G. May, R. Zell, P. Pring-Akerblom, W. Verhagen, and A. Heim.** 1999. Evolution of poliovirus type I during 5.5 years of prolonged enteral replication in an immunodeficient patient. *Virology* **265**:178-84.
34. **Belnap, D. M., B. M. McDermott, Jr., D. J. Filman, N. Cheng, B. L. Trus, H. J. Zuccola, V. R. Racaniello, J. M. Hogle, and A. C. Steven.** 2000. Three-dimensional structure of poliovirus receptor bound to poliovirus. *Proc Natl Acad Sci U S A* **97**:73-8.
35. **Bergelson, J. M.** 2008. New (fluorescent) light on poliovirus entry. *Trends Microbiol* **16**:44-7.
36. **Bergelson, J. M.** 2010. Receptors, p. 73-86. *In* E. Ehrenfeld, E. Domingo, and R. Roos (ed.), *The Picornaviruses*. ASM Press, Washington, DC.
37. **Bernhardt, G., J. A. Bibb, J. Bradley, and E. Wimmer.** 1994. Molecular characterization of the cellular receptor for poliovirus. *Virology* **199**:105-13.
38. **Bernhardt, G., J. Harber, A. Zibert, M. deCrombrughe, and E. Wimmer.** 1994. The poliovirus receptor: identification of domains and amino acid residues critical for virus binding. *Virology* **203**:344-56.
39. **Bevilacqua, J. M., L. Young, S. W. Chiu, J. D. Sparkes, and J. G. Kreeftenberg.** 1996. Rat immunogenicity assay of inactivated poliovirus. *Dev Biol Stand* **86**:121-7.

40. **Bhanuprakash, V., B. K. Indrani, M. Hosamani, V. Balamurugan, and R. K. Singh.** 2009. Bluetongue vaccines: the past, present and future. *Expert Rev Vaccines* **8**:191-204.
41. **Bienz, K., D. Egger, M. Troxler, and L. Pasamontes.** 1990. Structural organization of poliovirus RNA replication is mediated by viral proteins of the P2 genomic region. *J Virol* **64**:1156-63.
42. **Blomqvist, S., C. Savolainen, P. Laine, P. Hirttio, E. Lamminsallo, E. Penttila, S. Joks, M. Roivainen, and T. Hovi.** 2004. Characterization of a highly evolved vaccine-derived poliovirus type 3 isolated from sewage in estonia. *J Virol* **78**:4876-83.
43. **Bodian, D.** 1955. Emerging concept of poliomyelitis infection. *Science* **122**:105-8.
44. **Bodian, D.** 1972. Poliomyelitis, p. 2323-2344. *In* J. Minckler (ed.), *Pathology of the Nervous System*, vol. 3. McGraw-Hill, New York.
45. **Bodian, D.** 1955. Viremia, invasiveness, and the influence of injections. *Ann N Y Acad Sci* **61**:877-82.
46. **Bodian, D., I. M. Morgan, and H. A. Howe.** 1949. Differentiation of types of poliomyelitis viruses; the grouping of 14 strains into three basic immunological types. *Am J Hyg* **49**:234-45.
47. **Bolton, D. L., and M. Roederer.** 2009. Flow cytometry and the future of vaccine development. *Expert Rev Vaccines* **8**:779-89.
48. **Bonin, S., F. Petrera, B. Niccolini, and G. Stanta.** 2003. PCR analysis in archival postmortem tissues. *Mol Pathol* **56**:184-6.
49. **Bostina, M., D. Bubeck, C. Schwartz, D. Nicastro, D. J. Filman, and J. M. Hogle.** 2007. Single particle cryoelectron tomography characterization of the structure and structural variability of poliovirus-receptor-membrane complex at 30 A resolution. *J Struct Biol* **160**:200-10.
50. **Bostina, M., H. Levy, D. J. Filman, and J. M. Hogle.** 2011. Poliovirus RNA is released from the capsid near a twofold symmetry axis. *J Virol* **85**:776-83.
51. **Bottino, C., R. Castriconi, D. Pende, P. Rivera, M. Nanni, B. Carnemolla, C. Cantoni, J. Grassi, S. Marcenaro, N. Reymond, M. Vitale, L. Moretta, M. Lopez, and A. Moretta.** 2003. Identification of PVR (CD155) and Nectin-2 (CD112) as cell surface ligands for the human DNAM-1 (CD226) activating molecule. *J Exp Med* **198**:557-67.

52. **Bouchard, M. J., D. H. Lam, and V. R. Racaniello.** 1995. Determinants of attenuation and temperature sensitivity in the type 1 poliovirus Sabin vaccine. *J Virol* **69**:4972-8.
53. **Boutwell, R. K., N. H. Colburn, and C. C. Muckerman.** 1969. *In vivo* reactions of B-Propiolactone. *Annals of the New York Academy of Sciences* **2**:751-763.
54. **Brandenburg, B., L. Y. Lee, M. Lakadamyali, M. J. Rust, X. Zhuang, and J. M. Hogle.** 2007. Imaging poliovirus entry in live cells. *PLoS Biol* **5**:e183.
55. **Breindl, M.** 1971. The structure of heated poliovirus particles. *J Gen Virol* **11**:147-56.
56. **Broo, K., J. Wei, D. Marshall, F. Brown, T. J. Smith, J. E. Johnson, A. Schneemann, and G. Siuzdak.** 2001. Viral capsid mobility: a dynamic conduit for inactivation. *Proc Natl Acad Sci U S A* **98**:2274-7.
57. **Brookes, P., and P. D. Lawley.** 1964. Alkylating Agents. *Br Med Bull* **20**:91-5.
58. **Brown, D. M., C. T. Cornell, G. P. Tran, J. H. Nguyen, and B. L. Semler.** 2005. An authentic 3' noncoding region is necessary for efficient poliovirus replication. *J Virol* **79**:11962-73.
59. **Brown, D. M., S. E. Kauder, C. T. Cornell, G. M. Jang, V. R. Racaniello, and B. L. Semler.** 2004. Cell-dependent role for the poliovirus 3' noncoding region in positive-strand RNA synthesis. *J Virol* **78**:1344-51.
60. **Brown, F., B. Cartwright, and D. L. Stewart.** 1963. The effect of various inactivating agents on the viral and ribonucleic acid infectivities of foot-and-mouth disease virus and on its attachment to susceptible cells. *J Gen Microbiol* **31**:179-86.
61. **Brown, F., R. F. Meyer, M. Law, E. Kramer, and J. F. Newman.** 1998. A universal virus inactivant for decontaminating blood and biopharmaceutical products. *Biologicals* **26**:39-47.
62. **Brown, G. C., A. S. Rabson, and J. H. Schieble.** 1955. The effect of gamma globulin on sub clinical infection in familial associates of poliomyelitis cases. II. Serological studies and virus isolations from pharyngeal secretions. *J Immunol* **74**:71-80.
63. **Brusick, D. J.** 1977. The genetic properties of beta-propiolactone. *Mutat Res* **39**:241-55.
64. **Bubeck, D., D. J. Filman, N. Cheng, A. C. Steven, J. M. Hogle, and D. M. Belnap.** 2005. The structure of the poliovirus 135S cell entry intermediate at 10-angstrom

- resolution reveals the location of an externalized polypeptide that binds to membranes. *J Virol* **79**:7745-55.
65. **Bubeck, D., D. J. Filman, and J. M. Hogle.** 2005. Cryo-electron microscopy reconstruction of a poliovirus-receptor-membrane complex. *Nat Struct Mol Biol* **12**:615-8.
 66. **Budowsky, E. I.** 06.03.97 1997. Methods and compositions for the selective modification of nucleic acid. USA.
 67. **Budowsky, E. I.** 19.11.98 1998. Methods and compositions for the selective modification of nucleic acid. USA.
 68. **Budowsky, E. I.** 1991. Problems and prospects for preparation of killed antiviral vaccines. *Adv Virus Res* **39**:255-90.
 69. **Budowsky, E. I., E. A. Friedman, N. V. Zheleznova, and F. S. Noskov.** 1991. Principles of selective inactivation of viral genome. VI. Inactivation of the infectivity of the influenza virus by the action of beta-propiolactone. *Vaccine* **9**:398-402.
 70. **Budowsky, E. I., and M. A. Zalesskaya.** 1991. Principles of selective inactivation of viral genome. V. Rational selection of conditions for inactivation of the viral suspension infectivity to a given extent by the action of beta-propiolactone. *Vaccine* **9**:319-25.
 71. **Budowsky, E. I., M. A. Zalesskaya, N. M. Nepomnyashchaya, and R. G. Kostyanovsky.** 1996. Principles of selective inactivation of the viral genome: Dependence of the rate of viral RNA modification on the number of protonizable groups in ethyleneimine oligomers. *Vaccine Research* **5**:29-39.
 72. **Burnet, F. M., and J. Macnamara.** 1931. Immunological differences between strains of poliomyelitis virus *Br J Exp Pathol* **12**:57-61.
 73. **Burrage, T., E. Kramer, and F. Brown.** 2000. Inactivation of viruses by aziridines. *Dev Biol (Basel)* **102**:131-9.
 74. **Bussolati, G., L. Annaratone, E. Medico, G. D'Armento, and A. Sapino.** 2011. Formalin fixation at low temperature better preserves nucleic acid integrity. *PLoS One* **6**:e21043.
 75. **Cabasso, V. J., G. A. Jervis, A. W. Moyer, M. Roca-Garcia, E. V. Orsi, and H. R. Cox.** 1959. Presented at the Live Poliovirus Vaccines. First International Conference on Live Poliovirus Vaccines, Washington DC, USA.

76. **Canziani, G., W. Zhang, D. Cines, A. Rux, S. Willis, G. Cohen, R. Eisenberg, and I. Chaiken.** 1999. Exploring biomolecular recognition using optical biosensors. *Methods* **19**:253-69.
77. **Capodici, J., R. Maigetter, M. Revai, J. Latzo, F. Watson, J. Sung, J. Cramer, J. Tobing, J. Young, S. Caravoulias, S. Smith, and P. Lowry.** 2006. Large-scale Beta-propiolactone inactivation of HIV for vaccines. *BioProcess International* **4**:36-41.
78. **Cello, J., A. V. Paul, and E. Wimmer.** 2002. Chemical synthesis of poliovirus cDNA: generation of infectious virus in the absence of natural template. *Science* **297**:1016-8.
79. **Centers for Disease Control and Prevention.** 2001. Apparent Global Interruption of Wild Poliovirus Type 2 Transmission Morbidity and Mortality Weekly Report **50**:222-224.
80. **Centers for Disease Control and Prevention.** 2002. Certification of poliomyelitis eradication - European Region, June 2002. *Morbidity and Mortality Weekly Report* **51**:572-574.
81. **Centers for Disease Control and Prevention.** 1994. Certification of poliomyelitis eradication - the Americas, 1994. *Morbidity and Mortality Weekly Report* **43**:720-722.
82. **Centers for Disease Control and Prevention.** 2001. Certification of poliomyelitis eradication - Western Pacific Region, October 2000. *Morbidity and Mortality Weekly Report* **50**:1-3.
83. **Centers for Disease Control and Prevention.** 2000. Developing and expanding contributions of the Global Laboratory Network for Poliomyelitis Eradication, 1997-1999 *Morbidity and Mortality Weekly Report* **49**:156-160.
84. **Centers for Disease Control and Prevention.** 2009. Laboratory surveillance for wild and vaccine-derived polioviruses - worldwide, January 2008-June 2009. *Morbidity and Mortality Weekly Report* **58**:950-954.
85. **Centers for Disease Control and Prevention.** 2011. Poliomyelitis, p. 249-262. *In* W. Atkinson, S. Wolfe, and J. Hamborsky (ed.), *Epidemiology and Prevention of Vaccine-Preventable Diseases*, 12 ed. Public Health Foundation, Washington DC.
86. **Centers for Disease Control and Prevention.** 2009. Progress toward poliomyelitis eradication - Afghanistan and Pakistan, 2008. *Morbidity and Mortality Weekly Report* **58**:198-201.

87. **Centers for Disease Control and Prevention.** 2011. Progress towards poliomyelitis eradication - Afghanistan and Pakistan, January 2010 - September 2011. *Morbidity and Mortality Weekly Report* **60**:1523-1527.
88. **Centers for Disease Control and Prevention.** 2011. Progress towards poliomyelitis eradication - India, January 2010 - September 2011. *Morbidity and Mortality Weekly Report* **60**:1482-1486.
89. **Centers for Disease Control and Prevention.** 2006. Resurgence of wild poliovirus type 1 transmission and consequences of importation - 21 countries, 2002-2005. *Morbidity and Mortality Weekly Report* **55**:145-150.
90. **Centers for Disease Control and Prevention.** 2007. Update on vaccine-derived polioviruses-worldwide, January 2006-August 2007. *Morbidity and Mortality Weekly Report* **56**:996-1001.
91. **Centers for Disease Control and Prevention.** 2009. Update on vaccine-derived polioviruses - worldwide, January 2008-June 2009. *Morbidity and Mortality Weekly Report* **58**:1002-1006.
92. **Centers for Disease Control and Prevention.** 2009. Wild poliovirus type 1 and type 3 importations - 15 countries, Africa, 2008-2009. *Morbidity and Mortality Weekly Report* **58**:357-362.
93. **Cernakova, B., Z. Sobotova, I. Rovny, S. Blahova, M. Roivainen, and T. Hovi.** 2005. Isolation of vaccine-derived polioviruses in the Slovak Republic. *Eur J Clin Microbiol Infect Dis* **24**:438-9.
94. **Chen-Fu, Y., T. Naguib, S. Yang, E. Nasr, J. Jorba, N. Ahmed, R. Campagnoli, H. van der Avoort, H. Shimizu, T. Yoneyama, T. Miyamura, M. Pallansch, and O.M. Kew.** 2003. Circulation of endemic type 2 vaccine-derived poliovirus in Egypt from 1983 to 1993. *J Virol* **77**:8366-8377.
95. **Chen, C. H., R. Wu, L. G. Roth, S. Guillot, and R. Crainic.** 1997. Elucidating mechanisms of thermostabilization of poliovirus by D₂O and MgCl₂. *Arch Biochem Biophys* **342**:108-16.
96. **Chen, C. Y., and P. Sarnow.** 1995. Initiation of protein synthesis by the eukaryotic translational apparatus on circular RNAs. *Science* **268**:415-7.
97. **Chen, R., J. J. Mieyal, and D. A. Goldthwait.** 1981. The reaction of beta-propiolactone with derivatives of adenine and with DNA. *Carcinogenesis* **2**:73-80.

98. **Cho, M. W., N. Teterina, D. Egger, K. Bienz, and E. Ehrenfeld.** 1994. Membrane rearrangement and vesicle induction by recombinant poliovirus 2C and 2BC in human cells. *Virology* **202**:129-45.
99. **Christodoulou, C., F. Colbere-Garapin, A. Macadam, L. F. Taffs, S. Marsden, P. Minor, and F. Horaud.** 1990. Mapping of mutations associated with neurovirulence in monkeys infected with Sabin 1 poliovirus revertants selected at high temperature. *J Virol* **64**:4922-9.
100. **Chumakov, K., E. Dragunsky, A. Ivshina, J. Enterline, V. Wells, T. Nomura, M. Gromeier, and E. Wimmer.** 2001. Inactivated vaccines based on alternatives to wild-type seed virus. *Dev Biol (Basel)* **105**:171-7.
101. **Chumakov, K., and E. Ehrenfeld.** 2008. New generation of inactivated poliovirus vaccines for universal immunization after eradication of poliomyelitis. *Clin Infect Dis* **47**:1587-92.
102. **Chumakov, K., E. Ehrenfeld, E. Wimmer, and V. I. Agol.** 2007. Vaccination against polio should not be stopped. *Nat Rev Microbiol* **5**:952-8.
103. **Chumakov, K., and O. Kew.** 2010. The Poliovirus Eradication Initiative, p. 449-459. *In* E. Ehrenfeld, E. Domingo, and R. Roos (ed.), *The Picornaviruses*. ASM Press, Washington, DC.
104. **Chumakov, K. M.** 1999. Molecular consistency monitoring of oral poliovirus vaccine and other live viral vaccines. *Dev Biol Stand* **100**:67-74.
105. **Chumakov, K. M., L. B. Powers, K. E. Noonan, I. B. Roninson, and I. S. Levenbook.** 1991. Correlation between amount of virus with altered nucleotide sequence and the monkey test for acceptability of oral poliovirus vaccine. *Proc Natl Acad Sci U S A* **88**:199-203.
106. **Chung, J. Y., and S. M. Hewitt.** 2010. An optimized RNA extraction method from archival formalin-fixed paraffin-embedded tissue. *Methods Mol Biol* **611**:19-27.
107. **Clark, M. E., T. Hammerle, E. Wimmer, and A. Dasgupta.** 1991. Poliovirus proteinase 3C converts an active form of transcription factor III_C to an inactive form: a mechanism for inhibition of host cell polymerase III transcription by poliovirus. *EMBO J* **10**:2941-7.
108. **Colston, E., and V. R. Racaniello.** 1994. Soluble receptor-resistant poliovirus mutants identify surface and internal capsid residues that control interaction with the cell receptor. *Embo J* **13**:5855-62.

109. **Colston, E. M., and V. R. Racaniello.** 1995. Poliovirus variants selected on mutant receptor-expressing cells identify capsid residues that expand receptor recognition. *J Virol* **69**:4823-9.
110. **Committee on Typing of the National Foundation for Infantile Paralysis.** 1951. Immunologic classification of poliomyelitis viruses: a cooperative program for the typing of one hundred strains. *Am J Hyg* **54**:191-274.
111. **Cooper, G.** 2012. Unpublished data.
112. **Coyne, C. B., K. S. Kim, and J. M. Bergelson.** 2007. Poliovirus entry into human brain microvascular cells requires receptor-induced activation of SHP-2. *EMBO J* **26**:4016-28.
113. **Curry, S., M. Chow, and J. M. Hogle.** 1996. The poliovirus 135S particle is infectious. *J Virol* **70**:7125-31.
114. **Daijogo, S., and B. L. Semler.** Mechanistic intersections between picornavirus translation and RNA replication. *Adv Virus Res* **80**:1-24.
115. **Dalldorf, G., and S. Kelly.** 1956. Antigenic potency of poliovirus vaccines. *Am J Hyg* **64**:243-58.
116. **Danthi, P., M. Tosteson, Q. H. Li, and M. Chow.** 2003. Genome delivery and ion channel properties are altered in VP4 mutants of poliovirus. *J Virol* **77**:5266-74.
117. **De Jesus, N. H.** 2007. Epidemics to eradication: the modern history of poliomyelitis. *Virol J* **4**:70.
118. **De, L., B. Nottay, C. F. Yang, B. P. Holloway, M. Pallansch, and O. Kew.** 1995. Identification of vaccine-related polioviruses by hybridization with specific RNA probes. *J Clin Microbiol* **33**:562-71.
119. **De, L., C.F. Yang, E. da Silva, J. Boshell, P. Cáceres, J.R. Gomez, M. Pallansch, and O. Kew.** 1997. Genotype-specific RNA probes for the direct identification of wild polioviruses by blot hybridization. *J. Clin. Microbiol.* **35**:2834-2840.
120. **De Sena, J., and B. Mandel.** 1976. Studies on the in vitro uncoating of poliovirus. I. Characterization of the modifying factor and the modifying reaction. *Virology* **70**:470-83.
121. **De Sena, J., and B. Mandel.** 1977. Studies on the in vitro uncoating of poliovirus. II. Characteristics of the membrane-modified particle. *Virology* **78**:554-66.
122. **Dedhia, P., S. Tarale, G. Dhongde, R. Khadapkar, and B. Das.** 2007. Evaluation of DNA extraction methods and real time PCR optimization on formalin-fixed paraffin-embedded tissues. *Asian Pac J Cancer Prev* **8**:55-9.

123. **Delrue, I., P. L. Delputte, and H. J. Nauwynck.** 2009. Assessing the functionality of viral entry-associated domains of porcine reproductive and respiratory syndrome virus during inactivation procedures, a potential tool to optimize inactivated vaccines. *Vet Res* **40**:62.
124. **Dermer, O. C., and G. E. Ham.** 1969. *Ethylenimine and other Aziridines: Chemistry and Applications.* Academic press, New York.
125. **Desbat, B., E. Lancelot, T. Krell, M. C. Nicolai, F. Vogel, M. Chevalier, and F. Ronzon.** 2011. Effect of the beta-Propiolactone Treatment on the Adsorption and Fusion of Influenza A/Brisbane/59/2007 and A/New Caledonia/20/1999 Virus H1N1 on a Dimyristoylphosphatidylcholine/Ganglioside GM3 Mixed Phospholipids Monolayer at the Air-Water Interface. *Langmuir*.
126. **Deshpande, J. M., S. S. Nadkarni, and Z. A. Siddiqui.** 2003. Detection of MEF-1 laboratory reference strain of poliovirus type 2 in children with poliomyelitis in India in 2002 & 2003. *Indian J Med Res* **118**:217-23.
127. **Deshpande, J. M., S. J. Shetty, and Z. A. Siddiqui.** 2003. Environmental surveillance system to track wild poliovirus transmission. *Appl Environ Microbiol* **69**:2919-27.
128. **DeTulleo, L., and T. Kirchhausen.** 1998. The clathrin endocytic pathway in viral infection. *EMBO J* **17**:4585-93.
129. **di Tommaso, A., M. T. de Magistris, M. Bugnoli, I. Marsili, R. Rappuoli, and S. Abrignani.** 1994. Formaldehyde treatment of proteins can constrain presentation to T cells by limiting antigen processing. *Infect Immun* **62**:1830-4.
130. **Doedens, J. R., and K. Kirkegaard.** 1995. Inhibition of cellular protein secretion by poliovirus proteins 2B and 3A. *Embo J* **14**:894-907.
131. **Doel, T. R.** 1985. Inactivation of viruses produced in animal cell cultures, p. 129-149. *In* R. E. Spier and J. B. Griffiths (ed.), *Animal Cell Biotechnology*, vol. 2. Academic Press Inc., London.
132. **Doel, T. R., and P. J. Baccarini.** 1981. Thermal stability of foot-and-mouth disease virus. *Arch Virol* **70**:21-32.
133. **Doi, Y., S. Abe, H. Yamamoto, H. Horie, H. Ohyama, K. Satoh, Y. Tano, Y. Ota, M. Miyazawa, K. Wakabayashi, and S. Hashizume.** 2001. Progress with inactivated poliovirus vaccines derived from the Sabin strains. *Dev Biol (Basel)* **105**:163-9.

134. **Dorsch-Hasler, K., Y. Yogo, and E. Wimmer.** 1975. Replication of picornaviruses. I. Evidence from in vitro RNA synthesis that poly(A) of the poliovirus genome is genetically coded. *J Virol* **16**:1512-7.
135. **Dowdle, W. R.** 1998. The principles of disease elimination and eradication. *Bull World Health Organ* **76 Suppl 2**:22-5.
136. **Dowdle, W. R., and M. E. Birmingham.** 1997. The biologic principles of poliovirus eradication. *J Infect Dis* **175 Suppl 1**:S286-92.
137. **Dowdle, W. R., E. De Gourville, O. M. Kew, M. A. Pallansch, and D. J. Wood.** 2003. Polio eradication: the OPV paradox. *Rev Med Virol* **13**:277-91.
138. **Dragunsky, E., D. Gardner, R. Taffs, and I. Levenbook.** 1993. Transgenic PVR Tg-1 mice for testing of poliovirus type 3 neurovirulence: comparison with monkey test. *Biologicals* **21**:233-7.
139. **Dragunsky, E., R. Taffs, Y. Chernokhlostova, T. Nomura, K. Hioki, D. Gardner, L. Norwood, and I. Levenbook.** 1996. A poliovirus-susceptible transgenic mouse model as a possible replacement for the monkey neurovirulence test of oral poliovirus vaccine. *Biologicals* **24**:77-86.
140. **Dragunsky, E. M., A. P. Ivanov, S. Abe, S. G. Potapova, J. C. Enterline, S. Hashizume, and K. M. Chumakov.** 2006. Further development of a new transgenic mouse test for the evaluation of the immunogenicity and protective properties of inactivated poliovirus vaccine. *J Infect Dis* **194**:804-7.
141. **Dragunsky, E. M., A. P. Ivanov, V. R. Wells, A. V. Ivshina, G. V. Rezapkin, S. Abe, S. G. Potapova, J. C. Enterline, S. Hashizume, and K. M. Chumakov.** 2004. Evaluation of immunogenicity and protective properties of inactivated poliovirus vaccines: a new surrogate method for predicting vaccine efficacy. *J Infect Dis* **190**:1404-12.
142. **Duchene, M., J. Peetermans, E. D'Hondt, N. Harford, L. Fabry, and J. Stephenne.** 1990. Production of poliovirus vaccines: past, present, and future. *Viral Immunol* **3**:243-72.
143. **Duque, H., and A. C. Palmenberg.** 2001. Phenotypic characterization of three phylogenetically conserved stem-loop motifs in the mengovirus 3' untranslated region. *J Virol* **75**:3111-20.
144. **Earle, W. R., E. L. Schilling, T. H. Stark, N. P. Straus, M. F. Brown, and E. Shelton.** 1943. Production of malignancy in vitro. IV. The mouse fibroblast cultures and changes seen in the living cells. *J Natl Cancer Inst* **4**:165-212.

145. **Ehrenfeld, E., R. I. Glass, V. I. Agol, K. Chumakov, W. Dowdle, T. J. John, S. L. Katz, M. Miller, J. G. Breman, J. Modlin, and P. Wright.** 2008. Immunisation against poliomyelitis: moving forward. *Lancet* **371**:1385-7.
146. **Ehrenfeld, E., J. Modlin, and K. Chumakov.** 2009. Future of polio vaccines. *Expert Rev Vaccines* **8**:899-905.
147. **Ehrenfeld, E., and B. L. Semler.** 1995. Anatomy of the poliovirus internal ribosome entry site. *Curr Top Microbiol Immunol* **203**:65-83.
148. **el-Sayed, N., Y. el-Gamal, A. A. Abbassy, I. Seoud, M. Salama, A. Kandeel, E. Hossny, A. Shawky, H. A. Hussein, M. A. Pallansch, H. G. van der Avoort, A. H. Burton, M. Sreevatsava, P. Malankar, M. H. Wahdan, and R. W. Sutter.** 2008. Monovalent type 1 oral poliovirus vaccine in newborns. *N Engl J Med* **359**:1655-65.
149. **El Bassioni, L., I. Barakat, E. Nasr, E. M. de Gourville, T. Hovi, S. Blomqvist, C. Burns, M. Stenvik, H. Gary, O. M. Kew, M. A. Pallansch, and M. H. Wahdan.** 2003. Prolonged detection of indigenous wild polioviruses in sewage from communities in Egypt. *Am J Epidemiol* **158**:807-15.
150. **Elisberg, B. L.** 1984. Standardization of safety and potency tests of vaccines against poliomyelitis. *Rev Infect Dis* **6 Suppl 2**:S519-22.
151. **Embil Jr., J., L. Gervais, C. Hernandez Miyares, and G. Cardelle.** 1960. Presented at the Second International Conference on Live Poliovirus Vaccines, Washington, D.C.
152. **Enders, J. F., T. H. Weller, and F. C. Robbins.** 1949. Cultivation of the Lansing Strain of Poliomyelitis Virus in Cultures of Various Human Embryonic Tissues. *Science* **109**:85-7.
153. **European Pharmacopoeia.** 2011. 2.7.20. *In vivo* assay of poliomyelitis vaccine (inactivated), p. 226-227, European Pharmacopoeia 7.0.
154. **Everaert, L., R. Vrijssen, and A. Boeye.** 1989. Eclipse products of poliovirus after cold-synchronized infection of HeLa cells. *Virology* **171**:76-82.
155. **Evers, D. L., C. B. Fowler, B. R. Cunningham, J. T. Mason, and T. J. O'Leary.** 2011. The effect of formaldehyde fixation on RNA: optimization of formaldehyde adduct removal. *J Mol Diagn* **13**:282-8.
156. **Feldman, M. Y.** 1973. Reactions of nucleic acids and nucleoproteins with formaldehyde. *Prog Nucleic Acid Res Mol Biol* **13**:1-49.

157. **Felsenstein, J.** 2000. PHYLIP: phylogeny inference package, version 3.6a3 (computer program). Distributed by the author. Department of Genetics. University of Washington, Seattle.
158. **Fenner, F., D. A. Henderson, I. Arita, Z. Jezek, and I. D. Ladnyi.** 1988. Smallpox and its Eradication. World Health Organization, Geneva, Switzerland.
159. **Fenwick, M. L., and P. D. Cooper.** 1962. Early interactions between poliovirus and ERK cells: some observations on the nature and significance of the rejected particles. *Virology* **18**:212-23.
160. **Ferguson, M., D. J. Wood, and P. D. Minor.** 1993. Antigenic structure of poliovirus in inactivated vaccines. *J Gen Virol* **74**:685-90.
161. **Ferguson, M., Q. Yi-hua, P. D. Minor, D. I. Magrath, M. Spitz, and G. C. Schild.** 1982. Monoclonal antibodies specific for the Sabin vaccine strain of poliovirus 3. *Lancet* **2**:122-4.
162. **Filman, D. J., R. Syed, M. Chow, A. J. Macadam, P. D. Minor, and J. M. Hogle.** 1989. Structural factors that control conformational transitions and serotype specificity in type 3 poliovirus. *Embo J* **8**:1567-79.
163. **Fine, P. E.** 2009. Polio: measuring the protection that matters most. *J Infect Dis* **200**:673-5.
164. **Fine, P. E., and I. A. Carneiro.** 1999. Transmissibility and persistence of oral polio vaccine viruses: implications for the global poliomyelitis eradication initiative. *Am J Epidemiol* **150**:1001-21.
165. **Fine, P. E., G. Oblapenko, and R. W. Sutter.** 2004. Polio control after certification: major issues outstanding. *Bull World Health Organ* **82**:47-52.
166. **Fine, P. E., and S. Ritchie.** 2006. Perspective: determinants of the severity of poliovirus outbreaks in the post eradication era. *Risk Anal* **26**:1533-40.
167. **Flanagan, J. G., and P. Leder.** 1990. The kit ligand: a cell surface molecule altered in steel mutant fibroblasts. *Cell* **63**:185-94.
168. **Flanagan, J. B., R. F. Petterson, V. Ambros, N. J. Hewlett, and D. Baltimore.** 1977. Covalent linkage of a protein to a defined nucleotide sequence at the 5'-terminus of virion and replicative intermediate RNAs of poliovirus. *Proc Natl Acad Sci U S A* **74**:961-5.
169. **Fraenkel-Conrat, H.** 1981. Chemical modification of viruses, p. 245-283. *In* H. Fraenkel-Conrat and R. R. Wagner (ed.), *Comprehensive Virology*, vol. 17. Plenum, New York.

170. **Francis, T., Jr., and R. F. Korns.** 1955. Evaluation of 1954 field trial of poliomyelitis vaccine: synopsis of summary report. *Am J Med Sci* **229**:603-12.
171. **Frazatti-Gallina, N. M., R. M. Mourao-Fuches, R. L. Paoli, M. L. Silva, C. Miyaki, E. J. Valentini, I. Raw, and H. G. Higashi.** 2004. Vero-cell rabies vaccine produced using serum-free medium. *Vaccine* **23**:511-7.
172. **Freistadt, M. S., and V. R. Racaniello.** 1991. Mutational analysis of the cellular receptor for poliovirus. *J Virol* **65**:3873-6.
173. **Fricks, C. E., and J. M. Hogle.** 1990. Cell-induced conformational change in poliovirus: externalization of the amino terminus of VP1 is responsible for liposome binding. *J Virol* **64**:1934-45.
174. **Fricks, C. E., J. P. Icenogle, and J. M. Hogle.** 1985. Trypsin sensitivity of the Sabin strain of type 1 poliovirus: cleavage sites in virions and related particles. *J Virol* **54**:856-9.
175. **Friedrich, F., E. F. Da-Silva, and H. G. Schatzmayr.** 1996. Type 2 poliovirus recombinants isolated from vaccine-associated cases and from healthy contacts in Brazil. *Acta Virol* **40**:27-33.
176. **Fuchs, F., P. Minor, A. Daas, and C. Milne.** 2003. Establishment of European Pharmacopoeia BRP batch 2 for inactivated poliomyelitis vaccine for in vitro D antigen assay. *Pharmeuropa Bio* **2003**:23-50.
177. **Fujito, T., W. Ikeda, S. Kakunaga, Y. Minami, M. Kajita, Y. Sakamoto, M. Monden, and Y. Takai.** 2005. Inhibition of cell movement and proliferation by cell-cell contact-induced interaction of Necl-5 with nectin-3. *J Cell Biol* **171**:165-73.
178. **Furesz, J.** 2006. Developments in the production and quality control of poliovirus vaccines -- historical perspectives. *Biologicals* **34**:87-90.
179. **Furness, G.** 1961. The effect of environment on the replication of poliovirus in monkey kidney cells. *J Gen Microbiol* **25**:421-8.
180. **Gard, S.** 1957. Inactivation of poliovirus by formaldehyde: theoretical and practical aspects. *Bull World Health Organ* **17**:979-89.
181. **Gard, S., T. Wesslen, A. Fagraeus, A. Svedmyr, and G. Olin.** 1956. The use of guinea pigs in tests for immunogenic capacity of poliomyelitis virus preparations. *Arch Gesamte Virusforsch* **6**:401-11.
182. **Garlick, B., and R. J. Avery.** 1976. Inactivation of Newcastle disease virus by beta-propiolactone. *Arch Virol* **52**:175-9.

183. **Gavrilin, G. V., E. A. Cherkasova, G. Y. Lipskaya, O. M. Kew, and V. I. Agol.** 2000. Evolution of circulating wild poliovirus and of vaccine-derived poliovirus in an immunodeficient patient: a unifying model. *J Virol* **74**:7381-90.
184. **Geeraedts, F., N. Goutagny, V. Hornung, M. Severa, A. de Haan, J. Pool, J. Wilschut, K. A. Fitzgerald, and A. Huckriede.** 2008. Superior immunogenicity of inactivated whole virus H5N1 influenza vaccine is primarily controlled by Toll-like receptor signalling. *PLoS Pathog* **4**:e1000138.
185. **Ghendon, Y., S. Markushin, I. Akopova, I. Koptiaeva, and G. Krivtsov.** 2011. Chitosan as an adjuvant for poliovaccine. *J Med Virol* **83**:847-52.
186. **Gilman, A., and F. S. Philips.** 1946. The biological actions and therapeutic applications of the B-chloroethyl amines and sulfides. *Science* **103**:409-15.
187. **Gomez Yafal, A., G. Kaplan, V. R. Racaniello, and J. M. Hogle.** 1993. Characterization of poliovirus conformational alteration mediated by soluble cell receptors. *Virology* **197**:501-5.
188. **Gonzalez, G., L. Pfannes, R. Brazas, and R. Striker.** 2007. Selection of an optimal RNA transfection reagent and comparison to electroporation for the delivery of viral RNA. *J Virol Methods* **145**:14-21.
189. **Grassly, N. C., C. Fraser, J. Wenger, J. M. Deshpande, R. W. Sutter, D. L. Heymann, and R. B. Aylward.** 2006. New strategies for the elimination of polio from India. *Science* **314**:1150-3.
190. **Graves, J. H., and R. B. Arlinghaus.** 1967. Acetyleneimine in the preparation of inactivated food-and-mouth disease vaccines. *Proc Annu Meet U S Anim Health Assoc* **71**:396-403.
191. **Gromeier, M., and K. Wetz.** 1990. Kinetics of poliovirus uncoating in HeLa cells in a nonacidic environment. *J Virol* **64**:3590-7.
192. **Gromeier, M., and E. Wimmer.** 1998. Mechanism of injury-provoked poliomyelitis. *J Virol* **72**:5056-60.
193. **Groseil, C., P. Guerin, and P. Adamowicz.** 1995. Evaluation by polymerase chain reaction on the effect of beta-propiolactone and binary ethyleneimine on DNA. *Biologicals* **23**:213-20.
194. **Hahn, E. E. A.** 1972. Polioviruses. *In* S. A. Plotkin (ed.), *Strains of Human Viruses*. S. Karger AG, Basel, Switzerland.

195. **Hammon, W. M., L. L. Coriell, and J. Stokes, Jr.** 1952. Evaluation of Red Cross gamma globulin as a prophylactic agent for poliomyelitis. I. Plan of controlled field tests and results of 1951 pilot study in Utah. *J Am Med Assoc* **150**:739-49.
196. **Hammon, W. M., L. L. Coriell, P. F. Wehrle, and J. Stokes, Jr.** 1953. Evaluation of Red Cross gamma globulin as a prophylactic agent for poliomyelitis. IV. Final report of results based on clinical diagnoses. *J Am Med Assoc* **151**:1272-85.
197. **Hanecak, R., B. L. Semler, C. W. Anderson, and E. Wimmer.** 1982. Proteolytic processing of poliovirus polypeptides: antibodies to polypeptide P3-7c inhibit cleavage at glutamine-glycine pairs. *Proc Natl Acad Sci U S A* **79**:3973-7.
198. **Haque, A., and J. S. Blum.** 2005. New insights in antigen processing and epitope selection: development of novel immunotherapeutic strategies for cancer, autoimmunity and infectious diseases. *J Biol Regul Homeost Agents* **19**:93-104.
199. **Hara, M., Y. Saito, T. Komatsu, H. Kodama, W. Abo, S. Chiba, and T. Nakao.** 1981. Antigenic analysis of polioviruses isolated from a child with agammaglobulinemia and paralytic poliomyelitis after Sabin vaccine administration. *Microbiol Immunol* **25**:905-13.
200. **Harber, J., G. Bernhardt, H. H. Lu, J. Y. Sgro, and E. Wimmer.** 1995. Canyon rim residues, including antigenic determinants, modulate serotype-specific binding of polioviruses to mutants of the poliovirus receptor. *Virology* **214**:559-70.
201. **He, Y., V. D. Bowman, S. Mueller, C. M. Bator, J. Bella, X. Peng, T. S. Baker, E. Wimmer, R. J. Kuhn, and M. G. Rossmann.** 2000. Interaction of the poliovirus receptor with poliovirus. *Proc Natl Acad Sci U S A* **97**:79-84.
202. **Heinsbroek, E., and E. J. Ruitenberg.** 2010. The global introduction of inactivated polio vaccine can circumvent the oral polio vaccine paradox. *Vaccine* **28**:3778-83.
203. **Held, D. M., A. C. Shurtleff, S. Fields, C. Green, J. Fong, R. G. Jones, D. Sesardic, R. Buelow, and R. L. Burke.** 2010. Vaccination of rabbits with an alkylated toxoid rapidly elicits potent neutralizing antibodies against botulinum neurotoxin serotype B. *Clin Vaccine Immunol* **17**:930-6.
204. **Hemminki, K.** 1981. Reactions of beta-propiolactone, beta-butyrolactone and gamma-butyrolactone with nucleic acids. *Chem Biol Interact* **34**:323-31.
205. **Hemminki, K.** 1984. Reactions of ethyleneimine with guanosine and deoxyguanosine. *Chem Biol Interact* **48**:249-60.
206. **Hemminki, K., and D. B. Ludlum.** 1984. Covalent modification of DNA by antineoplastic agents. *J Natl Cancer Inst* **73**:1021-8.

207. **Herremans, T., J. H. Reimerink, T. G. Kimman, H. G. van Der Avoort, and M. P. Koopmans.** 2000. Antibody responses to antigenic sites 1 and 3 of serotype 3 poliovirus after vaccination with oral live attenuated or inactivated poliovirus vaccine and after natural exposure. *Clin Diagn Lab Immunol* **7**:40-4.
208. **Hogle, J. M.** 2002. Poliovirus cell entry: common structural themes in viral cell entry pathways. *Annu Rev Microbiol* **56**:677-702.
209. **Hogle, J. M., M. Chow, and D. J. Filman.** 1985. Three-dimensional structure of poliovirus at 2.9 Å resolution. *Science* **229**:1358-65.
210. **Hogle, J. M., and D. J. Filman.** 1989. The antigenic structure of poliovirus. *Philos Trans R Soc Lond B Biol Sci* **323**:467-78.
211. **Holland, J. J., and B. H. Hoyer.** 1962. Early stages of enterovirus infection. *Cold Spring Harb Symp Quant Biol* **27**:101-12.
212. **Holland, J. J., and E. D. Kiehn.** 1968. Specific cleavage of viral proteins as steps in the synthesis and maturation of enteroviruses. *Proc Natl Acad Sci U S A* **60**:1015-22.
213. **Holland, J. J., and L. L. Mc.** 1961. The location and nature of enterovirus receptors in susceptible cells. *J Exp Med* **114**:161-71.
214. **Holland, J. J., and L. L. Mc.** 1959. The mammalian cell-virus relationship. II. Adsorption, reception, and eclipse of poliovirus by HeLa cells. *J Exp Med* **109**:487-504.
215. **Holland, J. J., L. L. Mc, and J. T. Syverton.** 1959. Mammalian cell-virus relationship. III. Poliovirus production by non-primate cells exposed to poliovirus ribonucleic acid. *Proc Soc Exp Biol Med* **100**:843-5.
216. **Holland, J. J., L. L. Mc, and J. T. Syverton.** 1959. The mammalian cell-virus relationship. IV. Infection of naturally insusceptible cells with enterovirus ribonucleic acid. *J Exp Med* **110**:65-80.
217. **Horie, H., S. Koike, T. Kurata, Y. Sato-Yoshida, I. Ise, Y. Ota, S. Abe, K. Hioki, H. Kato, C. Taya, T. Nomura, S. Hashizume, H. Yonekawa, and A. Nomoto.** 1994. Transgenic mice carrying the human poliovirus receptor: new animal models for study of poliovirus neurovirulence. *J Virol* **68**:681-8.
218. **Horstmann, D. M.** 1955. Poliomyelitis: severity and type of disease in different age groups. *Ann N Y Acad Sci* **61**:956-67.
219. **Horstmann, D. M., R.W. McCollum, and A. D. Mascola.** 1954. Viremia in human poliomyelitis. *J Exp Med* **99**:355-69.
220. **Hovi, T.** 2006. Surveillance for polioviruses. *Biologicals* **34**:123-6.

221. **Hovi, T., S. Blomqvist, E. Nasr, C. C. Burns, T. Sarjakoski, N. Ahmed, C. Savolainen, M. Roivainen, M. Stenvik, P. Laine, I. Barakat, M. H. Wahdan, F. A. Kamel, H. Asghar, M. A. Pallansch, O. M. Kew, H. E. Gary, Jr., E. M. deGourville, and L. El Bassioni.** 2005. Environmental surveillance of wild poliovirus circulation in Egypt--balancing between detection sensitivity and workload. *J Virol Methods* **126**:127-34.
222. **Hovi, T., K. Cantell, A. Huovilainen, E. Kinnunen, T. Kuronen, K. Lapinleimu, T. Poyry, M. Roivainen, N. Salama, M. Stenvik, A. Silander, C.-J. Thoden, S. Salminen, and P. Weckstrom.** 1986. Outbreak of paralytic poliomyelitis in Finland: widespread circulation of antigenically altered poliovirus type 3 in a vaccinated population. *Lancet* **1**:1427-32.
223. **Hovi, T., L. M. Shulman, H. van der Avoort, J. Deshpande, M. Roivainen, and E.M. De Gourville.** 2012. Role of environmental poliovirus surveillance in global polio eradication and beyond. *Epidemiol Infect* **140**:1-13.
224. **Hovi, T., and M. Stenvik.** 1994. Selective isolation of poliovirus in recombinant murine cell line expressing the human poliovirus receptor gene. *J Clin Microbiol* **32**:1366-8.
225. **Howes, D. W.** 1959. The growth cycle of poliovirus in cultured cells. II. Maturation and release of virus in suspended cell populations. *Virology* **9**:96-109.
226. **Hsu, T. C., and D. J. Merchant.** 1961. Mammalian chromosomes in vitro. XIV. Genotypic replacement in cell populations. *J Natl Cancer Inst* **26**:1075-83.
227. **Huang, Y., J. M. Hogle, and M. Chow.** 2000. Is the 135S poliovirus particle an intermediate during cell entry? *J Virol* **74**:8757-61.
228. **Hull, H. F., N. A. Ward, B. P. Hull, J. B. Milstien, and C. de Quadros.** 1994. Paralytic poliomyelitis: seasoned strategies, disappearing disease. *Lancet* **343**:1331-7.
229. **Hulskotte, E. G., M. E. Dings, S. G. Norley, and A. D. Osterhaus.** 1997. Chemical inactivation of recombinant vaccinia viruses and the effects on antigenicity and immunogenicity of recombinant simian immunodeficiency virus envelope glycoproteins. *Vaccine* **15**:1839-45.
230. **Institute of Animal Health** 2011, posting date. Enterovirus. [Online.]
231. **Isomura, S., A. Mubina, A. Dure-samin, Y. Isihara, K. Sakae, T. Yamashita, O. Nishio, and A. Ahmed.** 1993. Virological and serological studies on poliomyelitis in Karachi, Pakistan. I. Outbreaks in 1990-91. *Acta Paediatrica Japonica* **35**:382-386.

232. **Ivanov, A. P., E. M. Dragunsky, and K. M. Chumakov.** 2006. 1,25-dihydroxyvitamin d3 enhances systemic and mucosal immune responses to inactivated poliovirus vaccine in mice. *J Infect Dis* **193**:598-600.
233. **Jacobson, M. F., and D. Baltimore.** 1968. Morphogenesis of poliovirus. I. Association of the viral RNA with coat protein. *J Mol Biol* **33**:369-78.
234. **Jacobson, S. J., D. A. Konings, and P. Sarnow.** 1993. Biochemical and genetic evidence for a pseudoknot structure at the 3' terminus of the poliovirus RNA genome and its role in viral RNA amplification. *J Virol* **67**:2961-71.
235. **Jang, S. K., M. V. Davies, R. J. Kaufman, and E. Wimmer.** 1989. Initiation of protein synthesis by internal entry of ribosomes into the 5' nontranslated region of encephalomyocarditis virus RNA in vivo. *J Virol* **63**:1651-60.
236. **Jang, S. K., H. G. Krausslich, M. J. Nicklin, G. M. Duke, A. C. Palmenberg, and E. Wimmer.** 1988. A segment of the 5' nontranslated region of encephalomyocarditis virus RNA directs internal entry of ribosomes during in vitro translation. *J Virol* **62**:2636-43.
237. **Jason-Moller, L., M. Murphy, and J. Bruno.** 2006. Overview of Biacore systems and their applications. *Curr Protoc Protein Sci* **Chapter 19**:Unit 19 13.
238. **Jenkins, H. E., R. B. Aylward, A. Gasasira, C. A. Donnelly, M. Mwanza, J. Corander, S. Garnier, C. Chauvin, E. Abanida, M. A. Pate, F. Adu, M. Baba, and N. C. Grassly.** 2010. Implications of a circulating vaccine-derived poliovirus in Nigeria. *N Engl J Med* **362**:2360-9.
239. **Jiang, S. D., D. Pye, and J. C. Cox.** 1986. Inactivation of poliovirus with beta-propiolactone. *J Biol Stand* **14**:103-9.
240. **Joachims, M., P. C. Van Breugel, and R. E. Lloyd.** 1999. Cleavage of poly(A)-binding protein by enterovirus proteases concurrent with inhibition of translation in vitro. *J Virol* **73**:718-27.
241. **Joklik, W. K., and J. E. Darnell, Jr.** 1961. The adsorption and early fate of purified poliovirus in HeLa cells. *Virology* **13**:439-47.
242. **Jones, R. G., Y. Liu, P. Rigsby, and D. Sesardic.** 2008. An improved method for development of toxoid vaccines and antitoxins. *J Immunol Methods* **337**:42-8.
243. **Jonsson, N., M. Gullberg, S. Israelsson, and A. M. Lindberg.** 2009. A rapid and efficient method for studies of virus interaction at the host cell surface using enteroviruses and real-time PCR. *Virology* **6**:217.

244. **Kalbfuss, B., Y. Genzel, M. Wolff, A. Zimmermann, R. Morenweiser, and U. Reichl.** 2007. Harvesting and concentration of human influenza A virus produced in serum-free mammalian cell culture for the production of vaccines. *Biotechnol Bioeng* **97**:73-85.
245. **Kamaraj, G., M. Lakshmi Narasu, and V. A. Srinivasan.** 2008. Validation of betapropiolactone (BPL) as an inactivant for infectious bovine rhinotracheitis (IBR) virus. *Res Vet Sci* **85**:589-94.
246. **Kaplan, G., M. S. Freistadt, and V. R. Racaniello.** 1990. Neutralization of poliovirus by cell receptors expressed in insect cells. *J Virol* **64**:4697-702.
247. **Kasermann, F., K. Wyss, and C. Kempf.** 2001. Virus inactivation and protein modifications by ethyleneimines. *Antiviral Res* **52**:33-41.
248. **Kato, H., O. Takeuchi, E. Mikamo-Satoh, R. Hirai, T. Kawai, K. Matsushita, A. Hiiragi, T. S. Dermody, T. Fujita, and S. Akira.** 2008. Length-dependent recognition of double-stranded ribonucleic acids by retinoic acid-inducible gene-I and melanoma differentiation-associated gene 5. *J Exp Med* **205**:1601-10.
249. **Katrak, K., B. P. Mahon, P. D. Minor, and K. H. Mills.** 1991. Cellular and humoral immune responses to poliovirus in mice: a role for helper T cells in heterotypic immunity to poliovirus. *J Gen Virol* **72**:1093-8.
250. **Kawamura, N., M. Kohara, S. Abe, T. Komatsu, K. Tago, M. Arita, and A. Nomoto.** 1989. Determinants in the 5' noncoding region of poliovirus Sabin 1 RNA that influence the attenuation phenotype. *J Virol* **63**:1302-9.
251. **Kemball, C. C., R. S. Fujinami, and J. L. Whitton.** 2010. Adaptive immune responses, p. 303-319. *In* E. Ehrenfeld, E. Domingo, and R. P. Roos (ed.), *The Picornaviruses*. ASM Press, Washington, DC.
252. **Kersten, G., T. Hazendonk, and C. Beuvery.** 1999. Antigenic and immunogenic properties of inactivated polio vaccine made from Sabin strains. *Vaccine* **17**:2059-66.
253. **Kew, O., V. Morris-Glasgow, M. Landaverde, C. Burns, J. Shaw, Z. Garib, J. Andre, E. Blackman, C. J. Freeman, J. Jorba, R. Sutter, G. Tambini, L. Venczel, C. Pedreira, F. Laender, H. Shimizu, T. Yoneyama, T. Miyamura, H. van Der Avoort, M. S. Oberste, D. Kilpatrick, S. Cochi, M. Pallansch, and C. de Quadros.** 2002. Outbreak of Poliomyelitis in Hispaniola Associated with Circulating Type 1 Vaccine-Derived Poliovirus. *Science* **296**:356-359.

254. **Kew, O. M., and M. A. Pallansch.** 2002. The Mechanism of Poliovirus Eradication, p. 481-491. *In* B. L. Semler and E. Wimmer (ed.), *Molecular Biology of Picornaviruses*. ASM Press, Washington, DC.
255. **Kew, O. M., R. W. Sutter, E. M. de Gourville, W. R. Dowdle, and M. A. Pallansch.** 2005. Vaccine-derived polioviruses and the endgame strategy for global polio eradication. *Annu Rev Microbiol* **59**:587-635.
256. **Kew, O. M., R. W. Sutter, B. K. Nottay, M. J. McDonough, D. R. Prevots, L. Quick, and M. A. Pallansch.** 1998. Prolonged replication of a type 1 vaccine-derived poliovirus in an immunodeficient patient. *J Clin Microbiol* **36**:2893-9.
257. **Khuri-Bulos, N., J. L. Melnick, M. H. Hatch, and S. T. Dawod.** 1984. The paralytic poliomyelitis epidemic of 1978 in Jordan: epidemiological implications. *Bull World Health Organ* **62**:83-8.
258. **Kilpatrick, D. R., B. Nottay, C. F. Yang, S. J. Yang, E. Da Silva, S. Penaranda, M. Pallansch, and O. Kew.** 1998. Serotype-specific identification of polioviruses by PCR using primers containing mixed-base or deoxyinosine residues at positions of codon degeneracy. *J Clin Microbiol* **36**:352-7.
259. **Kilpatrick, D. R., B. Nottay, C. F. Yang, S. J. Yang, M. N. Mulders, B. P. Holloway, M. A. Pallansch, and O. M. Kew.** 1996. Group-specific identification of polioviruses by PCR using primers containing mixed-base or deoxyinosine residue at positions of codon degeneracy. *J Clin Microbiol* **34**:2990-6.
260. **Kimball, A. C., R. N. Barr, H. Bauer, H. Kleinman, E. A. Johnson, and M. Cooney.** 1960. Presented at the Second International Conference on Live Poliovirus Vaccines, Washington, D.C.
261. **Kitamura, N., B. L. Semler, P. G. Rothberg, G. R. Larsen, C. J. Adler, A. J. Dorner, E. A. Emini, R. Hanecak, J. J. Lee, S. van der Werf, C. W. Anderson, and E. Wimmer.** 1981. Primary structure, gene organization and polypeptide expression of poliovirus RNA. *Nature* **291**:547-53.
262. **Kluger, J.** 2004. *Splendid Solution: Jonas Salk and the Conquest of Polio*. Penguin, New York.
263. **Knowles, N. J., T. Hovi, A. M. Q. King, and G. Stanway.** 2010. Overview of Taxonomy, p. 19-32. *In* E. Ehrenfeld, E. Domingo, and R. Roos (ed.), *The Picornaviruses*. ASM Press, Washington, DC.
264. **Kohara, M., T. Omata, A. Kameda, B. L. Semler, H. Itoh, E. Wimmer, and A. Nomoto.** 1985. In vitro phenotypic markers of a poliovirus recombinant constructed

- from infectious cDNA clones of the neurovirulent Mahoney strain and the attenuated Sabin 1 strain. *J Virol* **53**:786-92.
265. **Koike, S., H. Horie, I. Ise, A. Okitsu, M. Yoshida, N. Iizuka, K. Takeuchi, T. Takegami, and A. Nomoto.** 1990. The poliovirus receptor protein is produced both as membrane-bound and secreted forms. *EMBO J* **9**:3217-24.
266. **Koike, S., I. Ise, and A. Nomoto.** 1991. Functional domains of the poliovirus receptor. *Proc Natl Acad Sci U S A* **88**:4104-8.
267. **Koike, S., I. Ise, Y. Sato, H. Yonekawa, O. Gotoh, and A. Nomoto.** 1992. A second gene for the African green monkey poliovirus receptor that has no putative N-glycosylation site in the functional N-terminal immunoglobulin-like domain. *J Virol* **66**:7059-66.
268. **Koike, S., C. Taya, J. Aoki, Y. Matsuda, I. Ise, H. Takeda, T. Matsuzaki, H. Amanuma, H. Yonekawa, and A. Nomoto.** 1994. Characterization of three different transgenic mouse lines that carry human poliovirus receptor gene--influence of the transgene expression on pathogenesis. *Arch Virol* **139**:351-63.
269. **Koike, S., C. Taya, T. Kurata, S. Abe, I. Ise, H. Yonekawa, and A. Nomoto.** 1991. Transgenic mice susceptible to poliovirus. *Proc Natl Acad Sci U S A* **88**:951-5.
270. **Koprowski, H., G. A. Jervis, and T. W. Norton.** 1952. Immune responses in human volunteers upon oral administration of a rodent-adapted strain of poliomyelitis virus. *Am J Hyg* **55**:108-24.
271. **Koroleva, G. A., V. A. Lashkevich, and M. K. Voroshilova.** 1975. [Development of poliovirus infection in laboratory animals of different species]. *Vopr Virusol*:445-9.
272. **Koroleva, G. A., V. A. Lashkevich, and M. K. Voroshilova.** 1977. Differences in multiplication of virulent and vaccine strains of poliovirus type I, II, and III in laboratory animals. *Arch Virol* **54**:29-39.
273. **Koroleva, G. A., V. A. Lashkevich, and M. K. Voroshilova.** 1974. Study of poliovirus multiplication in different animal species using photosensitized virus strains. *Arch Gesamte Virusforsch* **46**:11-28.
274. **Koyama, S., K. J. Ishii, C. Coban, and S. Akira.** 2008. Innate immune response to viral infection. *Cytokine* **43**:336-41.
275. **Krausslich, H. G., M. J. Nicklin, H. Toyoda, D. Etchison, and E. Wimmer.** 1987. Poliovirus proteinase 2A induces cleavage of eucaryotic initiation factor 4F polypeptide p220. *J Virol* **61**:2711-8.

276. **Kreeftenberg, H., T. van der Velden, G. Kersten, N. van der Heuvel, and M. de Bruijn.** 2006. Technology transfer of Sabin-IPV to new developing country markets. *Biologicals* **34**:155-8.
277. **Krugman, S., J. Warren, M. S. Eiger, P. H. Berman, R. H. Michaels, and A. B. Sabin.** 1960. Presented at the Second International Conference on Live Poliovirus Vaccines, Washington, D.C.
278. **Kuyumcu-Martinez, N. M., M. Joachims, and R. E. Lloyd.** 2002. Efficient cleavage of ribosome-associated poly(A)-binding protein by enterovirus 3C protease. *J Virol* **76**:2062-74.
279. **La Monica, N., J. W. Almond, and V. R. Racaniello.** 1987. A mouse model for poliovirus neurovirulence identifies mutations that attenuate the virus for humans. *J Virol* **61**:2917-20.
280. **La Monica, N., C. Meriam, and V. R. Racaniello.** 1986. Mapping of sequences required for mouse neurovirulence of poliovirus type 2 Lansing. *J Virol* **57**:515-25.
281. **La Monica, N., and V. R. Racaniello.** 1989. Differences in replication of attenuated and neurovirulent polioviruses in human neuroblastoma cell line SH-SY5Y. *J Virol* **63**:2357-60.
282. **Laassri, M., K. Lottenbach, R. Belshe, M. Wolff, M. Rennels, S. Plotkin, and K. Chumakov.** 2005. Effect of different vaccination schedules on excretion of oral poliovirus vaccine strains. *J Infect Dis* **192**:2092-8.
283. **Landsteiner, K., and E. Popper.** 1908. Mikroskopische Präparate von einem menschlichen und zwei Affenrückenmarken. *Wien Klin Wochenschr* **21**.
284. **Landsteiner, K., and E. Popper.** 1909. Übertragung der Poliomyelitis acuta auf Affen. *Zeitschr. Immunitätsforsch Orig.* **2**:377-390.
285. **Lange, R., X. Peng, E. Wimmer, M. Lipp, and G. Bernhardt.** 2001. The poliovirus receptor CD155 mediates cell-to-matrix contacts by specifically binding to vitronectin. *Virology* **285**:218-27.
286. **Larkin, M. A., G. Blackshields, N. P. Brown, R. Chenna, P. A. McGettigan, H. McWilliam, F. Valentin, I. M. Wallace, A. Wilm, R. Lopez, J. D. Thompson, T. J. Gibson, and D. G. Higgins.** 2007. Clustal W and Clustal X version 2.0. *Bioinformatics* **23**:2947-8.
287. **Lavinder, C. H., A. W. Freeman, and W. H. Frost.** 1918. *Epidemiologic Studies of Poliomyelitis in New York City and the North-eastern United States During the Year 1916* US GPO, Washington, DC.

288. **Lawrence, S. A.** 2000. beta-Propiolactone: viral inactivation in vaccines and plasma products. *PDA J Pharm Sci Technol* **54**:209-17.
289. **Le Bouvier, G. L.** 1955. The modification of poliovirus antigens by heat and ultra violet light. *Lancet* **2**:1013-1016.
290. **Lee, Y. F., A. Nomoto, B. M. Detjen, and E. Wimmer.** 1977. A protein covalently linked to poliovirus genome RNA. *Proc Natl Acad Sci U S A* **74**:59-63.
291. **Lentz, K. N., A. D. Smith, S. C. Geisler, S. Cox, P. Buontempo, A. Skelton, J. DeMartino, E. Rozhon, J. Schwartz, V. Girjavallabhan, J. O'Connell, and E. Arnold.** 1997. Structure of poliovirus type 2 Lansing complexed with antiviral agent SCH48973: comparison of the structural and biological properties of three poliovirus serotypes. *Structure* **5**:961-78.
292. **Levy, H., M. Bostina, D. J. Filman, and J. M. Hogle.** 2010. Cell Entry: a Biochemical and Structural Perspective, p. 87-104. *In* E. Ehrenfeld, E. Domingo, and R. Roos (ed.), *The Picornaviruses*. ASM Press, Washington, DC.
293. **Levy, H. C., M. Bostina, D. J. Filman, and J. M. Hogle.** 2010. Catching a virus in the act of RNA release: a novel poliovirus uncoating intermediate characterized by cryo-electron microscopy. *J Virol* **84**:4426-41.
294. **Li, Q., A. G. Yafal, Y. M. Lee, J. Hogle, and M. Chow.** 1994. Poliovirus neutralization by antibodies to internal epitopes of VP4 and VP1 results from reversible exposure of these sequences at physiological temperature. *J Virol* **68**:3965-70.
295. **Liang, X., Y. Zhang, W. Xu, N. Wen, S. Zuo, L. A. Lee, and J. Yu.** 2006. An outbreak of poliomyelitis caused by type 1 vaccine-derived poliovirus in China. *J Infect Dis* **194**:545-51.
296. **Liao, S., and V. Racaniello.** 1997. Allele-specific adaptation of poliovirus VP1 B-C loop variants to mutant cell receptors. *J Virol* **71**:9770-7.
297. **Lindahl, T., and A. Andersson.** 1972. Rate of chain breakage at apurinic sites in double-stranded deoxyribonucleic acid. *Biochemistry* **11**:3618-23.
298. **Lipskaya, G., E. A. Chervonskaya, G. I. Belova, S. V. Maslova, T. N. Kutateladze, S. G. Drozdov, M. Mulders, M. A. Pallansch, O. M. Kew, and V. I. Agol.** 1995. Geographical genotypes (geotypes) of poliovirus case isolates from the former Soviet Union: relatedness to other known poliovirus genotypes. *J Gen Virol* **76** (Pt 7):1687-99.

299. **Liu, H. M., D. P. Zheng, L. B. Zhang, M. S. Oberste, M. A. Pallansch, and O. M. Kew.** 2000. Molecular evolution of a type 1 wild-vaccine poliovirus recombinant during widespread circulation in China. *J Virol* **74**:11153-61.
300. **Loo, Y. M., J. Fornek, N. Crochet, G. Bajwa, O. Perwitasari, L. Martinez-Sobrido, S. Akira, M. A. Gill, A. Garcia-Sastre, M. G. Katze, and M. Gale, Jr.** 2008. Distinct RIG-I and MDA5 signaling by RNA viruses in innate immunity. *J Virol* **82**:335-45.
301. **Lycke, E.** 1958. Studies of the inactivation of poliomyelitis virus by formaldehyde; the effect upon the rate of inactivation of temperature, pH and concentration of formaldehyde. *Arch Gesamte Virusforsch* **8**:267-84.
302. **Lyons, T., K. E. Murray, A. W. Roberts, and D. J. Barton.** 2001. Poliovirus 5'-terminal cloverleaf RNA is required in cis for VPg uridylylation and the initiation of negative-strand RNA synthesis. *J Virol* **75**:10696-708.
303. **Macadam, A. J., C. Arnold, J. Howlett, A. John, S. Marsden, F. Taffs, P. Reeve, N. Hamada, K. Wareham, J. Almond, N. Cammack, and P. D. Minor.** 1989. Reversion of the attenuated and temperature-sensitive phenotypes of the Sabin type 3 strain of poliovirus in vaccinees. *Virology* **172**:408-14.
304. **Macadam, A. J., G. Ferguson, C. Arnold, and P. D. Minor.** 1991. An assembly defect as a result of an attenuating mutation in the capsid proteins of the poliovirus type 3 vaccine strain. *J Virol* **65**:5225-31.
305. **Macadam, A. J., S. R. Pollard, G. Ferguson, R. Skuce, D. Wood, J. W. Almond, and P. D. Minor.** 1993. Genetic basis of attenuation of the Sabin type 2 vaccine strain of poliovirus in primates. *Virology* **192**:18-26.
306. **Mahon, B. P., K. Katrak, and K. H. Mills.** 1992. Antigenic sequences of poliovirus recognized by T cells: serotype-specific epitopes on VP1 and VP3 and cross-reactive epitopes on VP4 defined by using CD4⁺ T-cell clones. *J Virol* **66**:7012-20.
307. **Mahon, B. P., K. Katrak, A. Nomoto, A. J. Macadam, P. D. Minor, and K. H. Mills.** 1995. Poliovirus-specific CD4⁺ Th1 clones with both cytotoxic and helper activity mediate protective humoral immunity against a lethal poliovirus infection in transgenic mice expressing the human poliovirus receptor. *J Exp Med* **181**:1285-92.
308. **Manor, Y., R. Handsher, T. Halmut, M. Neuman, A. Bobrov, H. Rudich, A. Vonsover, L. Shulman, O. Kew, and E. Mendelson.** 1999. Detection of poliovirus circulation by environmental surveillance in the absence of clinical cases in Israel and the Palestinian authority. *J Clin Microbiol* **37**:1670-5.

309. **Martin, J.** 2011. Detection and Characterization of Polioviruses, p. 233-256. *In* J. R. Stephenson and A. Warnes (ed.), *Diagnostic Virology Protocols* 2ed. Humana Press, New York.
310. **Martin, J.** 2012. Unpublished results.
311. **Martin, J.** 2006. Vaccine-derived poliovirus from long term excretors and the end game of polio eradication. *Biologicals* **34**:117-22.
312. **Martin, J., G. Crossland, D. J. Wood, and P. D. Minor.** 2003. Characterization of formaldehyde-inactivated poliovirus preparations made from live-attenuated strains. *J Gen Virol* **84**:1781-8.
313. **Martin, J., G. Dunn, R. Hull, V. Patel, and P. D. Minor.** 2000. Evolution of the Sabin strain of type 3 poliovirus in an immunodeficient patient during the entire 637-day period of virus excretion. *J Virol* **74**:3001-10.
314. **Martin, J., G. L. Ferguson, D. J. Wood, and P. D. Minor.** 2000. The vaccine origin of the 1968 epidemic of type 3 poliomyelitis in Poland. *Virology* **278**:42-9.
315. **Masuda, N., T. Ohnishi, S. Kawamoto, M. Monden, and K. Okubo.** 1999. Analysis of chemical modification of RNA from formalin-fixed samples and optimization of molecular biology applications for such samples. *Nucleic Acids Res* **27**:4436-43.
316. **McLean, I.W. Jr., and A. R. Taylor.** 1958. Experiences in the production of poliovirus vaccines. *Prog Med Virol* **1**:122-64.
317. **McDermott, B. M., Jr., A. H. Rux, R. J. Eisenberg, G. H. Cohen, and V. R. Racaniello.** 2000. Two distinct binding affinities of poliovirus for its cellular receptor. *J Biol Chem* **275**:23089-96.
318. **McGoldrick, A., A. J. Macadam, G. Dunn, A. Rowe, J. Burlison, P. D. Minor, J. Meredith, D. J. Evans, and J. W. Almond.** 1995. Role of mutations G-480 and C-6203 in the attenuation phenotype of Sabin type 1 poliovirus. *J Virol* **69**:7601-5.
319. **McKay, H. W., A. R. Fodor, and U. P. Kokko.** 1963. Viremia Following the Administration of Live Poliovirus Vaccines. *Am J Public Health Nations Health* **53**:274-85.
320. **Melen, B., and R. Salenstedt.** 1959. Potency of inactivated poliovirus vaccines. The guinea pig test as a routine method. *Arch Gesamte Virusforsch* **9**:150-155.
321. **Melnick, J. L.** 1978. Advantages and disadvantages of killed and live poliomyelitis vaccines. *Bull World Health Organ* **56**:21-38.

322. **Melnick, J. L.** 1954. Attenuation of poliomyelitis viruses on passage through tissue culture. *Fed Proc* **13**:505.
323. **Melnick, J. L.** 1960. Problems associated with the use of live poliovirus vaccine. *Am J Public Health Nations Health* **50**:1013-31.
324. **Melnick, J. L.** 1960. Tests for safety of live poliovirus vaccine. *Acad Med N J Bull* **6**:146-167.
325. **Melnick, J. L.** 1996. Thermostability of poliovirus and measles vaccines. *Dev Biol Stand* **87**:155-60.
326. **Melnick, J. L.** 1991. Virus inactivation: lessons from the past. *Dev Biol Stand* **75**:29-36.
327. **Melnick, J. L., M. Benyesh-Melnick, and J. C. Brennan.** 1959. Studies on live poliovirus vaccine: its neurotrophic activity in monkeys and its increased neurovirulence after multiplication in vaccinated children. *JAMA* **171**:1165-1172.
328. **Mendelsohn, C., B. Johnson, K. A. Lionetti, P. Nobis, E. Wimmer, and V. R. Racaniello.** 1986. Transformation of a human poliovirus receptor gene into mouse cells. *Proc Natl Acad Sci U S A* **83**:7845-9.
329. **Mendelsohn, C. L., Wimmer, E. and Racaniello, V. R.** 1989. Cellular receptor for poliovirus: Molecular cloning, nucleotide sequence, and expression of a new member of the immunoglobulin superfamily. *Cell* **56**:855-865.
330. **Meredith, J. M., J. B. Rohll, J. W. Almond, and D. J. Evans.** 1999. Similar interactions of the poliovirus and rhinovirus 3D polymerases with the 3' untranslated region of rhinovirus 14. *J Virol* **73**:9952-8.
331. **Metz, B., G. F. Kersten, G. J. Baart, A. de Jong, H. Meiring, J. ten Hove, M. J. van Steenberg, W. E. Hennink, D. J. Crommelin, and W. Jiskoot.** 2006. Identification of formaldehyde-induced modifications in proteins: reactions with insulin. *Bioconjug Chem* **17**:815-22.
332. **Metz, B., G. F. Kersten, P. Hoogerhout, H. F. Brugghe, H. A. Timmermans, A. de Jong, H. Meiring, J. ten Hove, W. E. Hennink, D. J. Crommelin, and W. Jiskoot.** 2004. Identification of formaldehyde-induced modifications in proteins: reactions with model peptides. *J Biol Chem* **279**:6235-43.
333. **Minor, P.** 1998. Picornaviruses, p. 485-510. *In* L. Collier, A. Balows, M. Sussman, and B. W. J. Mahy (ed.), *Topley and Wilson's Microbiology and Microbial Infections*, 9 ed. Arnold, London.

334. **Minor, P.** 1990. Summary report of a meeting on the estimation of the potency of inactivated poliovaccine. Institute Pasteur, Paris 12-13 February 1990. *Biologicals* **18**:243-244.
335. **Minor, P.** 2009. Vaccine-derived poliovirus (VDPV): Impact on poliomyelitis eradication. *Vaccine* **27**:2649-52.
336. **Minor, P., and J. W. Almond.** 2002. Poliovirus Vaccines: Molecular Biology and Immune Response p. 381-390. *In* B. L. Semler and E. Wimmer (ed.), *Molecular Biology of Picornaviruses*. American Society for Microbiology Press, Washington DC, USA.
337. **Minor, P. D.** 1990. Antigenic structure of picornaviruses. *Curr Top Microbiol Immunol* **161**:121-54.
338. **Minor, P. D.** 2012. The Polio-Eradication programme and issues of the end game. *J Gen Virol* **93**: 457-474.
339. **Minor, P. D.** 2004. Polio eradication, cessation of vaccination and re-emergence of disease. *Nat Rev Microbiol* **2**:473-82.
340. **Minor, P. D.** 1997. Poliovirus, p. 555-577. *In* N. Nathanson, R. Ahmed, M. D. Gonzalez-Scarano, D. E. Griffin, K. V. Holmes, F. A. Murphy, and H. L. Robinson (ed.), *Viral Pathogenesis*. Lippincott-Raven Publishers, Philadelphia.
341. **Minor, P. D., and G. Dunn.** 1988. The effect of sequences in the 5' non-coding region on the replication of polioviruses in the human gut. *J Gen Virol* **69**:1091-6.
342. **Minor, P. D., M. Ferguson, K. Katrak, D. Wood, A. John, J. Howlett, G. Dunn, K. Burke, and J. W. Almond.** 1990. Antigenic structure of chimeras of type 1 and type 3 poliovirus involving antigenic site 1. *J Gen Virol* **71**:2543-51.
343. **Minor, P. D., M. Ferguson, K. Katrak, D. Wood, A. John, J. Howlett, G. Dunn, K. Burke, and J. W. Almond.** 1991. Antigenic structure of chimeras of type 1 and type 3 polioviruses involving antigenic sites 2, 3 and 4. *J Gen Virol* **72**:2475-81.
344. **Minor, P. D., and P. Muir.** 2009. Enteroviruses, p. 601-624. *In* A. J. Zuckerman, J. E. Banatvala, B. D. Schoub, P. D. Griffiths, and P. Mortimer (ed.), *Principles and Practice of Clinical Virology*, 6 ed. John Wiley and Sons, New York.
345. **Minor, P. D., P. A. Pipkin, D. Hockley, G. C. Schild, and J. W. Almond.** 1984. Monoclonal antibodies which block cellular receptors of poliovirus. *Virus Res* **1**:203-12.
346. **Mirzayan, C., and E. Wimmer.** 1994. Biochemical studies on poliovirus polypeptide 2C: evidence for ATPase activity. *Virology* **199**:176-87.

347. **Mohammed, A. J., S. AlAwaidy, S. Bawikar, P. J. Kurup, E. Elamir, M. M. Shaban, S. M. Sharif, H. G. van der Avoort, M. A. Pallansch, P. Malankar, A. Burton, M. Sreevatsava, and R. W. Sutter.** 2010. Fractional doses of inactivated poliovirus vaccine in Oman. *N Engl J Med* **362**:2351-9.
348. **Molla, A., K. S. Harris, A. V. Paul, S. H. Shin, J. Mugavero, and E. Wimmer.** 1994. Stimulation of poliovirus proteinase 3C_{pro}-related proteolysis by the genome-linked protein VPg and its precursor 3AB. *J Biol Chem* **269**:27015-20.
349. **Montagnon, B. J., B. Fanget, and J. C. Vincent-Falquet.** 1984. Industrial-scale production of inactivated poliovirus vaccine prepared by culture of Vero cells on microcarrier. *Rev Infect Dis* **6 Suppl 2**:S341-4.
350. **Montagnon, B. J., J. C. Vincent-Falquet, and J. F. Saluzzo.** 1999. Experience with vero cells at Pasteur Merieux Connaught. *Dev Biol Stand* **98**:137-40; discussion 167.
351. **Moore, A. E., L. Sabachewsky, and H. W. Toolan.** 1955. Culture characteristics of four permanent lines of human cancer cells. *Cancer Res* **15**:598-602.
352. **Morrison, M. E., Y. J. He, M. W. Wien, J. M. Hogle, and V. R. Racaniello.** 1994. Homolog-scanning mutagenesis reveals poliovirus receptor residues important for virus binding and replication. *J Virol* **68**:2578-88.
353. **Moynihan, M., and I. Petersen.** 1982. The durability of inactivated poliovirus vaccine: studies on the stability of potency in vivo and in vitro. *J Biol Stand* **10**:261-8.
354. **Mueller, S., D. Papamichail, J. R. Coleman, S. Skiena, and E. Wimmer.** 2006. Reduction of the rate of poliovirus protein synthesis through large-scale codon deoptimization causes attenuation of viral virulence by lowering specific infectivity. *J Virol* **80**:9687-96.
355. **Mueller, S., E. Wimmer, and J. Cello.** 2005. Poliovirus and poliomyelitis: a tale of guts, brains, and an accidental event. *Virus Res* **111**:175-93.
356. **Mulders, M. N., J. H. Reimerink, M. P. Koopmans, A. M. van Loon, and H. G. van der Avoort.** 1997. Genetic analysis of wild-type poliovirus importation into The Netherlands (1979-1995). *J Infect Dis* **176**:617-24.
357. **Murdin, A. D., A. Kameda, M. G. Murray, and E. Wimmer.** 1991. Phenotypic characterization of antigenic hybrids of poliovirus. *Microb Pathog* **10**:39-45.
358. **Murdin, A. D., C. Mirzayan, A. Kameda, and E. Wimmer.** 1991. The effect of site and mode of expression of a heterologous antigenic determinant on the properties of poliovirus hybrids. *Microb Pathog* **10**:27-37.

359. **Murdin, A. D., and E. Wimmer.** 1989. Construction of a poliovirus type 1/type 2 antigenic hybrid by manipulation of neutralization antigenic site II. *J Virol* **63**:5251-7.
360. **Murphy, M., L. Jason-Moller, and J. Bruno.** 2006. Using Biacore to measure the binding kinetics of an antibody-antigen interaction. *Curr Protoc Protein Sci* **Chapter 19**:Unit 19 14.
361. **Murray, R.** 1961. Standardization, licensing, and availability of live poliovirus vaccine. *JAMA* **175**:843-6.
362. **Murray, R., R. Kirchstein, G. Van Hoosier Jr, and S. Baron.** 1959. Presented at the First International Conference on Live Poliovirus Vaccines, Washington DC, USA.
363. **Nathanson, N., and D. Bodian.** 1962. Experimental poliomyelitis following intramuscular virus injection. III. The effect of passive antibody on paralysis and viremia. *Bull Johns Hopkins Hosp* **111**:198-220.
364. **Nathanson, N., and O. M. Kew.** 2010. From emergence to eradication: the epidemiology of poliomyelitis deconstructed. *Am J Epidemiol* **172**:1213-29.
365. **Nathanson, N., and A. D. Langmuir.** 1995. The Cutter incident. Poliomyelitis following formaldehyde-inactivated poliovirus vaccination in the United States during the Spring of 1955. II. Relationship of poliomyelitis to Cutter vaccine. 1963. *Am J Epidemiol* **142**:109-40; discussion 107-8.
366. **Nathanson, N., and A. D. Langmuir.** 1963. The Cutter incident: poliomyelitis following formaldehyde-inactivated poliovirus vaccination in the United States during the spring of 1955. I. Background. *Am. J. Epidemiol.* **78**:16-28.
367. **Nathanson, N., and A. D. Langmuir.** 1963. The Cutter incident: poliomyelitis following formaldehyde-inactivated poliovirus vaccination in the United States during the spring of 1955. II. Relationship of poliomyelitis to Cutter vaccine. *Am. J. Epidemiol.* **78**:29-60.
368. **Nathanson, N., and A. D. Langmuir.** 1963. The Cutter incident: poliomyelitis following formaldehyde-inactivated poliovirus vaccination in the United States during the spring of 1955. III. Comparison of the clinical character of vaccinated and contact cases occurring after use of high-rate lots of Cutter vaccine. *Am. J. Epidemiol.* **78**:61-81.
369. **Nathanson, N., and J. R. Martin.** 1979. The epidemiology of poliomyelitis: enigmas surrounding its appearance, epidemicity, and disappearance. *Am J Epidemiol* **110**:672-92.

370. **National Oceanic and Atmospheric Administration.** 1977. Local Climatological Data, Annual Summary With Comparative Data 1977. *In* Department of Commerce (ed.). National Oceanic and Atmospheric Administration, Washington, DC.
371. **National Research Council.** 2006. Workshop report. Exploring the role of antiviral drugs in the eradication of polio. National Academies Press, Washington, DC.
372. **Nelson, K. S., J. M. Janssen, S. B. Troy, and Y. Maldonado.** 2012. Intradermal fractional dose inactivated polio vaccine: A review of the literature. *Vaccine* **30**:121-5.
373. **Nomoto, A., B. Detjen, R. Pozzatti, and E. Wimmer.** 1977. The location of the polio genome protein in viral RNAs and its implication for RNA synthesis. *Nature* **268**:208-13.
374. **Nomoto, A., N. Kitamura, F. Golini, and E. Wimmer.** 1977. The 5'-terminal structures of poliovirion RNA and poliovirus mRNA differ only in the genome-linked protein VPg. *Proc Natl Acad Sci U S A* **74**:5345-9.
375. **Nomoto, A., T. Omata, H. Toyoda, S. Kuge, H. Horie, Y. Kataoka, Y. Genba, Y. Nakano, and N. Imura.** 1982. Complete nucleotide sequence of the attenuated poliovirus Sabin 1 strain genome. *Proc Natl Acad Sci U S A* **79**:5793-7.
376. **Odoom, J. K., Z. Yunus, G. Dunn, P. D. Minor, and J. Martin.** 2008. Changes in population dynamics during long-term evolution of sabin type 1 poliovirus in an immunodeficient patient. *J Virol* **82**:9179-90.
377. **Ohka, S., N. Matsuda, K. Tohyama, T. Oda, M. Morikawa, S. Kuge, and A. Nomoto.** 2004. Receptor (CD155)-dependent endocytosis of poliovirus and retrograde axonal transport of the endosome. *J Virol* **78**:7186-98.
378. **Ohka, S., W. X. Yang, E. Terada, K. Iwasaki, and A. Nomoto.** 1998. Retrograde transport of intact poliovirus through the axon via the fast transport system. *Virology* **250**:67-75.
379. **Omata, T., M. Kohara, S. Kuge, T. Komatsu, S. Abe, B. L. Semler, A. Kameda, H. Itoh, M. Arita, E. Wimmer, and A. Nomoto.** 1986. Genetic analysis of the attenuation phenotype of poliovirus type 1. *J Virol* **58**:348-58.
380. **Omata, T., M. Kohara, Y. Sakai, A. Kameda, N. Imura, and A. Nomoto.** 1984. Cloned infectious complementary DNA of the poliovirus Sabin 1 genome: biochemical and biological properties of the recovered virus. *Gene* **32**:1-10.

381. **Onorato, I. M., J. F. Modlin, A. M. McBean, M. L. Thoms, G. A. Losonsky, and R. H. Bernier.** 1991. Mucosal immunity induced by enhance-potency inactivated and oral polio vaccines. *J Infect Dis* **163**:1-6.
382. **Page, G. S., A. G. Mosser, J. M. Hogle, D. J. Filman, R. R. Rueckert, and M. Chow.** 1988. Three-dimensional structure of poliovirus serotype 1 neutralizing determinants. *J Virol* **62**:1781-94.
383. **Pallansch, M., and R. Roos.** 2007. Enteroviruses: Polioviruses, Coxsackieviruses, Echoviruses, and Newer Enteroviruses, p. 839-893. *In* D. M. Knipe, P. M. Howley, D. E. Griffin, R. A. Lamb, M. A. Martin, B. Roizman, and S. E. Straus (ed.), *Fields Virology*, 5 ed. Lippincott Williams and Wilkins, a Wolters Kluwer business, Philadelphia.
384. **Pallansch, M. A., and R. Roos.** 2001. Enteroviruses: polioviruses, coxsackieviruses, echoviruses, and newer enteroviruses, p. 723-775. *In* D. M. Knipe, P. M. Howley, D. E. Griffin, R. A. Lamb, M. A. Martin, B. Roizman, and S. E. Straus (ed.), *Fields Virology*, 4 ed, vol. 1. Lippincott Williams and Wilkins, Philadelphia.
385. **Palmenberg, A., D. Neubauer, and T. Skern.** 2010. Genome Organization and Encoded Proteins p. 3-17. *In* E. Ehrenfeld, E. Domingo, and R. Roos (ed.), *The Picornaviruses*. ASM Press, Washington, DC.
386. **Pan American Health Organization.** 1959. Proceedings of the First International Conference on Live Poliovirus Vaccines Pan American Sanitary Bureau, Washington, DC.
387. **Pan American Health Organization.** 1960. Proceedings of the Second International Conference on Live Poliovirus Vaccines. Pan American Health Organization, Washington, DC.
388. **Parsley, T. B., J. S. Towner, L. B. Blyn, E. Ehrenfeld, and B. L. Semler.** 1997. Poly (rC) binding protein 2 forms a ternary complex with the 5'-terminal sequences of poliovirus RNA and the viral 3CD proteinase. *RNA* **3**:1124-34.
389. **Patel, V., M. Ferguson, and P. D. Minor.** 1993. Antigenic sites on type 2 poliovirus. *Virology* **192**:361-4.
390. **Patriarca, P. A., P. F. Wright, and T. J. John.** 1991. Factors affecting the immunogenicity of oral poliovirus vaccine in developing countries: review. *Rev Infect Dis* **13**:926-39.
391. **Pattnaik, P.** 2005. Surface plasmon resonance: applications in understanding receptor-ligand interaction. *Appl Biochem Biotechnol* **126**:79-92.

392. **Paul, A. V.** 2002. Possible unifying mechanism of picornavirus genome replication, p. 227-246. *In* B. L. Semler and E. Wimmer (ed.), *Molecular Biology of Picornaviruses*. ASM Press, Washington, DC.
393. **Paul, A. V., X. Cao, K. S. Harris, J. Lama, and E. Wimmer.** 1994. Studies with poliovirus polymerase 3Dpol. Stimulation of poly(U) synthesis in vitro by purified poliovirus protein 3AB. *J Biol Chem* **269**:29173-81.
394. **Paul, A. V., J. Mugavero, J. Yin, S. Hobson, S. Schultz, J. H. van Boom, and E. Wimmer.** 2000. Studies on the attenuation phenotype of polio vaccines: poliovirus RNA polymerase derived from Sabin type 1 sequence is temperature sensitive in the uridylylation of VPg. *Virology* **272**:72-84.
395. **Paul, A. V., J. H. van Boom, D. Filippov, and E. Wimmer.** 1998. Protein-primed RNA synthesis by purified poliovirus RNA polymerase. *Nature* **393**:280-4.
396. **Paul, J. R.** 1971. *A History of Poliomyelitis*. Yale University Press, New Haven, Connecticut.
397. **Paul, J. R., D. M. Horstmann, J. T. Riordan, E. M. Opton, and R. H. Green.** 1960. Presented at the Second International Conference on Live Poliovirus Vaccines, Washington, D.C.
398. **Pelletier, J., G. Kaplan, V. R. Racaniello, and N. Sonenberg.** 1988. Cap-independent translation of poliovirus mRNA is conferred by sequence elements within the 5' noncoding region. *Mol Cell Biol* **8**:1103-12.
399. **Pelletier, J., and N. Sonenberg.** 1988. Internal initiation of translation of eukaryotic mRNA directed by a sequence derived from poliovirus RNA. *Nature* **334**:320-5.
400. **Perrin, P., and S. Morgeaux.** 1995. Inactivation of DNA by beta-propiolactone. *Biologicals* **23**:207-11.
401. **Pettersson, R. F., V. Ambros, and D. Baltimore.** 1978. Identification of a protein linked to nascent poliovirus RNA and to the polyuridylic acid of negative-strand RNA. *J Virol* **27**:357-65.
402. **Pfister, T., D. Egger, and K. Bienz.** 1995. Poliovirus subviral particles associated with progeny RNA in the replication complex. *J Gen Virol* **76 (Pt 1)**:63-71.
403. **Phillips, B. A., and R. Fennell.** 1973. Polypeptide composition of poliovirions, naturally occurring empty capsids, and 14S precursor particles. *J Virol* **12**:291-9.
404. **Pierangeli, A., M. Bucci, P. Pagnotti, A. M. Degener, and R. Perez Bercoff.** 1995. Mutational analysis of the 3'-terminal extra-cistronic region of poliovirus RNA:

- secondary structure is not the only requirement for minus strand RNA replication. FEBS Lett **374**:327-32.
405. **Pilipenko, E. V., V. M. Blinov, L. I. Romanova, A. N. Sinyakov, S. V. Maslova, and V. I. Agol.** 1989. Conserved structural domains in the 5'-untranslated region of picornaviral genomes: an analysis of the segment controlling translation and neurovirulence. *Virology* **168**:201-9.
406. **Pilipenko, E. V., A. P. Gmyl, S. V. Maslova, Y. V. Svitkin, A. N. Sinyakov, and V. I. Agol.** 1992. Prokaryotic-like cis elements in the cap-independent internal initiation of translation on picornavirus RNA. *Cell* **68**:119-31.
407. **Pilipenko, E. V., K. V. Poperechny, S. V. Maslova, W. J. Melchers, H. J. Slot, and V. I. Agol.** 1996. Cis-element, oriR, involved in the initiation of (-) strand poliovirus RNA: a quasi-globular multi-domain RNA structure maintained by tertiary ('kissing') interactions. *EMBO J* **15**:5428-36.
408. **Pipkin, P. A., D. J. Wood, V. R. Racaniello, and P. D. Minor.** 1993. Characterisation of L cells expressing the human poliovirus receptor for the specific detection of polioviruses in vitro. *J Virol Methods* **41**:333-40.
409. **Plotkin, S. A., and E. Vidor.** 2008. Poliovirus vaccine – inactivated, p. 605-629. *In* S. A. Plotkin, W. A. Orenstein, and P. A. Offit (ed.), *Vaccine*, 5 ed. Saunders Elsevier, Philadelphia.
410. **Poyry, T., M. Stenvik, and T. Hovi.** 1988. Viruses in sewage waters during and after a poliomyelitis outbreak and subsequent nationwide oral poliovirus vaccination campaign in Finland. *Appl Environ Microbiol* **54**:371-4.
411. **Qiagen.** 2010. QIAGEN® OneStep RT-PCR Kit Handbook. Qiagen.
412. **Qiagen.** 2008. QIAquick® Spin Handbook. Qiagen.
413. **Racaniello, V. R.** 2006. One hundred years of poliovirus pathogenesis. *Virology* **344**:9-16.
414. **Racaniello, V. R.** 2007. Picornaviridae: The viruses and their replication, p. 795-838. *In* D. M. Knipe, P. M. Howley, D. E. Griffin, R. A. Lamb, M. A. Martin, B. Roizman, and S. E. Straus (ed.), *Fields Virology*, 5 ed, vol. 1. Lippincott Williams and Wilkins, Philadelphia.
415. **Racaniello, V. R., and D. Baltimore.** 1981. Cloned poliovirus complementary DNA is infectious in mammalian cells. *Science* **214**:916-9.
416. **Racaniello, V. R., and R. Ren.** 1994. Transgenic mice and the pathogenesis of poliomyelitis. *Arch Virol Suppl* **9**:79-86.

417. **Race, E., C. A. Stein, M. D. Wigg, A. Baksh, M. Addawe, P. Frezza, and J. S. Oxford.** 1995. A multistep procedure for the chemical inactivation of human immunodeficiency virus for use as an experimental vaccine. *Vaccine* **13**:1567-75.
418. **Rait, V. K., L. Xu, T. J. O'Leary, and J. T. Mason.** 2004. Modeling formalin fixation and antigen retrieval with bovine pancreatic RNase A II. Interrelationship of cross-linking, immunoreactivity, and heat treatment. *Lab Invest* **84**:300-6.
419. **Rakoto-Andrianarivelo, M., S. Guillot, J. Iber, J. Balanant, B. Blondel, F. Riquet, J. Martin, O. Kew, B. Randriamanalina, L. Razafinimpiasa, D. Rousset, and F. Delpeyroux.** 2007. Co-circulation and evolution of polioviruses and species C enteroviruses in a district of Madagascar. *PLoS Pathog* **3**:e191.
420. **Rakoto-Andrianarivelo, M., N. Gumede, S. Jegouic, J. Balanant, S. N. Andriamamonjy, S. Rabemanantsoa, M. Birmingham, B. Randriamanalina, L. Nkolomoni, M. Venter, B. D. Schoub, F. Delpeyroux, and J. M. Reynes.** 2008. Reemergence of recombinant vaccine-derived poliovirus outbreak in Madagascar. *J Infect Dis* **197**:1427-35.
421. **Ramakrishnan, M. A., A. B. Pandey, K. P. Singh, R. Singh, S. Nandi, and M. L. Mehrotra.** 2006. Immune responses and protective efficacy of binary ethylenimine (BEI)-inactivated bluetongue virus vaccines in sheep. *Vet Res Commun* **30**:873-80.
422. **Ren, R., and V. R. Racaniello.** 1992. Poliovirus spreads from muscle to the central nervous system by neural pathways. *J Infect Dis* **166**:747-52.
423. **Ren, R. B., F. Costantini, E. J. Gorgacz, J. J. Lee, and V. R. Racaniello.** 1990. Transgenic mice expressing a human poliovirus receptor: a new model for poliomyelitis. *Cell* **63**:353-62.
424. **Ren, R. B., E. G. Moss, and V. R. Racaniello.** 1991. Identification of two determinants that attenuate vaccine-related type 2 poliovirus. *J Virol* **65**:1377-82.
425. **Resik, S., A. Tejada, P. M. Lago, M. Diaz, A. Carmenates, L. Sarmiento, N. Alemani, B. Galindo, A. Burton, M. Friede, M. Landaverde, and R. W. Sutter.** 2010. Randomized controlled clinical trial of fractional doses of inactivated poliovirus vaccine administered intradermally by needle-free device in Cuba. *J Infect Dis* **201**:1344-52.
426. **Rezapkin, G., J. Martin, and K. Chumakov.** 2005. Analysis of antigenic profiles of inactivated poliovirus vaccine and vaccine-derived polioviruses by block-ELISA method. *Biologicals* **33**:29-39.

427. **Rezapkin, G. V., L. Fan, D. M. Asher, M. R. Fibi, E. M. Dragunsky, and K. M. Chumakov.** 1999. Mutations in Sabin 2 strain of poliovirus and stability of attenuation phenotype. *Virology* **258**:152-60.
428. **Richards, O. C., and E. Ehrenfeld.** 1998. Effects of poliovirus 3AB protein on 3D polymerase-catalyzed reaction. *J Biol Chem* **273**:12832-40.
429. **Rieder, E., and E. Wimmer.** 2002. Cellular Receptors of Picornaviruses: an Overview, p. 61-70. *In* B. L. Semler and E. Wimmer (ed.), *Molecular Biology of Picornaviruses*. ASM Press, Washington, DC.
430. **Robbins, F. C.** 2004. The history of polio vaccine development, p. 17-30. *In* S. A. Plotkin and W. A. Orenstein (ed.), *Vaccines*, 4 ed. Saunders, Philadelphia.
431. **Roberts, A., E. W. Lamirande, L. Vogel, B. Baras, G. Goossens, I. Knott, J. Chen, J. M. Ward, V. Vassilev, and K. Subbarao.** 2010. Immunogenicity and protective efficacy in mice and hamsters of a beta-propiolactone inactivated whole virus SARS-CoV vaccine. *Viral Immunol* **23**:509-19.
432. **Roberts, J. J., and G. P. Warwick.** 1963. The Reaction of Beta-Propiolactone with Guanosine, Deoxyguanylic Acid and Rna. *Biochem Pharmacol* **12**:1441-2.
433. **Robertson, H. E., M. S. Acker, H. O. Dillenberg, R. Woodrow, R. J. Wilson, W. K. Ing, and D. R. Macleod.** 1962. Community-wide use of a "balanced" trivalent oral poliovirus vaccine (Sabin). A report of the 1961 trial at Prince Albert, Saskatchewan. *Can J Public Health* **53**:179-91.
434. **Roche Diagnostics** 2012, posting date. MagNA Pure LC Total Nucleic Acid Isolation Kit - Large Volume: Principle. [Online.]
435. **Rodriguez, P. L., and L. Carrasco.** 1995. Poliovirus protein 2C contains two regions involved in RNA binding activity. *J Biol Chem* **270**:10105-12.
436. **Roitt, I. M., and P. J. Delves.** 2001. *Roitt's Essential Immunology*, 10 ed. Blackwell Science, Oxford.
437. **Roivainen, M., S. Blomqvist, H. Al-Hello, A. Paananen, F. Delpeyroux, M. Kuusi, and T. Hovi.** 2010. Highly divergent neurovirulent vaccine-derived polioviruses of all three serotypes are recurrently detected in Finnish sewage. *Euro Surveill* **15**:pii/19566.
438. **Rothberg, P. G., T. J. Harris, A. Nomoto, and E. Wimmer.** 1978. O⁴-(5'-uridylyl)tyrosine is the bond between the genome-linked protein and the RNA of poliovirus. *Proc Natl Acad Sci U S A* **75**:4868-72.

439. **Rousset, D., M. Rakoto-Andrianarivelo, R. Razafindratsimandresy, B. Randriamanalina, S. Guillot, J. Balanant, P. Mauclere, and F. Delpeyroux.** 2003. Recombinant vaccine-derived poliovirus in Madagascar. *Emerg Infect Dis* **9**:885-7.
440. **Rowlands, D. J., and P. D. Minor.** 2010. Vaccine Strategies, p. 431-447. *In* E. Ehrenfeld, E. Domingo, and R. P. Roos (ed.), *The Picornaviruses*. American Society for Microbiology Press, Washington, D.C.
441. **Rowlands, D. J., D. V. Sangar, and F. Brown.** 1972. Stabilizing the immunizing antigen of foot-and-mouth disease virus by fixation with formaldehyde. *Arch Gesamte Virusforsch* **39**:274-83.
442. **Rozenand, S., and H. J. Skaletsky.** 2000. Primer3 on the WWW for general users and for biologist programmers, p. 365-386. *In* S. Krawetz and S. Misener (ed.), *Bioinformatics Methods and Protocols: Methods in Molecular Biology*. Humana Press, New Jersey.
443. **Rozovics, J. M., and B. L. Semler.** 2010. Genome Replication I: the Players, p. 107-125. *In* E. Ehrenfeld, E. Domingo, and R. Roos (ed.), *The Picornaviruses*. ASM Press, Washington, DC.
444. **Saalmuller, A.** 2006. New understanding of immunological mechanisms. *Vet Microbiol* **117**:32-8.
445. **Sabin, A. B.** 1985. Oral poliovirus vaccine: history of its development and use and current challenge to eliminate poliomyelitis from the world. *J Infect Dis* **151**:420-36.
446. **Sabin, A. B.** 1956. Pathogenesis of poliomyelitis; reappraisal in the light of new data. *Science* **123**:1151-7.
447. **Sabin, A. B.** 1956. Present status of attenuated live-virus poliomyelitis vaccine. *J Am Med Assoc* **162**:1589-96.
448. **Sabin, A. B., and L. R. Boulger.** 1973. History of Sabin attenuated poliovirus oral live vaccine strains. *J Biol Stand* **1**:115-118.
449. **Sabin, A. B., M. Ramos-Alvarez, J. Alvarez-Amezquita, W. Pelon, R. H. Michaels, I. Spigland, M. A. Koch, J. M. Barnes, and J. S. Rhim.** 1960. Live, orally given poliovirus vaccine. Effects of rapid mass immunization on population under conditions of massive enteric infection with other viruses. *JAMA* **173**:1521-6.
450. **Salk, J. E., and J. B. Gori.** 1960. A review of theoretical, experimental, and practical considerations in the use of formaldehyde for the inactivation of poliovirus. *Ann N Y Acad Sci* **83**:609-37.

451. **Salk, J. E., U. Krech, J. S. Youngner, B. L. Bennett, L. J. Lewis, and P. L. Bazeley.** 1954. Formaldehyde treatment and safety testing of experimental poliomyelitis vaccines. *Am J Public Health Nations Health* **44**:563-70.
452. **Salk, J. E., L. J. Lewis, B. L. Bennett, E. N. Ward, U. Krech, J. S. Younger, and P. L. Bazeley.** 1955. Antigenic activity of poliomyelitis vaccines undergoing field test. *Am J Public Health Nations Health* **45**:151-62.
453. **Sambrook, J., and D. Russell.** 2001. *Molecular Cloning. A Laboratory Manual*, 3 ed. Cold Spring Harbor Laboratory Press, New York.
454. **Sandoval, I. V., and L. Carrasco.** 1997. Poliovirus infection and expression of the poliovirus protein 2B provoke the disassembly of the Golgi complex, the organelle target for the antipoliovirus drug Ro-090179. *J Virol* **71**:4679-93.
455. **Sant, A. J., F. A. Chaves, S. A. Jenks, K. A. Richards, P. Menges, J. M. Weaver, and C. A. Lazarski.** 2005. The relationship between immunodominance, DM editing, and the kinetic stability of MHC class II:peptide complexes. *Immunol Rev* **207**:261-78.
456. **Schlesinger, R. W., I. M. Morgan, and P. K. Olitsky.** 1943. Transmission to Rodents of Lansing Type Poliomyelitis Virus Originating in the Middle East. *Science* **98**:452-4.
457. **Seder, R. A., and J. R. Mascola.** 2003. Immunology. Part A. Basic Immunology of Vaccine Development, p. 51-72. *In* B. R. Bloom and P.-H. Lambert (ed.), *The Vaccine Book*. Academic Press, London.
458. **Segal, A., J. J. Solomon, and U. Mate.** 1980. Isolation of 3-(2-carboxyethyl)thymine following in vitro reaction of beta-propiolactone with calf thymus DNA. *Chem Biol Interact* **29**:335-46.
459. **Segal, A., J. J. Solomon, J. Mignano, and J. Dino.** 1981. The isolation and characterization of 3-(2-carboxyethyl)cytosine following in vitro reaction of beta-propiolactone with calf thymus DNA. *Chem Biol Interact* **35**:349-61.
460. **Selinka, H. C., A. Zibert, and E. Wimmer.** 1992. A chimeric poliovirus/CD4 receptor confers susceptibility to poliovirus on mouse cells. *J Virol* **66**:2523-6.
461. **Selinka, H. C., A. Zibert, and E. Wimmer.** 1991. Poliovirus can enter and infect mammalian cells by way of an intercellular adhesion molecule 1 pathway. *Proc Natl Acad Sci U S A* **88**:3598-602.
462. **Serfling, R. E., and I. L. Sherman.** 1953. Poliomyelitis distribution in the United States. *Public Health Rep* **68**:453-66.

463. **Seth, S., M. K. Maier, Q. Qiu, I. Ravens, E. Kremmer, R. Forster, and G. Bernhardt.** 2007. The murine pan T cell marker CD96 is an adhesion receptor for CD155 and nectin-1. *Biochem Biophys Res Commun* **364**:959-65.
464. **Shearman, C. W., and L. A. Loeb.** 1979. Effects of depurination on the fidelity of DNA synthesis. *J Mol Biol* **128**:197-218.
465. **Shelokov, A., K. Habel, and D. W. McKinstry.** 1955. Relation of poliomyelitis virus types to clinical disease and geographic distribution: a preliminary report. *Ann N Y Acad Sci* **61**:998-1004.
466. **Shimizu, H., B. Thorley, F. J. Paladin, K. A. Brussen, V. Stambos, L. Yuen, A. Utama, Y. Tano, M. Arita, H. Yoshida, T. Yoneyama, A. Benegas, S. Roesel, M. Pallansch, O. Kew, and T. Miyamura.** 2004. Circulation of type 1 vaccine-derived poliovirus in the Philippines in 2001. *J Virol* **78**:13512-21.
467. **Shulman, L. M., R. Handsher, C. F. Yang, S. J. Yang, J. Manor, A. Vonsover, Z. Grossman, M. Pallansch, E. Mendelson, and O. M. Kew.** 2000. Resolution of the pathways of poliovirus type 1 transmission during an outbreak. *J Clin Microbiol* **38**:945-52.
468. **Shulman, L. M., Y. Manor, D. Sofer, R. Handsher, T. Swartz, F. Delpeyroux, and E. Mendelson.** 2006. Neurovirulent vaccine-derived polioviruses in sewage from highly immune populations. *PLoS One* **1**:e69.
469. **Shulman, L. M., Y. Manor, D. Sofer, T. Swartz, and E. Mendelson.** 2006. Oral poliovaccine: will it help eradicate polio or cause the next epidemic? *Isr Med Assoc J* **8**:312-5.
470. **Siegrist, C.-A.** 2008. Vaccine immunology, p. 17-36. *In* S. A. Plotkin, W. A. Orenstein, and P. A. Offit (ed.), *Vaccines*, 5 ed. Saunders Elsevier.
471. **Sigmundsson, K., G. Masson, R. Rice, N. Beauchemin, and B. Obrink.** 2002. Determination of active concentrations and association and dissociation rate constants of interacting biomolecules: an analytical solution to the theory for kinetic and mass transport limitations in biosensor technology and its experimental verification. *Biochemistry* **41**:8263-76.
472. **Simizu, B., S. Abe, H. Yamamoto, Y. Tano, Y. Ota, M. Miyazawa, H. Horie, K. Satoh, and K. Wakabayashi.** 2006. Development of inactivated poliovirus vaccine derived from Sabin strains. *Biologicals* **34**:151-4.

473. **Simmonds, P., C. McIntyre, C. Savolainen-Kopra, C. Tapparel, I. M. Mackay, and T. Hovi.** 2010. Proposals for the classification of human rhinovirus species C into genotypically assigned types. *J Gen Virol* **91**:2409-19.
474. **Singer, C., F. Knauert, G. Bushar, M. Klutch, R. Lundquist, and G. V. Quinnan, Jr.** 1989. Quantitation of poliovirus antigens in inactivated viral vaccines by enzyme-linked immunosorbent assay using animal sera and monoclonal antibodies. *J Biol Stand* **17**:137-50.
475. **Skinner, M. A., V. R. Racaniello, G. Dunn, J. Cooper, P. D. Minor, and J. W. Almond.** 1989. New model for the secondary structure of the 5' non-coding RNA of poliovirus is supported by biochemical and genetic data that also show that RNA secondary structure is important in neurovirulence. *J Mol Biol* **207**:379-92.
476. **Sloan, K. E., J. K. Stewart, A. F. Treloar, R. T. Matthews, and D. G. Jay.** 2005. CD155/PVR enhances glioma cell dispersal by regulating adhesion signaling and focal adhesion dynamics. *Cancer Res* **65**:10930-7.
477. **Slota, M., J. B. Lim, Y. Dang, and M. L. Disis.** 2011. ELISpot for measuring human immune responses to vaccines. *Expert Rev Vaccines* **10**:299-306.
478. **Smith, J., R. Leke, A. Adams, and R. H. Tangermann.** 2004. Certification of polio eradication: process and lessons learned. *Bull World Health Organ* **82**:24-30.
479. **Solecki, D., M. Gromeier, J. Harber, G. Bernhardt, and E. Wimmer.** 1998. Poliovirus and its cellular receptor: a molecular genetic dissection of a virus/receptor affinity interaction. *J Mol Recognit* **11**:2-9.
480. **Sonenberg, N.** 1987. Regulation of translation by poliovirus. *Adv Virus Res* **33**:175-204.
481. **Spector, D. H., and D. Baltimore.** 1974. Requirement of 3'-terminal poly(adenylic acid) for the infectivity of poliovirus RNA. *Proc Natl Acad Sci U S A* **71**:2983-7.
482. **Stern, L. J., and J. M. Calvo-Calle.** 2009. HLA-DR: molecular insights and vaccine design. *Curr Pharm Des* **15**:3249-61.
483. **Strategic Advisory Group of Experts on Immunization World Health Organization** 2010, posting date. Global Polio Eradication: Progress and Current Epidemiological / Operational Risks. [Online.]
484. **Strebel, P. M., R. W. Sutter, S. L. Cochi, R. J. Biellik, E. W. Brink, O. M. Kew, M. A. Pallansch, W. A. Orenstein, and A. R. Hinman.** 1992. Epidemiology of poliomyelitis in the United States one decade after the last reported case of indigenous wild virus-associated disease. *Clin Infect Dis* **14**:568-79.

485. **Sutter, R. W., O. M. Kew, and S. L. Cochi.** 2008. Poliovirus vaccine - live, p. 631-685. In S. A. Plotkin, W. A. Orenstein, and P. A. Offit (ed.), *Vaccines*, 5 ed. Saunders Elsevier, Philadelphia.
486. **Sutter, R. W., M. A. Pallansch, L. A. Sawyer, S. L. Cochi, and S. C. Hadler.** 1995. Defining surrogate serologic tests with respect to predicting protective vaccine efficacy: poliovirus vaccination. *Ann N Y Acad Sci* **754**:289-99.
487. **Svitkin, Y. V., N. Cammack, P. D. Minor, and J. W. Almond.** 1990. Translation deficiency of the Sabin type 3 poliovirus genome: association with an attenuating mutation C472----U. *Virology* **175**:103-9.
488. **Svitkin, Y. V., S. V. Maslova, and V. I. Agol.** 1985. The genomes of attenuated and virulent poliovirus strains differ in their in vitro translation efficiencies. *Virology* **147**:243-52.
489. **Svitkin, Y. V., T. V. Pestova, S. V. Maslova, and V. I. Agol.** 1988. Point mutations modify the response of poliovirus RNA to a translation initiation factor: a comparison of neurovirulent and attenuated strains. *Virology* **166**:394-404.
490. **Taffs, R., E. Dragunsky, T. Nomura, K. Hioki, I. Levenbook, and E. Fitzgerald.** 1998. Importance of experiments in poliovirus-susceptible transgenic mice for evaluating current potency tests of inactivated polio vaccine (IPV). *Dev Biol (Basel)* **86**:345.
491. **Taffs, R. E., Y. V. Chernokhvostova, E. M. Dragunsky, T. Nomura, K. Hioki, E. C. Beuvery, E. A. Fitzgerald, I. S. Levenbook, and D. M. Asher.** 1997. Inactivated poliovirus vaccine protects transgenic poliovirus receptor mice against type 3 poliovirus challenge. *J Infect Dis* **175**:441-4.
492. **Takeuchi, O., and S. Akira.** 2009. Innate immunity to virus infection. *Immunol Rev* **227**:75-86.
493. **Tano, Y., H. Shimizu, J. Martin, Y. Nishimura, B. Simizu, and T. Miyamura.** 2007. Antigenic characterization of a formalin-inactivated poliovirus vaccine derived from live-attenuated Sabin strains. *Vaccine* **25**:7041-6.
494. **Tardy-Panit, M., B. Blondel, A. Martin, F. Tekaiia, F. Horaud, and F. Delpeyroux.** 1993. A mutation in the RNA polymerase of poliovirus type 1 contributes to attenuation in mice. *J Virol* **67**:4630-8.
495. **Tebbens, R. J., M. A. Pallansch, O. M. Kew, V. M. Caceres, H. Jafari, S. L. Cochi, R. W. Sutter, R. B. Aylward, and K. M. Thompson.** 2006. Risks of

- paralytic disease due to wild or vaccine-derived poliovirus after eradication. *Risk Anal* **26**:1471-505.
496. **Teterina, N. L., A. E. Gorbalenya, D. Egger, K. Bienz, and E. Ehrenfeld.** 1997. Poliovirus 2C protein determinants of membrane binding and rearrangements in mammalian cells. *J Virol* **71**:8962-72.
497. **Tewari, M. K., G. Sinnathamby, D. Rajagopal, and L. C. Eisenlohr.** 2005. A cytosolic pathway for MHC class II-restricted antigen processing that is proteasome and TAP dependent. *Nat Immunol* **6**:287-94.
498. **The Cuba IPV Study Collaborative Group.** 2007. Randomized, Placebo-Controlled Trial of Inactivated Poliovirus Vaccine in Cuba. *N Engl J Med* **356**:1536-1544.
499. **The Global Polio Eradication Initiative** 10th January 2012 2010, posting date. Data and monitoring. Polio cases in the world in 2011. [Online.]
500. **Theiler, M.** 1946. Presented at the Mech. Immun. Poliomyelitis, Baltimore, M. D.
501. **Thompson, J. D., D. G. Higgins, and T. J. Gibson.** 1994. CLUSTAL W: improving the sensitivity of progressive multiple sequence alignment through sequence weighting, position-specific gap penalties and weight matrix choice. *Nucleic Acids Res* **22**:4673-80.
502. **Thompson, K. M., R. J. Tebbens, M. A. Pallansch, O. M. Kew, R. W. Sutter, R. B. Aylward, M. Watkins, H. E. Gary, Jr., J. Alexander, H. Jafari, and S. L. Cochi.** 2008. The risks, costs, and benefits of possible future global policies for managing polioviruses. *Am J Public Health* **98**:1322-30.
503. **Timm, E. A., I. W. McLean, Jr., C. H. Kupsky, and A. E. Hook.** 1956. The nature of the formalin inactivation of poliomyelitis virus. *J Immunol* **77**:444-52.
504. **Timm, E. A., E. Z. Rope, and L. I. Mc, Jr.** 1958. Chick potency tests of poliomyelitis vaccine: basic studies on response. *J Immunol* **80**:407-14.
505. **Tomlinson, A. J. H., and J. Davies.** 1961. Trial of living attenuated poliovirus vaccine. A report of the public health laboratory service to the poliomyelitis vaccines committee of the medical research council. *British Medical Journal* **2**:1037-1044.
506. **Toolan, H. W.** 1954. Transplantable human neoplasms maintained in cortisone-treated laboratory animals: H.S. No. 1; H.Ep. No. 1; H.Ep. No. 2; H.Ep. No. 3; and H.Emb.Rh. No. 1. *Cancer Res* **14**:660-6.
507. **Toyoda, H., M. J. Nicklin, M. G. Murray, C. W. Anderson, J. J. Dunn, F. W. Studier, and E. Wimmer.** 1986. A second virus-encoded proteinase involved in proteolytic processing of poliovirus polyprotein. *Cell* **45**:761-70.

508. **Tsang, S. K., P. Danthi, M. Chow, and J. M. Hogle.** 2000. Stabilization of poliovirus by capsid-binding antiviral drugs is due to entropic effects. *J Mol Biol* **296**:335-40.
509. **Tsvetkova, E. A., and N. M. Nepomnyaschaya.** 2001. Principles of selective inactivation of a viral genome. Comparative kinetic study of modification of the viral RNA and model protein with oligoaziridines. *Biochemistry (Mosc)* **66**:875-84.
510. **Tuthill, T. J., D. Bubeck, D. J. Rowlands, and J. M. Hogle.** 2006. Characterization of early steps in the poliovirus infection process: receptor-decorated liposomes induce conversion of the virus to membrane-anchored entry-intermediate particles. *J Virol* **80**:172-80.
511. **Tuthill, T. J., E. Groppelli, J. M. Hogle, and D. J. Rowlands.** 2010. Picornaviruses. *Curr Top Microbiol Immunol* **343**:43-89.
512. **Twomey, T., J. Newman, T. Burrage, P. Piatti, J. Lubroth, and F. Brown.** 1995. Structure and immunogenicity of experimental foot-and-mouth disease and poliomyelitis vaccines. *Vaccine* **13**:1603-10.
513. **Tydeman, M. S., and T. B. Kirkwood.** 1984. Design and analysis of accelerated degradation tests for the stability of biological standards I. Properties of maximum likelihood estimators. *J Biol Stand* **12**:195-206.
514. **Uittenbogaard, J. P., B. Zomer, P. Hoogerhout, and B. Metz.** 2011. Reactions of {beta}-Propiolactone with Nucleobase Analogues, Nucleosides, and Peptides: IMPLICATIONS FOR THE INACTIVATION OF VIRUSES. *J Biol Chem* **286**:36198-214.
515. **United States Department of Health Education and Welfare.** 1968. Biological Products Public Health Service, p. 32-44. *In* Public Health Service (ed.), 42. Division of Biological Standards National Institutes of Health, Maryland.
516. **Vaheri, A., and J. S. Pagano.** 1965. Infectious poliovirus RNA: a sensitive method of assay. *Virology* **27**:434-6.
517. **van der Avoort, H. G., B. P. Hull, T. Hovi, M. A. Pallansch, O. M. Kew, R. Crainic, D. J. Wood, M. N. Mulders, and A. M. van Loon.** 1995. Comparative study of five methods for intratypic differentiation of polioviruses. *J Clin Microbiol* **33**:2562-6.
518. **Van Regenmortel, M. H.** 2000. Binding measurements as surrogate biological assays: surface plasmon resonance biosensors for characterizing vaccine components. *Dev Biol (Basel)* **103**:69-74.

519. **van Rooyen, C. E. a. M., A.D.** 1943. Poliomyelitis. Experimental work in Egypt. *Edinburgh Medical Journal* **L**:705-720.
520. **van Steenis, G., A. L. van Wezel, and V. M. Sekhuis.** 1981. Potency testing of killed polio vaccine in rats. *Dev Biol Stand* **47**:119-28.
521. **van Wezel, A. L.** 1967. Growth of cell-strains and primary cells on micro-carriers in homogeneous culture. *Nature* **216**:64-5.
522. **van Wezel, A. L., and A. G. Hazendonk.** 1979. Intratypic serodifferentiation of poliomyelitis virus strains by strain-specific antisera. *Intervirology* **11**:2-8.
523. **Ventoso, I., S. E. MacMillan, J. W. Hershey, and L. Carrasco.** 1998. Poliovirus 2A proteinase cleaves directly the eIF-4G subunit of eIF-4F complex. *FEBS Lett* **435**:79-83.
524. **Verdijk, P., N. Y. Rots, and W. A. Bakker.** 2011. Clinical development of a novel inactivated poliomyelitis vaccine based on attenuated Sabin poliovirus strains. *Expert Rev Vaccines* **10**:635-44.
525. **Voloshchuk, T. P., V. Patskovskii Iu, and A. I. Potopal'skii.** 1999. [Alkylation of nucleic acid components with ethylenimine and its derivatives. IV. Alkylation of homopolynucleotides and DNA]. *Bioorg Khim* **25**:464-73.
526. **Voloshchuk, T. P., Y. V. Patskovskii, and A. I. Potopal'skii.** 1993. *Bioorganicheskaya khimiya* **19**:484-493.
527. **von Ahlfen, S., A. Missel, K. Bendrat, and M. Schlumpberger.** 2007. Determinants of RNA quality from FFPE samples. *PLoS One* **2**:e1261.
528. **Voroshilova, M. K., V. I. Zhevandrova, E. A. Tolskaya, G. A. Koroleva, and G. P. Taranova.** 1960. Presented at the Second International Conference on Live Poliovirus Vaccines, Washington, D.C.
529. **Wang, B., X. Zhang, Z. Cai, L. Ma, Z. Gao, M. Sun, S. D. Jiang, W. Li, J. Yang, and G. Liao.** 2010. Inactivation effect of binary ethylenimine on type II poliovirus. *Chinese Journal of Biologicals*:649-653.
530. **Wang, C. Y., S. Lynn, M.-H. Jong, Y.-L. Lin, T.-Y. Chang, A. Walfield, A. Wang, J. Wang, and C. Sia.** 2004. Appendix 58: Full protection in pigs against FMDV challenge following single dose of synthetic emergency FMD vaccine.
531. **Wassilak, S., M. A. Pate, K. Wannemuehler, J. Jenks, C. Burns, P. Chenoweth, E. A. Abanida, F. Adu, M. Baba, A. Gasasira, J. Iber, P. Mkanda, A. J. Williams, J. Shaw, M. Pallansch, and O. Kew.** 2011. Outbreak of type 2 vaccine-derived

- poliovirus in Nigeria: emergence and widespread circulation in an underimmunized population. *J Infect Dis* **203**:898-909.
532. **Westdijk, J., D. Brugmans, J. Martin, A. van't Oever, W. A. Bakker, L. Levels, and G. Kersten.** 2011. Characterization and standardization of Sabin based inactivated polio vaccine: proposal for a new antigen unit for inactivated polio vaccines. *Vaccine* **29**:3390-7.
533. **Westrop, G. D., K. A. Wareham, D. M. Evans, G. Dunn, P. D. Minor, D. I. Magrath, F. Taffs, S. Marsden, M. A. Skinner, G. C. Schild, and J. W. Almond.** 1989. Genetic basis of attenuation of the Sabin type 3 oral poliovirus vaccine. *J Virol* **63**:1338-44.
534. **Wetz, K.** 1987. Cross-linking of poliovirus with bifunctional reagents: biochemical and immunological identification of protein neighbourhoods. *J Virol Methods* **18**:143-51.
535. **White, J. M., and D. R. Littman.** 1989. Viral receptors of the immunoglobulin superfamily. *Cell* **56**:725-8.
536. **WHO Collaborative Study Group on Oral and Inactivated Poliovirus Vaccines.** 1996. Combined immunization of infants with oral and inactivated poliovirus vaccines: results of a randomized trial in the Gambia, Oman, and Thailand. *Bull World Health Organ* **74**:253-268.
537. **Wigler, M., S. Silverstein, L. S. Lee, A. Pellicer, Y. Cheng, and R. Axel.** 1977. Transfer of purified herpes virus thymidine kinase gene to cultured mouse cells. *Cell* **11**:223-32.
538. **Wimmer, E.** 1982. Genome-linked proteins of viruses. *Cell* **28**:199-201.
539. **Wood, D. J.** 1997. New approaches to oral poliovirus vaccine neurovirulence tests: transgenic mice susceptible to poliovirus and molecular analysis of poliovirus. A meeting of the WHO Global Programme for Vaccines and Immunization and the WHO Biologicals Unit, Geneva, Switzerland, 26-28 September 1996. *Vaccine* **15**:341-345.
540. **Wood, D. J., and A. B. Heath.** 1995. A WHO collaborative study of immunogenicity assays of inactivated poliovirus vaccines. *Biologicals* **23**:301-11.
541. **Wood, D. J., A. B. Heath, and L. A. Sawyer.** 1995. A WHO Collaborative study on assays of the antigenic content of inactivated poliovirus vaccines. *Biologicals* **23**:83-94.

542. **Wood, D. J., and B. Hull.** 1999. L20B cells simplify culture of polioviruses from clinical samples. *J Med Virol* **58**:188-92.
543. **Wood, D. J., and A. J. Macadam.** 1997. Laboratory tests for live attenuated poliovirus vaccines. *Biologicals* **25**:3-15.
544. **Wood, D. J., R. W. Sutter, and W. R. Dowdle.** 2000. Stopping poliovirus vaccination after eradication: issues and challenges. *Bull World Health Organ* **78**:347-57.
545. **World Health Organization.** 2002. Annex 2. Recommendations for the production and control of poliomyelitis vaccine (inactivated). World Health Organization.
546. **World Health Organization.** 2008. Eliminating needles, Polio Pipeline, vol. 1.
547. **World Health Organization.** 2004. Global Polio Eradication Initiative, Strategic Plan 2004-2008. *Weekly Epidemiological Record* **79**:55-57.
548. **World Health Organization.** 2008. Improving IPV, Polio Pipeline, vol. 1.
549. **World Health Organization.** 2006. Inactivated poliovirus vaccine following oral poliovirus vaccine cessation. Supplement to the WHO position paper. *Weekly Epidemiological Record* **81**:137-144.
550. **World Health Organization.** 1997. Manual for the Virological Investigation of Poliomyelitis WHO/EP/GEN/97.01. World Health Organization.
551. **World Health Organization** 9th January 2012 2012, posting date. Polio Case Count. [Online.]
552. **World Health Organization.** 2004. Polio Laboratory Manual. World Health Organization.
553. **World Health Organization.** 2010. Poliomyelitis in Tajikistan: first importation since Europe certified polio-free. *Weekly Epidemiological Record* **85**:157-158.
554. **World Health Organization.** 2003. Poliovirus type 2 (MEF-1) found in Northern India. Polio Lab Network Quartely Update, September 2003 **Vol IX**:1-2.
555. **World Health Organization.** 2004. Progress towards global poliomyelitis eradication: preparation for the oral poliovirus vaccine cessation era. *Weekly Epidemiological Record* **79**:349-356.
556. **World Health Organization.** 2002. Progress towards the global eradication of poliomyelitis, 2001. *Wkly Epidemiol Rec* **77**:98-107.
557. **World Health Organization.** 2009. Update on improving IPV, Polio Pipeline, vol. 3.
558. **World Health Organization.** 2006. Vaccine-derived polioviruses - update. *Weekly Epidemiological Record* **81**:398-404.

559. **World Health Organization.** 2009. Vaccine-derived polioviruses detected worldwide, January 2008-June 2009. *Weekly Epidemiological Record* **84**:390-396.
560. **World Health Organization.** 2011. Vaccine-derived polioviruses detected worldwide, July 2009-March 2011. *Weekly Epidemiological Record* **86**:277-286.
561. **World Health Organization.** 2003. WHO global action plan for laboratory containment of wild polioviruses, 2nd ed, Geneva:WHO.
562. **Wyman, O.** 2009. Global post-eradication IPV supply and demand assessment: integrated findings. Bill & Melinda Gates Foundation.
563. **Xing, L., K. Tjarnlund, B. Lindqvist, G. G. Kaplan, D. Feigelstock, R. H. Cheng, and J. M. Casasnovas.** 2000. Distinct cellular receptor interactions in poliovirus and rhinoviruses. *EMBO J* **19**:1207-16.
564. **Yakovenko, M. L., E. A. Cherkasova, G. V. Rezapkin, O. E. Ivanova, A. P. Ivanov, T. P. Eremeeva, O. Y. Baykova, K. M. Chumakov, and V. I. Agol.** 2006. Antigenic evolution of vaccine-derived polioviruses: changes in individual epitopes and relative stability of the overall immunological properties. *J Virol* **80**:2641-53.
565. **Yalamanchili, P., K. Harris, E. Wimmer, and A. Dasgupta.** 1996. Inhibition of basal transcription by poliovirus: a virus- encoded protease (3Cpro) inhibits formation of TBP-TATA box complex in vitro. *J Virol* **70**:2922-9.
566. **Yang, C., H. Shi, J. Zhou, Y. Liang, and H. Xu.** 2009. CpG oligodeoxynucleotides are a potent adjuvant for an inactivated polio vaccine produced from Sabin strains of poliovirus. *Vaccine* **27**:6558-63.
567. **Yang, C. F., H. Y. Chen, J. Jorba, H. C. Sun, S. J. Yang, H. C. Lee, Y. C. Huang, T. Y. Lin, P. J. Chen, H. Shimizu, Y. Nishimura, A. Utama, M. Pallansch, T. Miyamura, O. Kew, and J. Y. Yang.** 2005. Intratypic recombination among lineages of type 1 vaccine-derived poliovirus emerging during chronic infection of an immunodeficient patient. *J Virol* **79**:12623-34.
568. **Yang, C. F., L. De, B. P. Holloway, M. A. Pallansch, and O. M. Kew.** 1991. Detection and identification of vaccine-related polioviruses by the polymerase chain reaction. *Virus Res* **20**:159-79.
569. **Yang, C. F., L. De, S. J. Yang, J. Ruiz Gomez, J. R. Cruz, B. P. Holloway, M. A. Pallansch, and O. M. Kew.** 1992. Genotype-specific in vitro amplification of sequences of the wild type 3 polioviruses from Mexico and Guatemala. *Virus Res* **24**:277-96.

570. **Yang, C. F., T. Naguib, S. J. Yang, E. Nasr, J. Jorba, N. Ahmed, R. Campagnoli, H. van der Avoort, H. Shimizu, T. Yoneyama, T. Miyamura, M. Pallansch, and O. Kew.** 2003. Circulation of endemic type 2 vaccine-derived poliovirus in Egypt from 1983 to 1993. *J Virol* **77**:8366-77.
571. **Yogo, Y., and E. Wimmer.** 1975. Sequence studies of poliovirus RNA. III. Polyuridylic acid and polyadenylic acid as components of the purified poliovirus replicative intermediate. *J Mol Biol* **92**:467-77.
572. **Yoshida, H., H. Horie, K. Matsuura, T. Kitamura, S. Hashizume, and T. Miyamura.** 2002. Prevalence of vaccine-derived polioviruses in the environment. *J Gen Virol* **83**:1107-11.
573. **Zamora, M., W. E. Marrison, and R. E. Lloyd.** 2002. Poliovirus-mediated shutoff of host translation: an indirect effect, p. 313-320. *In* B. L. Semler and E. Wimmer (ed.), *Molecular Biology of Picornaviruses*. ASM Press, Washington, DC.
574. **Zhang, P., S. Mueller, M. C. Morais, C. M. Bator, V. D. Bowman, S. Hafenstein, E. Wimmer, and M. G. Rossmann.** 2008. Crystal structure of CD155 and electron microscopic studies of its complexes with polioviruses. *Proc Natl Acad Sci U S A* **105**:18284-9.
575. **Zhdanov, V. M., M. P. Chumakov, and A. A. Smorodintsev.** 1960. Presented at the Second International Conference on Live Poliovirus Vaccines, Washington, D.C.